MONASH University

Endosome NOX2 oxidase promotes viral pathogenicity and provides a potential target for novel antiviral therapies

Eunice Elizabeth To

Bachelor of Science (Honours)

A Thesis submitted to the Faculty of Medicine, Nursing and Health Sciences in total fulfillment of the requirements of the degree of

DOCTOR OF PHILOSOPHY

2017

Department of Pharmacology

Monash University

Melbourne, Victoria

Australia

Table of Contents

General Declaration

Monash University

Monash Research Graduate School

In accordance with Monash University Doctorate Regulation 17.2 Doctor of Philosophy the following declarations are made:

I hereby declare that this thesis contains no material that has been accepted for the award of any other degree or diploma at any university or equivalent institution and that, to the very best of my knowledge and belief, this thesis contains no material previously published or written by another person, except where due reference is made in the text of the thesis.

This thesis contains two original papers published in a peer-reviewed journal and one unpublished manuscript. The core theme of the thesis examines the cellular biology of reactive oxygen species (ROS) in viral pathology. The ideas, development and writing up of all the papers in the thesis were the principal responsibility of myself, the candidate, working within the Department of Pharmacology under the supervision of Dr Stavros Selemidis.

The inclusion of co-authors reflects the fact that the work came from active collaboration between researchers and acknowledge input into team-based research.

In the case of chapters 2 and 3 my contribution to the work involved the following:

Thesis chapter	Publication title	Publication status	Nature and extent of candidate's contribution	Co-author name(s) and % of Co-author's contribution	Co-author(s), Monash student Y/N*
2	Influenza A virus and TLR7 activation potentiate NOX2 oxidase-dependent ROS production in macrophages	Published	Conducted all experiments, analysed results and wrote manuscript, with intellectual advice and editorial assistance from co-	1) Brad Broughton- N/A 2) Keshia Hendricks - N/A 3) Ross Vlahos - N/A 4) Stavros Selemidis -N/A	1) No 2) Yes 3) No 4) No

			authors -**95%**		
3	Endosomal NOX2 oxidase exacerbates virus pathogenicity and is a target for antiviral therapy	Accepted for publication	Conducted all experiments except the high content radiometric FRET imaging assay and designing/creating conjugation of Nox2 inhibitors, analysed results and wrote manuscript, with intellectual advice and editorial assistance from co-authors – **85%**	1) Ross Vlahos - N/A 2) Raymond Luong - 10% 3) Michelle L. Halls - N/A 4) Patrick Reading - N/A 5) Paul King - N/A 6) Christopher Chan - 1% 7) Grant Drummond - N/A 8) Chris Sobey - N/A 9) Brad Broughton - N/A 10) Malcolm Starkey - N/A 11) Renee V. Sluis - N/A 12) Sharon Lewin - N/A 13) Steven Bozinovski - N/A 14) Luke O'Neil - N/A 15) Tim Quach - N/A 16) Chris Porter - N/A 17) Doug A. Brooks - N/A 18) John O'Leary - N/A 19) Stavros Selemidis- N/A	1) No 2) Yes 3) No 4) No 5) No 6) Yes 7) No 8) No 9) No 10) No 11) No 12) No 13) No, 14) No 15) No 16) No 17) No 18) No 19) No

I have renumbered sections of submitted or published papers in order to generate a consistent presentation with the thesis.

Student signature: [redacted] Date: 17-02-2017

The undersigned hereby certify that the above declaration correctly reflects the nature and extent of the student and co-authors' contributions to this work. In instances where I am not the responsible author I have consulted with the responsible author to agree on the respective contributions of the authors.

[redacted]

Main Supervisor signature: Date: 17-02-2017

Acknowledgements

First and foremost, I would like express the deepest appreciation to my supervisor, Dr. Stavros Selemidis, not only for the his scholarly advice, patience and immense support in guiding me throughout this project, but also for his prompt inspirations, meticulous scrutiny and continual dedication towards research that has moulded my enthusiasm to achieve something of merit. I feel privileged and extremely grateful to have been given this opportunity for personal development and professional enhancement; something less tangible but far more precious than the qualifications gained.

The experience and knowledge gained from learning a wide array of experimental techniques has been invaluable. Needless to say, this would not have been possible without the help of A/Prof. Ross Vlahos, who spent countless hours teaching me various aspects of the *in vivo* models; Dr. Brad Broughton, for providing advice and technical suggestions regarding immunohistochemistry; Dr. Michelle Halls for performing and teaching me site-directed mutagenesis and cell transfection assays; Ray and Keshia, who I have worked closely with throughout the past few years and have been fantastic lab mates. Thank you!

I would like to extend my gratitude to my family, especially my sister (Deborah) for their unwavering support and encouragement, and friends (Kaki, Monika, Chau, Jane, Huey Wen, Jack, Dumindi and Shaz) for their comfort and unwavering support, who have carried me through the storms and has gotten me through this roller coaster ride.

Last but not least I would like to thank my fellow colleagues and friends, for the friendships made, entertaining conversations in the student room, are memories that I will always cherish. A special thanks to Prof. Robert Widdop for his support, it has been a great pleasure to work in the Department of Pharmacology. Definitely have made this journey a blast and an unforgettable experience!

Summary

The ever present threat of viral epidemics and pandemics, emerging anti-viral resistance, and long lag times for vaccine development highlight an urgent need for novel approaches to target viral pathology. Almost all of the current immunisation and therapeutic strategies depend on strain specific features of the virus to provide specificity. Thus, identifying a strain-dependent mechanism that targets a common process of pathogenesis across all viral strains is essential. The experiments described in this thesis use both *in vitro* and *in vivo* models to explore and identify potential novel therapeutic targets in viral infections, with a focus on influenza A viruses. The over production of reactive oxygen species (ROS) are known to be key contributors to lung injury during influenza A virus infection, mainly being produced by the NOX2 containing NADPH oxidase (NOX) enzyme complex. However, the subcellular sites of ROS generation and how ROS exerts their effects to influence lung inflammation remain ill defined.

In Chapter 2, we demonstrated the influenza A virus (IAV) internalises in RAW264.7 macrophage cells and mouse alveolar macrophages, causing an elevation in NOX2-oxidase dependent oxidative burst. Toll-like receptors play an important role in the recognition of microbial pathogen associated molecular patterns and function as a crucial line of defense against microbial infection. TLR7 activation with imiquimod increased basal superoxide and similar to influenza A virus, enhanced the NOX2-oxidase dependent oxidative burst. In contrast, stimulation with the TLR3 agonist poly I:C failed to impact the oxidative burst. Moreover, a custom synthesised peptide corresponding to the region 337-348 on p47phox conjugated to a HIV-tat, designed to inhibit the phosphorylation of Ser346 on p47phox suppressed the IAV and imiquimod-induced enhancement in the oxidative burst. Taken together, this study demonstrated for the first time that IAV infection and TLR7 activation enhance the NOX2 oxidase dependent oxidative burst in macrophages, highlighting the importance of Ser346 for a functional NOX2 enzyme. These data may underpin the lung inflammation associated with IAV infections.

Having established that virus infection enhanced the oxidative burst, we next examined the subcellular sites of ROS production in reponse to viruses. In Chapter 3, we have made the profound discovery that viral replication and pathogenesis is heavily reliant on the production of ROS in endosomes. Here, we identified that ssRNA viruses including IAV, HIV, Dengue (flaviviridae type and related to *Zika virus*), Respiratory Synctitial Virus, Rhinovirus, Human Parainfluenza Virus, Human Metapneumovirus Viruses and DNA viruses including Herpes Simplex and Vaccinia Virus generated large quantities of ROS in endosomes. ROS generation triggered by ssRNA and DNA viruses involved a highly specific endosome signalling platform

that relies on either recognition by TLR7-MyD88 for ssRNA viruses or TLR9 for DNA viruses. This has direct significance for improved understanding of the pathogenesis of major RNA viral infections in humans. Furthermore, we showed that the NOX enzymes are directly involved in viral-induced ROS production in endosomes. Downstream activation of protein kinase C and NOX2 oxidase assembly/activity is directly responsible for ROS generation, and specifically superoxide/H_2O_2 production. We identify that the molecular target of endosomal H_2O_2 involves a single essential and unique cysteine residue on the ectodomain of TLR7 (i.e. Cys98), which suppressed host humoral immunity against the infecting virus. This is the first ever demonstration of a molecular signalling target of ROS that resides *within* endosomal compartments and unravels a new paradigm of organelle-dependent cell signalling. In light of these findings, we subsequently synthesised an innovative molecular targeting system, to deliver a specific NOX2 oxidase inhibitor (Cgp91) directly to endosomes thereby disrupting the viral signalling platform via abrogation of ROS production. We provide pre-clinical data that demonstrated that this molecular construct is effective at reducing endosomal ROS production, airway inflammation and expression of anti-viral cytokines in Hkx-31 infected mice, which has a significant downstream impact on humoral immunity and viral clearance.

Having shown that Cgp91 provides protection against the low pathogenic Hkx-31 strain in a prevention model, we also determined whether it provides protection against both Hkx-31 and the more virulent PR8 strain in an intervention model of virus infection. In Chapter 4, we demonstrated that administration of Cgp91 via prevention was effective in reducing airway inflammation, neutrophil influx, pulmonary inflammationin, ROS generation and viral mRNA expression in PR8 infected-mice. However, administration of Cgp91 via intervention was not as effective in relieving influenza symptoms in PR8-infected, but did reduce airway inflammation and neutrophil infiltration in Hkx-31-infected mice. Collectively, these data suggested that targeting endosomal ROS using Cgp91 may be used as a potential adjuvant for treating viral infections.

In summary, the findings suggest that endosomal NOX2-derived ROS are essential mediators of a fundamental molecular mechanism of viral pathogenicity that impacts on innate immunity and the capacity of the host to fight and clear viral infections. This discovery is significant since it provides a new paradigm in fundamental understanding of viral infection and at the same time has great potential for translation into a therapeutic strategy. The specific targeting of this pathogenic process with our novel endosomal targeted ROS inhibitor has major implications for the management and treatment of globally devastating viruses.

Abbreviations

ANOVA	analysis of variance
AM	alveolar macrophage
Apocynin	4-hydroxy-3-methoxyacetophenone/acetovanillone
Baf-A	bafilomycin A
BALF	bronchoalveolar lavage fluid
BMDM	bone marrow-derived macrophages
BSA	bovine serum albumin
CCP	clathrin-coated pits
CGD	chronic granulomatous disease
Cgp91	cholestanol-conjugated gp91ds-TAT
CME	clathrin-mediated endocytosis
CYBB	cytochrome B-245 Beta Chain
DAPI	4', 6-diamidino-2-phenylindole
DIPEA	N,N-diisopropylethylamine
DMSO	dimethyl sulfoxide
DNA	deoxyribonucleic acid
DMF	N,N-dimethylformamide
Duox	dual oxidase
dsRNA	double-stranded ribonucleic acid
EDT	1,2-ethanedithiol
EEA1	early endosome antigen 1
Egp91	ethyl conjugated gp91ds-TAT
ERK	extracellular signal regulated kinase
FBS	fetal bovine serum
FRET	fluorescence resonance energy transfer
Fe^{2+}	iron (II)
FITC	fluorescein isothiocyanate

GAPDH	glyceraldehyde 3-phosphate dehydrogenase
Gp91ds-tat	glycoprotein 91 double stranded-tat
GPx	glutathione peroxidase
GTP	guanosine triphosphate
HA	heamagluttinin
HCl	hydrochloric acid
HCTU	O-(6-chlorobenzotriazol-1-yl)-N,N,N',N'-tetramethyluronium hexafluorophosphate
HEPES	4-(2-hydroxyethyl)-1-piperazineethanesulfonic acid
HIV	human immunodeficiency virus
Hk x-31	Hong Kong x-31
HMPV	human metapneumovirus
HPIV	human parainfluenza virus
HRP	horseradish peroxidase
HSV	herpes simplex virus
H_2O_2	hydrogen peroxide
H_2O	water
IAV	influenza A virus
IFN-α	interferon alpha
IFN-β	interferon beta
IL-1β	interluekin-1 beta
i.n	intranasal
i.p	intraperitoneal
IRF-7	interferon regulatory factor 7
IL-6	interleukin-6
L-012	8-amino-5-chloro-7-phenylpyrido[3,4-d]pyridazine-1,4(2H,3H)dione
mAb	monoclonal antibody
MAPK	mitogen-activated protein kinase
MAVS	mitochondrial antiviral-signaling protein

MCP-1	monocyte chemoattractant protein-1
MIP-2	macrophage inflammatory protein-2
mRNA	messenger ribonucleic acid
MTS	[3-(4,5-dimethylthiazol-2-yl)-5-(3-carboxymethoxyphenyl)-2-(4-sulfophenyl)-2H-tetrazolium]
MyD88	myeloid Differentiation Primary Response 88
NA	neuraminidase
NAC	N-Acetyl-L-cysteine
NDV	newcastle disease virus
NADPH	nicotinamide adenine dinucleotide phosphate
NLR	nucleotide-binding oligomerization domain-like receptor
NF-κB	nuclear factor κB
NLR	nucleotide-binding oligomerization domain-like receptor
NLRP3	NACHT, LRR and PYD domains-containing protein 3
NTHI	non-typeable haemophilus influenzae
NO	nitric oxide
NOX	NADPH oxidase
NP	nucleoprotein
O_2	molecular oxygen
$O_2^{-\cdot}$	superoxide
ODN	oligodeoxynucleotide
OH^-	hydroxide
$ONOO^-$	peroxynitrite
PAMP	pathogen associated molecular pattern
PDB	phorbol dibutyrate
PEI	polyethyleneimine
PBS	phosphate buffered saline
Poly I:C	polyinosinic-polycytidylic acid
PKC	protein kinase C

PFA	paraformaldehyde
PR8	Puerto Rico 8
PRR	pattern recognition receptor
PTP	protein tyrosine phosphatases
RAC	ras-related C3 botulinum toxin substrate
RIG-I	retinoic acid inducible gene I
RNA	ribonucleic acid
ROS	reactive oxygen species
RSV	respiratory syncytial virus
siRNA	small interfering ribonucleic acid
SP	streptococcus pneumoniae
ssRNA	single-stranded ribonucleic acid
TBS-T	tris buffered saline containing 0.1% tween 20
TNBS	2,4,6-trinitrobenzenesulfonic acid
SOD	superoxide dismutase
TFA	trifluoroacaetic acid
TNF-α	tumour necrosis factor alpha
TLR	toll-like receptor
TRITC	tetramethylrhodamine
TREML4	triggering receptor expressed on myeloid cells Like 4
Ugp91	unconjugated gp91ds-TAT
UV	ultraviolet
vRNP	viral ribonucleoprotein
V-ATPase	vacuolar (H^+)-ATPase
QPCR	quantitative polymerase chain reaction
3-NT	3-Nitrotyrosine

Units of measure

g	gram
h	hour
min	minute
mg	milligram
µg	microgram
µL	microlitre
M	molar
mM	millimolar
µM	micromolar
U	units
U/ml	units per millilitre
RLU	relative light units
rpm	revolutions per minute
SEM	standard error of the mean
MW	molecular weight
%	percentage
°C	degrees celsius

Chapter 1:
General introduction

Influenza A virus and the socio-economic burden it imposes

Influenza A viruses belong to the *Orthomyxoviridae* family, which possess several unique characteristics. They are composed of a genome of eight single-stranded ribonucleic acids that encodes 12 viral proteins (Palese and Shaw, 2007). Influenza A viruses are classified based upon the antigenic properties of key viral surface proteins, namely haemagglutinin (HA) and neuraminidase (NA) that are arranged mostly outside the lipid membrane (Boulo *et al.*, 2007). HA is a multifunctional influenza A virus (IAV) protein and has an important role in determining the way in which the virus specifically interacts with the host, by binding onto host cell sialic acid receptors (Marsh *et al.*, 2007). Upon infection, the HA protein undergoes irreversible conformational changes to allow fusion of the viral envelope with the host membrane, thus mediating viral entry into the cell (Eierhoff *et al.*, 2010). NA functions by eliminating the sialic acid-containing receptors of the host and viral membranes, a process that is required for proper release of newly assembled virions from the host cell surface (Watanabe *et al.*, 2010). The M1 and M2 viral proteins interact with viral ribonucleoproteins (vRNPs) and the viral membrane, which is necessary for complete uncoating of the virus, promoting the transport of RNPs to the nucleus (Noton *et al.*, 2007; Roberts *et al.*, 1998; Ruigrok *et al.*, 2000). To date, there has been identification of 16 and 9 types of HA and NA, respectively, which differentiate the various strains of influenza viruses. While these virus strains circulate in birds and mammals, three have gained the capability to infect humans and cause significant mortality and morbidity, namely the H1N1, H2N2 and H3N2 strains. Indeed, over the last decade, these three virus strains have caused four major overwhelming pandemics: the 1918 H1N1 'Spanish flu', 1957 H2N2 'Asian flu', 1968 H3N2 'Hong Kong flu' and more recently the 2009 H1N1 'Swine flu' (Doherty *et al.*, 2006; Neumann *et al.*, 2009). As a result, the 1918 H1N1 'Spanish flu' caused 20-50 million fatalities worldwide, making it the largest known outbreak of infectious disease (La Gruta *et al.*, 2007). In addition to these pandemics, the H1N1 and H3N2 strains continue to cause seasonal epidemics, during which millions of people are infected, being responsible for approximately 50,000 deaths annually (Yang *et al.*, 2012). Infections are characterized by upper respiratory distress accompanied by fever, myalgia, nasal congestion and rhinitis. Infection is usually confined within the respiratory tract, but it is possible for it to become systemic depending on the strain of virus. For example, the highly pathogenic H5N1 subtype preferentially infects the lower respiratory tract, which can result in severe pneumonia and thus a higher mortality rate (Fukuyama *et al.*, 2011). In order for influenza virus to spread from the respiratory tract to other susceptible organs, it must enter the circulation, get transported and exit the tissue-blood junctions (Seo *et al.*, 2002). In cases where extreme severity of the disease causes death, is mainly associated with the adolescent, elderly and individuals who are immunocompromised (Fleming *et al.*, 2000). Due to the segmented nature

of the genomes, if a host cell is simultaneously infected with two different influenza strains, the gene segments of one virus can recombine with those of another virus during replication, a process known as genetic re-assortment, subsequently generating a novel influenza virus strain (Medina *et al.*, 2011). The emergence of new strains from the rapidly evolving and mutating viral genomic contents is predicted to be the cause of the next global outbreak (Müller *et al.*, 2012). The ease in which multiple virus strains transmit and spread to a broad spectrum of hosts, highlights the urgent requirement for effective therapies.

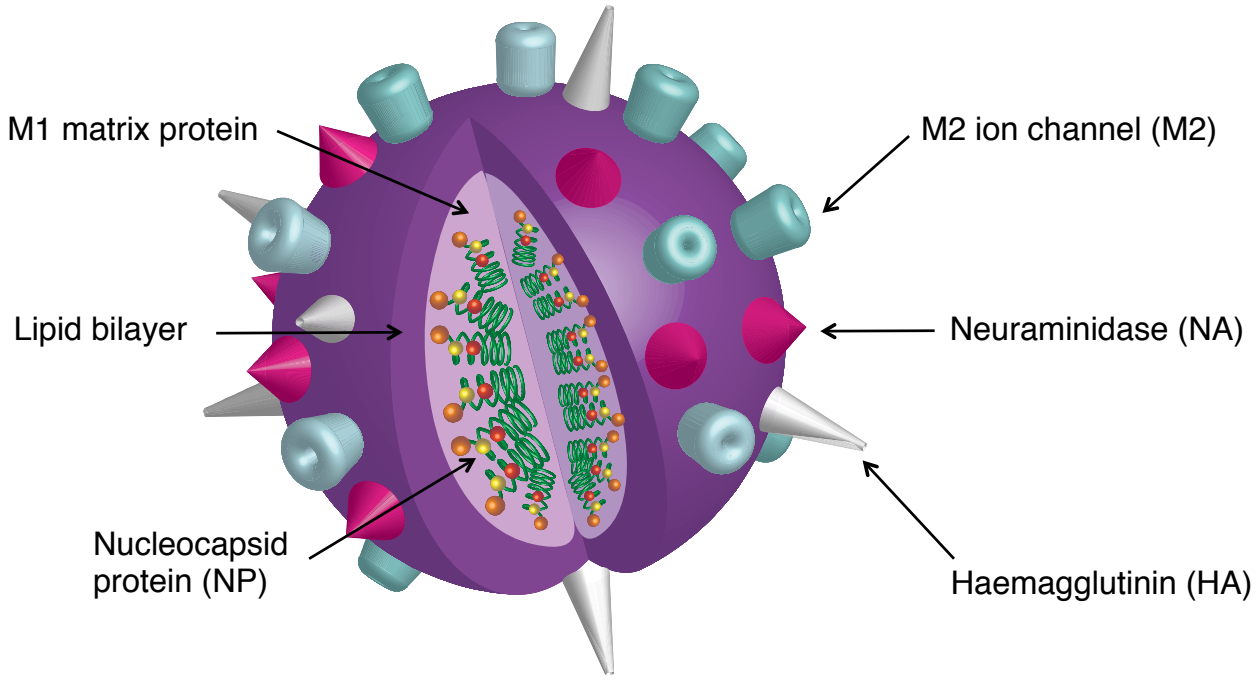

Figure 1: Schematic diagram displaying the different components of the influenza A virus structure. The virus consists of multiple negative sense single-stranded RNA segments, encoding various viral proteins including the surface glycoproteins embedded in the lipid bilayer, namely haemagglutinin (HA) and neuraminidase (NA). The M2 ion channels are a component of the viral envelope that is regulated by pH. Underneath the viral lipid membrane is the M1 matrix protein, holding the nucleocapsid protein.

Vaccines and the emergence of anti-influenza drug resistant viruses

Currently, vaccines and prophylactic antiviral therapeutics continue to be the most effective methods of containing the spread of IAV (Rumschlag-Booms *et al.*, 2013), although these therapies are largely ineffective against emerging strains of virus. Influenza vaccines are composed of antigens that function to initiate the production of antibodies when injected into humans, to neutralise the activity of the virus, and therefore preventing attachment of the virus

to susceptible cells (Yang *et al.*, 2012). However, the special feature of the influenza viruses having a segmented RNA genome that mutates frequently makes it almost impossible to produce an adequate and sufficiently effective vaccine. Furthermore, in the scenario of a pandemic, mass production of vaccines has found to be problematic, with current technology not being able to produce enough in a timely manner to halt the progress of a new strain (Moscona, 2005).

Antivirals are a means of prophylaxis and treatment for influenza virus infections, consisting of two drug classes that target the viral envelope: the adamantane and neuraminidase inhibitors (Bullough *et al.*, 1994). Adamantanes (amantadine and rimantadine) block the ion channel formed by the M2 protein to interfere with viral uncoating, which is critical for the release of viral ribonucleoprotein complexes into the cytoplasm. In addition, uncoating is required for activation of viral trafficking and provides signals to the cell to initiate innate immune system responses (Mercer *et al.*, 2013; Saxena *et al.*, 2012). Despite these ion channel inhibitors displaying effectiveness against influenza virus infection, they have been reported to cause adverse effects in the central nervous system and more than 99% of circulating IAV strains have become resistant, thus leading to the discontinuation of their use (Abed *et al.*, 2005; Rumschlag-Booms *et al.*, 2013; Yang *et al.*, 2012). The neuraminidase inhibitors (oseltamivir and zanamivir) interfere with the release of newly assembled progeny virions, thus preventing spread of the virus both within infected host cells and consequently to other cells (Moscona, 2005). Nonetheless, this drug class is also associated with the emergence of resistant virus strains (Lackenby *et al.*, 2008). The currently approved treatments that target key mechanisms of viral infection and replication are problematic due to drug resistance and have been demonstrated to be ineffective when administered two days post infection (Sheu *et al.*, 2011), which emphasizes the need for new effective therapeutics, in particular those that target the key mechanisms of the host immune response that occurs upon infection with IAV.

Internalisation of virus into endosomes

It has previously been mentioned that IAV can bind on the sialic acid receptors on the cell surface, although specific transmembrane receptors mediating IAV entry has not been fully elucidated and multiple receptors may exist. More recently, a C-type lectin langerin receptor was shown to act as an attachment for influenza A virus entry (Ng *et al.*, 2016). Other C-type lectin receptors that may not necessarily bear sialic acid residues have also been implicated for influenza A virus entry (Ng *et al.*, 2014; Upham *et al.*, 2010). A process known as clathrin-mediated endocytosis (CME) has been identified to be the main mechanism by which IAV is endocytosed (Matlin *et al.*, 1981; Patterson *et al.*, 1979; Yoshimura *et al.*, 1982). This involves the formation of clathrin-coated pits (CCPs) upon viral attachment, whereby the virus is

sequestered into these CCPs. CME is completely dependent on the guanosine triphosphate (GTPase) dynamin, which mediates the 'pinching off' of newly formed vesicles, allowing the virus to get internalised into the endosome (Scott *et al.*, 2002). To reinforce this, Banerjee *et al.* (2013) demonstrated that the dynamin inhibitor (Dynasore) was able to efficiently block influenza A viral endocytosis in the carcinomic human alveolar basal epithelial cell line (A549 cells). de Vries *et al.* (2011) made similar observations with the use of Dynasore in HeLa cells. Despite the outlook of inhibiting virus endocytosis by Dynasore to be of great clinical use, high concentrations of the inhibitor have exhibited cytotoxic effects in tissue culture and are therefore not suitable for clinical use (Bachran *et al.*, 2011). As the virus gets internalized, it passes through different stages of the endocytic network, where it is firstly transported into early endosomes (Helenius, 2013; Huotari *et al.*, 2011).

Once virus enters the endocytic pathway, it is subjected to an acidic environment, where the pH falls from 7.0 to 6.0-6.5 within early endosomes, and then further to 5.0-6.0 in late endosomes (White *et al.*, 1982). This acidic state is required for fusion of the viral membrane with endosomal membranes to cause a proton influx into the lumen of the virus, resulting in the release of viral ribonucleoprotein segments into the cytosol (Martin *et al.*, 1991; Wang *et al.*, 2009). Banerjee *et al* (2013) revealed using automated high-content fluorescence microscopy and a cell-permeable pH probe, that cells pretreated with the vacuolar (H+)-ATPase (V-ATPase) channel inhibitor Bafilomycin A1 blocked endosomal acidification, suggesting that the endocytic pathway is pH-sensitive. V-ATPase channels are proton pumps that maintain acidification of early and late endosomes (Forgac, 2007; Qi *et al.*, 2007). Evidently, the V-ATPase activity is found to be elevated during IAV infection (Marjuki *et al.*, 2011). In addition to facilitating release of contents into the cytosol, the fall in pH occurring in endosomes is crucial for IAV sensing by endosomal toll-like receptors (Diebold *et al.*, 2004; Marjuki *et al.*, 2011). This thesis focuses on the role of various host cellular targets, including pattern recognition receptors and NADPH oxidases, and their contribution to immunopathology following influenza A virus infection.

Pathological pathways of the host immune response

Unraveling the underlying mechanisms of the host immune response is crucial for understanding the pathogenesis of influenza A viruses. Influenza A viruses enter the lungs, where they primarily bind α-2,6 sialic acid receptors on airway epithelium and resident alveolar macrophages in the respiratory tract, leading to internalisation of the virus and viral replication (Heui *et al.*, 2008; Julkunen *et al.*, 2000). Infection of these cells leads to activation of the transcription factor nuclear factor kappa B (NF-kB), in turn producing cytokines, including tumor necrosis factor alpha (TNFα), interleukin-6 (IL-6) and chemokines, namely IL-8, monocyte

chemoattractant protein-1 (MCP-1) and macrophage inflammatory protein-2 (MIP-2) (Bußfeld *et al.*, 1998; Elsharkawy *et al.*, 2010; Julkunen *et al.*, 2000; Matsukura *et al.*, 1996). In contrast, Type I-interferons (i.e. IFNα/β) use an alternative pathway for signaling and generation, which occurs through interferon regulatory factor-3 (IRF-3) (Collins *et al.*, 2004). These cytokines and chemokines serve to perpetrate the inflammatory response by recruiting immune cells, including neutrophils, T lymphocytes and monocytes/macrophages, which is the basis of the host antiviral defense system (Baggiolini, 1998; Sallusto *et al.*, 2008). These processes must be tightly regulated to promote viral clearance whilst avoiding excessive inflammation to the surrounding tissue.

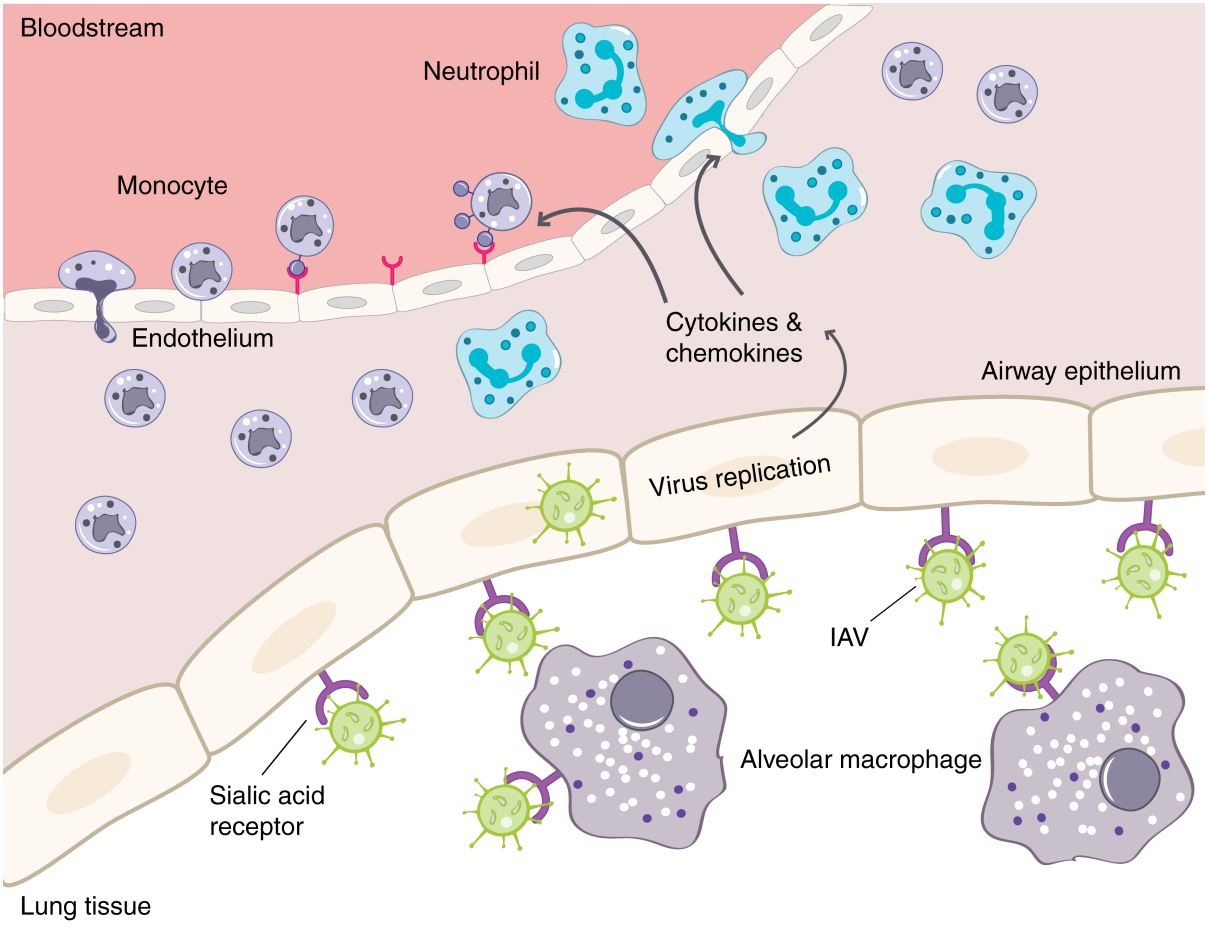

This work by Chau Khuong is licensed under a Creative Commons Attribution-NonCommercial-NoDerivatives 4.0 International License.

Figure 2: Schematic diagram depicting the major components of the innate immune response. Influenza A virus infects airway epithelium, in which virus replication occurs, triggering the release of cytokines and chemokines. Additionally, alveolar macrophages on the respiratory tract are also infected, resulting in activation of transcription factors that are necessary for the production of cytokines and chemokines. This enhanced lung inflammation results in the recruitment of other inflammatory cells, including monocytes and neutrophils.

Role of endosomal toll-like receptors

Toll-like receptors (TLRs) play a key role in the recognition of microbial pathogen associated molecular patterns (PAMPs) and function as a crucial line of defense against microbial infection, which ultimately bridges an effective innate and adaptive response (Bowie *et al.*, 2005). Currently, 10 human TLRs have been identified and are broadly expressed on antigen presenting cells, preferentially expressed on macrophages and dendritic cells (Liew *et al.*, 2005). Based on the cellular location, the TLR family can be divided into two subpopulations. TLR1-2, TLR4-6 and TLR10-11 are expressed on the cell surface, where they detect microbial components such as lipoproteins and lipids. On the other hand, TLR3 and TLR7-9 are expressed exclusively in intracellular vesicles, including endosomes and lysosomes where they mainly detect viral structures such as nucleic acids (Kawai *et al.*, 2009; Takeda *et al.*, 2015) (Refer to Table 1 for a list of all the TLRs and their ligands). The nucleic acid-recognizing TLRs are unresponsive to their ligands at the cell surface, but rather in endosomal compartments to mediate signaling cascades that upregulate inflammatory pathways (Akira *et al.*, 2001; Kagan, 2012). Importantly, TLR3 and TLR7 are located in the endosomal compartments where they detect viral nucleic acids (Nishiya *et al.*, 2004). Specifically, TLR3 and TLR7 recognise double-stranded RNA and single-stranded RNA (ssRNA), respectively (Diebold *et al.*, 2004; Muzio *et al.*, 2000).

Previous studies have shown that acidification within the endosome, results in the release of ssRNA from IAV, which can bind TLR7 via a MyD88-dependent pathway, and trigger an inflammatory response characterised by cytokine (IL-1β, IFN-β, IL-6 and IL-12) release (Diebold *et al.*, 2004; Hemmi *et al.*, 2002). This gives rise to one of the most important mechanisms of host-defense against viral infection. Activation of TLR7 can occur by stimulation with the synthetic agonist imiquimod. Imiquimod is known to be highly selective for TLR7, but can have dual effects on TLR7 and TLR8 in certain species (Zhu *et al.*, 2008). It has been used in a variety of diseased states, including superficial basal cell carcinoma, genital warts and cancer therapy (Ito *et al.*, 2015; von Krogh *et al.*, 2000).

To elucidate the importance of TLR7, Lund *et al.* (2004a) demonstrated that mice deficient in TLR7 and MyD88 had failed to secrete IL-12 and IFN-α and displayed impaired antiviral clearance mechanisms. For example, Thomas *et al.* (2009) showed that production of the antiviral cytokine IL-1β in response to IAV promotes survival in mice, as opposed to being associated with lethal immunopathology. In addition to this, Pang *et al.* (2013) demonstrated that TLR7 was required for proper viral replication. To further support the notion that TLR7 plays a protective role in promoting antiviral immunity, the use of the TLR7 ligand (loxoribine) inhibited replication of the highly pathogenic PR8 influenza A virus both *in vitro* and *in vivo*. In contrast, other studies did not find a requirement for TLR7 or its adaptor protein MyD88 in immune

defence or *in vivo* adaptive T cell responses against influenza virus challenge (Heer *et al.*, 2007; Le Goffic *et al.*, 2006; Seo *et al.*, 2010). The reasons for the discrepancies amongst these studies are unclear, which requires a deeper understanding of the biochemical pathways and signalling mechanisms of TLR7. Taken together, the use of TLR7 agonists for immunotherapy appears to provide a promising approach in developing novel antiviral treatments.

A key knowledge gap that needs to be addressed is the mechanism of TLR7 activation. TLR7 trafficking is regulated by the multi-transmembrane-domain containing Unc93B1, which was demonstrated to be indispensible for TLR7 responses (Fukui *et al.*, 2011; Kim *et al.*, 2008). Moreover, proteolytic cleavage of the ectodomain of TLR7 by asparagine endopeptidase (AEP) or a member of the cathepsin family is required for TLR7 signalling (Ewald *et al.*, 2011). Mechanistically, the N-terminal part of the ectodomain on TLR7 (TLR7N) forms intramolecular disulphide bonds with the truncated TLR7 (TLR7C) via unique cysteine residues. Specifically, the conserved Cys98 residue on TLR7N and Cys475 were necessary to form disulphide bonds to evoke TLR7 responses (Kanno *et al.*, 2013b).

Similar to TLR7, TLR8 also recognises ssRNA in the endosome. The way in which TLR7 and 8 discriminate between self and non-self RNA is unclear. TLR8 is expressed by human macrophages and monocytes. It is stimulated by its ligand ssRNA, which results in the production of IL-12 (Ablasser *et al.*, 2009). However, the relevance of TLR8 in influenza virus infection is largely unknown. In contrast, TLR9 is recognised by unmethylated CpG-containing oligodeoxynucleotide motifs (CpG ODNs) from bacteria and senses a genome of DNA viruses, including Herpes Simplex virus (HSV) and murine cytomegalovirus (MCMV). The ability for TLR9 to stimulate a Th-1 like response makes them a suitable target for the development of vaccines. Treatment with CpG-ODN (agonist of TLR9) provided a high level of protection against lethal doses of influenza A virus in mice (Wong *et al.*, 2009). Similarly, Han *et al.* (2014) demonstrated the use of a TLR9 agonist resulted in a significant reduction of viral and cytokine mRNA expression in lung epithelial cells. A deeper understanding of the cellular and molecular mechanisms behind TLR9 ligands as immunomodulants may uncover novel therapeutics to combat viral infections.

In regards to TLR3, a fundamental question of whether or not it is involved in the recognition of influenza A viruses has yet to be fully elucidated. Activation of TLR3 by a synthetic analogue polyinosinic-polycytidylic acid (poly I:C) triggered the release of TNF-α and IFN-β through signaling to the transcription factor NF-kB (Yang *et al.*, 2013). The use of this synthetic analogue has been widely used to mimic viral infections as dsRNA is generated as a byproduct during IAV replication. Although cytokines are generated in a TLR3-dependent manner in lung epithelial cells upon infection with IAV, the precise role of TLR3 *in vivo* is still undefined (Guillot *et al.*, 2005). In an experimental murine model, it was evident that mice

lacking the TLR3 gene showed an unexpected survival advantage despite a higher accumulation of viral load in the lungs compared to the wild-type controls challenged with IAV infection (Le Goffic *et al.*, 2006). However, this does not hold true for all viral infections one study using TLR3 genetically deficient mice demonstrated that TLR3 was not required for the generation of effective antiviral responses (Edelmann *et al.*, 2004). No alterations in viral pathogenesis were observed, nor did deletion of TLR3 impair the host's generation of adaptive antiviral responses to lymphocytic choriomeningitis virus or vesicular stomatitis virus (Edelmann *et al.*, 2004). Although it appears that TLR3 may play a role in contributing to antiviral immunity, it still remains unclear whether TLR3 contributes to the host antiviral response during IAV infection, which therefore warrants further investigation.

Viral and bacterial cytosolic sensors

The detection of microbial pathogens involves host cell sensors that recognise microbial components within endosomes, namely TLRs or within the cytosol such as the nucleotide-binding oligomerization domain-like receptors (NLRs) (Kimbrell *et al.*, 2001). An example of this is the inflammasome complex, which is a cytoplasmic multiprotein complex that mediate proteolytic processing of IL-1 proteins to their active form (Agostini *et al.*, 2004; Broz *et al.*, 2011). The apoptotic speck-like protein containing a caspase activation (ASC) and NLRP3 are required for proper activation of inflammatory caspase-1, a protease identified to be responsible for the release of IL-1β (Agostini *et al.*, 2004). Inflammasome activation is a two-step process beginning with a priming step. This can be achieved by activating the transcription factor NF-kB, which mediates the synthesis of pro- IL-1β and causes the upregulation of the NLRP3 inflammasome. Secondly, a multitude of stimuli that cause membrane pertubations induce IL-1β maturation that is necessary for the formation of the complex (Halle *et al.*, 2008; Martinon *et al.*, 2009). The formation of the inflammasome can be set off by various microbial stimuli, including dsRNA, bacterial RNA and synthetic imidazoquinoline (Marina-García *et al.*, 2008). The role of NLRP3 inflammasome in response to viral infections *in vivo* has not been widely investigated. There is evidence that demonstrates the importance of activating the inflammasome complex during a viral infection, as mice deficient in caspase-1, ASC and IL-1R displayed a delayed clearance of IAV infection (Ichinohe *et al.*, 2009a). Moreover, mice lacking NLRP3 or caspase-1 exhibited dramatically increased mortality and a reduced immune response after exposure to the influenza A virus (Allen *et al.*, 2009b). Mechanistically, Allen *et al.* (2009b) demonstrated that the activation of the NLRP3 complex was dependent on lysosomal maturation. Collectively, these studies have eluded that sensing of cellular stress due to the imbalances in ionic concentrations in intracellular vesicles serve as a viral recognition pathway.

In addition to the NLRP3 complex possessing a broad spectrum of stimuli, in vitro studies have revealed an additional cytosolic system of retinoic acid inducible gene-1 (RIG-1)-like receptor proteins (RLRs), which are involved in the sensing of viral genomic RNA (Kato *et al.*, 2006; Loo *et al.*, 2008; Rehwinkel *et al.*, 2010). RIG-I possess two N-terminal caspase activation domains that allow for interaction with the mitochondrial adaptor protein (MAVS) (Yoneyama *et al.*, 2009). MAVS triggers the activation of NF-kB, IRF-3, and IRF-7, which in turn induces the transcription of Type I and III interferons that can contribute to subsequent antigen-specific adaptive immune responses, including induction of protective antibodies (Collins *et al.*, 2004; Kato *et al.*, 2006; Samuel, 2001). Another cytoplasmic sensor that detects dsRNA is the melanoma differentiation-associated protein 5 (MDA-5) and is induced by IFN-β and TNF-α. Notably, mice deficient in RIG-I, MAVS and MDA-5 readily succumb to infection with RNA viruses, emphasizing the importance of RLRs in antiviral immunity (Gitlin *et al.*, 2006; Kato *et al.*, 2006). The ability of these specific endosomal and viral cytosolic sensors to contribute to lung pathology caused by IAV infection, as well as their link to these subcellular compartments generating ROS remains largely unidentified.

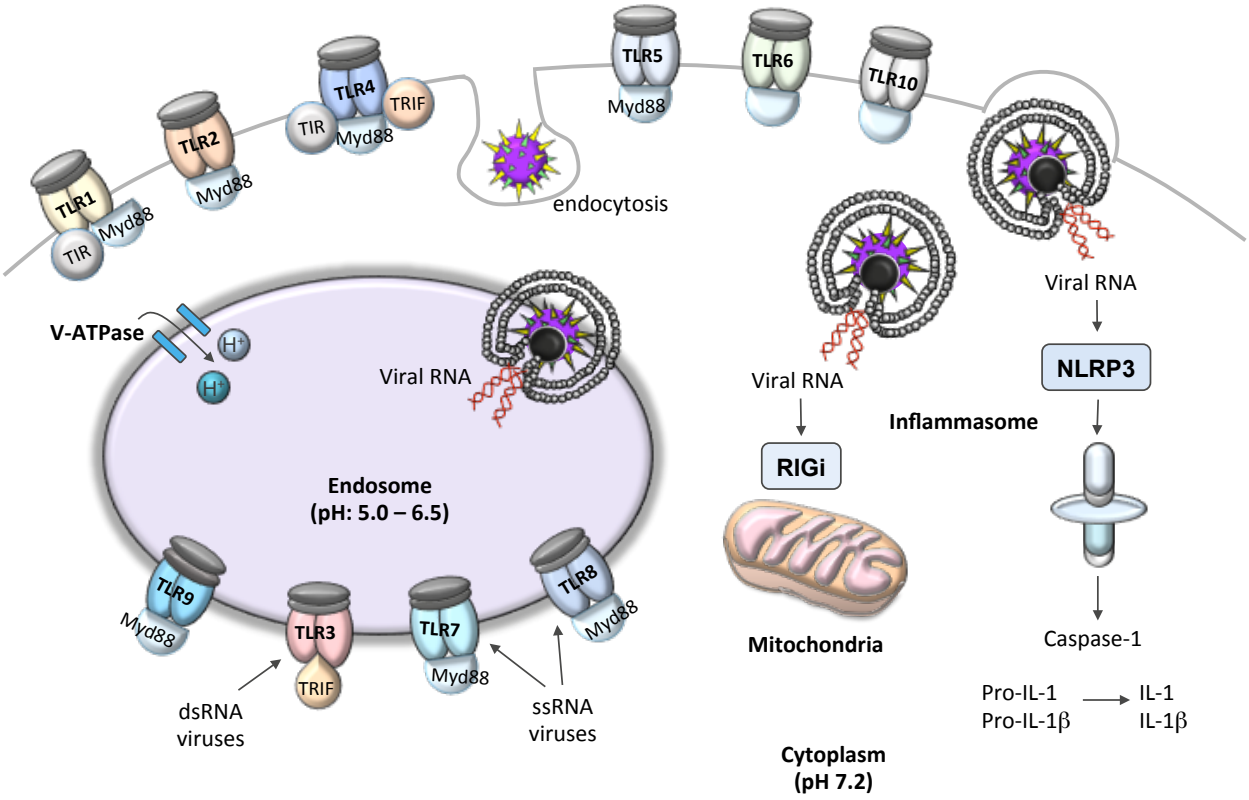

Figure 3: Schematic diagram displaying various toll-like receptors (TLRs), viral cytosolic sensors and their cellular distribution within a cell. TLR1-2, TLR4-6 and TLR10 are expressed on the cell surface where they are activated by various bacterial stimuli. On the other hand, TLR3 and TLR7-9 are localized within endosomal compartments where they detect viral nucleic acids. The cytosolic sensors RIG-I and NLRP3 are capable of sensing viral RNA after the virus has undergone replication.

	Adaptor protein	Cellular location	Ligand/activator	References
TLR1	MyD88, TIRAP (TIR)	Cell surface	Tri-acyl lipopeptides (bacteria, mycobacteria)	Takeuchi *et al.* (2002), Jin *et al.* (2007)
TLR2	MyD88	Cell surface	Lipoprotein/lipopeptides (bacteria), Peptidoglycan (gram-positive bacteria)	Aliprantis *et al.* (1999), Campos *et al.* (2001) Jin *et al.* (2007), Takeuchi *et al.* (2000)
TLR3	TRIF	Endosomes	dsRNA (virus)	Choe *et al.* (2005), Nishiya *et al.* (2005), Yang *et al.* (1995)
TLR4	MyD88, TIR, TRIF	Cell surface	LPS (gram-negative bacteria)	Hoshino *et al.* (1999) Poltorak *et al.* (1998), Tanimura *et al.* (2008)
TLR5	MyD88	Cell surface	Flagellin (bacteria)	(Batah *et al.*, 2016) (Hayashi *et al.*, 2001)
TLR6	Unknown	Cell surface	Di-acyl lipopeptides (mycoplasma)	Omueti *et al.* (2005), (Takeuchi *et al.*, 2002)
TLR7	MyD88	Endosomes	ssRNA (virus), Imidazoquinoline (synthetic compounds),	Diebold *et al.* (2004), Heil *et al.* (2004), Hemmi *et al.* (2002), Nishiya *et al.* (2005)
TLR8	MyD88	Cell surface	ssRNA (virus)	Heil *et al.* (2004), Ishii *et al.* (2014), Tanji *et al.* (2015)
TLR9	MyD88	Endosomes	CpG DNA (bacteria), DNA (virus)	Hemmi *et al.* (2000), Ohto *et al.* (2015)

TLR10	Unknown	Cell surface	Unknown	Chuang *et al.* (2001)
TLR11	MyD88	Cell surface	Toxoplasma gondii (protozoa)	Plattner *et al.* (2008), Yarovinsky *et al.* (2005)
RIG-I	IPS-1	Cytosol	ssRNA and dsRNA (virus)	Hornung *et al.* (2006), Kato *et al.* (2006), Yoneyama *et al.* (2009)
NLRP3	ASC	Cytosol	RNA	Allen *et al.* (2009b), Idris (2014)

Table 1: A list of toll-like receptors, RIG-I-like receptor, and NOD-like receptor showing the appropriate adaptor proteins, cellular location and their ligands in pattern recognition.

Protective antibody responses during a viral infection

The generation of protective antibodies during IAV infection is primarily mediated by the humoral immune response (Graham *et al.*, 1997). Secretion of IgA by the mucosal immune system accounts for approximately 70% of the body's total Ig production (Lamm, 1997; Woof *et al.*, 2005). Secretion of IgA in the mucociliary blanket is believed to provide protection by preventing the attachment of viruses (Kirkeby *et al.*, 2000). However, a study using IgA KO mouse mice demonstrated a decrease in both nasal and pulmonary viral replication, which suggests that IgA is not necessarily required for prevention of influenza virus infection in the murine nose (Mbawuike *et al.*, 1999). Studies have suggested an important role for TLR7 in antiviral resistance as it regulates the instruction of B cells to elicit appropriate antibody production, and indirectly through the induction of IFN-α by plasmacytoid dendritic cells (Koyama *et al.*, 2007; Lopez *et al.*, 2004). Koyoma *et al* (2007) demonstrated TLR7 and MyD88 were required for generation of Th1-mediated responses, including the virus-specific total IgG and IgG2a. Moreover, deficiency in TLR7 and MyD88 revealed dysregulation of influenza-specific antibody isotype switching. In parallel, another study showed reduced levels of IgG2a and IgG2c when challenged with influenza in mice lacking MyD88 (Heer *et al.*, 2007). Based on these studies, it appears that TLR7 is required to orchestrate the generation of protective antibodies, which could be used as a therapeutic target to alleviate the severity of influenza virus infections.

Reactive oxygen species (ROS)

Generation of ROS has been implicated in a variety of physiological responses such as cell proliferation, cell signaling and apoptosis (Peshavariya *et al.*, 2009; Tammariello *et al.*, 2000). Sources of ROS production include xanthine oxidase, nicotinamide adenine dinucleotide phosphate reduced (NADPH) oxidase family of enzymes and the mitochondrial electron transport chain, as a result of aerobic metabolism (Forman *et al.*, 2002). The term "respiratory burst" was derived from the generation of ROS in phagocytic cells, namely neutrophils and macrophages, due to the transient consumption of oxygen. Later evidence revealed that ROS generation also occurred in a variety of non-phagocytic cells (Bayraktutan *et al.*, 2000; Griendling *et al.*, 2000). As depicted in Figure 4, superoxide is formed by the catalysed reduction of molecular oxygen, which can either form peroxynitrite ($ONOO^-$) by reacting with nitric oxide (NO) or converted to hydrogen peroxide (H_2O_2) *via* the superoxide dismutase (SOD) family of enzymes. H_2O_2 can be metabolised by catalase or glutathione peroxidase (GPx) to form water (H_2O), or reduced by iron (II) (Fe^{2+}) to form hydroxyl radical ($OH^{\bullet}$) (Vlahos *et al.*, 2012b). The generation of ROS has shown to play an important role in the hosts' ability to combat invading pathogens. Therefore, an emerging area of research implicates ROS as a target for influenza infections.

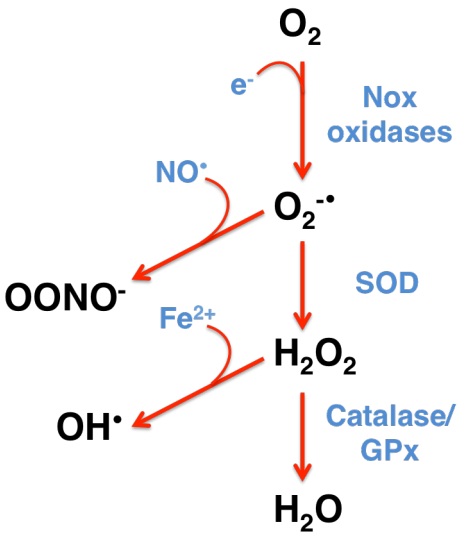

Figure 4: Pathways of ROS production and metabolism. One electron reduction gives rise to superoxide anions (O_2^-), which can be converted to hydrogen peroxide (H_2O_2) by superoxide dismutase (SOD) or can react with nitric oxide (NO) to form peroxynitrie ($ONOO^-$). H_2O_2 can be further reduced into water with catalase/glutathione peroxidase or be reduced to form hydroxyl radicals (OH).

ROS and implications in influenza A virus infection

ROS, most predominantly superoxide, H_2O_2 and $ONOO^-$ are key contributors to the lung injury due to IAV infection (Vlahos *et al.*, 2012b). The excessive production of ROS causes enhanced regulation of redox-sensitive pathways that promote over-exuberant inflammatory responses (Akaike, 2001; Snelgrove *et al.*, 2004). Thus, the blockade of superoxide production will decrease the production of the downstream derivatives, as previously outlined in Figure 4. ROS were found to be elevated in lung tissue and serum of virus-infected mice that was suppressed by the administration of SOD (Oda *et al.*, 1989). This highlights the importance of superoxide anion in the pathogenesis of influenza virus infections. Subsequently, this would effectively decrease the production of H_2O_2 and $ONOO^-$ that are found to exert toxic effects to cells, causing oxidative stress, lipid oxidation and DNA damage, thereby promoting lung injury and tissue damage (Akaike *et al.*, 1996). As previously mentioned, H_2O_2 can also activate the transcription factor NF-kB to upregulate the production of pro-inflammatory mediators (Anrather *et al.*, 2006). In parallel with this, virus-infected mice administered with catalase demonstrated a reduction in inflammatory cell infiltration, inflammatory cytokines and NF-kB expression (Shi *et al.*, 2014), highlighting that H_2O_2 needs to be tightly regulated during influenza infections.

Antioxidants have been employed to reduce superoxide and H_2O_2 levels with the goal of inhibiting oxidative stress-dependent cell and tissue injury. To support this, Beck *et al.* (2013) showed selenium-deficient mice displayed enhanced lung pathology in response to influenza virus infections. N-Acetyl-L-cysteine (NAC) is a precursor to the amino acid L-cysteine that acts to stimulate glutathione synthesis (Uchide *et al.*, 2008). Therefore, glutathione peroxidase (GPx), a selenium-dependent antioxidant enzyme was put into focus. This enzyme functions to reduce the detrimental effects of H_2O_2 by converting it to water, and has been demonstrated to play a protective role in disease states where oxidative stress has been implicated, including Huntington's and Parkinson's disease (Brigelius-Flohé, 2006; Zhang *et al.*, 2000). Evidently, in comparison to GPx-1-deficient mice that had increased airways and lung inflammation compared to WT mice, administration of GPx-1 mimetic ebselen had attenuated IAV-induced lung inflammation (Yatmaz *et al.*, 2013). Herein, ROS has shown to be important in combating pathogens and promoting viral clearance. However, the toxicity of these molecules and their lack of specificity mean they can be detrimental by damaging the surrounding tissue area (Schwarz, 1996). These lines of evidence highlight the importance of ROS in the pathogenesis of IAV. With respect to this, therapeutically an alternative to antioxidants would be to target the most abundant source of superoxide production, namely the NADPH oxidases (Akaike *et al.*, 1990).

NADPH oxidase family of enzymes

The NOX family of NADPH oxidases, are a highly regulated, membrane-bound group of multi-subunit enzyme complexes found in a variety of phagocytic and non-phagocytic cells in which their primary function is to generate ROS (Bedard *et al.*, 2007a). They are expressed in key cell types of the airways, including endothelial, epithelial and inflammatory cells (alveolar macrophages, monocytes, neutrophils and T lymphocytes). Various NOX isoforms have different roles in the inflammatory response, each having unique expression pattern and subunit requirement (Drummond *et al.*, 2011a). For the purpose of this thesis, we will focus on the critical NADPH oxidase isoform i.e. NOX2 oxidase that is expressed in macrophages within the respiratory tract, which is mainly associated with promoting lung oxidative stress, apoptosis, lung inflammation and dysfunction during influenza A virus infections (Imai *et al.*, 2008b; Vlahos *et al.*, 2011b).

NOX2 and other NOX isoforms

The key NOX isoform with the highest abundance in macrophages is NOX2 oxidase. As displayed in Figure 5, the NOX2 oxidase complex is composed of the following regulatory subunits that form a ternary complex: p40phox, p47phox and p67phox. In addition, there is a membrane-bound heterodimer consisting of NOX2 and p22phox. Phosphorylation of p47phox leads to a conformational change allowing the ternary complex to interact with the membrane-bound NOX2-p22phox heterodimer. In addition, two GTP-binding proteins Ras-related C3 botulinum toxin substrate 1 and 2 (RAC1 and RAC2) are involved in activation of the complex (Groemping *et al.*, 2003). NOX2 oxidase is expressed in inflammatory cells that are resident and are recruited to the lungs, including macrophages and neutrophils (Ermert *et al.*, 2009).

Heightened activity of NOX2 oxidase following influenza A infection, leads to increased oxidative stress causing mild to moderate lung injury (Imai *et al.*, 2008b; Snelgrove *et al.*, 2006b). In comparison to naïve uninfected WT mice, WT mice infected with the Hkx-31 IAV had significantly increased production of superoxide that was virtually abolished in $NOX2^{-/y}$ mice (Vlahos *et al.*, 2011b). Blockade of superoxide production will in turn decrease production of its downstream derivatives (ie. H_2O_2 and $ONOO^-$), which was previously mentioned to exert toxic effects to cells (Akaike *et al.*, 1996). The deletion of the NOX2 gene not only inhibited ROS production, but also decreased the number of infiltrating immune cells (Vlahos *et al.*, 2011b). Moreover, by the use of $NOX2^{-/-}$ mice, Snelgrove *et al.* (2006b) demonstrated that following infection with the Hkx-31 IAV, there was a significant improvement in lung function and reduced level of lung tissue damage. Owing to the fact NOX2-derived ROS plays an essential role in contributing to the lung pathology associated with IAV infections, it is important to establish the

subcellular compartments of ROS generation, which may be used as a potential drug target for reducing IAV-induced lung inflammation.

Other NOX isoforms that have been implicated in virus infections include NOX1. Evidently, Selemidis *et al.* (2013) demonstrated that lungs of NOX1$^{-/-}$ mice infected with the Hkx-31 IAV displayed greater levels of airway inflammation, indicating a protective role of NOX1. This protective effect of NOX1 is surprising, given the vast amount of evidence implicating ROS in promoting lung injury in response to IAV infection. Although members of the NADPH oxidase family of enzymes appear to be promising targets, further investigation is warranted, as there is no evidence to implicate NOX3, NOX4, NOX5 oxidases and DUOX1/DUOX2 (see Figure 5 for structure) in the pathology caused by IAV.

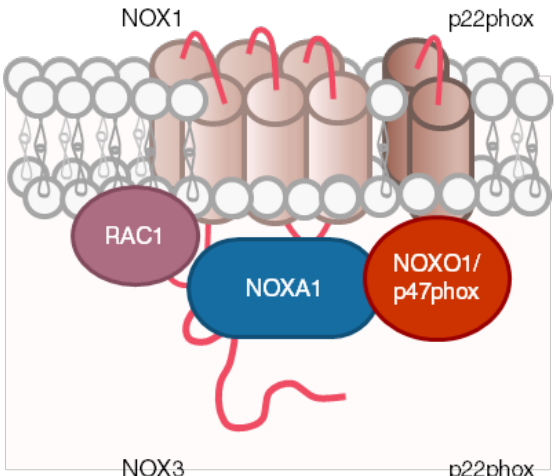
NOX1
p22phox
RAC1
NOXA1
NOXO1/
p47phox

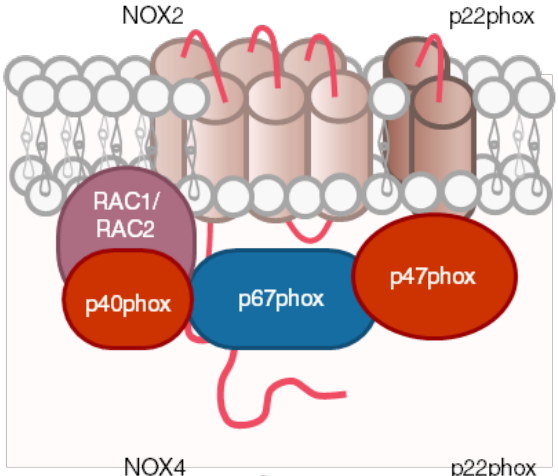
NOX2
p22phox
RAC1/
RAC2
p40phox
p67phox
p47phox

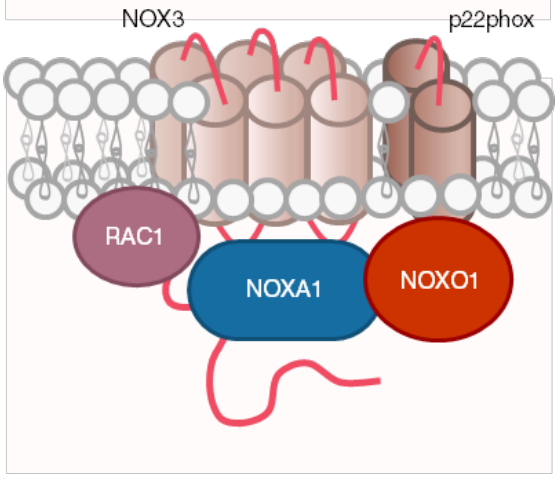
NOX3
p22phox
RAC1
NOXA1
NOXO1

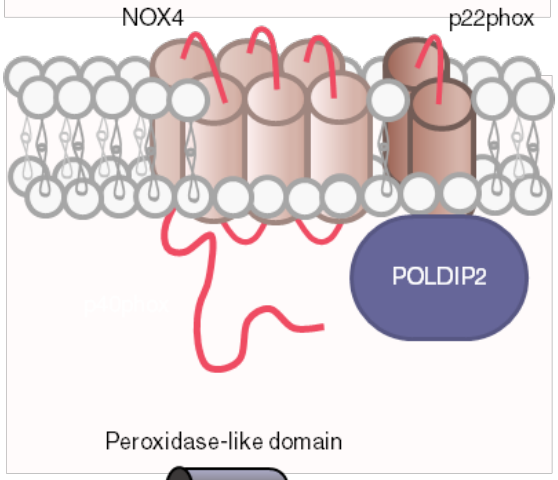
NOX4
p22phox
POLDIP2
Peroxidase-like domain

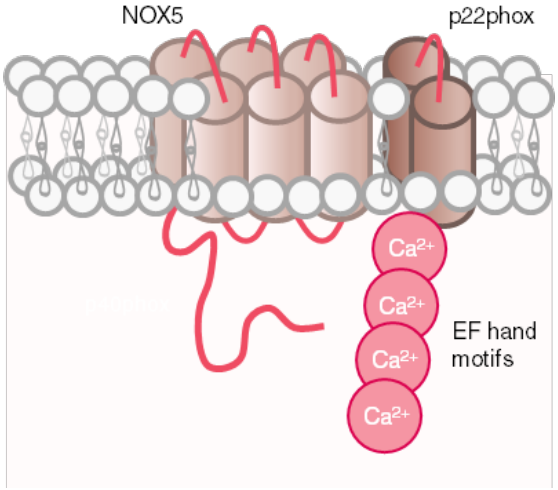
NOX5
p22phox
Ca2+
Ca2+
Ca2+
Ca2+
EF hand
motifs

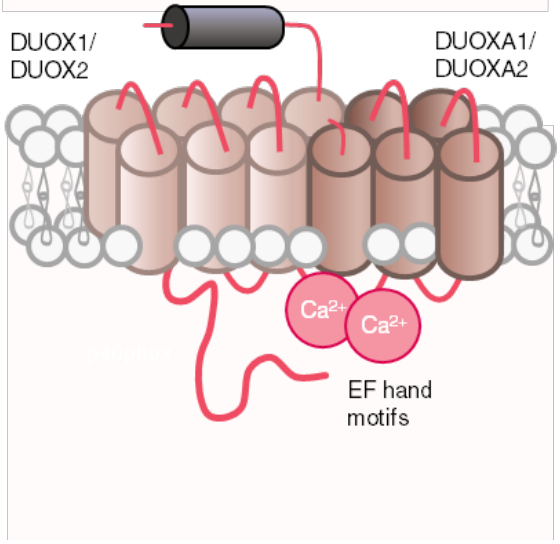
DUOX1/
DUOX2
DUOXA1/
DUOXA2
Ca2+
Ca2+
EF hand
motifs

Figure 5. The subunit composition of various NADPH oxidase isoforms. The catalytic core subunits of the enzymes Nox1-5 and Duox1-2 are displayed in pink. Stabilization partner (p22phox) for Nox1-5 and DuoxA1/DuoxA2 for Duox1/2 are shown in beige. The cytosolic organisers (p40phox, p47phox and NOX01) in red; cytosolic activators (p67phox and NOX activator (NOXA1)) are displayed in blue and small GTPases (RAC1 and RAC2) in purple. Polymerase δ-interacting protein 2 (POLDIP2) is linked to Nox4 and regulated the activity of the enzyme (purple). Nox5 and Duox1/Duox2 do not require subunits and are activated by Ca2+. The schematic also shows the extracellular peroxidase-like region (shown in black) on DUOX1 and DUOX2.

NADPH oxidase in health and disease

An important line of study leading to the discovery of the phagocyte NADPH oxidase stemmed from clinical research, where patients with a rare genetic condition who suffered from recurrent life-threatening bacterial and fungal infections due to the lack of functional NADPH oxidase complexes, also referred to as chronic granulomatous disease (CGD) (Berendes *et al.*, 1957). Chronic or over stimulation of ROS can result in oxidative stress, but likewise, reduced or abolished ROS generating capacity can be harmful (van den Berg *et al.*, 2009). CGD is characterised by a genetic mutation in a component of the NOX2 oxidase complex, with the major genetic form being X-linked that is caused by mutations in the cytochrome B-245 beta chain (CYBB) gene encoding $gp91^{phox}$, comprising of approximately 70% of all reported cases (Segal *et al.*, 1978). Other autosomal recessive forms of CGD transpire from mutations in the genes encoding p22phox, p47phox or p67phox (Roos *et al.*, 2010). The overall consequence is reduced induction of neutrophil apoptosis to limit inflammation and reduced ability of macrophages to engulf apoptotic cells, resulting in an increase in toxic oxygen-derived components that contribute to heightened local inflammation (Hartl *et al.*, 2012). This indicates that host defense is a key function of Nox2 oxidase. Although, it is important to note that phagocytes possess oxygen-independent killing mechanisms, as studies have shown that Nox2 was not required for killing some types of bacterium (Abuaita *et al.*, 2015; Ziltener *et al.*, 2016). Collectively, these observations suggest that maintaining homeostasis between the generation and elimination of ROS is crucial to health.

Mechanism whereby NOX2 regulates ROS and cytokines

The subcellular mechanisms that lead to NOX2 activation and the signaling pathways of the ensuing inflammatory response to IAV remain poorly understood. The most widely

investigated pathway by which ROS regulates cellular and physiological function is through redox-sensitive cysteine residues. Amongst the 20 amino acids that form proteins, cysteines have gained particular interest because of their sensitivity to oxidation. It possesses a thiol moiety in the side chain that is chemically active, allowing it to form disulfide bonds with another thiol (Meng *et al.*, 2013; Miki *et al.*, 2012; Östman *et al.*, 2011). A classic example is signaling through protein tyrosine phosphatases (PTPs), as they regulate the phosphorylation state of many proteins required for cell proliferation and survival (Hunter, 2000). The catalytic regions of PTPs have cysteines that are prone to oxidative inactivation, whereby ROS, specifically H_2O_2 decreases phosphatase activity (Rhee, 2006; Salmeen *et al.*, 2005). Numerous studies have supported this biochemical mechanism *in vitro* and *in vivo* (Lee et al., 1998; Mahadev et al., 2001; Yan et al., 1996), implicating cysteines as important targets for regulating ROS-mediated signal transduction pathways. Another possible pathway is signaling that is taking place within the endosome. In fact, NOX2 is expressed on the endosomal membrane (Oakley *et al.*, 2009). Recently, NOX2-derived ROS are increasingly recognised as key elements of intracellular signaling, where endosomal signaling may present a central coordinating point in this process. For example, NOX2 oxidase was shown to produce endosomal superoxide that is required for IL-1β-dependent activation of NF-kB. The source of this endosomal superoxide was regulated through RAC-1-dependent internalisation of NOX2, implicating this as a crucial step in allowing NOX2 oxidase to be catalytically active (Li *et al.*, 2006b). To further support the notion that ROS signaling occurs within the endosome, Li *et al.* (2009) demonstrated that inhibiting endocytosis reduced the ability of IL-1β to induce NOX2-dependent generation of superoxide as well as abrogating the activation of NF-kB, thus decreasing the detrimental effects of multiple pro-inflammatory cytokines. Both studies provide evidence that NOX2 oxidase mediated ROS production occurs in the endosomal compartment, which may indicate an important role of targeting endosomes in regulating the lung pathology associated with IAV infection.

Pharmacological inhibitors of NADPH oxidases

Given the substantial evidence that NADPH oxidases are key culprits in contributing to the pathogenesis and progression of viral and bacterial infections, targeting ROS generation by inhibiting NADPH oxidase may be a viable therapeutic approach in alleviating disease severity and inflammation. Due to the high degree of homology between the NOX isoforms, inhibitors for specific NOX isoforms do not exist. Instead, inhibitors vary in the degree of selectivity for different isoforms (Drummond *et al.*, 2011a). The main focus of this thesis is to study the role of NOX2 oxidase, therefore we utilised two inhibitors, including apocynin and gp91ds-tat. Apocynin (4-hydroxy-3-methoxyacetophenone) acts by blocking the assembly of a functional NADPH oxidase complex, in turn blocking the release of superoxide free radicals (Johnson *et al.*, 2002).

It has been beneficial in a plethora of disease models. For instance, treatment with apocynin improved the survival rate and necrotic area in rats with severe liver disease (Kimura *et al.*, 2016), reduced IAV-induced lung inflammation (Oostwoud *et al.*, 2016; Vlahos *et al.*, 2011b) and abolished hippocampal oxidative stress in septic animals (Hernandes *et al.*, 2014). Despite the positive outlook for the use of apocynin therapeutically, caution must be taken as high concentrations of apocynin inhibit NOX4 (Rouhanizadeh *et al.*, 2005) and NOX5 (Fu *et al.*, 2006) activity.

Gp91ds-tat is a peptide inhibitor that was designed to specifically block NOX2 oxidase. It does so by mimicking a sequence of NOX2 that is required for interaction with the catalytic subunit $p47^{phox}$ (Bedard *et al.*, 2007a). It also contains a specific 9-amino acid peptide (HIV-TAT) from the human immunodeficiency virus (HIV) coat, which promotes internalization into the cell (Rey *et al.*, 2001). Using electron paramagnetic resonance, Csányi *et al.* (2011) confirmed the selectivity of gp91ds-tat for NOX2 oxidase by showing that it blocked superoxide generation from NOX2 oxidase, but not NOX1 or NOX4 isoforms. Furthermore, this peptide is beneficial in reversing vascular pathology and neointimal hyperplasia by suppressing superoxide generation (Jacobson *et al.*, 2003; Quesada *et al.*, 2015). Therefore, it may be possible to use this compound during an influenza virus infection to inhibit ROS-mediated lung inflammation. We postulated that endosomes could be an important intracellular site for ROS generation in triggering redox-sensitive pathways that contribute to an enhanced diseased state. Thus, we sought out to design a compound that can be delivered into endosomal compartments and have the ability to block NOX2 oxidase. To bring this idea forward, three versions of the specific NOX2 inhibitor gp91ds-tat were synthesised to investigate the role of endosomal NOX2 oxidase in influenza virus disease; an unconjugated gp91ds-tat, ethyl ester gp91ds-tat and a cholestanol conjugated gp91ds-TAT (refer to Figure 6 for the chemical structure of these compounds). Lipid rafts form a dynamic platform in controlling membrane functions (Simons *et al.*, 1997). These rafts are abundant in cholesterol-rich regions, which are involved in the transport of fatty acids and glucose, and serve as platforms for signaling proteins in the plasma membrane (Rajendran *et al.*, 2005). Cholestanol is an analogue of cholesterol that was conjugated to the NOX2 inhibitor (gp91ds-tat) to function as a lipid anchor to the plasma membrane. The addition of the HIV-tat allows for penetration through the cell membrane, promoting the trafficking of the drug into endosomes. This concept of endosomal targeting of drugs had arisen from a study conducted by Halima *et al.* (2011), which designed an endosomal β-secretase inhibitor for the treatment of Alzheimer's disease. It is possible that directly linking the gp91ds-tat to the cholestanol (lipid anchor) may hinder the compounds interaction with the target because it may be too close to the lipid bilayer. Therefore, it is appropriate that a linker is utilised. To do this, cholestanol conjugation via a polyethylene glycol linker (PEG-linker) was

used to allow for maximal movement of the drug in the lipid bilayer and the anchor can be strategically positioned in order for successful delivery of drug into endosomal compartments (Rajendran *et al.*, 2008b).

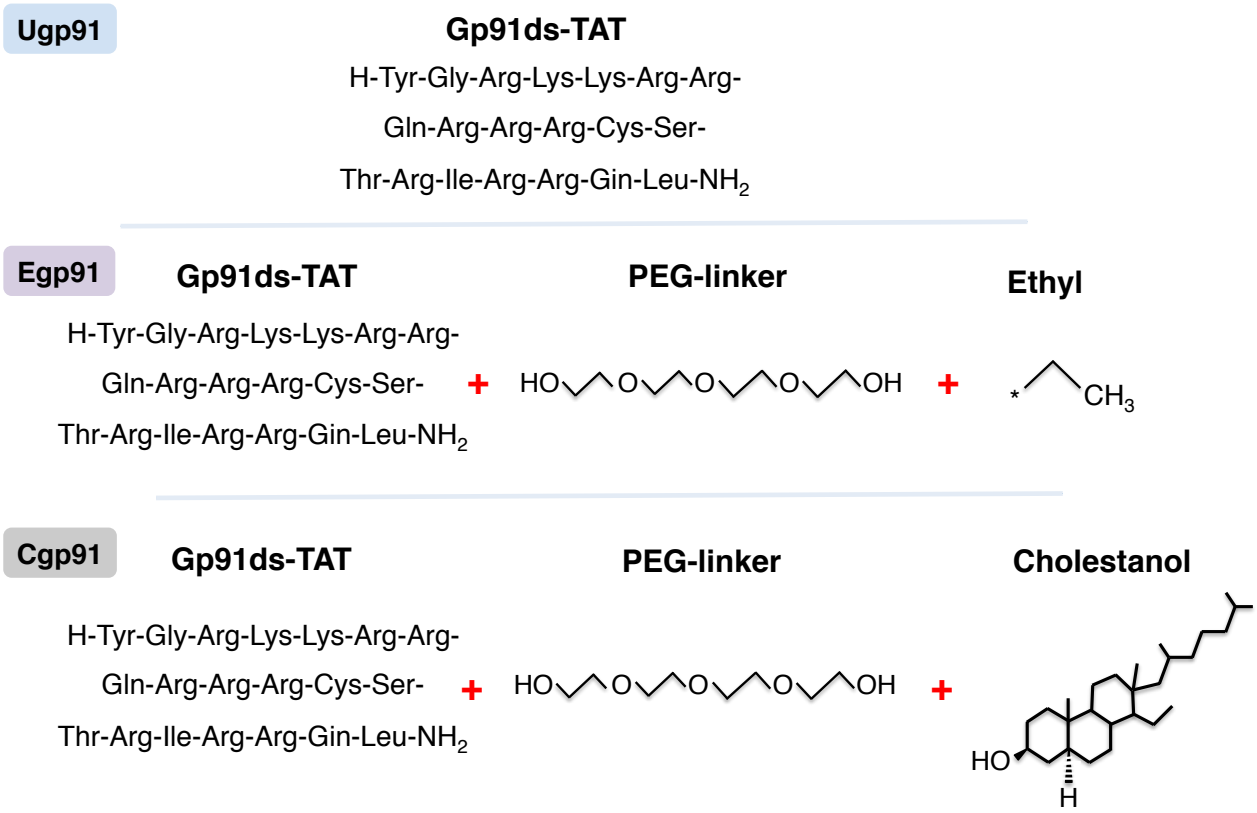

Figure 6: Structural variations of the specific NOX2 inhibitor gp91ds-tat. The chemical structures of three versions of the inhibitor are displayed. Firstly, an unconjugated gp-91 (Ugp91) (top panel), secondly an ethyl ester conjugated version (Egp91)(middle panel) and thirdly a cholestanol-conjugated version (Cgp91)(bottom panel). Note that a flexible PEG linker holds egp91 and cgp91 together.

Working Hypothesis

There are several key knowledge gaps that need to be addressed, 1) the impact of IAV on altering ROS levels 2) the subcellular sites of ROS generation and how it contributes to lung inflammation and 3) the molecular targets of ROS. In this thesis we hypothesise firstly, that the priming effect by influenza virus and TLR7 activation may involve phosphorylation of specific serine residues on the p47phox subunit. Secondly, NOX2-derived ROS as a key culprit in the pathogenesis of viral infections and viruses internalise into endosomes, resulting in increases in endosomal ROS generation. Thirdly, genetic ablation of NOX2 or pharmacological inhibition of NOX2 will improve viral pathology. Finally, the targeted inhibition of endosomal ROS will be more superior than that of the unconjugated NOX2 inhibitor in attenuating viral pathogenicity.

Aims of this Thesis

1) To determine whether influenza A virus infection alters the levels of ROS generation in macrophages
2) To elucidate the subcellular site of ROS generation that occurs following influenza A virus infection
3) To examine the cell signaling pathways leading to NOX2 activation following influenza A virus infection and to identify the molecular targets of the ensuing ROS.
4) To establish the effect of endosome targeting of a NOX2 oxidase inhibitor i.e. gp91ds-TAT on its potency at suppressing ROS production and the severity of influenza A virus infection in vivo.

References

Abed Y, Goyette N, Boivin G (2005). Generation and characterization of recombinant influenza A (H1N1) viruses harboring amantadine resistance mutations. *Antimicrob. Agents Chemother.* **49**(2)**:** 556-559.

Ablasser A, Poeck H, Anz D, Berger M, Schlee M, Kim S*, et al.* (2009). Selection of molecular structure and delivery of RNA oligonucleotides to activate TLR7 versus TLR8 and to induce high amounts of IL-12p70 in primary human monocytes. *Journal of Immunology* **182**(11)**:** 6824-6833.

Agostini L, Martinon F, Burns K, McDermott MF, Hawkins PN, Tschopp J (2004). NALP3 forms an IL-1β-processing inflammasome with increased activity in Muckle-Wells autoinflammatory disorder. *Immunity* **20**(3)**:** 319-325.

Aguirre J, Lambeth JD (2010). Nox enzymes from fungus to fly to fish and what they tell us about Nox function in mammals. *Free radical biology & medicine* **49**(9)**:** 1342-1353.

Akaike T (2001). Role of free radicals in viral pathogenesis and mutation. *Rev. Med. Virol.* **11**(2)**:** 87-101.

Akaike T, Ando M, Oda T, Doi T, Ijiri S, Araki S*, et al.* (1990). Dependence on O2 - generation by xanthine oxidase of pathogenesis of influenza virus infection in mice. *Journal of Clinical Investigation* **85**(3)**:** 739-745.

Akaike T, Noguchi Y, Ijiri S, Setoguchi K, Suga M, Zheng YM*, et al.* (1996). Pathogenesis of influenza virus-induced pneumonia: Involvement of both nitric oxide and oxygen radicals. *Proc. Natl. Acad. Sci. U. S. A.* **93**(6)**:** 2448-2453.

Akira S, Takeda K, Kaisho T (2001). Toll-like receptors: Critical proteins linking innate and acquired immunity. *Nat. Immunol.* **2**(8)**:** 675-680.

Aliprantis AO, Yang RB, Mark MR, Suggett S, Devaux B, Radolf JD*, et al.* (1999). Cell activation and apoptosis by bacterial lipoproteins through Toll- like receptor-2. *Science* **285**(5428)**:** 736-739.

Allen IC, Scull MA, Moore CB, Holl EK, McElvania-TeKippe E, Taxman DJ*, et al.* (2009a). The NLRP3 inflammasome mediates in vivo innate immunity to influenza A virus through recognition of viral RNA. *Immunity* **30**(4)**:** 556-565.

Allen IC, Scull MA, Moore CB, Holl EK, McElvania-TeKippe E, Taxman DJ*, et al.* (2009b). The NLRP3 Inflammasome Mediates In Vivo Innate Immunity to Influenza A Virus through Recognition of Viral RNA. *Immunity* **30**(4)**:** 556-565.

Anrather J, Racchumi G, Iadecola C (2006). NF-κB regulates phagocytic NADPH oxidase by inducing the expression of gp91phox. *Journal of Biological Chemistry* **281**(9)**:** 5657-5667.

Bachran D, Schneider S, Bachran C, Weng A, Melzig MF, Fuchs H (2011). The endocytic uptake pathways of targeted toxins are influenced by synergistically acting Gypsophila saponins. *Mol. Pharm.* **8**(6)**:** 2262-2272.

Baggiolini M (1998). Chemokines and leukocyte traffic. *Nature* **392**(6676)**:** 565-568.

Banerjee I, Yamauchi Y, Helenius A, Horvath P (2013). High-Content Analysis of Sequential Events during the Early Phase of Influenza A Virus Infection. *PLoS ONE* **8**(7).

Batah J, Denève-Larrazet C, Jolivot PA, Kuehne S, Collignon A, Marvaud JC*, et al.* (2016). Clostridium difficile flagella predominantly activate TLR5-linked NF-κB pathway in epithelial cells. *Anaerobe* **38:** 116-124.

Bayraktutan U, Blayney L, Shah AM (2000). Molecular characterization and localization of the NAD(P)H oxidase components gp91-phox and p22-phox in endothelial cells. *Arterioscler. Thromb. Vasc. Biol.* **20**(8)**:** 1903-1911.

Beck CR, Sokal R, Arunachalam N, Puleston R, Cichowska A, Kessel A*, et al.* (2013). Neuraminidase inhibitors for influenza: A review and public health perspective in the aftermath of the 2009 pandemic. *Influenza and other Respiratory Viruses* **7**(1 SUPPL.1)**:** 14-24.

Bedard K, Krause KH (2007a). The NOX family of ROS-generating NADPH oxidases: Physiology and pathophysiology. *Physiological Reviews* **87**(1)**:** 245-313.

Bedard K, Krause KH (2007b). The NOX family of ROS-generating NADPH oxidases: physiology and pathophysiology. *Physiological reviews* **87**(1)**:** 245-313.

Berendes H, Bridges RA, Good RA (1957). A fatal granulomatosus of childhood: the clinical study of a new syndrome. *Minn Med* **40**(5)**:** 309-312.

Boulo S, Akarsu H, Ruigrok RWH, Baudin F (2007). Nuclear traffic of influenza virus proteins and ribonucleoprotein complexes. *Virus Res.* **124**(1-2)**:** 12-21.

Bowie AG, Haga IR (2005). The role of Toll-like receptors in the host response to viruses. *Mol. Immunol.* **42**(8)**:** 859-867.

Brigelius-Flohé R (2006). Glutathione peroxidases and redox-regulated transcription factors. *Biological Chemistry* **387**(10-11)**:** 1329-1335.

Broz P, Monack DM (2011). Molecular mechanisms of inflammasome activation during microbial infections. *Immunol. Rev.* **243**(1)**:** 174-190.

Buffinton GD, Christen S, Peterhans E, Stocker R (1992). Oxidative stress in lungs of mice infected with influenza a virus. *Free Radic. Res.* **16**(2)**:** 99-110.

Bullough PA, Hughson FM, Skehel JJ, Wiley DC (1994). Structure of influenza haemagglutinin at the pH of membrane fusion. *Nature* **371**(6492)**:** 37-43.

Bußfeld D, Kaufmann A, Meyer RG, Gemsa D, Sprenger H (1998). Differential mononuclear leukocyte attracting chemokine production after stimulation with active and inactivated influenza A virus. *Cell. Immunol.* **186**(1)**:** 1-7.

Campbell AM, Kashgarian M, Shlomchik MJ (2012). NADPH oxidase inhibits the pathogenesis of systemic lupus erythematosus. *Science translational medicine* **4**(157)**:** 157ra141.

Campos MAS, Almeida IC, Takeuchi O, Akira S, Valente EP, Procópio DO*, et al.* (2001). Activation of toll-like receptor-2 by glycosylphosphatidylinositol anchors from a protozoan parasite. *Journal of Immunology* **167**(1)**:** 416-423.

Chan MCW, Cheung CY, Chui WH, Tsao GSW, Nicholls JM, Chan YO*, et al.* (2005). Proinflammatory cytokine responses induced by influenza A (H5N1) viruses in primary human alveolar and bronchial epithelial cells. *Respir. Res.* **6**.

Chandler JD, Hu X, Ko EJ, Park S, Lee YT, Orr M*, et al.* (2016). Metabolic pathways of lung inflammation revealed by high-resolution metabolomics (HRM) of H1N1 influenza virus infection in mice. *Am. J. Physiol. Regul. Integr. Comp. Physiol.* **311**(5)**:** R906-R916.

Chen T, Hu Y, Liu B, Huang X, Gao N, Jin Z*, et al.* (2016). Synthetic toll-like receptor 7 agonist as a conjugated adjuvant enhances the Th1 type immunogenicity of influenza virus vaccine. *Int. J. Clin. Exp. Pathol.* **9**(4)**:** 4790-4795.

Choe J, Kelker MS, Wilson IA (2005). Structural biology: Crystal structure of human toll-like receptor 3 (TLR3) ectodomain. *Science* **309**(5734)**:** 581-585.

Chu Y, Piper R, Richardson S, Watanabe Y, Patel P, Heistad DD (2006). Endocytosis of extracellular superoxide dismutase into endothelial cells: role of the heparin-binding domain. *Arteriosclerosis, thrombosis, and vascular biology* **26**(9)**:** 1985-1990.

Chuang TH, Ulevitch RJ (2001). Identification of hTLR10: A novel human Toll-like receptor preferentially expressed in immune cells. *Biochim. Biophys. Acta Gene Struct. Expr.* **1518**(1-2)**:** 157-161.

Collins SE, Noyce RS, Mossman KL (2004). Innate Cellular Response to Virus Particle Entry Requires IRF3 but Not Virus Replication. *Journal of Virology* **78**(4)**:** 1706-1717.

Cossart P, Helenius A (2014). Endocytosis of viruses and bacteria. *Cold Spring Harbor perspectives in biology* **6**(8).

Csányi G, Cifuentes-Pagano E, Al Ghouleh I, Ranayhossaini DJ, Egaña L, Lopes LR*, et al.* (2011). Nox2 B-loop peptide, Nox2ds, specifically inhibits the NADPH oxidase Nox2. *Free Radic. Biol. Med.* **51**(6)**:** 1116-1125.

Dang PMC, Stensballe A, Boussetta T, Raad H, Dewas C, Kroviarski Y*, et al.* (2006). A specific p47phox-serine phosphorylated by convergent MAPKs mediates neutrophil NADPH oxidase priming at inflammatory sites. *Journal of Clinical Investigation* **116**(7)**:** 2033-2043.

de Vries E, Tscherne DM, Wienholts MJ, Cobos-Jiménez V, Scholte F, García-Sastre A*, et al.* (2011). Dissection of the influenza a virus endocytic routes reveals macropinocytosis as an alternative entry pathway. *PLoS Pathogens* **7**(3).

Diebold SS, Kaisho T, Hemmi H, Akira S, Reis E Sousa C (2004). Innate Antiviral Responses by Means of TLR7-Mediated Recognition of Single-Stranded RNA. *Science* **303**(5663)**:** 1529-1531.

Doherty PC, Turner SJ, Webby RG, Thomas PG (2006). Influenza and the challenge for immunology. *Nat. Immunol.* **7**(5)**:** 449-455.

Drummond GR, Selemidis S, Griendling KK, Sobey CG (2011a). Combating oxidative stress in vascular disease: NADPH oxidases as therapeutic targets. *Nature reviews. Drug discovery* **10**(6)**:** 453-471.

Drummond GR, Selemidis S, Griendling KK, Sobey CG (2011b). Combating oxidative stress in vascular disease: NADPH oxidases as therapeutic targets. *Nat. Rev. Drug Discov.* **10**(6)**:** 453-471.

Edelmann KH, Richardson-Burns S, Alexopoulou L, Tyler KL, Flavell RA, Oldstone MBA (2004). Does Toll-like receptor 3 play a biological role in virus infections? *Virology* **322**(2)**:** 231-238.

Eierhoff T, Hrincius ER, Rescher U, Ludwig S, Ehrhardt C (2010). The epidermal growth factor receptor (EGFR) promotes uptake of influenza a viruses (IAV) into host cells. *PLoS Pathogens* **6**(9).

El Benna J, Faust LRP, Johnson JL, Babior BM (1996). Phosphorylation of the burst oxidase subunit p47phox as determined by two-dimensional phosphopeptide mapping: Phosphorylation by protein kinase C, protein kinase A, and a mitogen-activated protein kinase. *Journal of Biological Chemistry* **271**(11)**:** 6374-6378.

El-Benna J, Dang PMC, Gougerot-Pocidalo MA (2008). Priming of the neutrophil NADPH oxidase activation: Role of p47phox phosphorylation and NOX2 mobilization to the plasma membrane. *Seminars in Immunopathology* **30**(3)**:** 279-289.

Elsharkawy AM, Oakley F, Lin F, Packham G, Mann DA, Mann J (2010). The NF-κB p50:p50:HDAC-1 repressor complex orchestrates transcriptional inhibition of multiple pro-inflammatory genes. *J. Hepatol.* **53**(3)**:** 519-527.

Ely JTA (2007). Ascorbic acid role in containment of the world avian flu pandemic. *Exp. Biol. Med.* **232**(7)**:** 847-851.

Ermert D, Urban CF, Laube B, Goosmann C, Zychlinsky A, Brinkmann V (2009). Mouse neutrophil extracellular traps in microbial infections. *J. Innate Immun.* **1**(3)**:** 181-193.

Ewald SE, Engel A, Lee J, Wang M, Bogyo M, Barton GM (2011). Nucleic acid recognition by Toll-like receptors is coupled to stepwise processing by cathepsins and asparagine endopeptidase. *J. Exp. Med.* **208**(4)**:** 643-651.

Fleming DM, Zambon M, Bartelds AIM (2000). Population estimates of persons presenting to general practitioners with influenza-like illness, 1987-96: A study of the demography of influenza-like illness in sentinel practice networks in England and Wales, and in The Netherlands. *Epidemiol. Infect.* **124**(2)**:** 245-253.

Forgac M (2007). Vacuolar ATPases: Rotary proton pumps in physiology and pathophysiology. *Nat. Rev. Mol. Cell Biol.* **8**(11)**:** 917-929.

Forman HJ, Torres M (2002). Reactive oxygen species and cell signaling: Respiratory burst in macrophage signaling. *American Journal of Respiratory and Critical Care Medicine* **166**(12 II)**:** S4-S8.

Fu X, Beer DG, Behar J, Wands J, Lambeth D, Cao W (2006). cAMP-response element-binding protein mediates acid-induced NADPH oxidase NOX5-S expression in Barrett esophageal adenocarcinoma cells. *Journal of Biological Chemistry* **281**(29)**:** 20368-20382.

Fukui R, Saitoh SI, Kanno A, Onji M, Shibata T, Ito A*, et al.* (2011). Unc93B1 restricts systemic lethal inflammation by orchestrating toll-like receptor 7 and 9 trafficking. *Immunity* **35**(1)**:** 69-81.

Fukuyama S, Kawaoka Y (2011). The pathogenesis of influenza virus infections: The contributions of virus and host factors. *Curr. Opin. Immunol.* **23**(4)**:** 481-486.

García-Sastre A, Biron CA (2006). Type 1 interferons and the virus-host relationship: A lesson in détente. *Science* **312**(5775)**:** 879-882.

Geiler J, Michaelis M, Naczk P, Leutz A, Langer K, Doerr HW*, et al.* (2010). N-acetyl-l-cysteine (NAC) inhibits virus replication and expression of pro-inflammatory molecules in A549 cells infected with highly pathogenic H5N1 influenza A virus. *Biochem. Pharmacol.* **79**(3)**:** 413-420.

Gitlin L, Barchet W, Gilfillan S, Cella M, Beutler B, Flavell RA*, et al.* (2006). Essential role of mda-5 in type I IFN responses to polyriboinosinic: polyribocytidylic acid and encephalomyocarditis picornavirus. *Proc. Natl. Acad. Sci. U. S. A.* **103**(22)**:** 8459-8464.

Goff PH, Hayashi T, Martínez-Gil L, Corr M, Crain B, Yao S*, et al.* (2015). Synthetic toll-like receptor 4 (TLR4) and TLR7 ligands as influenza virus vaccine adjuvants induce rapid, sustained, and broadly protective responses. *Journal of Virology* **89**(6)**:** 3221-3235.

Graham MB, Braciale TJ (1997). Resistance to and recovery from lethal influenza virus infection in B lymphocyte-deficient mice. *J. Exp. Med.* **186**(12)**:** 2063-2068.

Griendling KK, Sorescu D, Ushio-Fukai M (2000). NAD(P)H oxidase: Role in cardiovascular biology and disease. *Circ. Res.* **86**(5)**:** 494-501.

Groemping Y, Lapouge K, Smerdon SJ, Rittinger K (2003). Molecular basis of phosphorylation-induced activation of the NADPH oxidase. *Cell* **113**(3)**:** 343-355.

Guillot L, Le Goffic R, Bloch S, Escriou N, Akira S, Chignard M*, et al.* (2005). Involvement of Toll-like receptor 3 in the immune response of lung epithelial cells to double-stranded RNA and influenza A virus. *Journal of Biological Chemistry* **280**(7)**:** 5571-5580.

Hai R, Schmolke M, Leyva-Grado VH, Thangavel RR, Margine I, Jaffe EL*, et al.* (2013). Influenza A(H7N9) virus gains neuraminidase inhibitor resistance without loss of in vivo virulence or transmissibility. *Nat. Commun.* **4**.

Halima SB, Rajendran L (2011). Membrane anchored and lipid raft targeted β-secretase inhibitors for alzheimer's disease therapy. *J. Alzheimer's Dis.* **24**(SUPPL. 2)**:** 143-152.

Halle A, Hornung V, Petzold GC, Stewart CR, Monks BG, Reinheckel T*, et al.* (2008). The NALP3 inflammasome is involved in the innate immune response to amyloid-β. *Nat. Immunol.* **9**(8)**:** 857-865.

Halls ML, Poole DP, Ellisdon AM, Nowell CJ, Canals M (2015). Detection and Quantification of Intracellular Signaling Using FRET-Based Biosensors and High Content Imaging. *Methods in molecular biology* **1335:** 131-161.

Han Y, Bo ZJ, Xu MY, Sun N, Liu DH (2014). The protective role of TLR3 and TLR9 ligands in human pharyngeal epithelial cells infected with influenza A virus. *Korean J. Physiol. Pharmacol.* **18**(3)**:** 225-231.

Hartl D, Rieber N, Hector A, Kuijpers T, Roos D (2012). Current concepts of hyperinflammation in chronic granulomatous disease. *Clin. Dev. Immunol.* **2012**.

Hayashi F, Smith KD, Ozinsky A, Hawn TR, Yi EC, Goodlett DR*, et al.* (2001). The innate immune response to bacterial flagellin is mediated by Toll-like receptor 5. *Nature* **410**(6832)**:** 1099-1103.

Hayden FG, Fritz RS, Lobo MC, Alvord WG, Strober W, Straus SE (1998). Local and systemic cytokine responses during experimental human influenza A virus infection. Relation to symptom formation and host defense. *Journal of Clinical Investigation* **101**(3)**:** 643-649.

Heer AK, Shamshiev A, Donda A, Uematsu S, Akira S, Kopf M*, et al.* (2007). TLR signaling fine-tunes anti-influenza B cell responses without regulating effector T cell responses. *Journal of Immunology* **178**(4)**:** 2182-2191.

Heil F, Hemmi H, Hochrein H, Ampenberger F, Kirschning C, Akira S*, et al.* (2004). Species-Specific Recognition of Single-Stranded RNA via Till-like Receptor 7 and 8. *Science* **303**(5663)**:** 1526-1529.

Helenius A (2013). Virus entry: What has pH got to do with it? *Nature Cell Biology* **15**(2)**:** 125.

Hemmi H, Kaisho T, Takeuchi O, Sato S, Sanjo H, Hoshino K*, et al.* (2002). Small-antiviral compounds activate immune cells via the TLR7 MyD88-dependent signaling pathway. *Nat. Immunol.* **3**(2)**:** 196-200.

Hemmi H, Takeuchi O, Kawai T, Kaisho T, Sato S, Sanjo H*, et al.* (2000). A Toll-like receptor recognizes bacterial DNA. *Nature* **408**(6813)**:** 740-745.

Hernandes MS, D'Avila JC, Trevelin SC, Reis PA, Kinjo ER, Lopes LR*, et al.* (2014). The role of Nox2-derived ROS in the development of cognitive impairment after sepsis. *J. Neuroinflamm.* **11**.

Herold S, Steinmueller M, Von Wulffen W, Cakarova L, Pinto R, Pleschka S*, et al.* (2008). Lung epithelial apoptosis in influenza virus pneumonia: The role of macrophage-expressed TNF-related apoptosis-inducing ligand. *J. Exp. Med.* **205**(13)**:** 3065-3077.

Herold S, Von Wulffen W, Steinmueller M, Pleschka S, Kuziel WA, Mack M*, et al.* (2006). Alveolar epithelial cells direct monocyte transepithelial migration upon influenza virus infection: Impact of chemokines and adhesion molecules. *Journal of Immunology* **177**(3)**:** 1817-1824.

Heui MK, Lee YW, Lee KJ, Hyun SK, Sung WC, Van Rooijen N*, et al.* (2008). Alveolar macrophages are indispensable for controlling influenza viruses in lungs of pigs. *Journal of Virology* **82**(9)**:** 4265-4274.

Hofmann P, Sprenger H, Kaufmann A, Bender A, Hasse C, Nain M*, et al.* (1997). Susceptibility of mononuclear phagocytes to influenza A virus infection and possible role in the antiviral response. *J. LEUKOCYTE BIOL.* **61**(4)**:** 408-414.

Hornung V, Ellegast J, Kim S, Brzózka K, Jung A, Kato H*, et al.* (2006). 5′ -Triphosphate RNA is the ligand for RIG-I. *Science* **314**(5801)**:** 994-997.

Hoshino K, Takeuchi O, Kawai T, Sanjo H, Ogawa T, Takeda Y*, et al.* (1999). Cutting edge: Toll-like receptor 4 (TLR4)-deficient mice are hyporesponsive to lipopolysaccharide evidence for TLR4 as the Lps gene product. *Journal of Immunology* **162**(7)**:** 3749-3752.

Hunter T (2000). Signaling - 2000 and beyond. *CELL* **100**(1)**:** 113-127.

Huotari J, Helenius A (2011). Endosome maturation. *EMBO Journal* **30**(17)**:** 3481-3500.

Ichinohe T, Lee HK, Ogura Y, Flavell R, Iwasaki A (2009). Inflammasome recognition of influenza virus is essential for adaptive immune responses. *The Journal of experimental medicine* **206**(1)**:** 79-87.

Idris A (2014). Cellular responses to cytosolic double-stranded RNA—the role of the infammasome. *Immunol. Immunogenet.* **6:** 7-11.

Imai Y, Kuba K, Neely GG, Yaghubian-Malhami R, Perkmann T, van Loo G*, et al.* (2008a). Identification of oxidative stress and Toll-like receptor 4 signaling as a key pathway of acute lung injury. *Cell* **133**(2)**:** 235-249.

Imai Y, Kuba K, Neely GG, Yaghubian-Malhami R, Perkmann T, van Loo G*, et al.* (2008b). Identification of Oxidative Stress and Toll-like Receptor 4 Signaling as a Key Pathway of Acute Lung Injury. *CELL* **133**(2)**:** 235-249.

Ishii N, Funami K, Tatematsu M, Seya T, Matsumoto M (2014). Endosomal localization of TLR8 confers distinctive proteolytic processing on human myeloid cells. *Journal of Immunology* **193**(10)**:** 5118-5128.

Ishikawa E, Nakazawa M, Yoshinari M, Minami M (2005). Role of tumor necrosis factor-related apoptosis-inducing ligand in immune response to influenza virus infection in mice. *Journal of Virology* **79**(12)**:** 7658-7663.

Ito H, Ando T, Ogiso H, Arioka Y, Seishima M (2015). Inhibition of induced nitric oxide synthase enhances the anti-tumor effects on cancer immunotherapy using TLR7 agonist in mice. *Cancer Immunol. Immunother.* **64**(4)**:** 429-436.

Iwasaki A, Pillai PS (2014). Innate immunity to influenza virus infection. *Nature reviews. Immunology* **14**(5)**:** 315-328.

Jacobson GM, Dourron HM, Liu J, Carretero OA, Reddy DJ, Andrzejewski T*, et al.* (2003). Novel NAD(P)H oxidase inhibitor suppresses angioplasty-induced superoxide and neointimal hyperplasia of rat carotid artery. *Circ. Res.* **92**(6)**:** 637-643.

Jensen DD, Halls ML, Murphy JE, Canals M, Cattaruzza F, Poole DP*, et al.* (2014). Endothelin-converting enzyme 1 and beta-arrestins exert spatiotemporal control of substance P-induced inflammatory signals. *The Journal of biological chemistry* **289**(29)**:** 20283-20294.

Jin MS, Kim SE, Heo JY, Lee ME, Kim HM, Paik SG*, et al.* (2007). Crystal Structure of the TLR1-TLR2 Heterodimer Induced by Binding of a Tri-Acylated Lipopeptide. *CELL* **130**(6)**:** 1071-1082.

Johnson DK, Schillinger KJ, Kwait DM, Hughes CV, McNamara EJ, Ishmael F*, et al.* (2002). Inhibition of NADPH oxidase activation in endothelial cells by ortho-methoxy-substituted catechols. *Endothelium J. Endothelial Cell Res.* **9**(3)**:** 191-203.

Judkins CP, Diep H, Broughton BR, Mast AE, Hooker EU, Miller AA*, et al.* (2010). Direct evidence of a role for Nox2 in superoxide production, reduced nitric oxide bioavailability, and early atherosclerotic plaque formation in ApoE-/- mice. *American journal of physiology. Heart and circulatory physiology* **298**(1)**:** H24-32.

Julkunen I, Melén K, Nyqvist M, Pirhonen J, Sareneva T, Matikainen S (2000). Inflammatory responses in influenza A virus infection. *Vaccine* **19**(SUPPL. 1)**:** S32-S37.

Kagan JC (2012). Signaling organelles of the innate immune system. *CELL* **151**(6)**:** 1168-1178.

Kanno A, Yamamoto C, Onji M, Fukui R, Saitoh S, Motoi Y*, et al.* (2013a). Essential role for Toll-like receptor 7 (TLR7)-unique cysteines in an intramolecular disulfide bond, proteolytic cleavage and RNA sensing. *International immunology* **25**(7)**:** 413-422.

Kanno A, Yamamoto C, Onji M, Fukui R, Saitoh SI, Motoi Y*, et al.* (2013b). Essential role for Toll-like receptor 7 (TLR7)-unique cysteines in an intramolecular disulfide bond, proteolytic cleavage and RNA sensing. *Int. Immunol.* **25**(7)**:** 413-422.

Kato H, Takeuchi O, Sato S, Yoneyama M, Yamamoto M, Matsui K*, et al.* (2006). Differential roles of MDA5 and RIG-I helicases in the recognition of RNA viruses. *Nature* **441**(1)**:** 101-105.

Kawahara T, Quinn MT, Lambeth JD (2007). Molecular evolution of the reactive oxygen-generating NADPH oxidase (Nox/Duox) family of enzymes. *BMC evolutionary biology* **7:** 109.

Kawai T, Akira S (2009). The roles of TLRs, RLRs and NLRs in pathogen recognition. *Int. Immunol.* **21**(4)**:** 317-337.

Kelkka T, Kienhofer D, Hoffmann M, Linja M, Wing K, Sareila O*, et al.* (2014). Reactive oxygen species deficiency induces autoimmunity with type 1 interferon signature. *Antioxidants & redox signaling* **21**(16)**:** 2231-2245.

Kim YM, Brinkmann MM, Paquet ME, Ploegh HL (2008). UNC93B1 delivers nucleotide-sensing toll-like receptors to endolysosomes. *Nature* **452**(7184)**:** 234-238.

Kimbrell DA, Beutler B (2001). The evolution and genetics of innate immunity. *Nat. Rev. Gen.* **2**(4)**:** 256-267.

Kimura K, Shirabe K, Yoshizumi T, Takeishi K, Itoh S, Harimoto N*, et al.* (2016). Ischemia-reperfusion injury in fatty liver is mediated by activated NADPH oxidase 2 in rats. *Transplantation* **100**(4)**:** 791-800.

King PT, Lim S, Pick A, Ngui J, Prodanovic Z, Downey W*, et al.* (2013). Lung T-cell responses to nontypeable Haemophilus influenzae in patients with chronic obstructive pulmonary disease. *The Journal of allergy and clinical immunology* **131**(5)**:** 1314-1321 e1314.

Kirkeby L, Rasmussen TT, Reinholdt J, Kilian M (2000). Immunoglobulins in nasal secretions of healthy humans: Structural integrity of secretory immunoglobulin A1 (IgA1) and occurrence of neutralizing antibodies to IgA1 proteases of nasal bacteria. *Clin. Diagn. Lab. Immunol.* **7**(1)**:** 31-39.

Koyama S, Ishii KJ, Kumar H, Tanimoto T, Coban C, Uematsu S*, et al.* (2007). Differential role of TLR- and RLR-signaling in the immune responses to influenza A virus infection and vaccination. *Journal of Immunology* **179**(7)**:** 4711-4720.

La Gruta NL, Kedzierska K, Stambas J, Doherty PC (2007). A question of self-preservation: Immunopathology in influenza virus infection. *Immunology and Cell Biology* **85**(2)**:** 85-92.

Lackenby A, Hungnes O, Dudman SG, Meijer A, Paget WJ, Hay AJ*, et al.* (2008). Emergence of resistance to oseltamivir among influenza A(H1N1) viruses in Europe. *Euro Surveill.* **13**(5).

Lamm ME (1997). Interaction of antigens and antibodies at mucosal surfaces. In: *Annual Review of Microbiology* Vol. 51, pp 311-340.

Le Goffic R, Balloy V, Lagranderie M, Alexopoulou L, Escriou N, Flavell R*, et al.* (2006). Detrimental contribution of the Toll-like receptor (TLR)3 to influenza A virus-induced acute pneumonia. *PLoS Pathogens* **2**(6)**:** 0526-0535.

Lee SR, Kwont KS, Kim SR, Rhee SG (1998). Reversible inactivation of protein-tyrosine phosphatase 1B in A431 cells stimulated with epidermal growth factor. *Journal of Biological Chemistry* **273**(25)**:** 15366-15372.

Li Q, Harraz MM, Zhou W, Zhang LN, Ding W, Zhang Y*, et al.* (2006a). Nox2 and Rac1 regulate H2O2-dependent recruitment of TRAF6 to endosomal interleukin-1 receptor complexes. *Molecular and Cellular Biology* **26**(1)**:** 140-154.

Li Q, Harraz MM, Zhou W, Zhang LN, Ding W, Zhang Y*, et al.* (2006b). Nox2 and Rac1 regulate H2O2-dependent recruitment of TRAF6 to endosomal interleukin-1 receptor complexes. *Molecular and cellular biology* **26**(1)**:** 140-154.

Li Q, Spencer NY, Oakley FD, Buettner GR, Engelhardt JF (2009). Endosomal Nox2 facilitates redox-dependent induction of NF -kB by TNF α. *Antioxidants and Redox Signaling* **11**(6)**:** 1249-1263.

Liew FY, Xu D, Brint EK, O'Neill LAJ (2005). Negative regulation of toll-like receptor-mediated immune responses. *Nature Reviews Immunology* **5**(6)**:** 446-458.

Loo YM, Fornek J, Crochet N, Bajwa G, Perwitasari O, Martinez-Sobrido L*, et al.* (2008). Distinct RIG-I and MDA5 signaling by RNA viruses in innate immunity. *Journal of Virology* **82**(1)**:** 335-345.

Lopez CB, Moltedo B, Alexopoulou L, Bonifaz L, Flavell RA, Moran TM (2004). TLR-independent induction of dendritic cell maturation and adaptive immunity by negative-strand RNA viruses. *Journal of Immunology* **173**(11)**:** 6882-6889.

Lund JM, Alexopoulou L, Sato A, Karow M, Adams NC, Gale NW*, et al.* (2004a). Recognition of single-stranded RNA viruses by Toll-like receptor 7. *Proceedings of the National Academy of Sciences of the United States of America* **101**(15)**:** 5598-5603.

Lund JM, Alexopoulou L, Sato A, Karow M, Adams NC, Gale NW*, et al.* (2004b). Recognition of single-stranded RNA viruses by Toll-like receptor 7. *Proc. Natl. Acad. Sci. U. S. A.* **101**(15)**:** 5598-5603.

Mahadev K, Zilbering A, Zhu L, Goldstein BJ (2001). Insulin-stimulated Hydrogen Peroxide Reversibly Inhibits Protein-tyrosine Phosphatase 1B in Vivo and Enhances the Early Insulin Action Cascade. *Journal of Biological Chemistry* **276**(24)**:** 21938-21942.

Marina-García N, Franchi L, Kim YG, Miller D, McDonald C, Boons GJ*, et al.* (2008). Pannexin-1-mediated intracellular delivery of muramyl dipeptide induces caspase-1 activation via cryopyrin/NLRP3 independently of Nod2. *Journal of Immunology* **180**(6)**:** 4050-4057.

Marjuki H, Gornitzky A, Marathe BM, Ilyushina NA, Aldridge JR, Desai G*, et al.* (2011). Influenza A virus-induced early activation of ERK and PI3K mediates V-ATPase-dependent intracellular pH change required for fusion. *Cellular Microbiology* **13**(4)**:** 587-601.

Marsh GA, Hatami R, Palese P (2007). Specific residues of the influenza A virus hemagglutinin viral RNA are important for efficient packaging into budding virions. *Journal of Virology* **81**(18)**:** 9727-9736.

Martin K, Helenius A (1991). Nuclear transport of influenza virus ribonucleoproteins: The viral matrix protein (M1) promotes export and inhibits import. *CELL* **67**(1)**:** 117-130.

Martinon F, Mayor A, Tschopp J (2009). The inflammasomes: Guardians of the body. In: *Annual Review of Immunology* Vol. 27, pp 229-265.

Matlin KS, Reggio H, Helenius A, Simons K (1981). Infectious entry pathway of influenza virus in a canine kidney cell line. *J. CELL BIOL.* **91**(3 I)**:** 601-613.

Matsukura S, Kokubu F, Noda H, Tokunaga H, Adachi M (1996). Expression of IL-6, IL-8, and RANTES on human bronchial epithelial cells, NCI-H292, induced by influenza virus A. *J. ALLERGY CLIN. IMMUNOL.* **98**(6 I)**:** 1080-1087.

Mbawuike IN, Pacheco S, Acuna CL, Switzer KC, Zhang Y, Harriman GR (1999). Mucosal immunity to influenza without IgA: An IgA knockout mouse model. *Journal of Immunology* **162**(5)**:** 2530-2537.

Medina RA, García-Sastre A (2011). Influenza A viruses: New research developments. *Nature Reviews Microbiology* **9**(8)**:** 590-603.

Meng FG, Zhang ZY (2013). Redox regulation of protein tyrosine phosphatase activity by hydroxyl radical. *Biochim. Biophys. Acta Proteins Proteomics* **1834**(1)**:** 464-469.

Mercer J, Greber UF (2013). Virus interactions with endocytic pathways in macrophages and dendritic cells. *Trends Microbiol.* **21**(8)**:** 380-388.

Miki H, Funato Y (2012). Regulation of intracellular signalling through cysteine oxidation by reactive oxygen species. *J. Biochem.* **151**(3)**:** 255-261.

Mishina NM, Tyurin-Kuzmin PA, Markvicheva KN, Vorotnikov AV, Tkachuk VA, Laketa V*, et al.* (2011). Does cellular hydrogen peroxide diffuse or act locally? *Antioxidants & redox signaling* **14**(1)**:** 1-7.

Moscona A (2005). Neuraminidase inhibitors for influenza. *New Engl. J. Med.* **353**(13)**:** 1363-1373.

Müller KH, Kakkola L, Nagaraj AS, Cheltsov AV, Anastasina M, Kainov DE (2012). Emerging cellular targets for influenza antiviral agents. *Trends in Pharmacological Sciences* **33**(2)**:** 89-99.

Muzio M, Bosisio D, Polentarutti N, D'Amico G, Stoppacciaro A, Mancinelli R*, et al.* (2000). Differential expression and regulation of toll-like receptors (TLR) in human leukocytes: Selective expression of TLR3 in dendritic cells. *Journal of Immunology* **164**(11)**:** 5998-6004.

Neumann G, Noda T, Kawaoka Y (2009). Emergence and pandemic potential of swine-origin H1N1 influenza virus. *Nature* **459**(7249)**:** 931-939.

Ng WC, Liong S, Tate MD, Irimura T, Denda-Nagai K, Brooks AG*, et al.* (2014). The macrophage galactose-type lectin can function as an attachment and entry receptor for influenza virus. *Journal of Virology* **88**(3)**:** 1659-1672.

Ng WC, Londrigan SL, Nasr N, Cunningham AL, Turville S, Brooks AG*, et al.* (2016). The C-type lectin langerin functions as a receptor for attachment and infectious entry of influenza A virus. *Journal of Virology* **90**(1)**:** 206-221.

Nishiya T, DeFranco AL (2004). Ligand-regulated Chimeric Receptor Approach Reveals Distinctive Subcellular Localization and Signaling Properties of the Toll-like Receptors. *Journal of Biological Chemistry* **279**(18)**:** 19008-19017.

Nishiya T, Kajita E, Miwa S, DeFranco AL (2005). TLR3 and TLR7 are targeted to the same intracellular compartments by distinct regulatory elements. *Journal of Biological Chemistry* **280**(44)**:** 37107-37117.

Nitsch-Osuch A, Brydak LB (2015). Treatment and prophylaxis of influenza and the problem of resistance to neuraminidase inhibitors. *Postepy Hig Med Dosw (Online)* **69:** 1087-1095.

Noton SL, Medcalf E, Fisher D, Mullin AE, Elton D, Digard P (2007). Identification of the domains of the influenza A virus M1 matrix protein required for NP binding, oligomerization and incorporation into virions. *J. GEN. VIROL.* **88**(8)**:** 2280-2290.

Oakley FD, Abbott D, Li Q, Engelhardt JF (2009). Signaling components of redox active endosomes: The redoxosomes. *Antioxidants and Redox Signaling* **11**(6)**:** 1313-1333.

Oda T, Akaike T, Hamamoto T, Suzuki F, Hirano T, Maeda H (1989). Oxygen radicals in influenza-induced pathogenesis and treatment with pyran polymer-conjugated SOD. *Science* **244**(4907)**:** 974-976.

Ohto U, Shibata T, Tanji H, Ishida H, Krayukhina E, Uchiyama S*, et al.* (2015). Structural basis of CpG and inhibitory DNA recognition by Toll-like receptor 9. *Nature* **520**(7549)**:** 702-705.

Omueti KO, Beyer JM, Johnson CM, Lyle EA, Tapping RI (2005). Domain exchange between human Toll-like receptors 1 and 6 reveals a region required for lipopeptide discrimination. *Journal of Biological Chemistry* **280**(44)**:** 36616-36625.

Oostwoud LC, Gunasinghe P, Seow HJ, Ye JM, Selemidis S, Bozinovski S*, et al.* (2016). Apocynin and ebselen reduce influenza A virus-induced lung inflammation in cigarette smoke-exposed mice. *Sci. Rep.* **6**.

Östman A, Frijhoff J, Sandin Å, Böhmer FD (2011). Regulation of protein tyrosine phosphatases by reversible oxidation. *J. Biochem.* **150**(4)**:** 345-356.

Pang IK, Pillai PS, Iwasaki A (2013). Efficient influenza A virus replication in the respiratory tract requires signals from TLR7 and RIG-I. *Proc. Natl. Acad. Sci. U. S. A.* **110**(34)**:** 13910-13915.

Patterson S, Oxford JS, Dourmashkin RR (1979). Studies on the mechanism of influenza virus entry into cells. *J. GEN. VIROL.* **43**(1)**:** 223-229.

Perrone LA, Plowden JK, García-Sastre A, Katz JM, Tumpey TM (2008). H5N1 and 1918 pandemic influenza virus infection results in early and excessive infiltration of macrophages and neutrophils in the lungs of mice. *PLoS Pathogens* **4**(8).

Peshavariya H, Dusting GJ, Jiang F, Halmos LR, Sobey CG, Drummond GR*, et al.* (2009). NADPH oxidase isoform selective regulation of endothelial cell proliferation and survival. *Naunyn-Schmiedeberg's Arch. Pharmacol.* **380**(2)**:** 193-204.

Plattner F, Yarovinsky F, Romero S, Didry D, Carlier MF, Sher A*, et al.* (2008). Toxoplasma Profilin Is Essential for Host Cell Invasion and TLR11-Dependent Induction of an Interleukin-12 Response. *Cell Host and Microbe* **3**(2)**:** 77-87.

Poltorak A, He X, Smirnova I, Liu MY, Van Huffel C, Du X*, et al.* (1998). Defective LPS signaling in C3H/HeJ and C57BL/10ScCr mice: Mutations in Tlr4 gene. *Science* **282**(5396)**:** 2085-2088.

Qi J, Wang Y, Forgac M (2007). The vacuolar (H+)-ATPase: Subunit arrangement and in vivo regulation. *J. Bioenerg. Biomembr.* **39**(5-6)**:** 423-426.

Quesada IM, Lucero A, Amaya C, Meijles DN, Cifuentes ME, Pagano PJ*, et al.* (2015). Selective inactivation of NADPH oxidase 2 causes regression of vascularization and the size and stability of atherosclerotic plaques. *Atherosclerosis* **242**(2)**:** 469-475.

Rajendran L, Schneider A, Schlechtingen G, Weidlich S, Ries J, Braxmeier T*, et al.* (2008a). Efficient inhibition of the Alzheimer's disease beta-secretase by membrane targeting. *Science* **320**(5875)**:** 520-523.

Rajendran L, Schneider A, Schlechtingen G, Weidlich S, Ries J, Braxmeier T*, et al.* (2008b). Efficient inhibition of the Alzheimer's disease β-secretase by membrane targeting. *Science* **320**(5875)**:** 520-523.

Rajendran L, Simons K (2005). Lipid rafts and membrane dynamics. *J. Cell Sci.* **118**(6)**:** 1099-1102.

Ramirez-Ortiz ZG, Prasad A, Griffith JW, Pendergraft WF, 3rd, Cowley GS, Root DE*, et al.* (2015). The receptor TREML4 amplifies TLR7-mediated signaling during antiviral responses and autoimmunity. *Nature immunology* **16**(5)**:** 495-504.

Rehwinkel J, Tan CP, Goubau D, Schulz O, Pichlmair A, Bier K*, et al.* (2010). RIG-I Detects Viral Genomic RNA during Negative-Strand RNA Virus Infection. *CELL* **140**(3)**:** 397-408.

Rey FE, Cifuentes ME, Kiarash A, Quinn MT, Pagano PJ (2001). Novel competitive inhibitor of NAD(P)H oxidase assembly attenuates vascular O2 - and systolic blood pressure in mice. *Circ. Res.* **89**(5)**:** 408-414.

Rhee SG (2006). H2O2, a necessary evil for cell signaling. *Science* **312**(5782)**:** 1882-1883.

Roberts PC, Lamb RA, Compans RW (1998). The M1 and M2 proteins of influenza a virus are important determinants in filamentous particle formation. *Virology* **240**(1)**:** 127-137.

Roos D, Kuhns DB, Maddalena A, Bustamante J, Kannengiesser C, de Boer M*, et al.* (2010). Hematologically important mutations: The autosomal recessive forms of chronic granulomatous disease (second update). *Blood Cells Mol. Dis.* **44**(4)**:** 291-299.

Rouhanizadeh M, Hwang J, Clempus RE, Marcu L, Lassègue B, Sevanian A*, et al.* (2005). Oxidized-1-palmitoyl-2-arachidonoyl-sn-glycero-3-phosphorylcholine induces vascular endothelial superoxide production: Implication of NADPH oxidase. *Free Radic. Biol. Med.* **39**(11)**:** 1512-1522.

Ruigrok RWH, Barge A, Durrer P, Brunner J, Ma K, Whittaker GR (2000). Membrane interaction of influenza virus M1 protein. *Virology* **267**(2)**:** 289-298.

Rumschlag-Booms E, Rong L (2013). Influenza A virus entry: Implications in virulence and future therapeutics. *Adv. Virol.* **2013**.

Sakai S, Kawamata H, Mantani N, Kogure T, Shimada Y, Terasawa K*, et al.* (2000). Therapeutic effect of anti-macrophage inflammatory protein 2 antibody on influenza virus-induced pneumonia in mice. *Journal of Virology* **74**(5)**:** 2472-2476.

Sallusto F, Baggiolini M (2008). Chemokines and leukocyte traffic. *Nat. Immunol.* **9**(9)**:** 949-952.

Salmeen A, Barford D (2005). Functions and mechanisms of redox regulation of cysteine-based phosphatases. *Antioxidants and Redox Signaling* **7**(5-6)**:** 560-577.

Samuel CE (2001). Antiviral actions of interferons. *Clin. Microbiol. Rev.* **14**(4)**:** 778-809.

Saxena RK, Tripathi P, Rawat G (2012). Pandemism of swine flu and its prospective drug therapy. *European Journal of Clinical Microbiology and Infectious Diseases* **31**(12)**:** 3265-3279.

Schappi M, Deffert C, Fiette L, Gavazzi G, Herrmann F, Belli D*, et al.* (2008). Branched fungal beta-glucan causes hyperinflammation and necrosis in phagocyte NADPH oxidase-deficient mice. *The Journal of pathology* **214**(4)**:** 434-444.

Schindelin J, Arganda-Carreras I, Frise E, Kaynig V, Longair M, Pietzsch T*, et al.* (2012). Fiji: an open-source platform for biological-image analysis. *Nature methods* **9**(7)**:** 676-682.

Schoggins JW, Wilson SJ, Panis M, Murphy MY, Jones CT, Bieniasz P*, et al.* (2011). A diverse range of gene products are effectors of the type i interferon antiviral response. *Nature* **472**(7344)**:** 481-485.

Schwarz KB (1996). Oxidative stress during viral infection: A review. *Free Radic. Biol. Med.* **21**(5)**:** 641-649.

Scott DJ, Grossmann JG, Tame JRH, Byron O, Wilson KS, Otto BR (2002). Low resolution solution structure of the apo form of Escherichia coli haemoglobin protease Hbp. *J. Mol. Biol.* **315**(5)**:** 1179-1187.

Segal A, Jones OG, Webster D, Allison A (1978). ABSENCE OF A NEWLY DESCRIBED CYTOCHROME b FROM NEUTROPHILS OF PATIENTS WITH CHRONIC GRANULOMATOUS DISEASE. *Lancet* **312**(8087)**:** 446-449.

Selemidis S, Seow HJ, Broughton BRS, Vinh A, Bozinovski S, Sobey CG*, et al.* (2013). Nox1 Oxidase Suppresses Influenza A Virus-Induced Lung Inflammation and Oxidative Stress. *PLoS ONE* **8**(4).

Selemidis S, Sobey CG, Wingler K, Schmidt HH, Drummond GR (2008). NADPH oxidases in the vasculature: molecular features, roles in disease and pharmacological inhibition. *Pharmacology & therapeutics* **120**(3)**:** 254-291.

Seo SH, Hoffmann E, Webster RG (2002). Lethal H5N1 influenza viruses escape host anti-viral cytokine responses. *Nat. Med.* **8**(9)**:** 950-954.

Seo SH, Webby R, Webster RG (2004). No apoptotic deaths and different levels of inductions of inflammatory cytokines in alveolar macrophages infected with influenza viruses. *Virology* **329**(2)**:** 270-279.

Seo SU, Kwon HJ, Song JH, Byun YH, Seong BL, Kawai T*, et al.* (2010). MyD88 signaling is indispensable for primary influenza A virus infection but dispensable for secondary infection. *Journal of Virology* **84**(24)**:** 12713-12722.

Sheu TG, Fry AM, Garten RJ, Deyde VM, Shwe T, Bullion L*, et al.* (2011). Dual resistance to adamantanes and oseltamivir among seasonal influenza A(H1N1) viruses: 2008-2010. *J. Infect. Dis.* **203**(1)**:** 13-17.

Shi X, Shi Z, Huang H, Zhu H, Zhou P, Zhu H*, et al.* (2014). Ability of recombinant human catalase to suppress inflammation of the murine lung induced by influenza A. *Inflammation* **37**(3)**:** 809-817.

Simons K, Ikonen E (1997). Functional rafts in cell membranes. *Nature* **387**(6633)**:** 569-572.

Snelgrove R, Williams A, Thorpe C, Hussell T (2004). Manipulation of immunity to and pathology of respiratory infections. *Expert Rev. Anti-Inf.* **2**(3)**:** 413-426.

Snelgrove RJ, Edwards L, Rae AJ, Hussell T (2006a). An absence of reactive oxygen species improves the resolution of lung influenza infection. *Eur J Immunol* **36**(6)**:** 1364-1373.

Snelgrove RJ, Edwards L, Rae AJ, Hussell T (2006b). An absence of reactive oxygen species improves the resolution of lung influenza infection. *Eur. J. Immunol.* **36**(6)**:** 1364-1373.

Sun K, Yajjala VK, Bauer C, Talmon GA, Fischer KJ, Kielian T*, et al.* (2016). Nox2-derived oxidative stress results in inefficacy of antibiotics against post-influenza S. aureus pneumonia. *J. Exp. Med.* **213**(9)**:** 1851-1864.

Takeda K, Akira S (2015). Toll-Like receptors. *Curr. Protoc. Immunol.* **2015:** 14.12.11-14.12.10.

Takeuchi O, Kaufmann A, Grote K, Kawai T, Hoshino K, Morr M*, et al.* (2000). Cutting edge: Preferentially the R-stereoisomer of the mycoplasmal lipopeptide macrophage-activating lipopeptide-2 activates immune cells through a toll-like receptor 2- and MyD88-dependent signaling pathway. *Journal of Immunology* **164**(2)**:** 554-557.

Takeuchi O, Sato S, Horiuchi T, Hoshino K, Takeda K, Dong Z*, et al.* (2002). Cutting edge: Role of Toll-like receptor 1 in mediating immune response to microbial lipoproteins. *Journal of Immunology* **169**(1)**:** 10-14.

Tammariello SP, Quinn MT, Estus S (2000). NADPH oxidase contributes directly to oxidative stress and apoptosis in nerve growth factor-deprived sympathetic neurons. *J. Neurosci.* **20**(1).

Tanimura N, Saitoh S, Matsumoto F, Akashi-Takamura S, Miyake K (2008). Roles for LPS-dependent interaction and relocation of TLR4 and TRAM in TRIF-signaling. *Biochem. Biophys. Res. Commun.* **368**(1)**:** 94-99.

Tanji H, Ohto U, Shibata T, Taoka M, Yamauchi Y, Isobe T*, et al.* (2015). Toll-like receptor 8 senses degradation products of single-stranded RNA. *Nature Structural and Molecular Biology* **22**(2)**:** 109-116.

Tate MD, Deng YM, Jones JE, Anderson GP, Brooks AG, Reading PC (2009). Neutrophils ameliorate lung injury and the development of severe disease during influenza infection. *Journal of Immunology* **183**(11)**:** 7441-7450.

Tate MD, Schilter HC, Brooks AG, Reading PC (2011). Responses of mouse airway epithelial cells and alveolar macrophages to virulent and avirulent strains of influenza a virus. *Viral Immunol.* **24**(2)**:** 77-88.

Thomas PG, Dash P, Aldridge Jr JR, Ellebedy AH, Reynolds C, Funk AJ*, et al.* (2009). The Intracellular Sensor NLRP3 Mediates Key Innate and Healing Responses to Influenza A Virus via the Regulation of Caspase-1. *Immunity* **30**(4)**:** 566-575.

To EE, Broughton BR, Hendricks KS, Vlahos R, Selemidis S (2014). Influenza A virus and TLR7 activation potentiate NOX2 oxidase-dependent ROS production in macrophages. *Free radical research* **48**(8)**:** 940-947.

Tumpey TM, García-Sastre A, Taubenberger JK, Palese P, Swayne DE, Pantin-Jackwood MJ*, et al.* (2005). Pathogenicity of influenza viruses with genes from the 1918 pandemic virus: Functional roles of alveolar macrophages and neutrophils in limiting virus replication and mortality in mice. *Journal of Virology* **79**(23)**:** 14933-14944.

Uchide N, Toyoda H (2008). Potential of selected antioxidants for influenza chemotherapy. *Anti-Infective Agents in Medicinal Chemistry* **7**(2)**:** 73-83.

Upham JP, Pickett D, Irimura T, Anders EM, Reading PC (2010). Macrophage receptors for influenza a virus: Role of the macrophage galactose-type lectin and mannose receptor in viral entry. *Journal of Virology* **84**(8)**:** 3730-3737.

van den Berg JM, van Koppen E, Åhlin A, Belohradsky BH, Bernatowska E, Corbeel L*, et al.* (2009). Chronic granulomatous disease: The European experience. *PLoS ONE* **4**(4).

Violin JD, Zhang J, Tsien RY, Newton AC (2003). A genetically encoded fluorescent reporter reveals oscillatory phosphorylation by protein kinase C. *The Journal of cell biology* **161**(5)**:** 899-909.

Vlahos R, Selemidis S (2014). NADPH Oxidases as Novel Pharmacologic Targets against Influenza A Virus Infection. *Molecular pharmacology* **86**(6)**:** 747-759.

Vlahos R, Stambas J, Bozinovski S, Broughton BR, Drummond GR, Selemidis S (2011a). Inhibition of Nox2 oxidase activity ameliorates influenza A virus-induced lung inflammation. *PLoS pathogens* **7**(2)**:** e1001271.

Vlahos R, Stambas J, Bozinovski S, Broughton BRS, Drummond GR, Selemidis S (2011b). Inhibition of Nox2 oxidase activity ameliorates influenza a virus-induced lung inflammation. *PLoS Pathogens* **7**(2).

Vlahos R, Stambas J, Selemidis S (2012a). Suppressing production of reactive oxygen species (ROS) for influenza A virus therapy. *Trends in pharmacological sciences* **33**(1)**:** 3-8.

Vlahos R, Stambas J, Selemidis S (2012b). Suppressing production of reactive oxygen species (ROS) for influenza A virus therapy. *Trends Pharmacol. Sci.* **33**(1)**:** 3-8.

von Krogh G, Lacey CJN, Gross G, Barrasso R, Schneider A (2000). European course on HPV associated pathology: Guidelines for primary care physicians for the diagnosis and management of anogenital warts. *Sex. Transm. Infect.* **76**(3)**:** 162-168.

Wang H, Jiang C (2009). Influenza A virus H5N1 entry into host cells is through clathrin-dependent endocytosis. *Science in China, Series C: Life Sciences* **52**(5)**:** 464-469.

Wareing MD, Lyon AB, Lu B, Gerard C, Sarawar SR (2004). Chemokine expression during the development and resolution of a pulmonary leukocyte response to influenza A virus infection in mice. *J. LEUKOCYTE BIOL.* **76**(4)**:** 886-895.

Watanabe T, Watanabe S, Kawaoka Y (2010). Cellular networks involved in the influenza virus life cycle. *Cell Host and Microbe* **7**(6)**:** 427-439.

West AP, Brodsky IE, Rahner C, Woo DK, Erdjument-Bromage H, Tempst P*, et al.* (2011). TLR signalling augments macrophage bactericidal activity through mitochondrial ROS. *Nature* **472**(7344)**:** 476-480.

White J, Kartenbeck J, Helenius A (1982). Membrane fusion activity of influenza virus. *EMBO Journal* **1**(2)**:** 217-222.

Wijburg OLC, Dinatale S, Vadolas J, Van Rooijen N, Strugnell RA (1997). Alveolar macrophages regulate the induction of primary cytotoxic T- lymphocyte responses during influenza virus infection. *Journal of Virology* **71**(12)**:** 9450-9457.

Wong JP, Christopher ME, Viswanathan S, Karpoff N, Dai X, Das D*, et al.* (2009). Activation of toll-like receptor signaling pathway for protection against influenza virus infection. *Vaccine* **27**(25-26)**:** 3481-3483.

Woof JM, Mestecky J (2005). Mucosal immunoglobulins. *Immunol. Rev.* **206:** 64-82.

Xu L, Yoon H, Zhao MQ, Liu J, Ramana CV, Enelow RI (2004). Cutting edge: Pulmonary immunopathology mediated by antigen-specific expression of TNF-α by antiviral CD8+ T cells. *Journal of Immunology* **173**(2)**:** 721-725.

Yan SR, Berton G (1996). Regulation of Src family tyrosine kinase activities in adherent human neutrophils. Evidence that reactive oxygen intermediates produced by adherent neutrophils increase the activity of the p58(c-fgr) and p53/56(lyn) tyrosine kinases. *Journal of Biological Chemistry* **271**(38)**:** 23464-23471.

Yang CS, Kim JJ, Lee SJ, Hwang JH, Lee CH, Lee MS*, et al.* (2013). TLR3-triggered reactive oxygen species contribute to inflammatory responses by activating signal transducer and activator of transcription-1. *Journal of Immunology* **190**(12)**:** 6368-6377.

Yang J, Li M, Shen X, Liu S (2012). Influenza A virus entry inhibitors targeting the hemagglutinin. *Viruses* **5**(1)**:** 352-373.

Yang YL, Reis LFL, Paylovic J, Aguzzi S, Schäfer R, Kumar A*, et al.* (1995). Deficient signaling in mice devoid of double-stranded RNA-dependent protein kinase. *EMBO Journal* **14**(24)**:** 6095-6106.

Yarovinsky F, Zhang D, Andersen JF, Bannenberg GL, Serhan CN, Hayden MS*, et al.* (2005). Immunology: TLR11 activation of dendritic cells by a protozoan profilin-like protein. *Science* **308**(5728)**:** 1626-1629.

Yatmaz S, Seow HJ, Gualano RC, Wong ZX, Stambas J, Selemidis S*, et al.* (2013). Glutathione peroxidase-1 reduces influenza A virus-induced lung inflammation. *American Journal of Respiratory Cell and Molecular Biology* **48**(1)**:** 17-26.

Yewdell JW, Bennink JR, Smith GL, Moss B (1985). Influenza A virus nucleoprotein is a major target antigen for cross-reactive anti-influenza A virus cytotoxic T lymphocytes. *Proc. Natl. Acad. Sci. U. S. A.* **82**(6)**:** 1785-1789.

Yoneyama M, Fujita T (2009). RNA recognition and signal transduction by RIG-I-like receptors. *Immunol. Rev.* **227**(1)**:** 54-65.

Yoshimura A, Kuroda K, Kawasaki K, Yamashina S, Maeda T, Ohnishi S (1982). Infectious cell entry mechanism of influenza virus. *Journal of Virology* **43**(1)**:** 284-293.

Zhang J, Graham DG, Montine TJ, Ho YS (2000). Enhanced N-methyl-4-phenyl-1,2,3,6-tetrahydropyridine toxicity in mice deficient in CuZn-superoxide dismutase or glutathione peroxidase. *Journal of Neuropathology and Experimental Neurology* **59**(1)**:** 53-61.

Zhang RH, Li CH, Wang CL, Xu MJ, Xu T, Wei D*, et al.* (2014). N-acetyl-l-cystine (NAC) protects against H9N2 swine influenza virus-induced acute lung injury. *Int. Immunopharmacol.* **22**(1)**:** 1-8.

Zhu J, Lai K, Brownile R, Babiuk LA, Mutwiri GK (2008). Porcine TLR8 and TLR7 are both activated by a selective TLR7 ligand, imiquimod. *Mol. Immunol.* **45**(11)**:** 3238-3243.

Chapter 2:
Influenza A virus and TLR7 activation potentiate NOX2 oxidase-dependent ROS production in macrophages

Declaration for Thesis Chapter 2- *Influenza A virus and TLR7 activation potentiate NOX2 oxidase-dependent ROS production in macrophages*

Declaration by candidate

In the case of Chapter 2, the nature and extent of my contribution to the work was as follows:

Nature of contribution	**Extent of contribution (%)**
Intellectual input into the design of experiments, performed all experiments, cell culture, confocal microscopy, L-012 enhanced chemiluminescence; analysed results, prepared figures and wrote the manuscript	95 %

The following co-authors have contributed to this study. If co-authors are students at Monash University, the extent of their contribution must be stated:

Name	**Nature of contribution**	**Extent of contribution (%)**
Keshia S Hendricks	Provided intellectual advice during experiments	N/A
Brad RS Broughton Ross Vlahos	Provided intellectual advice during experimental and manuscript preparation	N/A
Stavros Selemidis	Intellectual input into the design of experiments, preparation of manuscript, management of the project and provided funding to support the project	N/A

The undersigned hereby certify that the above declaration correctly reflects the nature and extent of candidate's and co-authors' contribution to this work.

Candidate's signature: Date: 17-02-2017

Main supervisor's signature: [redacted] Date: 17-02-2017

Free Radical Research, August 2014; 48(8): 940–947
© 2014 Informa UK, Ltd.
ISSN 1071-5762 print/ISSN 1029-2470 online
DOI: 10.3109/10715762.2014.927579

informa
healthcare

ORIGINAL ARTICLE

Influenza A virus and TLR7 activation potentiate NOX2 oxidase-dependent ROS production in macrophages

E. E. To[1], B. R. S. Broughton[1], K. S. Hendricks[1], R. Vlahos[2] & S. Selemidis[1]

[1]*Department of Pharmacology, Monash University, Victoria, Australia, and* [2]*Department of Pharmacology & Therapeutics, Respiratory Research Group, Lung Health Research Centre, The University of Melbourne, Victoria, Australia*

Abstract

Influenza A virus infects resident alveolar macrophages in the respiratory tract resulting in Toll like receptor 7 (TLR7) activation that triggers an inflammatory response to resolve the infection. Macrophages are also major sources of reactive oxygen species (ROS) *via* the NOX2-containing NADPH oxidase. Although ROS are crucial for pathogen clearance, in response to influenza A virus, ROS are touted as being culprit mediators of the lung tissue injury. The aim of the present study was to determine whether influenza A virus infection and TLR7 activation of macrophages, results in alterations in their ROS production. Here we demonstrate using immunofluorescence that influenza A virus (Hong Kong X-31 strain; H3N2) internalizes in RAW264.7 cells and mouse alveolar macrophages within 1 h, resulting in a significant enhancement in the stimulated NOX2 oxidase-dependent oxidative burst, although virus had no effect on basal ROS. The specific TLR7 agonist imiquimod (10 μg/ml) elevated basal superoxide production and, in a similar fashion to influenza A virus, enhanced NOX2 oxidase-dependent oxidative burst. By contrast, the TLR3 agonist, poly I:C (1–100 μg/ml) failed to influence the oxidative burst to NOX2 oxidase. A peptide corresponding to the region 337–348 on p47phox conjugated to a HIV-tat, designed to inhibit the phosphorylation of Ser346 on p47phox suppressed the influenza A virus- and imiquimod-induced enhancement in the oxidative burst. In conclusion, this study demonstrates *for the first time* that influenza A virus and TLR7 activation enhance the NOX2 oxidase-dependent oxidative burst in macrophages, which might underpin the acute lung injury to influenza A virus infection.

Keywords: superoxide, imiquimod, poly I:C, lung pathology, oxidative stress

Introduction

Influenza A virus infections continue to represent a major social and economic burden worldwide with estimations of ~5 million cases annually and about 10% resulting in death. This is compounded by the problems with current classes of therapeutics to treat influenza. The major classes of antiviral compounds, the neuraminidase inhibitors, have been demonstrated to lack efficacy against certain strains of influenza A virus. Vaccination is highly specific for circulating viruses, however, to generate sufficient amounts of vaccine against new emerging strains of virus for which the population possess no immunity against, takes about 6 months, putting the population at high risk. Therefore, there is a pressing need for novel pharmacological strategies that target the lung pathology, which might be achieved by targeting key processes of the host immune response.

A typical host immune response to influenza A virus in the absence of pre-existing immunity is generally characterised by epithelial and resident macrophage infection and activation [1]. This causes cytokine and chemokine release and the infiltration of blood borne inflammatory cells such as monocytes, neutrophils and macrophages into the lung and airways [1]. Strong evidence suggests that this inflammatory response is responsible for the inappropriate lung tissue injury following influenza A virus infection [2]. Recent evidence by our and other laboratories have clearly demonstrated that reactive oxygen species (ROS), most predominantly superoxide, hydrogen peroxide (H_2O_2) and peroxynitrite ($ONOO^-$) are key contributors to the lung injury due to influenza A virus infection [2–7]. Indeed, the excessive production of ROS causes enhanced regulation of redox-sensitive pathways, oxidative stress, lipid oxidation and DNA damage, thereby promoting lung injury and tissue damage [2,3]. In keeping with this, key antioxidant enzyme systems such as GPX-1 that promote H_2O_2 inactivation protect against airways and lung inflammation and oxidative stress [8]. These lines of evidence highlight the importance of ROS in the pathogenesis of influenza A virus and suggest that drugs that target the most abundant source of ROS production, namely the NADPH oxidases, might be useful for alleviating the oxidative stress burden and the consequences of it.

The NOX family of NADPH oxidases are a highly regulated, membrane-bound group of multi-subunit enzyme complexes found in a variety of phagocytic and non-phagocytic cells in which their primary function is to generate ROS [9–11]. They are expressed in key cell types of the airways, including endothelial, epithelial and

Correspondence: Dr. Stavros Selemidis, Department of Pharmacology, Oxidant and Inflammation Biology Group, Monash University, Clayton, Victoria 3800, Australia. Tel: +613-9905-5756. E-mail: Stavros.selemidis@monash.edu

(Received date: 8 January 2014; Accepted date: 20 May 2014; Published online: 19 June 2014)

inflammatory cells (alveolar macrophages, monocytes, neutrophils and T lymphocytes). Various NOX isoforms and their splice variants have different roles in the inflammatory response, each having unique expression pattern and subunit requirement [10–12]. The key NOX isoform with the highest abundance in macrophages is the NOX2 oxidase. NOX2 oxidase is composed of the following regulatory subunits that form a ternary complex: p40phox, p47phox and p67phox. Phosphorylation of p47phox leads to a conformational change allowing the ternary complex to interact with the membrane-bound NOX2-p22phox heterodimer. In addition, two GTP-binding proteins RAC1 and RAC2 are involved in activation of the complex [13]. NOX2 oxidase is expressed in inflammatory cells that are resident and are recruited to the lungs, including macrophages and neutrophils.

NOX2 oxidase activation following influenza A virus infection, leads to increased oxidative stress causing mild to moderate lung injury [4,7,14]. In comparison to naïve uninfected WT mice, WT mice infected with the X-31 influenza A virus had significantly increased production of superoxide, which was virtually abolished in NOX2$^{-/y}$ mice [7]. The deletion of the *NOX2* gene not only limited ROS production, but also decreased the number of infiltrating immune cells, which would reduce the over exuberant lung inflammation observed in influenza A virus infection [7]. Owing to the fact NOX2 plays a crucial role in the lung pathology associated with influenza A virus infections, it is important to establish which of the key cell types of the airways are contributing to the oxidative stress and whether there is regulation of NOX2 oxidase activity within these cells by influenza A virus.

Toll-like receptors (TLRs) play a key role in the recognition of microbial pathogen associated molecular patterns (PAMPs) and function as a crucial line of defence against microbial infection. Currently, there are 10 known human TLRs (12 mouse) that are broadly expressed on immune cells, preferentially expressed on macrophages and dendritic cells [15,16]. Importantly, TLR3 and TLR7 are located in the endosomal compartments where they detect viral nucleic acids [15]. Specifically, TLR3 and TLR7 recognise double-stranded RNA and single-stranded RNA (ssRNA), respectively [17,18]. The interaction between TLRs and viruses within endosomes mediates signalling cascades to upregulate proinflammatory pathways. Activation of TLR3 by its synthetic analogue polyinosinic-polycytidylic acid (poly I:C) increased ROS production, and release of TNF-α and IFN-β through signalling to NF-kB [19]. Previous studies have shown that acidification within the endosome results in the release of ssRNA from influenza A virus, which can bind TLR7, triggering an inflammatory response characterised by cytokine (IL-β, IFN-β, IL-6 and IL-12) release [17]. This gives rise to one of the most important mechanisms of host-defence against viral infection. Therefore the aim of the present study was to determine whether influenza A virus infection increases the NOX2 oxidase-dependent oxidative burst of macrophages and also whether similar effects are evident following activation of the most likely sensors of influenza A viral RNA, that is, TLR3 and TLR7.

Methods

Virus

The mouse-adapted Hong Kong X-31 (H3N2) influenza A virus was provided by Dr John Stambas (School of Medicine, Deakin University, CSIRO, Australia). The virus was provided in phosphate buffered saline (PBS) as a stock solution of 1×10^8 plaque forming units per ml (PFUs/ml) and stored at -80°C until used. On the day of use, virus was thawed quickly and incubated at 37°C prior to infection.

Animal ethics statement

The experiments described in this manuscript were approved by the Animal Experimentation Ethics Committee of Monash University and conducted in compliance with the guidelines of the National Health and Medical Research Council (NHMRC) of Australia on animal experimentation.

Cell culture and primary cell isolation

The immortalized cell line RAW 264.7 cells (derived from mouse peritoneum) were maintained in Dulbecco's Modified Eagle's Medium (Sigma) supplemented with L-glutamine, glucose (4500 mg/L), sodium pyruvate (110 mg/L) and fetal bovine serum (FBS; 10%) and kept in a 37°C incubator with a humidified mixture of 5% CO_2 and 95% air. The medium was changed two to three times a week, cells were sub-cultured by scraping upon being ~80–90% confluent, and counted using the Countess® automated cell counter (Invitrogen). Alveolar macrophages were isolated by lung lavage from age-matched (8–10 weeks) male C57Bl/6J (WT) and NOX2$^{-/y}$ mice as previously published [7]. Cell suspensions were spun down by centrifugation (1500 rpm at 4°C for 5 min). Supernatant was removed, and then cells were resuspended in 1 ml of sterile PBS and counted using the Countess® automated cell counter. Cells were then seeded into 96-well (4×10^4 cells/well) or 6-well (5×10^5 cells/well) plates for ROS production assay and immunocytochemistry, as stated below.

Immunofluorescence microscopy

RAW264.7 cells were seeded onto glass coverslips in 6-well plates, and allowed to adhere for 24 h in DMEM. Cells were then incubated in the absence or presence of X-31 influenza A virus (MOI 1, 3 or 10) in serum-free medium at varying time points (30 min, 1 h). In v cases, cells were pre-treated for 30 min prior to infection with the dynamin inhibitor, dynasore (100 μM), or the vehicle for dynasore, dimethyl sulfoxide (DMSO; 0.1%). Next, the cells were washed with PBS (0.01 M) and fixed with 4%

paraformaldehyde (PFA) for 15 min. Cells were treated for 10 min with PBS-containing Triton X-100 (0.25%) and then washed out three times over 15 min with PBS. The samples were then incubated with 10% goat serum-containing PBS for 1 h. This was followed by the addition of a primary antibody for nucleoprotein (1:1000) to localise influenza A virus for 24 h at 4°C. Cells were washed three times over 30 min with PBS (0.01 M). Following the washes, a goat anti-mouse IgG (1:1000) secondary antibody was added to the wells for 2 h and kept in the dark. Finally, the cells were washed three times over 30 min with PBS (0.01 M); cover slips were mounted onto microscope slides with 0.1–1 μg of diamidino-2-phenylindole (DAPI) for 3 min. Slides were viewed and photographed on an Olympus fluorescence microscope. Importantly, secondary antibody control experiments were performed to ensure primary antibody specific immunoreactivity.

ROS production by L-012-enhanced chemiluminescence

Total ROS production was measured using L-012-enhanced chemiluminescence. RAW264.7 cells and primary mouse alveolar macrophages were seeded into a 96-well Opti Viewplate (4×10^4 cells/well). Cells were either treated with PBS (control), imiquimod (1–10 μg/ml) or TLR3 agonist poly I:C (1–100 μg/ml) or infected with X-31 influenza A virus at a multiplicity of infection (MOI; 1, 3 or 10) for 1 h. In some cases, cells were pretreated for 30 min with the mouse Ser346 HIV-tat containing peptide inhibitor (50 μM) prior to virus infection or imiquimod treatment. Cells were then washed of media with warm 37°C Krebs-HEPES buffer or PBS, then exposed to a Krebs-HEPES buffer containing L-012 (10^{-4} mol/L) in the absence (i.e. basal ROS production) or presence (stimulated ROS production) of the protein kinase C (PKC) and NADPH oxidase activator phorbol dibutyrate (PDB; 10^{-7} mol/L). The same treatments were performed in blank wells (i.e. with no cells), which served as controls for background luminescence. All treatment groups were performed in triplicates. Photon emission [relative light units (RLU)/s] was detected using the Chameleon™ luminescence detector (Hidex, model 425105, Finland) and recorded from each well for 1 s over 40 cycles. Individual data points for each group were derived from the average values of the three replicates minus the respective blank controls.

Statistical analysis

For studies that examined the effects of TLR agonists on basal ROS production, data were normalised by expressing as a percentage of the control response. These ROS data are expressed as mean ± standard error of the mean (SEM) with statistical comparisons made using the non-parametric Kruskal–Wallis one-way analysis of variance (ANOVA) test followed by Dunnets *post hoc* test. For studies that investigated the effect of TLR agonists and influenza A virus on the PDB-dependent oxidative burst, raw data were presented to display the time course of the response. For these data, statistical comparisons of the mean peak response were performed with parametric tests, including Student's unpaired t-test and one-way ANOVA followed by Tukey's *post hoc* test for multiple comparisons. All statistical tests were performed using GraphPad Prism (GraphPad Software Version 6.0, San Diego CA, USA). $P < 0.05$ was taken to indicate significance. Note, *n* is representative of a separate experiment where cells were used from a different passage upon splitting.

Drugs and their suppliers

Imiquimod (Invivogen) and poly I:C (Sigma) were dissolved in endotoxin-free water and prepared as stock solutions of 10 mM in aliquots of 30 μL and stored at −20°C. L-012 (WAKO chemicals, Japan), PDB (Sigma), and dynasore (Sigma) were dissolved in DMSO (100%) and prepared as 10 mM stock solutions in aliquots of 10, 25 and 50 μL, stored at −20°C. FBS (Sigma) was made into 50 ml aliquots and stored at −20°C. The Ser346 peptide inhibitor (Genecbio Limited) corresponding to amino acids 337–348 (RRPGRPGQLSTD-NH2) of p47phox tagged at the N-terminus to a HIV-tat based peptide (YGRKKRRQRRR) to permit membrane translocation was dissolved in distilled water at concentrations of 10 mM and stored at −20°C. The nucleoprotein antibody (AbCAM) and DAPI (Vector Laboratories) were stored at − 20°C.

Results

Internalization of influenza A virus

Immunohistochemistry was used to localise the nucleoprotein of influenza A virus in RAW264.7 cells and mouse alveolar macrophages. Influenza A virus infection for 1 h resulted in a strong punctate pattern of fluorescence using the nucleoprotein specific antibody in both RAW264.7 cells (Figure 1) and alveolar macrophages (data not shown). By contrast, there was no obvious fluorescence for nucleoprotein in the control-uninfected group (Figure 1). Addition of the dynamin inhibitor dynasore (100 μM) abolished the influenza A virus-induced increase in nucleoprotein fluorescence (Figure 1), indicating endocytosis as the primary mechanism of viral entry in macrophages. The vehicle used for dynasore [i.e. DMSO (0.1%)] had no effect on nucleoprotein fluorescence caused by influenza A virus (Figure 1).

Effect of influenza A virus on basal ROS production and the stimulated oxidative burst

Using L-012-enhanced-chemiluminescence, we examined whether X-31 influenza A virus affects both basal and PDB-stimulated superoxide production in RAW 264.7. We have previously shown that this basal and

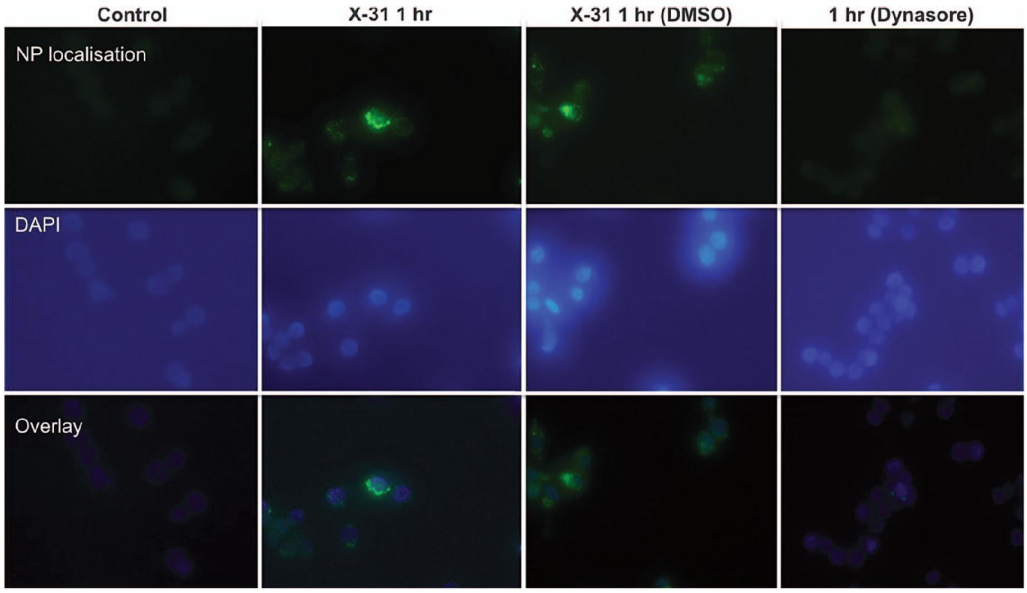

Figure 1. Influenza A virus enters macrophages *via* endocytosis. Representative immunofluorescence images using an antibody for nucleoprotein (NP; 1:1000), which is specific for IAV followed by fluorescein isothiocyanate-goat anti-mouse secondary antibody (1:1000; green fluorescence). Slides were then mounted in a 4′,6-diamidino-2-phenylindole (DAPI) containing media to stain for nuclei (blue fluorescence). The top panel of images show NP fluorescence alone, middle panel shows DAPI alone and lower panel shows merged images of the virus (NP) and nuclei (DAPI). RAW264.7 cells were either left untreated (no virus; phosphate buffered saline) or exposed to X-31 virus (MOI 10) for 1 h in the absence or presence of dynasore (100 μM). These images are representative of $n = 4$ experiments. Magnification 40×.

PDB-stimulated L-012 enhanced signal to be suppressed by addition of SOD and abolished by deletion of the *NOX2* gene (i.e. NOX2$^{-/y}$ cells) [7]. Addition of X-31 virus (MOI of 1, 3 and 10) failed to significantly alter basal superoxide production in RAW 264.7 cells (Figure 2). In the absence of virus, PDB (10^{-7} M) caused a rapid and large burst of superoxide production (Figure 2). However, the peak superoxide production to PDB was significantly ($P < 0.05$, $n = 5$) enhanced by X-31 (MOI of 10) compared to the control group (Figure 2). Lower concentrations of virus (i.e. MOI of 1 and 3) failed to enhance superoxide production to PDB (Figure 2). We also tested whether influenza A virus affects the oxidative burst of alveolar macrophages. In the absence of virus, PDB (10^{-7} M) caused a rather modest increase in superoxide production in alveolar macrophages when compared to RAW264.7 cells (Figure 2). However, like in RAW264.7 cells, X-31 influenza A virus infection at MOI 10 resulted in a significant ($P < 0.05$) enhancement in the peak superoxide response to PDB in alveolar macrophages (Figure 2).

Effect of TLR7 and TLR3 activation on the oxidative burst

We assessed whether imiquimod treatment influenced both basal and PDB-stimulated superoxide production in macrophages. Imiquimod (3 and 10 μg/ml) exposure resulted in a significant ($P < 0.05$, $n = 7$) increase (~2.5-fold; maximum response 677 ± 250 RLU/s, $n = 6$) in superoxide production compared to the untreated control (250 ± 90 RLU/s, $n = 6$) in RAW264.7 cells (Figure 3). Also, similar to what was observed with the virus, imiquimod (1 and 10 μg/ml) exposure for 1 h caused a significant ($P < 0.05$) enhancement in the subsequent PDB (10^{-7} M)-stimulated oxidative burst compared to the control (Figure 3). In parallel, a 1-h imiquimod (10 μg/ml) pre-treatment of alveolar macrophages significantly ($P < 0.05$) increased the subsequent response to PDB (10^{-7} M; Figure 3).

We investigated the effect of stimulating TLR3 with the agonist poly I:C on superoxide production. Poly I:C (50 and 100 μg/ml) significantly ($P < 0.05$) increased superoxide production (maximum 298 ± 70 RLU/s, $n = 6$) in RAW264.7 cells compared to the control (maximum 117 ± 32 RLU/s, $n = 6$) (Figure 3). However, unlike both the influenza A virus and imiquimod pre-treatment, poly I:C (3 and 100 μg/ml) exposure for 1 h did not enhance the PDB (10^{-7} M)-stimulated response compared to the control (Figure 3).

Effect of Ser346 peptide inhibitor on influenza A virus and imiquimod PDB-stimulated oxidative burst

Along with other serine residues on p47phox, phosphorylation of the Ser346 residue is crucial for activation of the fully assembled NADPH oxidase complex. Therefore, we designed a short peptide conjugated to HIV-tat to enable cell permeation, to inhibit phosphorylation of Ser346 on the p47phox subunit and priming of NOX2 oxidase by influenza A virus. This approach is analogous to that taken by Dang et al. (2006), to suppress

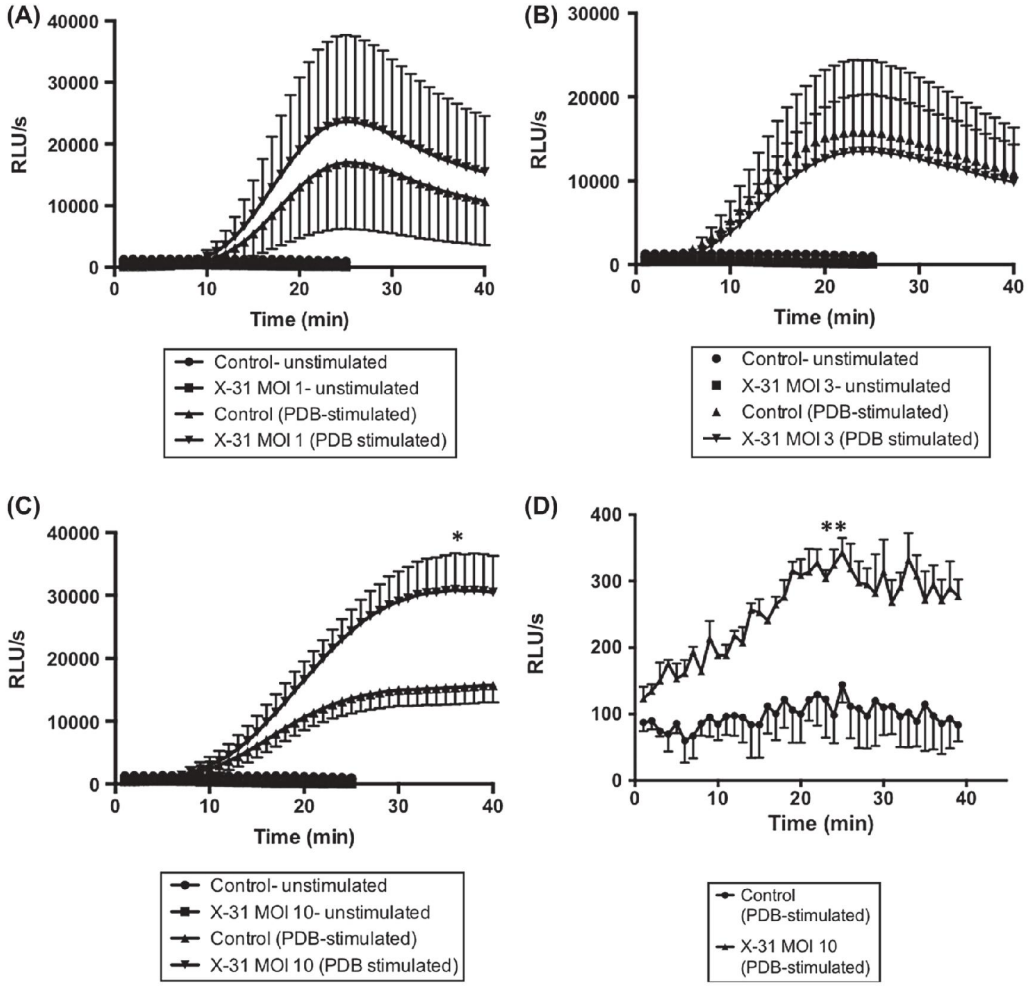

Figure 2. Influenza A virus potentiates the NOX2 oxidase-dependent superoxide generation in macrophages. Phorbol dibutyrate (PDB) (10^{-7} M)-stimulated superoxide production in the absence (no virus) or presence of X-31 IAV at the indicated MOI in (A–C) RAW264.7 cells, (D) alveolar macrophages as measured by L-012 (100 μM)-enhanced chemiluminescence. Data at each time point are the mean ± SEM in relative light units per second (RLU/s) from $n = 5$ experiments (except for d; $n = 3$). Statistical analyses were conducted using unpaired Student's t-test comparing the mean peak response of each curve of each experiment. Statistical significance was taken when the $P < 0.05$. *Indicates $P < 0.05$ and **denotes $P < 0.01$.

phosphorylation of Ser345 (human sequence) and NOX2 oxidase priming in neutrophils [20]. Addition of this Ser346 peptide (50 μM) significantly ($P < 0.05$) inhibited the enhancement of the PDB (10^{-7} M)-induced superoxide production caused by the virus (MOI 10) and imiquimod (10 μg/ml) in macrophages (Figure 4). The peptide did not affect the PDB response in the absence of the virus or imiquimod (Figure 4).

Discussion

Excessive host innate responses to influenza A virus infection characterised by an overproduction of ROS by inflammatory cells is believed to be a key contributor to the lung injury [2,4]. However, the specific type of inflammatory cell involved is largely unknown. Therefore, the present study examined whether short-term (i.e. 1 h) influenza A virus infection results in elevations in NOX2 oxidase-dependent superoxide generation in macrophages. In the first instance, using a specific antibody to detect nucleoprotein of influenza A virus the present study showed that X-31 virus enters macrophages *via* a dynamin-dependent process. This finding is consistent with previous studies showing that dynamin-dependent endocytosis was the main pathway of viral entry [21], and this appears to hold true irrespective of the genetic makeup and pathogenicity of the infecting strain. For instance, Wang and Jiang (2009) demonstrated that the highly pathogenic and lethal virus H5N1 strain also enters *via* dynamin-dependent endocytosis [22]. Mechanistically, the formation of clathrin-coated pits at viral binding sites enables the virus to target endocytic machinery, allowing internalisation of the virus into cells [23]. However, there are alternative routes whereby viruses can enter, including both clathrin- and caveolin-mediated endocytosis, as well as clathrin- and caveolin-independent pathways [21,24]. This body of evidence demonstrates the importance of endocytosis in the

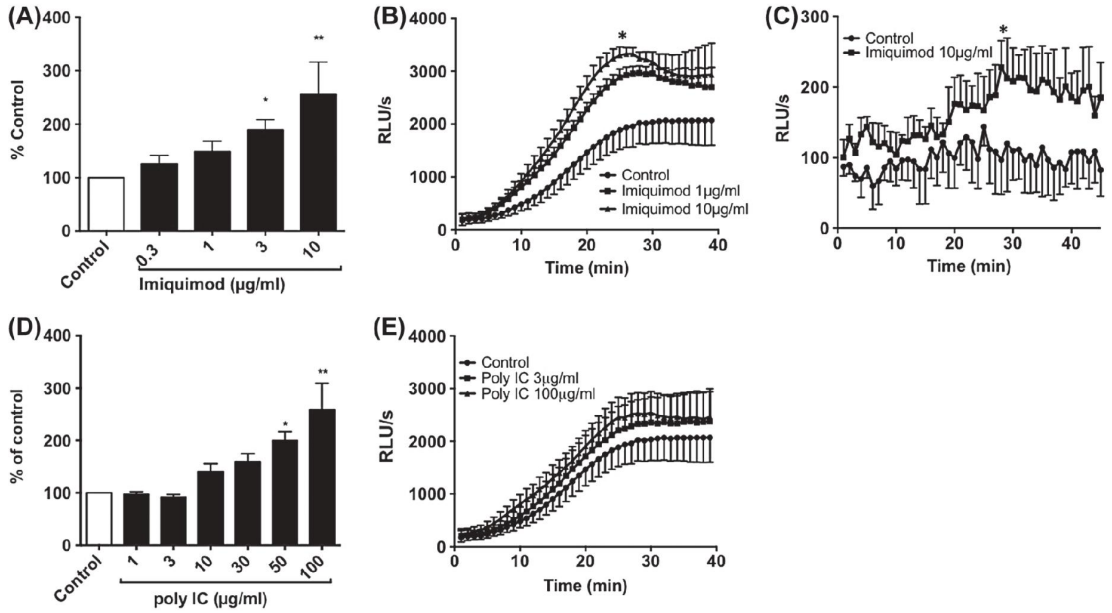

Figure 3. Effect of TLR7 and TLR3 activation on superoxide production in macrophages. Superoxide production was measured using L-012 (100 μM)-enhanced chemiluminescence in (A) RAW264.7 cells exposed to increasing concentrations of imiquimod (0.3–10 μg/ml). PDB-stimulated (10–7 M) superoxide production in (B) RAW264.7 cells and (C) alveolar macrophages in the absence (control) or presence of imiquimod (1, 10 μg/ml) for 1 h. (D) Superoxide production was measured using L-012 (100 μM)-enhanced chemiluminescence in RAW264.7 cells exposed to increasing concentrations of poly I:C (1–100 μg/ml) or a control (PBS). (E) PDB-stimulated (10^{-7} M) superoxide production in RAW264.7 cells in the absence (control; PBS) and presence of poly I:C (3, 100 μg/ml) for an hour. Data are represented as mean ± SEM of $n = 5$–10 experiments (except for c; $n = 3$). In A and D, data are expressed as a % of the control group and statistical analyses were conducted using one-way ANOVA Kruskal–Wallis test followed by Dunnets *post hoc* test for multiple comparisons. In B, C and E, the mean peak responses of each curve of each experiment were compared using unpaired Student's t-test. Statistical significance was taken when the $P < 0.05$. *Indicates $P < 0.05$ and **denotes $P < 0.01$.

progression of the influenza A virus pathway for proper viral infection.

Having established that virus becomes internalized in macrophages within 1 h, we wanted to examine whether the presence of virus resulted in alterations in ROS production. Both RAW264.7 cells and alveolar macrophages exposed to influenza A virus for 1 h displayed a significantly enhanced PDB-stimulated oxidative burst that was chiefly characterized by an exacerbated peak response. This observation is analogous to the "priming effect" seen in human neutrophils, where an initial exposure to TNF-α resulted in significantly greater superoxide production to

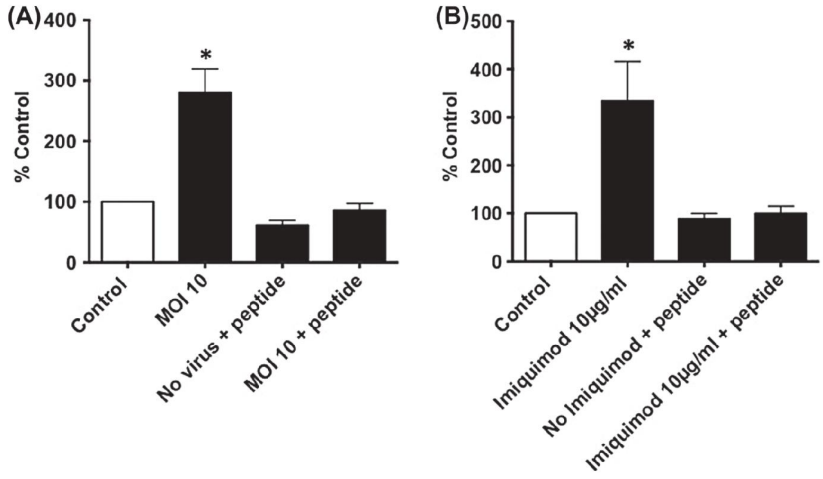

Figure 4. Ser346 peptide inhibits the influenza A virus and imiquimod-dependent enhancement in the PDB-stimulated superoxide production in macrophages. Superoxide production was measured using L-012 (100 μM)-enhanced chemiluminescence in RAW264.7 cells in the absence (control; PBS) or presence of X-31 IAV (MOI 10) or (B) imiquimod (10 μg/ml). RAW264.7 cells were exposed to the Ser346 peptide inhibitor (50 μM) for 30 min prior to being exposed to IAV and imiquimod. Data are represented as mean ± SEM for $n = 4$–5 experiments and are expressed as a % of the control group. Statistical analyses were conducted using one-way ANOVA Kruskal–Wallis test followed by Dunnets *post hoc* test for multiple comparisons. Statistical significance was taken when the $P < 0.05$. *Indicates a $P < 0.05$ and **denotes $P < 0.01$.

a second stimulus [i.e. N-formyl-methionyl-leucyl-phenylalanine (fMLF)] [25]. Such a primed state for NOX2 oxidase has been described as a "ready to go" state, which ultimately results in a higher and faster response to a second stimulus [26]. From a mechanistic point of view, several hypotheses have been proposed to explain how priming of NOX2 oxidase occurs. However, to understand this, it is important to emphasize how the regulatory subunit for NOX2 activation that is, p47phox is regulated by phosphorylation. Generally, it is widely regarded that phosphorylation of the multiple serine residues on p47phox induces conformational changes in the protein that allow it and its associated subunits, that is, p67phox and p40phox, to assemble with NOX2 to form a fully functional oxidase unit capable of superoxide generation. The effect of priming agents on p47phox phosphorylation have recently been deciphered by site-directed mutagenesis, mass spectroscopy and Western blotting, and it is believed to be due to partial phosphorylation of p47phox, in particular its serine residue at position 345 on the peptide sequence [25,27]. This partial phosphorylation status of p47phox then results in a greater increase in phosphorylation of the remaining serine residues on p47phox upon subsequent stimulation with the second stimulus and a greater superoxide response. We hypothesized that the priming effect of the virus shown in the present study may involve phosphorylation of serine346 (mouse sequence differs from human which is serine 345) on the p47phox subunit, analogous to what occurs in human neutrophils [20,25,27]. Therefore, to evaluate this, we custom designed in the same manner as Dang et al., (2006), a peptide inhibitor corresponding to amino acids 337–348 of p47phox tagged at the N-terminus to a HIV-tat based peptide (YGRKKRRQRRR) to permit membrane translocation [20]. It is expected that the peptide will compete against serine 346 of p47phox for the substrate that causes phosphorylation in response to influenza A virus. It has been shown that both extracellular signal-regulated kinases 1/2 (ERK1/2) and p38 mitogen-activated protein kinase (p38 MAPK) are responsible for phosphorylation induced by granulocyte-macrophage colony-stimulating factor (GMCSF) and TNF-α in the priming of human neutrophils [20,28]. Our study showed that this Ser346 peptide inhibitor significantly suppressed the influenza A virus-dependent enhancement in the oxidative burst in macrophages. Importantly, the peptide alone did not alter the control response, indicating it does not have non-specific effects and is most probably blocking the enhancement of the oxidative burst caused by the virus.

Endosomal TLRs, in particular TLR7 and TLR3, are considered to be targets for viral RNA, however, there appears to be some degree of selectivity in the type of RNA that they detect. For instance, there is a growing consensus that TLR7 is the main sensor for ssRNA type viruses such as influenza A virus and that by contrast, TLR3 is a sensor for double stranded RNA. Despite this, there is some evidence that appears to challenge this dogma and suggests that TLR3 does sense influenza A virus to regulate a pro-inflammatory response [29]. Therefore, we evaluated whether activation of TLR7 and TLR3 could also elicit ROS production and by implication is responsible for the superoxide production caused by influenza A virus. The present study showed the TLR7 agonist imiquimod, like influenza A virus significantly enhanced the PDB-stimulated oxidative burst, indicative of a TLR7-dependent priming effect of NOX2 oxidase. Consistent with this, Makni-Maalej et al. (2012) provided evidence that the TLR7/8 agonist CL097 primed fMLP-dependent NOX2 oxidase in human neutrophils [30]. Again, partial phosphorylation of the serine residues on the p47phox subunit appears to be the mechanism of this priming effect of TLR7 activation. Indeed, in the present study, the Ser346 peptide inhibitor blocked the imiquimod-dependent enhancement in superoxide generation in macrophages. Although our findings that TLR7 activation results in priming of NOX2 oxidase are similar to those of Makni-Maalej et al. (2012), these authors showed that TLR7 activation resulted in phosphorylation of Ser328 and Ser315 in human neutrophils, in addition to Ser 345 as opposed to Ser346 that our data would suggest to be the relevant serine. We are not ruling out Ser328 and Ser315 as additional targets to influenza A virus in macrophages, but this area warrants further investigation. In addition we found that activation of TLR3 also elicits ROS production, which is consistent with the findings of Yang et al. (2013). However, unlike both influenza A virus and imiquimod, poly I:C failed to enhance the PDB-stimulated oxidative burst. This inability of poly I:C to prime NOX2 oxidase makes TLR3 less likely to be a target for influenza A virus infection in macrophages.

We agree with previous studies that have suggested that the effect of NOX2 priming could be viewed as a "double-edged sword" [25]. Priming could promote rapid clearance of the pathogen, however, excessive and uncontrolled priming may induce the generation of large quantities of toxic ROS by hyperactivating NADPH oxidase, which can damage surrounding tissues and participate in an inflammatory reaction. The present study demonstrates for the first time that influenza A virus infection of macrophages results in an exacerbated oxidative burst. This is likely to be a consequence of TLR7 activation by the virus, although a role for TLR3 cannot be ruled out. A better understanding of the different mechanisms and transduction pathways involved in NADPH oxidase activation by influenza A virus and TLRs in the endosome is necessary. Moreover, it would be of interest to decipher whether influenza A virus infection of epithelial and endothelial cells results in similar enhancement in ROS production. Finally, these studies have shed new light into the mechanisms *via* which influenza A virus infection leads to cell and tissue injury.

Acknowledgments

The authors wish to thank the Australian Research Council for fellowship and funding support (FT120100876) for Dr Stavros Selemidis and the National Health and Medical Research Council of Australia for funding

support (APP1027112). Also the authors wish to thank Dr John Stambas for providing stocks of X-31 influenza A virus.

Declaration of interest

The authors report no declarations of interest. The authors alone are responsible for the content and writing of the paper.

References

[1] La Gruta NL, Kedzierska K, Stambas J, Doherty PC. A question of self-preservation: immunopathology in influenza virus infection. Immunol Cell Biol 2007;85:85–92.

[2] Vlahos R, Stambas J, Selemidis S. Suppressing production of reactive oxygen species (ROS) for influenza A virus therapy. Trends Pharmacol Sci 2012;33:3–8.

[3] Akaike T, Noguchi Y, Ijiri S, Setoguchi K, Suga M, Zheng YM, et al. Pathogenesis of influenza virus-induced pneumonia: involvement of both nitric oxide and oxygen radicals. Proc Natl Acad Sci U S A 1996;93:2448–2453.

[4] Imai Y, Kuba K, Neely GG, Yaghubian-Malhami R, Perkmann T, van Loo G, et al.. Identification of oxidative stress and toll-like receptor 4 signaling as a key pathway of acute lung injury. Cell 2008;133:235–249.

[5] Kash JC, Xiao Y, Davis AS, Walters KA, Chertow DS, Easterbrook JD, et al. Treatment with the reactive oxygen species scavenger EUK-207 reduces lung damage and increases survival during 1918 influenza virus infection in mice. Free Radic Biol Med 2014;67:235–247.

[6] Lee YH, Lai CL, Hsieh SH, Shieh CC, Huang LM, Wu-Hsieh BA. Influenza A virus induction of oxidative stress and MMP-9 is associated with severe lung pathology in a mouse model. Virus Res 2013;178:411–422.

[7] Vlahos R, Stambas J, Bozinovski S, Broughton BRS, Drummond GR, Selemidis S. Inhibition of Nox2 oxidase activity ameliorates influenza a virus-induced lung inflammation. PLoS Pathog 2011;7:e 1001271.

[8] Yatmaz S, Seow HJ, Gualano RC, Wong ZX, Stambas J, Selemidis S, et al. Glutathione Peroxidase-1 (GPx-1) reduces Influenza A virus-induced lung inflammation. Am J Respir Cell Mol Biol 2013;48:17–26.

[9] Bedard K, Krause KH. The NOX family of ROS-generating NADPH oxidases: physiology and pathophysiology. Physiol Rev 2007;87:245–313.

[10] Drummond GR, Selemidis S, Griendling KK, Sobey CG. Combating oxidative stress in vascular disease: NADPH oxidases as therapeutic targets. Nat Rev Drug Discov 2011;10: 453–471.

[11] Selemidis S, Sobey CG, Wingler K, Schmidt HH, Drummond GR. NADPH oxidases in the vasculature: molecular features, roles in disease and pharmacological inhibition. Pharmacol Ther 2008;120:254–291.

[12] Harrison CB, Selemidis S, Guida E, King PT, Sobey CG, Drummond GR. NOX2beta: a novel splice variant of NOX2 that regulates NADPH oxidase activity in macrophages. PLoS One 2012;7:e48326.

[13] Groemping Y, Lapouge K, Smerdon SJ, Rittinger K. Molecular basis of phosphorylation-induced activation of the NADPH oxidase. Cell 2003;113:343–355.

[14] Snelgrove RJ, Edwards L, Rae AJ, Hussell T. An absence of reactive oxygen species improves the resolution of lung influenza infection. Eur J Immunol 2006;36:1364–1373.

[15] Casanova JL, Abel L, Quintana-Murci L. Human TLRs and IL-1Rs in host defense: natural insights from evolutionary, epidemiological, and clinical genetics. Annu Rev Immunol 2011;29:447–491.

[16] Liew FY, Xu D, Brint EK, O'Neill LAJ. Negative regulation of toll-like receptor-mediated immune responses. Nat Rev Immunol 2005;5:446–458.

[17] Diebold SS, Kaisho T, Hemmi H, Akira S, Reis e Sousa C. Innate antiviral responses by means of TLR7-mediated recognition of single-stranded RNA. Science 2004;303:1529–1531.

[18] Muzio M, Bosisio D, Polentarutti N, D'Amico G, Stoppacciaro A, Mancinelli R, et al. Differential expression and regulation of toll-like receptors (TLR) in human leukocytes: selective expression of TLR3 in dendritic cells. J Immunol 2000;164:5998–6004.

[19] Yang CS, Kim JJ, Lee SJ, Hwang JH, Lee CH, Lee MS, Jo EK. TLR3-triggered reactive oxygen species contribute to inflammatory responses by activating signal transducer and activator of transcription-1. J Immunol 2013;190:6368–6377.

[20] Dang PMC, Stensballe A, Boussetta T, Raad H, Dewas C, Kroviarski Y, et al. A specific p47phox-serine phosphorylated by convergent MAPKs mediates neutrophil NADPH oxidase priming at inflammatory sites. J Clin Invest 2006;116: 2033–2043.

[21] de Vries E, Tscherne DM, Wienholts MJ, Cobos-Jiménez V, Scholte F, García-Sastre A, et al. Dissection of the influenza A virus endocytic routes reveals macropinocytosis as an alternative entry pathway. PLoS Pathog 2011;7:e1001329.

[22] Wang H, Jiang C. Influenza A virus H5N1 entry into host cells is through clathrin-dependent endocytosis. Sci China C Life Sci 2009;52:464–469.

[23] Rust MJ, Lakadamyali M, Zhang F, Zhuang X. Assembly of endocytic machinery around individual influenza viruses during viral entry. Nat Struct Mol Biol 2004;11:567–573.

[24] Sieczkarski SB, Whittaker GR. Influenza virus can enter and infect cells in the absence of clathrin-mediated endocytosis. J Virol 2002;76:10455–10464.

[25] El-Benna J, Dang PMC, Gougerot-Pocidalo MA. Priming of the neutrophil NADPH oxidase activation: role of p47phox phosphorylation and NOX2 mobilization to the plasma membrane. Semin Immunopathol 2008;30:279–289.

[26] Clark RA, Volpp BD, Leidal KG, Nauseef WM. Two cytosolic components of the human neutrophil respiratory burst oxidase translocate to the plasma membrane during cell activation. J Clin Invest 1990;85:714–721.

[27] Sheppard FR, Kelher MR, Moore EE, McLaughlin NJD, Banerjee A, Silliman CC. Structural organization of the neutrophil NADPH oxidase: phosphorylation and translocation during priming and activation. J Leukoc Biol 2005;78: 1025–1042.

[28] Dewas C, Dang PMC, Gougerot-Pocidalo MA, El-Benna J. TNF-α induces phosphorylation of p47phox in human neutrophils: partial phosphorylation of p47phox is a common event of priming of human neutrophils by TNF-α and granulocyte-macrophage colony-stimulating factor. J Immunol 2003;171:4392–4398.

[29] Le Goffic R, Pothlichet J, Vitour D, Fujita T, Meurs E, Chignard M, Si-Tahar M. Cutting edge: Influenza A virus activates TLR3-dependent inflammatory and RIG-I-dependent antiviral responses in human lung epithelial cells. J Immunol 2007;178:3368–3372.

[30] Makni-Maalej K, Boussetta T, Hurtado-Nedelec M, Belambri SA, Gougerot-Pocidalo MA, El-Benna J. The TLR7/8 agonist CL097 primes N-formyl-methionyl-leucyl-phenylalanine- stimulated NADPH oxidase activation in human neutrophils: critical role of p47phox phosphorylation and the proline isomerase Pin1. J Immunol 2012;189: 4657–4665.

Chapter 3:
Endosomal NOX2 oxidase exacerbates virus pathogenicity and is a target for antiviral therapy

Declaration for Thesis Chapter 3- *Endosomal NOX2 oxidase exacerbates virus pathogenicity and is a target for antiviral therapy*

Declaration by candidate

In the case of Chapter 3 the nature and extent of my contribution to the work was as follows:

Nature of contribution	**Extent of contribution (%)**
Intellectual input into the design of experiments, performed all experiments (infections and treatments of animals), tissue collection, QPCR, ELISA, cell culture, transfections, L-012 enhanced chemiluminsence, western blot, confocal microscopy, antibody determination with the exception of site-directed mutagenesis and high-content ratiometric FRET imaging; analysed results, prepared figures and wrote the manuscript	85 %

The following co-authors have contributed to this study. If co-authors are students at Monash University, the extent of their contribution must be stated:

Name	**Nature of contribution**	**Extent of contribution (%)**
Raymond Luong	Performed and assisted the candidate with experiments	10 %
Christopher Chan	Assisted the candidate with experiments	1 %
Michelle L Halls	Performed the site-directed mutagenesis and high-content ratiometric FRET imaging assays	N/A
Tim Quach	Synthesised peptides for use in experiments	N/A

Patrick C Reading Paul T King Grant Drummond Brad RS Broughton Malcolm R Starkey Ross Vlahos Steven Bozinovski Renee van der Sluis Sharon R Lewin Christopher JH Porter Doug A Brooks John J O'Leary	Provided materials and/or intellectual advice during experimental and manuscript preparation	N/A
Stavros Selemidis	Intellectual input into the design of experiments, preparation of manuscript, management of the project and provided funding to support the project	N/A

The undersigned hereby certify that the above declaration correctly reflects the nature and extent of candidate's and co-authors' contribution to this work.

Candidates signature: Date: 17-02-2017

Main supervisor's signature: [redacted] Date: 17-02-2017

[Accepted for publication in Nature Communications on the 30/3/2017]

ARTICLE

Endosomal NOX2 oxidase exacerbates virus pathogenicity and is a target for antiviral therapy

Eunice E. To[1], Ross Vlahos[2], Raymond Luong[1], Michelle L. Halls[3], Patrick C. Reading[4], Paul T. King[5], Christopher Chan[1], Grant R. Drummond[1], Christopher G. Sobey[1], Brad R.S. Broughton[1], Malcolm R. Starkey[6], Renee van der Sluis[7], Sharon R. Lewin[7,8], Steven Bozinovski[2], Luke A.J. O'Neill[9], Tim Quach[10,11], Christopher J.H. Porter[10,12], Doug A. Brooks[13], John J. O'Leary[14,15] and Stavros Selemidis[1]

1 Department of Pharmacology, Infection and Immunity Program, Biomedicine Discovery Institute, Monash University, Clayton, Victoria, Australia, 3800.

2 School of Health Sciences and Health Innovations Research Institute, RMIT University, Bundoora, Victoria, Australia, 3083.

3 Drug Discovery Biology, Monash Institute of Pharmaceutical Sciences, Monash University, Parkville, Victoria, Australia, 3052.

4 Department of Microbiology and Immunology, The University of Melbourne, The Peter Doherty Institute for Infection and Immunity, Melbourne, Victoria, Australia, 3000.

5 Department of Medicine, Monash Medical Centre, Monash University, Clayton, Victoria, Australia, 3168.

6 Priority Research Centre's Grow Up Well and Lung Health, School of Biomedical Sciences and Pharmacy, Faculty of Health and Medicine, The University of Newcastle, and Hunter Medical research Institute, New South Wales, Australia, 2305.

7 The Peter Doherty Institute for Infection and Immunity, Melbourne, Victoria, Australia, 3000.

8 Department of Infectious Diseases, Alfred Hospital and Monash University, Melbourne, Australia 3004.

9 School of Biochemistry and Immunology, Trinity Biomedical Sciences Institute, Trinity College Dublin, Dublin 2, Ireland.

10 ARC Centre of Excellence in Convergent Bio-Nano Science and Technology, Monash Institute of Pharmaceutical Sciences, Monash University, Parkville, Victoria, Australia, 3052.

11 Medicinal Chemistry, Monash Institute of Pharmaceutical Sciences, Monash University, Parkville, Victoria, Australia, 3052.

12 Drug Delivery Disposition and Dynamics, Monash Institute of Pharmaceutical Sciences, Monash University, Parkville, Victoria, Australia, 3052.

13 School of Pharmacy and Medical Sciences, Sansom Institute for Health Research, Division of Health Sciences, University of South Australia, Australia, 5001.

14 Department of Histopathology Trinity College Dublin, Ireland, Sir Patrick Dun's Laboratory, Central Pathology Laboratory, St James's Hospital, Dublin 8, Ireland.

15 Molecular Pathology Laboratory, Coombe Women and Infants' University Hospital, Dublin 8, Ireland.

Author for Correspondence:

Dr Stavros Selemidis

Oxidant and Inflammation Biology Group, Department of Pharmacology, Infection and Immunity Program, Biomedicine Discovery Institute, Monash University, Clayton, Victoria, Australia, 3800.

Tel: 613 9905 5756

Email: Stavros.selemidis@monash.edu

ABSTRACT

Viral pandemics pose an imminent global health threat, and with emerging anti-viral resistance and delays in vaccine development, there is an urgent need for novel therapeutic approaches to target viral-cell-immune interactions, irrespective of the infecting strain. Reactive oxygen species (ROS) evolved ~1.5 billion years ago in eukaryotes and are ancient processes that protect plants, fungi and animals against invading pathogens such as bacteria. However, in mammals ROS production by inflammatory cells paradoxically promotes virus pathogenicity by mechanisms not yet defined. Here we identify that the primary enzymatic source of ROS, NOX2 oxidase, is activated after the internalization of single stranded RNA and DNA viruses into endocytic compartments. Activation of endosomal NOX2 results in the spatially targeted generation of hydrogen peroxide, which suppresses key antiviral and humoral signaling networks *via* modification of a unique, highly conserved cysteine residue (Cys98) on the ectodomain of the Toll-like receptor-7. Accordingly, targeted inhibition of endosomal ROS production abrogates influenza A virus pathogenicity. We conclude that endosomal ROS are essential mediators of a fundamental molecular mechanism of viral pathogenicity, which involves suppression of RNA immunity. Specific targeting of this pathogenic process with endosomal targeted ROS inhibitors has major implications for the treatment of globally devastating viruses.

INTRODUCTION

The production of reactive oxygen species (ROS) is a highly coordinated process achieved by enzymes of the NADPH oxidase (NOX) family. NOX enzymes are not present in prokaryotes but evolved in single cell eukaroytes and are present in most eukaryotic groups including amoeba, fungi, algae and plants, nemotodes, echinoderms, urochordates, insects, fish, reptiles and mammals (Aguirre *et al.*, 2010; Kawahara *et al.*, 2007). The functions of NADPH oxidases within eukaryotes are diverse, however, a common functional theme is the generation of ROS by innate immune cells in response to pathogen attack. Indeed, orthologs of NADPH oxidase in plants *(ArtbohD and ArtbohF)*, fungi (*NOXA/B*), and invertebrates *C-elegans (*Duox orthologs), *Drosophila melongaster (NOX5 homolog, d-NOX and DUOX*) and mosquito *aedes aegypti (NOXM and DUOX)* generate ROS with bactericidal activity that protects the host (Aguirre *et al.*, 2010; Kawahara *et al.*, 2007). Vertebrates including teleosts, amphibians, birds and mammals possess a NOX2 NADPH oxidase that generates a burst of ROS within phagosomes to kill invading pathogens especially bacteria. However, the impact of ROS on virus infection is largely unknown.

ROS, such as superoxide anion and hydrogen peroxide (H_2O_2), are produced by mouse and human inflammatory cells in response to viral infection and ROS production and enhance the

pathology caused by viruses of low to high pathogenicity, including influenza A (Imai *et al.*, 2008a; Snelgrove *et al.*, 2006a; To *et al.*, 2014; Vlahos *et al.*, 2014; Vlahos *et al.*, 2011a; Vlahos *et al.*, 2012a). The primary source of inflammatory cell ROS is the NOX2 oxidase enzyme (Bedard *et al.*, 2007b; Drummond *et al.*, 2011b; Selemidis *et al.*, 2008; Vlahos *et al.*, 2014). Although NOX2 oxidase plays a role in the killing of bacteria and fungi *via* phagosomal ROS production, NOX2 oxidase does not appear to eliminate viruses in a manner analogous to that for bacteria. In fact, in the absence of NOX2, influenza A virus causes substantially less lung injury and dysfunction, and leads to lower viral burden suggesting that NOX2 oxidase-derived ROS *promotes* rather than inhibits viral infection (Imai *et al.*, 2008a; Snelgrove *et al.*, 2006a; To *et al.*, 2014; Vlahos *et al.*, 2014; Vlahos *et al.*, 2011a; Vlahos *et al.*, 2012a). However, it remains unknown how viruses cause ROS production and how these highly reactive oxygen molecules, which appear to be largely confined to their site of generation, contribute to disease.

After binding to the plasma membrane (Cossart *et al.*, 2014), viruses enter cells and ultimately endosomes by a variety of mechanisms resulting in viral RNA detection by endosomal pattern recognition receptors, including toll-like receptor 3 (TLR3), TLR7 and TLR9 (Iwasaki *et al.*, 2014). The specific receptor interaction depends upon either the Group (I to V) or genomic orientation (i.e. ssRNA, dsRNA or DNA) of the virus and triggers an immune response characterised by Type I IFN and IL-1β production, and B-cell dependent antibody production (Iwasaki *et al.*, 2014). Host nucleic acids and self-antigens are also detected by endosomal TLRs, and in autoimmune disease, mediate similar Type I IFN responses and stimulate antibody production against self-RNA and antigen. Notably, mice that are chronically deficient in NOX2 oxidase have an increased tendency to develop self-antibodies (Campbell *et al.*, 2012) and patients with chronic granulomatous disease, who have a defective capacity to generate ROS *via* the NOX2 oxidase, have elevated circulating Type I IFNs and autoantibodies (Kelkka *et al.*, 2014). These observations are supportive of the notion that low levels of ROS result in an enhanced immune response. However, it remains unknown how ROS modulates inflammation and the pathology caused by viruses and whether targeted (and acute) abrogation of ROS may actually be beneficial in treating viral infection. Here we hypothesise firstly, that the internalization of virus into endosomes results in ROS production and that this subdues essential immune pathways that would otherwise clear the virus; and secondly that the targeted inhibition of endosomal ROS markedly reduces viral pathogenicity. The identification of a mechanism to explain the paradoxical effect of ROS on viruses versus other pathogens such as bacteria has the potential to facilitate the development of specific endosome-targeted antiviral therapies.

RESULTS

Influenza viruses drive endosomal ROS

To address the potential role of endosomal ROS production in virus pathology we first focussed on influenza A viruses, which belong to the Group IV negative sense, ssRNA viruses of the *Orthomyxoviridae* family and are internalized by endocytosis. Exposure of mouse alveolar macrophages (AMs), mouse peritoneal RAW264.7 cells or bone marrow-derived macrophages (BMMs) to influenza A virus strain HKx31 (H3N2) resulted in a dose and time-dependent increase in influenza nucleoprotein (NP) fluorescence (Supplementary Fig. 1a), which was almost abolished by the dynamin inhibitor, Dynasore (100 μM) indicating a clathrin-coated pit or caveolin-dependent mechanism of internalization (Supplementary Fig. 1b). Internalised virus displayed a strong co-location with the early endosomal marker EEA1 (Fig. 1a). However, not all of the NP was co-located with EEA1 indicating that influenza A virus was not present exclusively in early endosomes (Fig. 1a) and might have already entered late endosomes and/or lysosomes. NOX2 co-located with EEA1 in control and influenza infected cells (Fig. 1b, Supplementary Fig. 1c). Thus, the enzymatic machinery for ROS generation is present in early endosomes and this is significantly enhanced in influenza A virus infection, promoting co-localisation with internalized virus.

Endosomal ROS production in response to viral uptake was assessed with OxyBURST (Li *et al.*, 2006a). Exposure to a series of low to high pathogenic seasonal and pandemic influenza A viruses resulted in rapid and dose-dependent increases in OxyBURST fluorescence in mouse primary AMs (Fig. 1 c,d and Supplementary Fig. 2 a,b,e,f), RAW264.7 cells (data not shown), BMMs (data not shown) and human alveolar macrophages (Fig. 1h). This OxyBURST-derived signal was abolished by addition of superoxide dismutase (SOD; 300 U/mL), which internalizes into the endosome along with the virus (Chu *et al.*, 2006) and converts superoxide to H_2O_2 (Fig. 1e,f). In contrast the ROS signal was significantly increased in AMs from mice deficient in endosomal SOD ($SOD3^{-/-}$ mice), establishing the detection of a superoxide derivative (Supplementary Fig. 2 c,d). For confirmation that ROS production occurred in acidified endosomes we demonstrated a co-location of OxyBURST fluorescence with Lysotracker in the presence of influenza virus (Fig. 1g). Inhibition of the vacuolar V-ATPase pump with bafilomycin A (100 nM), and thus inhibition of endosomal acidification, abolished the Lysotracker fluorescence and endosomal ROS production in response to influenza A virus infection (Fig. 1g). Endosomal ROS was minimal in $NOX2^{-/y}$ alveolar macrophages, but was unaffected in $NOX4^{-/-}$ macrophages and in macrophages treated with the NOX1 inhibitor ML171 (100 nM) (Fig. 1e,f and Supplementary Fig. 2h,i). Internalization of influenza A virus into AMs was not impaired in $NOX2^{-/y}$ cells (Supplementary Fig. 2g), indicating that reduced endosomal ROS production was not due to reduced viral entry. In addition, heat- and UV-inactivated forms of influenza

(replication-deficient) caused an increase in endosomal ROS production that was similar to the live virus control (Fig. 1i,j). Therefore, influenza A viruses, irrespective of subtype, strain and pathogenicity, stimulate NOX2, but not NOX4 or NOX1 oxidase-dependent ROS production in endosomes, and this involves endosomal acidification, but does not require viral replication.

Endosome TLR7-NOX2 signaling axis

RNA viruses are recognized by endosomal TLR7 (for ssRNA viruses) (Diebold *et al.*, 2004; Lund *et al.*, 2004b) and TLR3 (dsRNA viruses), as well as the cytosolic sensors retinoic acid inducible gene I (RIG-I) (which can detect viral RNA bearing 5' triphosphates [18] and NOD-like receptors (NLRs) (Iwasaki *et al.*, 2014)·(Allen *et al.*, 2009a; Ichinohe *et al.*, 2009b). We hypothesized that influenza A virus entry into acidified endosomes results in the liberation of viral RNA, activation of TLR7 and stimulation of NOX2 oxidase-dependent ROS production. Consistent with this suggestion, TLR7 co-locates with influenza A virus (Fig. 2a), NOX2 (Fig. 2b) and EEA1 (Fig. 2c and Supplementary Fig. 3a) and primary AMs from TLR7$^{-/-}$ mice, and TLR7- and MyD88-deficient BMDM, display minimal endosomal ROS production in response to influenza A virus (Fig. 2d, and Supplementary Fig. 3 b-e). The lack of endosomal ROS production in response to virus in TLR7$^{-/-}$ and MyD88$^{-/-}$ cells was not due to a reduced capacity of the NOX2 oxidase *per se*, as NOX2 activation by the PKC activator phorbol dibutyrate (PDB; 10^{-6}M) was similar in these cells and WT control cells (Supplementary Fig. 3c). Moreover, the expression of NOX2 was unaffected in TLR7$^{-/-}$ cells (data not shown). As a second measure of NOX2 oxidase activity, we assessed enzyme assembly by examining the degree of association of the NOX2 catalytic subunit with the p47^{phox} regulatory subunit. In unstimulated cells, there was very little co-localization of NOX2 and p47^{phox} (Fig. 2e). However, influenza virus caused strong co-location of NOX2 and p47^{phox}, which was reduced by Dynasore or bafilomycin A pre-treatment, and almost abolished in TLR7$^{-/-}$ cells (Fig. 2e). To provide further evidence that the activation of TLR7 leads to endosomal ROS production, we used the specific TLR7 agonist, imiquimod (10 μg/mL). Imiquimod markedly increased endosomal ROS in AMs from human and WT mice, but not from NOX2$^{-/y}$ mice (Fig. 2f) or macrophages deficient in TLR7 or MyD88 (Supplementary Fig. 3b). Finally, we pulsed AMs or RAW264.7 cells with a guanidine- and uridine-rich ssRNA sequence (ssRNA40; 100 μM). In concentrations capable of increasing IL-1β, IL-6 and TNF-α mRNA *via* a TLR7-dependent mechanism (Supplementary Fig. 4), ssRNA40 caused elevated endosomal ROS production (Fig. 2g). In contrast, endosomal ROS production in response to influenza virus was preserved in RIG-I$^{-/-}$, NLRP3$^{-/-}$, TLR2$^{-/-}$ and TLR4$^{-/-}$ macrophages and in macrophages treated with the TLR3 inhibitor (50 μM) (Supplementary Fig. 3d-h).

We subsequently examined how TLR7 elicits the assembly and activation of endosomal NOX2 oxidase. NOX2 oxidase can be activated by protein kinase C, which triggers robust phosphorylation of key serine residues on $p47^{phox}$, resulting in a NOX2 oxidase-dependent oxidative burst (Drummond *et al.*, 2011b). To define the spatiotemporal regulation of PKC signalling and to assess its regulation by TLR7, we expressed the FRET biosensor cytoCKAR, to detect cytosolic PKC (Halls *et al.*, 2015; Jensen *et al.*, 2014; Violin *et al.*, 2003) in WT and $TLR7^{-/-}$ macrophages. The treatment of WT macrophages with influenza A virus or imiquimod elevated cytosolic PKC activity within 5 min, but this response was absent in $TLR7^{-/-}$ macrophages and in WT macrophages treated with Dynasore or bafilomycin A (Fig. 2h,i). A FRET biosensor method for cytosolic pERK1/2 activity [21,24] showed that both influenza virus and imiquimod increased cytosolic pERK1/2 in a TLR7-dependent manner. In contrast, blocking pERK1/2 with PD98059 (30 μM) did not influence endosomal ROS production (Supplementary Fig. 5a,b) or the association of NOX2 with $p47^{phox}$ in response to influenza (data not shown). These data indicate that influenza A virus increases endosomal NOX2 oxidase activity *via* TLR7 and the downstream activation of PKC but not *via* pERK1/2.

We conclude that virus infection triggers a NOX2 oxidase-dependent production of ROS in endosomes using a process that is dependent on low pH. Indeed this conclusion is supported by the following experimental evidence. First it is known that reduced endosome acidification impairs the activation of TLR7 by viral RNA (Diebold *et al.*, 2004; Lund *et al.*, 2004b). Our study is in agreement with this finding, showing that NOX2 dependent ROS production to virus infection and to the TLR7 agonist imiquimod was abolished in $TLR7^{-/-}$ cells and also by pretreatment with bafilomycin A. Second, bafilomycin A suppressed PKC activation due to influenza virus and imiquimod treatment, and PKC is upstream of acute NOX2 activation (Bedard *et al.*, 2007; Drummond *et al.*, 2011). Third, bafilomycin A suppressed the association of p47phox-NOX2, which is a critical step for NOX2 assembly and activation.

Viral strain independence of endosomal ROS

Exposure of macrophages to rhinovirus *(picornaviridae, Group IV),* respiratory syncytial virus (*paramyxoviridae, Group V*), human parainfluenza virus (*paramyxoviridae, Group V*), human metapneumovirus (*paramyxoviridae, Group V*), Sendai virus (*paramyxoviridae, Group V*), Dengue virus (*flavoviridae Group IV*), or HIV (*retroviridae*, Group VI, ssRNA-RT virus) resulted in a significant elevation of endosomal ROS that was markedly suppressed in $TLR7^{-/-}$ macrophages, but unaffected in $TLR9^{-/-}$ cells (Fig. 3a,b). Both mumps virus (*paramyxoviridae Group V*) and Newcastle disease virus (NDV, *paramyxoviridae Group V*) failed to generate significant endosomal ROS (Fig. 3a,b), and it is noteworthy that these viruses primarily enter

cells by a cell membrane fusion process and not *via* endocytosis. Rotavirus (rhesus monkey strain or bovine UK strain, (*reoviridae Group III*)) exposure of macrophages also failed to generate endosomal ROS (Fig. 3a,b). The DNA viruses Herpes simplex virus 2 *(herpesviridae, Group I)* and vaccinia virus *(poxyviridae, Group I)* each caused an elevation in endosomal ROS in WT macrophages and TLR7$^{-/-}$ macrophages, but not in TLR9$^{-/-}$ macrophages (Fig. 3a,b). We conclude that the specific recognition of either ssRNA viruses by TLR7, or DNA viruses by TLR9, leads to a NOX2 oxidase-dependent burst of endosomal ROS.

Bacteria and viruses activate distinct ROS pathways

Plasma membrane TLRs, especially TLR1, TLR2 and TLR4, and not those present within endosomes (such as TLR7), sense bacteria resulting in the recruitment of mitochondria to macrophage phagosomes and mitochondrial dependent ROS production (West *et al.*, 2011). However, the stimulation of endosomal TLRs failed to augment mitochondrial ROS (West *et al.*, 2011). We confirmed that TLR7 activation with imiquimod, which caused a significant elevation in endosomal ROS (Fig. 2f), failed to increase macrophage mitochondrial superoxide production (Supplementary Fig. 3i). We examined the production of phagosomal ROS in response to the gram-positive bacteria *Streptococcus pneumoniae* (SP) or gram-negative *non-typeable Haemophilus influenzae* (NTHI). Both SP and NTHI caused ROS production in WT mouse macrophages (Fig. 3c), which was significantly enhanced in SOD3$^{-/-}$ cells (data not shown), but unaffected in TLR7$^{-/-}$ macrophages (Fig. 3c). Thus, endosomal ROS production is not a characteristic of endocytosis *per se,* but a '*pathogen (cargo)-specific*' response. ROS produced for antibacterial purposes involves an obligatory role of mitochondria, which serves as a central hub to promote innate immune signalling. By contrast, ssRNA viruses do not employ these antibacterial ROS generating pathways.

Endosomal H_2O_2 suppresses TLR7 immunity

To establish the functional importance of endosomal ROS, we assessed the impact of NOX2 inhibition on the production of cytokines that are endosome TLR7-dependent and thus relevant to virus pathogenicity (Diebold *et al.*, 2004). We first confirmed an endosome- and TLR7-dependent signal by showing that imiquimod caused a significant elevation in IFN-β, IL-1β, TNF-α and IL-6 expression in WT macrophages, but not in TLR7$^{-/-}$ macrophages (Fig. 4a) or in macrophages treated with bafilomycin A (100 nM) (Fig. 4b). Second, pre-treatment with the NOX2 oxidase inhibitor and H_2O_2 scavenger, apocynin (300 μM) significantly enhanced IFN-β, IL-1β, TNF-α and IL-6 expression in response to imiquimod, in WT macrophages but not in TLR7$^{-/-}$ macrophages, indicating that the suppressive effect of NOX2 oxidase-derived ROS on cytokine expression is dependent on TLR7 (Fig. 4a). In contrast, IFN-β, IL-1β, TNF-α and IL-6

expression in response to the TLR3 agonist, poly I:C (25 μg/mL), was suppressed by apocynin pre-treatment (Supplementary Fig. 6a) whereas increases in these same cytokines triggered by the TLR9 agonist CpG (10 μg/mL), were unaffected by apocynin (Supplementary Fig. 6b). We further tested whether NOX2 oxidase influences TLR7 immunity *in vivo.* WT and NOX2$^{-/y}$ mice were treated with a single dose of imiquimod (50 μg/mouse, intranasally) for measurements of lung IFN-β, IL-1β and IL-6 after 24 h. This time point was chosen to reflect early phases of RNA infection. There were no discernible alterations in airway inflammation in response to imiquimod (Supplementary Fig. 4c), however, imiquimod treatment resulted in elevated levels of IFN-β, IL-1β, IL-6 and TNF-α in NOX2$^{-/y}$ mice (Fig. 4d).

We sought to establish how endosomal NOX2 oxidase activity results in the suppression of TLR7-dependent responses and hypothesized that the parent species superoxide and its immediate downstream product, H_2O_2 are culprit mediators. Inactivation of superoxide by SOD failed to influence either basal or imiquimod-stimulated expression of IFN-β, IL-1β, TNF-α and IL-6, suggesting little role for superoxide *itself* in modulating TLR7 responses (Supplementary Fig. 7). To examine H_2O_2, we utilized catalase to inactivate the H_2O_2 generated within endosomes. We found that within 30 min, exposure to a FITC-labelled catalase resulted in co-localisation with LysoTracker, confirming internalization into acidified endosomal compartments (Fig. 4e). A 1hr "pulse" exposure to catalase (1000 U/mL) resulted in significant elevations in IFN-β and IL-1β expression after 24h in WT macrophages, but not in TLR7$^{-/-}$ macrophages (Fig. 4f). Moreover, imiquimod-dependent responses were significantly increased in the presence of catalase (Fig. 4g). The catalase-dependent increase in cytokines was significantly suppressed in WT macrophages treated with Dynasore (Fig. 4h) but unaffected in TLR2$^{-/-}$ macrophages (Supplementary Fig. 8a). The translocation of TLR7 to endosomes is governed by the actions of the chaperone protein, UNCB93. Indeed in the absence of UNCB93 there are substantial signalling defects due to the failure of the nucleotide-sensing TLRs to reach the endolysosomes, where they initiate MyD88/TRIF-dependent signalling pathways. In UNCB93$^{-/-}$ cells, the increase in cytokines to catalase treatment was significantly smaller than that observed in WT cells (Supplementary Fig. 8b). Thus, the suppressive actions of H_2O_2 are most likely occurring when TLR7 is located within the endosomal compartment. Catalase had no effect on TLR7, TREML4 or NLRP3 expression indicating that H_2O_2 does not modulate the expression of TLR7, a positive regulator of TLR7 activity (i.e. TREML4 (Ramirez-Ortiz *et al.*, 2015)) or NLRP3 that drives similar anti-viral cytokines to TLR7 (Supplementary Fig. 8c-f). Therefore the effect of H_2O_2 is likely to be post-translational. We then examined whether endosomal NOX2 oxidase-derived H_2O_2 influences TLR7 responses *in vivo.* We administered catalase (1000 U/mouse) intranasally to WT mice and showed a 3 to 4 fold increase in lung IFN-β, IL-1β, TNF-α and IL-6 after 24 h and this occurred prior to overt airway inflammation (Fig. 4i,j).

We questioned whether H_2O_2 released by endosomal NOX2 oxidase targets cysteine residues on protein domains of TLR7 that regulate receptor activity and are exposed upon activation within endosomal compartments (Kanno *et al.*, 2013a). These include Cys260, Cys263, Cys270 and Cys273 within the leucine repeat region as well as two additional cysteines, Cys98 and Cys445 that are unique to TLR7 (Supplementary Fig. 9-11). We performed site-directed mutagenesis to create a series of TLR7 mutants including 1) a mutant with all six of these cysteine residues replaced with alanine, 2) mutants with a dual mutation of Cys98 and Cys445 ($TLR7^{C98A/C445A}$) and 3) single mutations of Cys98 ($TLR7^{C98A}$) and Cys445 ($TLR7^{C445A}$). Transfection of WT TLR7 or $TLR7^{C445A}$ into $TLR7^{-/-}$ macrophages restored the ability of imiquimod to stimulate cytokine expression in these cells; however, transfection with the TLR7 containing the 6 mutations, the $TLR7^{C98A/C445A}$ or the $TLR7^{C98A}$ did not (Fig. 4k). Catalase (1000 U/mL) treatment had little or no effect on cytokine expression in cells expressing the mutated TLR7, $TLR7^{C98A/C445A}$ or $TLR7^{C98A}$ whereas it markedly increased cytokine expression in cells with WT TLR7 or $TLR7^{C445A}$ (Fig. 4k). Protein expression levels were equivalent for the WT and mutated receptors and they also appeared to be similarly localised within early endosomes (data not shown).

We performed sequence analysis using both multiple sequence analysis algorithms (i.e. CLUSTAL OMEGA) and pair-wise sequence analysis (NCBI, Blast) with human TLR7 as a reference point. Using the multiple sequence analysis we identified that Cys98 was unique to TLR7 and fully conserved in vertebrate TLR7 including from teleosts to man (Fig 4l and Supplementary Fig. 9-10). Pair-wise sequence alignment showed that Cys98 was the only cysteine residue of the 27 cysteines on TLR7 that was unique to TLR7 and fully conserved in vertebrates (Supplementary Fig. 11). We suggest that H_2O_2 produced by endosomal NOX2 oxidase is likely to modify a single and evolutionary conserved unique cysteine residue i.e. Cys98 located on the endosomal face of TLR7, resulting in a dampened antiviral cytokine response. Potentially this signifies Cys98 of TLR7 as a novel redox sensor that controls immune function during viral infections. The precise type of molecular modification of this cysteine by H_2O_2, however, is currently unknown and certainly warrants further investigation.

NOX2 oxidase dampens antibody production

We examined if the suppressive effect of endosomal NOX2 oxidase activity on Type I IFN and IL-1β expression also occurs following influenza A virus infection. Firstly, virus triggered translocation of the transcription factor, IRF-7, to the nucleus of WT BMMs, but not $TLR7^{-/-}$ BMMs, indicating that influenza A virus activates TLR7-dependent antiviral signaling in macrophages (Supplementary Fig. 12). Second, virus elevated IFN-β, IL-1β, IL-6, and TNF-α expression to a greater extent in $NOX2^{-/y}$ AMs (Fig. 5a). Third, influenza A virus (Hkx31; 10^5 PFU/mouse) infection in mice *in vivo* for 24h resulted in greater increases in lung IFN-β (mRNA

and protein), IL-1β, TNF-α and IL-6 in NOX2$^{-/y}$ mice (Fig. 5b,c). Thus a fully functional NOX2 oxidase suppresses anti-viral cytokine production triggered by influenza A virus.

TLR7 is essential for the activation of B-cells and for antibody production. To test whether NOX2 oxidase suppresses TLR7-dependent immunity to influenza A virus *in vivo*, we used heat-inactivated, replication-deficient influenza A virus as a stimulus, and hence a form of virus expected to mainly trigger engagement of the TLR7 PRR with very little contribution of RIG-I and NLRP3 (Ichinohe *et al.*, 2009b). Intranasal inoculation with inactivated virus had no effect on weight loss over 7-days (Fig. 5d) or airways BALF inflammation (Fig. 5e). NOX2 deletion resulted in a significant elevation in lung levels of IFN-β, IL-1β and TNF-α mRNA (Fig. 5f) and in both serum and BALF levels of IgA, total IgG, IgG1, IgG2b and IgG3 (Fig. 5g,h). Therefore, activation of endosomal NOX2 oxidase following influenza A virus infection results in the suppression of antiviral cytokines and humoral immunity *via* the suppression of antibody production – processes that are required for optimal clearance of the virus and resistance to re-infection.

Endosomal targeted NOX2 inhibitor

We synthesized an innovative molecular targeting system, to deliver a specific NOX2 oxidase inhibitor (i.e. gp91ds-TAT) directly to endosomes, so as to disrupt the viral signaling platform by abrogating ROS production. To do this we generated a tripartite structure comprising gp91ds-tat conjugated to the membrane anchor cholestanol *via* a PEG-linker at the N-terminal region of the peptide. Similar constructs have been shown previously to enhance endosome localisation for inhibitors of the enzyme beta secretase (Rajendran *et al.*, 2008a). A Cy5 fluorophore conjugated to cholestanol using the same PEG linker resulted in cytosolic fluorescence in the peri-nuclear region and co-localisation with EEA1, NOX2 and influenza virus NP following viral infection in a dynasore-sensitive manner providing evidence for endocytosis as its primary mode of cell entry (Fig. 6a-e). Superoxide generation in macrophages *in vitro* was suppressed with at least a 10-fold greater potency by cholestanol-conjugated gp91ds-TAT (Cgp91ds-TAT) when compared to the unconjugated drug (Ugp91ds-TAT; Fig. 6f), which is not attributed to enhanced ROS scavenging properties of the compound (Fig. 6g).

We examined whether Cgp91ds-TAT suppresses disease severity following influenza A virus infection *in vivo*. Daily intranasal administration of Cgp91ds-TAT (0.02 mg/kg/d) from 1 day prior, until day 3 post-influenza A virus infection resulted in a ~40% reduction in airways inflammation (Fig. 6h), whereas Ugp91ds-TAT had no effect (Fig. 6h). Cgp91ds-TAT significantly increased lung Type I IFN-β mRNA levels compared to the control virus group, whereas Ugp91ds-TAT failed to do so (Fig. 6i). To eliminate the possibility that this improvement in NOX2 inhibition by

cholestanol conjugation of gp91ds-TAT was attributed to cholestanol-PEG linker *per se*, we conjugated the cholestanol PEG-linker to a scrambled gp91ds-TAT (Sgp91ds-TAT) and examined its effect against influenza infection *in vivo*. Sgp91ds-TAT had no effect on airway inflammation, lung IFN-β mRNA levels and superoxide production (Supplementary Fig. 13). Increasing the dose of the Ugp91ds-TAT by 10-fold to 0.2 mg/kg/day significantly reduced the weight loss caused by influenza A virus at day 3 and almost abolished airway inflammation, as well superoxide production in BALF inflammatory cells, similar to Cgp91ds-TAT at the same dose (Fig. 6j-l). Strikingly, both Cgp91ds-TAT (0.2 mg/kg/day) and Ugp91ds-TAT (0.2 mg/kg/day) caused an almost 10,000-fold, decrease in lung influenza A viral burden (Fig. 6m). Thus, suppression of endosome NOX2 oxidase *via* nasal administration of gp91ds-TAT results in a substantial reduction in influenza A virus pathogenicity. This is an innovative approach for suppressing NOX2 oxidase activity that occurs within the endosome compartment. We would like to emphasize that our novel NOX2 inhibitor is unlikely to solely suppress endosome NOX2. However, our inhibitor is specifically and preferentially delivered via the endocytic compartment owing to the cholestanol conjugation. In support of this, our findings of Figs 6A and B show that cholestanol conjugation results in a drug delivery system that promotes endosome delivery i.e our drug displayed a strong degree of co-location with EEA1+ endosomes that was abolished by dynasore pretreatment. This property is a novel delivery system that brings a NOX2 inhibitor to the predominant site of action that relates to virus infection (see Fig 6D showing strong co-location of viral nucleoprotein and our NOX2 inhibitor). We speculate that following internalization into the endosome the drug is most likely on the luminal face of the endosome membrane and due to the TAT portion can penetrate the membrane and suppress NOX2 activity. The drug might still be able to diffuse towards other sites or locations of NOX2, however, we believe the immediate and primary site of action will be NOX2 activity at the endosome, given that the drug appears to be selectively delivered *via* the endocytic pathway.

Discussion

We have accumulated evidence that virus entry into endosomal compartments triggers a NOX2 oxidase- dependent production of ROS in endosomes. However, some ROS may have possibly been generated in sites outside of the endosome, which may have then diffused into the endosomes. As such the site of ROS generation and site of detection in some instances might be distinct. We suggest that the major contributor to endosomal concentrations of superoxide will be superoxide generated directly in this compartment. Superoxide is the primary product of NOX2 and it will only be generated within the endosome compartment owing to the topology of the NOX2 and the unidirectional transfer of electrons through this catalytic subunit. In keeping with this, it is well regarded that superoxide does not travel far from its site of generation due to

its negative charge. By contrast to superoxide, hydrogen peroxide has some capacity to permeate membranes and diffuse, and as such, it can be envisaged that some endosome H_2O_2 might have been generated elsewhere by NOX2 expressed in other sites of the cell such as the plasma membrane. However for several lines of evidence we suggest that it is very likely that little remotely generated H_2O_2 is finding its way into the endosome compartment. First we demonstrate that PKC activation following virus infection, which is critical for NOX2 activation, is significantly impaired if: 1) the virus is prevented from entering cells (Fig 2H and 2I); 2) endosome acidification is blocked by Bafilomycin A (Fig 2H and 2I) or 3) if TLR7 is absent (i.e. $TLR7^{-/-}$ macrophages are used). Therefore, endosomal NOX2 derived ROS generation occurs only after virus has entered endosomes and activates endosome-specific pathways, lending further credence to endosome NOX2 as the predominant site of H_2O_2 generation. Second, elegant studies addressing spatial-temporal aspects of H_2O_2 diffusion clearly demonstrate that H_2O_2 diffusion in the cytoplasm is strongly limited, but is instead localized to near the sites of its generation (Mishina *et al.*, 2011), providing evidence that endosome H_2O_2 is unlikely to have been generated at a remote site.

Here we demonstrate that endosomal ROS are essential negative regulators of a fundamental molecular mechanism of viral pathogenicity that impacts on antiviral immunity and the capacity of the host to fight and clear viral infections. Importantly, this effect is conserved, regardless of viral classification, for all viruses that enter cells via the endocytic pathway, and is TLR7 dependent. This provides a potential target for antiviral therapy for a range of viruses that cause significant morbidity and mortality worldwide. Previous work has demonstrated that a deficiency in the phagocyte NADPH oxidase can result in exacerbated inflammation and necrosis in response to fungal components including β-glucans that activate TLR2 and dectin-1 (Schappi *et al.*, 2008). Our study is not a universal mechanism that defines how NOX2 oxidase might be regulating inflammation to fungi and other pathogens but certainly provides strong mechanistic insight into ROS dependent regulation of antiviral immunity.

Intriguingly, our study raises a broader paradox: Why does a mammalian cell generate ROS that may ultimately cause harm (i.e. by promoting viral pathogenicity)? We hypothesize that suppression of TLR7 activation by endosomal NOX2 is a hitherto unrecognized mechanism that has evolved to inhibit an inflammatory response against self-RNA/antigens and the development of autoimmunity, but which in a very similar manner results in a host response to viral RNA that inadvertently exacerbates viral pathogenicity. Realizing the delicate balance between viral clearance and the induction of an autoimmune response, the current data suggest the potential to employ short term (during the course of infection) suppression of endosomal ROS as a means of reducing viral pathogenicity without causing long term problems with

autoimmunity.

EXPERIMENTAL PROCEDURES

Viruses

The influenza A virus vaccine strains HKx31 (H3N2) and BJx109 (H3N2) were kindly provided by A/Prof. John Stambas (School of Medicine, Deakin University, CSIRO). Human strains of influenza A virus, including seasonal H3N2 (A/New York/55/2004, A/Brisbane/9/2007), seasonal H1N1 (A/Brazil/11/1978, A/New Caledonia/20/1999, A/Solomon Islands/3/2006), A(H1N1)pdm09 strains (A/California/7/2009, A/Auckland/1/2009), rhinovirus, respiratory synctitial virus (strain A2), human parainfluenza virus type-3, human metapneumovirus (strain CAN97-83), mumps virus (strain Enders) and Newcastle disease virus (strain V4) were provided by A/Prof Patrick Reading (Department of Immunology and Microbiology, University of Melbourne, The Peter Doherty Institute for Infection and Immunity). Additional viruses were provided by the following people: dengue virus serotype 2; Vietnam 2005 (Associate Professor Elizabeth McGraw; Monash University); rotavirus (Rhesus and UK strains, A/Prof Barbara Coulson, Department of Microbiology and Immunology, The Peter Doherty Institute for Infection and Immunity); sendai virus (Cantell strain, Dr Ashley Mansell from Hudson Institute of Medical Research, Monash University), herpes simplex virus type-2 (strain 186; Dr Niahm Mangan, Hudson Institute of Medical Research, Monash University), vaccinia virus (Western Reserve strain, WR NIH-TC; A/Prof. David Tscharke, Australia National University) and HIV (NL4-3(AD8)-EGFP strain, Professor Sharon Lewin, The Peter Doherty Institute for Infection and Immunity, The University of Melbourne). The viruses were provided in phosphate buffered saline (PBS) and stored at -80°C until used. On the day of use, virus was thawed quickly and incubated at 37°C prior to infection. In some cases HKx31 virus was inactivated by heat (56°C) for 30 min or UV light (30 min).

Bacteria

Streptococcus pneumoniae EF3030 (capsular type 19F) was used as the parent *S. pneumoniae* strain in all experiments. *S. pneumoniae* EF3030 is a clinical isolate that is frequently used as a model of human carriage as it typically colonizes the nasopharynx in the absence of bacteremia. For infection experiments, pneumococci were grown statically at 37°C in Todd-Hewitt broth, supplemented with 0.5% yeast extract, to an optical density (600 nm) of 0.4–0.45. Cultures were placed on wet ice for 5 min and frozen in 8% (v/v) glycerol at -70°C. Live bacterial counts were confirmed prior to each experiment. A defined strain of *non-typeable Haemophilus influenzae* (NTHi; MU/MMC-1) was previously typed and sequenced and demonstrated to be NTHi, as we have previously shown (King *et al.*, 2013).

Conjugation of NOX2 oxidase inhibitors

Gp91 ds-tat: YGRKK-RRQRR-RCSTR-IRRQL-NH_2

Preparation of gp91 ds-tat was carried out by standard Fmoc solid-phase peptide synthesis (SPPS) on Fmoc-PAL-PEG-PS resin (Life Technologies, loading 0.17 mmol/g). Fmoc deprotection reactions were carried out using 20% *v*/*v* piperidine in *N*,*N*-dimethylformamide (DMF). Coupling reactions were carried out using Fmoc-protected amino acids with *O*-(6-chlorobenzotriazol-1-yl)-*N*,*N*,*N*′,*N*′-tetramethyluronium hexafluorophosphate (HCTU) as coupling agent and *N*,*N*-diisopropylethylamine (DIPEA) as activating agent. Reactions were monitored using the 2,4,6-trinitrobenzenesulfonic acid (TNBS) test to indicate the absence or presence of free amino groups. The alternating sequence of deprotection and coupling reactions was carried out manually for all 20 amino acid residues using the appropriate Fmoc- and side-chain protected amino acids. After a final de-protection step, a small portion of the peptide was cleaved from resin using trifluoroacaetic acid (TFA)/triisopropylsilane (TIPS)/1,2-ethanedithiol (EDT)/water (92.5:2.5:2.5:2.5) for 4 h, during which time the side-chain protecting groups were simultaneously removed. The crude peptide was then purified by reverse-phase high-pressure liquid chromatography (HPLC) using a Phenomenex Luna 5 C8 (2) 100 Å AXIA column (10 Å, 250 × 21.2 mm) with 0.1% TFA/water and 0.1% TFA/ACN as the buffer solutions. The purified gp91 ds-tat peptide was confirmed as having the correct molecular weight by ESI-MS analysis: calcd. for $C_{109}H_{207}N_{52}O_{25}S$ [M + $5H^+$] *m/z* 535.3, obs. *m/z* 535.7; calcd. for $C_{109}H_{208}N_{52}O_{25}S$ [M + $6H^+$] *m/z* 446.3, obs. *m/z* 446.6; calcd. for $C_{109}H_{209}N_{52}O_{25}S$ [M + $7H^+$] *m/z* 382.7, obs. *m/z* 382.9.

Cgp91 ds-tat: Ac-Asp(OChol)-PEG4-PEG3-PEG4-gp91-NH_2

Preparation of cholestanol-conjugated gp91 ds-tat (cgp91 ds-tat) was carried out by manual SPPS from resin-bound gp91 ds-tat (as described above), using Fmoc-PEG4-OH, Fmoc-PEG3-OH, Fmoc-PEG4-OH and Fmoc-Asp(OChol)-OH as the amino acids. After the final deprotection step, the *N*-terminus was capped using a mixture of acetic anhydride and DIPEA in DMF and the peptide construct was cleaved from resin using TFA/TIPS/EDT/water (92.5:2.5:2.5:2.5). The crude peptide was purified as described previously to give cgp91 ds-tat: calcd. for $C_{173}H_{319}N_{56}O_{43}S$ [M + $5H^+$] *m/z* 780.3, obs. *m/z* 780.6; calcd. for $C_{173}H_{320}N_{56}O_{43}S$ [M + $6H^+$] *m/z* 650.4, obs. *m/z* 650.7; calcd. for $C_{173}H_{321}N_{56}O_{43}S$ [M + $7H^+$] *m/z* 557.6, obs. *m/z* 558.0.

Egp91 ds-tat: Ac-Asp(OEt)-PEG4-PEG3-PEG4-gp91-NH_2

Preparation of ethyl ester-conjugated gp91 ds-tat (egp91 ds-tat) was carried out in the same

way as for cgp91 ds-tat, except for replacement of Fmoc-Asp(OChol)-OH with Fmoc-Asp(OEt)-OH in the final coupling step: calcd. for $C_{148}H_{277}N_{56}O_{43}S$ [M + $5H^+$] *m/z* 711.8, obs. *m/z* 712.1; calcd. for $C_{148}H_{278}N_{56}O_{43}S$ [M + $6H^+$] *m/z* 593.3, obs. *m/z* 593.7; calcd. for $C_{148}H_{279}N_{56}O_{43}S$ [M + $7H^+$] *m/z* 508.7, obs. *m/z* 509.0.

Sgp91 ds-tat: Ac-Asp(OChol)-PEG4-PEG3-PEG4-RKK-RRQRR-RCLRI-TRQSR-NH_2

Preparation of the 18 amino acid scrambled gp91 ds-tat (Sgp91 ds-tat) peptide was carried out by manual SPPS as described above for unscrambled gp91 ds-tat. The resin-bound sgp91 ds-tat was then conjugated to cholestanol via a PEG linker using the same method described above for unscrambled cgp91 ds-tat. The crude peptide was purified in the same way to give cgp91 ds-tat: calcd. for $C_{162}H_{307}N_{54}O_{40}S$ [M + $5H^+$] *m/z* 736.3, obs. *m/z* 736.5; calcd. for $C_{162}H_{308}N_{54}O_{40}S$ [M + $6H^+$] *m/z* 613.7, obs. *m/z* 614.0; calcd. for $C_{162}H_{309}N_{54}O_{40}S$ [M + $7H^+$] *m/z* 526.2, obs. *m/z* 526.3

Animal ethics statement

The mouse experiments described in this manuscript were approved by the Animal Experimentation Ethics Committee of The University of Melbourne and conducted in compliance with the guidelines of the National Health and Medical Research Council (NHMRC) of Australia on animal experimentation.

In vivo infection with influenza A virus and intranasal delivery of pharmacological agents

Aged matched littermate male naïve WT control and $NOX2^{-/y}$ mice were anaesthetized by penthrane inhalation and infected intranasally (*i.n.*) 1×10^4 or 1×10^5 plaque forming units (PFU) of Hk-x31 in a 50 μL volume, diluted in PBS as described previously (Vlahos *et al.*, 2011a). Mice were euthanised at Day 1, 3 or 7 following influenza infections. In some experiments, anaesthetized mice were treated via intranasal delivery with either DMSO (control), unconjugated gp91dstat (0.02mg/kg, 0.2mg/kg), cholestanol conjugated-gp91dstat (0.02mg/kg, 0.2mg/kg) or cholestanol conjugated-scrambled gp91ds-TAT (0.02mg/kg) one day prior to infection with Hk-x31 and everyday thereafter for 3 days. In additional experiments, anaesthetized mice were treated with imiquimod (50 μg/mouse, *i.n.*) or catalase (1000U /mouse, *i.n.*) and then euthanised for analysis at Day 1.

Airways inflammation and differential cell counting

Mice were killed by sodium pentobarbitone (*i.p* injection at 360 mg/kg) and bronchoalveolar lavage (BAL) differential cell counting performed as we have previously described (Vlahos *et al.*, 2011a).

Cell culture and primary cell isolation

Human alveolar macrophages were obtained from subjects undergoing a bronchoscopy at Monash Medical Centre to investigate underlying lung disease with approval from the ethics committee of Southern Health/Monash Medical Centre. Written consent was obtained from all subjects. The bronchoscope was wedged in the right middle lobe and 25–50 mL of saline was washed into the airway then aspirated. Cells were washed twice with PBS before being suspended in culture medium (RPMI with 10% fetal calf serum with 100 U/mL penicillin and 100 μg/mL streptomycin) for ~24 h before use.

Alveolar macrophages were isolated by lung lavage from age-matched (6-10 weeks) male C57Bl/6J (WT), NOX2$^{-/y}$, NOX4$^{-/-}$, TLR7$^{-/-}$, TLR9$^{-/-}$ or SOD3$^{-/-}$ mice. A thin shallow midline incision from the lower jaw to the top of the rib cage was made and the larynx was separated to expose the top of the trachea. The layer of smooth muscle covering the trachea was removed, a small incision made and a sheathed 21-gauge needle was inserted into the lumen. The lungs were repeatedly (3 times) lavaged with 300-400 μL of phosphate-buffered saline (PBS; Sigma). Cell suspensions were spun down by centrifugation (1500 rpm at 4^{o}C for 5 min). Supernatant was removed, then cells were re-suspended in 1 mL of sterile PBS and counted using the Countess® automated cell counter. Cells were then seeded into 24-well plates (1x10^{5} cells/well) for immunocytochemistry and fluorescence microscopy, as stated below.

The immortalized cell line RAW 264.7 cells (derived from mouse peritoneum) and immortalized bone marrow-derived macrophages (BMMs; courtesy of Dr Ashley Mansell of the Hudson Institute of Medical Research Monash University and Prof Eicke Latz of the Institute of Innate Immunity, University of Bonn, Germany) were maintained in Dulbecco's Modified Eagle's Medium (DMEM: Sigma) supplemented with L-glutamine, glucose (4500 mg/L), sodium pyruvate (110 mg/L) and fetal bovine serum (FBS; 10%). The TLR2$^{-/-}$, TLR3$^{-/-}$, TLR4$^{-/-}$, TLR7$^{-/-}$, TRIF$^{-/-}$, RIG-I$^{-/-}$, MyD88$^{-/-}$, NLRP3$^{-/-}$ and UNC93B1$^{-/-}$ immortalized bone marrow-derived macrophages were maintained in RPMI medium supplemented with glucose (4500 mg/L), non essential amino acids, sodium pyruvate streptomycin and FBS (10%) and DMEM (20%) (containing all supplements as stated above). All cells were kept at 37°C with a humidified mixture of 5% CO_2 and 95% air. The medium was changed two to three times a week, cells were sub-cultured by scraping when ~80-90% confluent, and counted using the Countess® automated cell counter (Invitrogen).

Confocal fluorescence microscopy

Cells were seeded onto glass cover slips in 24-well plates, and allowed to adhere for 24 h in DMEM. Cells were then incubated in the absence or presence of HKx31 influenza A virus (MOI 0.1, 1 or 10) in serum-free medium at varying time points (5 min, 15 min, 30 min and 1 h). In some cases, cells were pretreated for 30 min prior to infection with Dynasore (100 µM) or the vehicle for Dynasore, dimethyl sulfoxide (DMSO; 0.1%). Next, the cells were washed with PBS (0.01 M) and fixed with 4% paraformaldehyde (PFA) for 15 min. Cells were treated for 10 min with PBS-containing Triton X-100 (0.25%) and then washed three times over 15 min with PBS. The samples were then incubated with 10% goat serum-containing PBS for 2 h and/or mouse on mouse IgG blocking reagent. This was followed by the addition of a primary antibody for nucleoprotein (1:1000) to localize influenza A virus, purified mouse anti-NOX2 (1:500) to localize NOX2, rabbit anti-TLR7 (1:1000) to localize TLR7, or mouse anti-early endosome antigen 1 (EEA1; 1000) to localize early endosomes for 24 h at 4°C. In some experiments, combinations of antibodies were used at the indicated concentrations to determine protein co-localization. Cells were washed three times over 30 min with PBS (0.01 M). Following the washes, a secondary antibody goat anti-rabbit alexa 594 (1:1000), goat anti rabbit red 647 (1:500, 1:1000) and/or biotinylated anti-mouse IgG was added to appropriate wells in the dark for 2 h. Finally, the cells were washed three times over 30 min with PBS (0.01 M); and where appropriate (mouse primary and secondary anti Fluroscein Avidin DCS was applied for 5 minutes). Cover slips were mounted onto microscope slides with 10-20 μL of diamidino-2-phenylindole (DAPI) for 3 min. Slides were viewed and photographed on a Nikon upright inverted confocal fluorescence microscope. All immunohistochemistry was assessed by two observers blinded as to the treatment groups throughout the analysis process and all of the appropriate controls were performed, in that all combinations of primary and secondary antibodies were used to ensure no cross reactivity occurred.

We verified the specificity of both the TLR7 and NOX2 antibodies by examining the degree of staining in WT macrophages and in TLR7$^{-/-}$ and NOX2$^{-/-}$ macrophages respectively. There was no staining for TLR7 in the TLR7$^{-/-}$ macrophages (Fig 2c). Similarly with the NOX2 antibody we observed no staining in alveolar macrophages of NOX2$^{-/y}$ mice compared to the WT cells (Supplementary Fig 1D). Further evidence for the specificity of this NOX2 antibody can be found in Judkins *et al.*, 2010 (Judkins *et al.*, 2010).

Endosomal ROS production

Human alveolar macrophages; WT, TLR7$^{-/-}$, TLR2$^{-/-}$, TLR3$^{-/-}$, TLR4$^{-/-}$, TRIF$^{-/-}$, MyD88$^{-/-}$, RIG-I$^{-/-}$ and NLRP3$^{-/-}$ BMMs; mouse primary WT, NOX2$^{-/y}$, NOX4$^{-/-}$, TLR7$^{-/-}$, TLR9$^{-/-}$ or SOD3$^{-/-}$ alveolar

macrophages and RAW264.7 cells were seeded (1×10^5 cells/well) onto glass coverslips in 24-well plates allowing the cells to adhere for 24h in DMEM or RPMI medium before being pretreated with OxyBURST Green H2HFF (100 μM) and/or LysoTracker Deep Red (50 μM) for 5 min. This was followed by incubation with PBS (control group; 0.01 M), imiquimod (10 μg/mL), single stranded RNA (100 μM), or infected with either H3N2 influenza viruses (A/New York/55/2004, A/Brisbane/9/2007), seasonal H1N1 influenza A viruses (A/Brazil/11/1978, A/New Caledonia/20/1999, A/Solomon Islands/3/2006), A(H1N1)pdm influenza A viruses (A/California/7/2009, A/Auckland/1/2009), or with re-assortant vaccine strains HKx31 (MOI 0.1-10) or BJx109 (MOI 10) in serum-free medium at varying time points (5 min, 15 min, 30 min and 1 hr). Other wells were infected with dengue virus (MOI 10), Sendai virus (40HAU/mL), human parainfluenza virus (MOI 10), human metapneumovirus (MOI 10), rhinovirus (MOI 10), respiratory syncytial virus (MOI 10), HIV (MOI 10), Newcastle disease virus (MOI 10), mumps virus (MOI 10), rhesus or UK rotaviruses (each at MOI 10) or herpes simplex virus-2 (MOI 10) under similar conditions. In some cases, cells were pretreated with superoxide dismutase (SOD; 300 U/mL), apocynin (300 μM), gp91dstat (50 μM) or bafilomycin A (100 nM), for 30 min prior to infection. Next, the cells were washed with PBS (0.01 M) and fixed with 4% PFA for 15 min. After fixation, cells were then washed three times with PBS over 30 min. Cover slips were then mounted onto microscope slides with 10-20 μL of DAPI for 3 min, then analysed and photographed on an Nikon upright or inverted confocal fluorescence microscope.

NOX2 oxidase assembly

To measure NOX2 oxidase activity we assessed p47phox and NOX2 assembly using confocal fluorescence microscopy. Control and HKx31 virus-infected WT and TLR7$^{-/-}$ alveolar macrophages were processed as indicated above under “confocal fluorescence microscopy”. In additional experiments, WT cells were treated with Dynasore (100μM) or bafilomycin A (100nM) for 30 min prior to virus infection. After exposing samples with 10% goat serum-containing PBS for 2 h, the rabbit anti-p47phox antibody and the mouse anti-NOX2 antibody were added followed by addition of appropriate secondary antibodies, as specified above.

L-O12-enhanced chemiluminescence

ROS production was quantified using L-O12-enhanced chemiluminescence. RAW264.7 cells and primary mouse alveolar macrophages were seeded into a 96-well OptiView plate ($5x10^4$ cells/well). RAW264.7 cells were either treated with DMSO (control, appropriate concentration), unconjugated gp91dstat (100nM-30μM), cholestanol-conjugated gp91dstat (100nM-30μM) or ethyl-conjugated gp91dstat (100nM-30μM) for 1h. BALF was collected from mice treated with

DMSO (control), unconjugated gp91dstat (0.02mg/kg, 0.2mg/kg), cholestanol conjugated-gp91dstat (0.02mg/kg, 0.2mg/kg) and/or infected with X-31 influenza A virus ($1X10^5$ PFUs). Cells were then washed of media with 37 °C Krebs-HEPES buffer, then exposed to a Krebs-HEPES buffer containing L-O12 (10^{-4} mol/L) in the absence (i.e. basal ROS production) or presence (stimulated ROS production) of the PKC and NADPH oxidase activator phorbol dibutyrate (PDB; 10^{-6} mol/L). The same treatments were performed in blank wells (i.e. with no cells), which served as controls for background luminescence. All treatment groups were performed in triplicates. Photon emission [relative light units (RLU)/s] was detected using the Chameleon™ luminescence detector (Hidex, model 425105, Finland) and recorded from each well for 1 s over 60 cycles. Individual data points for each group were derived from the average values of the three replicates minus the respective blank controls. Data are represented as a % of the control in the dose-response curves or as raw values (ex vivo experiments).

To test whether the unconjugated or cholestanol conjugated gp91dstat exhibited ROS scavenging properties, the xanthine oxidase cell free assay was used. Briefly, Krebs-HEPES buffer containing L-012 (10^{-4} mol/L) was added into a 96-well Optiview plate. Following this, 0.1% DMSO, unconjugated gp91dstat (Ugp91ds-TAT, 1µM) or cholestanol conjugated gp91ds-TAT (1 µM) were added in combination with Xanthine (100 µM). Immediately after xanthine oxidase (0.03 U/mL) was added, photon emission [relative light units (RLU)/s] was detected using the Chameleon™ luminescence detector (Hidex, model 425105, Finland) and recorded from each well for 1 s over 60 cycles. Individual data points for each group were derived from the average values of the three replicates minus the respective blank controls. Data are represented as raw values.

Site directed mutagenesis, sequencing and transfections

HA-TLR7 cDNA was purchased from Sino Biological. Mutation of the key cysteine residues in TLR7 (Cys260, Cys263, Cys270, Cys273, Cys98 and Cys445) to alanine was performed using the QuikChange Multi Site-Directed Mutagenesis kit. Sequences of WT and mutant HA-TLR7 were confirmed by the Australian Genome Research Facility. Cells were transfected using linear polyethyleneimine (PEI)(Halls *et al.*, 2015)

High-content ratiometric FRET imaging

Cells were plated and transfected in suspension with 200 ng/well FRET biosensor DNA using PEI, in black, optically clear 96-well plates for 48 hr. Prior to the experiment, cells were partially

serum-starved overnight in 0.5% FBS media. Fluorescence imaging was performed using a high-content GE Healthcare INCell 2000 Analyzer with a Nikon Plan Fluor ELWD 40x (NA 0.6) objective and FRET module as described *(22)*. For CFP/YFP (CKAR) emission ratio analysis, cells were sequentially excited using a CFP filter (430/24) with emission measured using YFP (535/30) and CFP (470/24) filters, and a polychroic optimized for the CFP/YFP filter pair (Quad3). For GFP/RFP (EKAR) emission ratio analysis, cells were sequentially excited using a FITC filter (490/20) with emission measured using dsRed (605/52) and FITC (525/36) filters, and a polychroic optimized for the FITC/dsRed filter pair (Quad4). Cells were imaged every 100 sec for 20 min (image capture of 2 fields of view in 12 wells per 100 sec). Data were analysed using in-house scripts written for the FIJI distribution of ImageJ (Schindelin *et al.*, 2012), as described (Halls *et al.*, 2015).

Quantification of mRNA by QPCR

Whole lungs were perfused free of blood *via* right ventricular perfusion with 10 mL of pre-warmed saline, rapidly excised en bloc, blotted and snap frozen in liquid nitrogen. 15 mg of whole lung tissue pooled from 5 mice per treatment group or from cells that have been treated with imiquimod (10 µg/ml), poly I:C (100 ng/ml), CpG (10 µg/mL)), ssRNA (500 µg/mL) or catalase (1000 U/ml) for 24 hours. In some cases, cells were pre-treated with apocynin (300 µM), SOD (300 U/mL) or bafilomycin A (100 nM) for 30 mins. Total RNA was extracted using RNeasy kits (Qiagen), reverse transcribed with SuperScript III (Invitrogen), and triplicate real time PCR reactions were performed with Applied Biosystems pre-developed assay reagents and 18S rRNA internal control as previously described(Vlahos *et al.*, 2011a). QPCR analysis of mRNA of gene encoding segment 3 polymerase (*PA*) of influenza virus strain PR8 (sequence) from a custom designed forward and reverse primer (Life Technologies) in the lungs of mice treated with DMSO (control), unconjugated gp91dstat (0.02mg/kg, 0.2mg/kg), cholestanol conjugated-gp91dstat (0.02mg/kg, 0.2mg/kg) and/or infected with X-31 influenza A virus ($1X10^5$ PFUs) 3 days post infection with the virus. Data are presented relative to the GAPDH mRNA and normalised to the X-31 infected control.

ELISA and multiplex immunoassay

Protein levels of IFN-β, IL-1β, TNF-α and IL-6 secreted into the BALF of HKx31-infected ($1x10^4$ PFUs) wild-type and $NOX2^{-/y}$ mice were measured using ELISAs and performed using commercially available kits according to the manufacturer's instructions (R&D system, Minneapolis, MN). The cytokine titres in samples were determined by plotting the optical densities using a 4-parameter fit for the standard curve.

Antibody determination

Serum and BALF levels of various antibody isotypes (IgA, IgE, IgG1, Ig2a, IgG2b, IgG3, IgM and total IgG) were quantified in HKx31-infected ($1x10^4$ PFUs) WT and $NOX2^{-/y}$ mice using the ProcartaPlex Multiplex Immunoassay (Mouse antibody isotyping panel; eBioscience, USA) according to the manufacturer's instructions. Briefly, antibody-conjugated magnetic beads were added into each well of a 96-well plate. Antibody standards were serially diluted (1:4) in universal assay buffer (eBioscience, USA) to construct a 7-point standard curve. Serum and BALF samples (diluted 1:20,000 in universal assay buffer) and/or standards were added to appropriate wells of the 96-well plate containing the antibody-conjugated magnetic beads. Following this, a detection antibody mix (eBioscience, USA) was added to each well and the plate was incubated for 30 min at room temperature on a microplate shaker (500 rpm) in the dark. After washing, a reading buffer (eBioscience, USA) was added to all wells. The plate was read by a Magpix® multiplex reader (Luminex, USA) with xPONENT® software (Luminex, USA). Procartaplex™ Analyst 1.0 software (eBioscience, USA) was used to interpolate serum and BALF antibody concentrations in each sample from the standard curve.

Western blotting

Total protein was extracted from BMDM cells using a mixture of 1.5X Laemmli buffer containing 25% Glycerol, 7.5% SDS, 250mM Tris-HCl at pH 6.8, and 0.001g bromophenol blue. Samples were sonicated then heated at 37°C for 20 minutes, followed by centrifugation at 13,000rpm for 30 minutes at 4°C. An RCDC (reducing agent and detergent compatible) protein assay (BioRad, Australia) was performed and the protein content was quantified using ProteinQuant-Lowry software (SoftMax Pro) at 750nm.

10% gels (15 wells) were made up using TGX Stain-Free FastCast Acrylamide starter kit, 10% (#161-0183, BioRad). 10μg of protein per sample was electrophoresed at 200V for ~45 minutes in the presence of Running buffer (diluted from 10x buffer, #161-0732, BioRad). Protein was then transferred in the Transfer-Blot Turbo transfer system (7 minutes), membranes were washed in Tris-buffered saline-tween (TBS-T) (0.1% Tween-20 in 1X TBS) followed by blocking with TBS-T/5% skim milk for at least 1 hour at room temperature whilst shaking. Primary antibodies (rabbit HA (1:5000), mouse GAPDH (1:20000)) were probed and allowed to be incubated overnight at 4ºC on a mechanical shaker. Membranes were then washed and incubated with either anti-rabbit or anti-mouse secondary antibodies conjugated with HRP for an hour at room temperature on a shaker. Membranes were developed with ECL reagents (ClarityTM Western ECL Blotting Substrate, BioRad) for 5 minutes, and imaged using a digital imager ChemiDoc MP imaging system. Adjusted volume of bands were analyzed using Image

Lab software, with individual bands then normalized to the adjusted volume of the housekeeping gene GAPDH.

Statistical analysis and image analysis

In order to quantify the fluorescence microscopy data, images acquired from confocal systems were analysed in Image J. Approximately 100 cells per treatment group from at least three independent experiments were analyzed unless otherwise stated in the figure legend to calculate the fluorescence in each cell, which was then averaged and expressed as a percentage of the area fluorescence. All statistical tests were performed using GraphPad Prism (GraphPad Software Version 6.0, San Diego CA, USA). $P<0.05$ was taken to indicate significance. For isolated cell culture work, *n* is representative of a separate experiment where cells were used from a different passage upon splitting.

Chemicals

Imiquimod (Invivogen) and H.M.W poly I:C (Invivogen) were dissolved in endotoxin-free water and prepared as stock solutions of 10 mg/mL in aliquots of 30 μL and 100 μL and stored at -20°C. ssRNA (Invivogen) was dissolved in endotoxin-free water and prepared as a stock solution of 5mM in aliquots of 50 μL and stored at -20°C. Dynasore (Sigma) (freshly prepared on the day) was dissolved in DMSO (100%) and prepared as 10 mM stock solutions. FBS (Sigma) was stored in 50 ml aliquots at -20°C. SOD (Sigma) was dissolved in distilled water and prepared as stock solutions (10μl) of 30,000 units/ml and stored at -20°C. OxyBURST Green H2HFF bovine serum albumin (BSA)(Molecular probes) and LysoTracker Deep Red)(Molecular probes) in stock solutions (1 mg/mL) were generated immediately before use by dissolving in PBS. Bafilomycin A (Sigma) was prepared as a stock solution of 100 μM in aliquots of 10 μL and stored at -20°C. Apocynin (Sigma) made freshly on the day of use and gp91dstat (Anaspec) were prepared as stock solutions of 100 mM and 50 mM respectively, in 100% DMSO. The antibodies nucleoprotein (AbCAM), early endosome antigen 1 (AbCAM), purified mouse anti-gp91phox (BD Transduction Laboratories, Purified Mouse Anti gp91[phox] Clone 53/gp91[phox](RUO), rabbit anti-TLR7 (AbCAM), rabbit anti-p47phox antibody (AbCAM), FITC goat anti-mouse IgG (Molecular probes), goat anti-rabbit alexa 594 (Molecular probes), goat anti-rabbit far red 647 (Molecular probes) and DAPI (Vector Laboratories) were stored at -20°C.

AUTHOR CONTRIBUTIONS

E.E.T., R.L., M.L.H., C.C., B.R.S.B, R.V.S., T.Q., S.B., R.V., S.S. performed experiments. E.E.T. and S.S wrote the manuscript. P.C.R., P.T.K., S.R.L., G.R.D., C.G.S., B.R.S.B, M.R.S.,

C.J.H.P., S.B., R.V., L. A.J. O'N., D.A.B, J. J. O'L and S.S provided intellectual input and edited the manuscript. P. C.R provided influenza viruses and P.T.K. provided human alveolar macrophages. S.S supervised and managed the overall study.

ACKNOWLEDGMENTS

This work was supported by the Australian Research Council (ARC) Future Fellowship Scheme for SS (I.D. FT120100876) and SB (I.D. FT130100654); The National Health and Medical Research Council of Australia (NHMRC) RD Wright Fellowship scheme for MLH (I.D 1061687); The NHMRC Senior Research Fellowship Scheme for GRD (I.D APP1006017) and CGS (I.D. APP1079467), The NHMRC practitioner fellowship for SRL (I.D APP 1042654); The NHMRC Early Career Fellowship for MRS (I.D APP1072000); The NHMRC project grant schemes (Project I.D 1122506, 1128276, 1027112, 1041795, 1052979); the ARC Centre of Excellence in Bio-Nano Science and Technology (Project CE140100036) and The Australian Postgraduate Award for EET. The authors also wish to thank the following people for providing viruses including Associate Professor Elizabeth McGraw (Monash University); A/Prof Barbara Coulson (The Peter Doherty Institute for Infection and Immunity, The University of Melbourne); Dr Ashley Mansell (Hudson Institute of Medical Research, Monash University), Dr Niahm Mangan (Hudson Institute of Medical Research, Monash University), A/Prof David Tscharke (Australia National University), Professor Sharon Lewin (The Peter Doherty Institute for Infection and Immunity, The University of Melbourne) and A/Prof John Stambas (CSIRO, Deakin University, Geelong, Australia). We thank Professor Karlheinz Peter (Baker IDI Heart and Diabetes Institute, Melbourne, Australia) for providing TLR9$^{-/-}$ mice and Professor Philip Hansbro (Hunter Medical School, University of Newcastle, Australia). Also the authors wish to thank Professor Arthur Christopoulos (Drug Discovery Biology, Monash institute of Pharmaceutical Sciences, Monash University, Australia) for providing feedback on the manuscript.

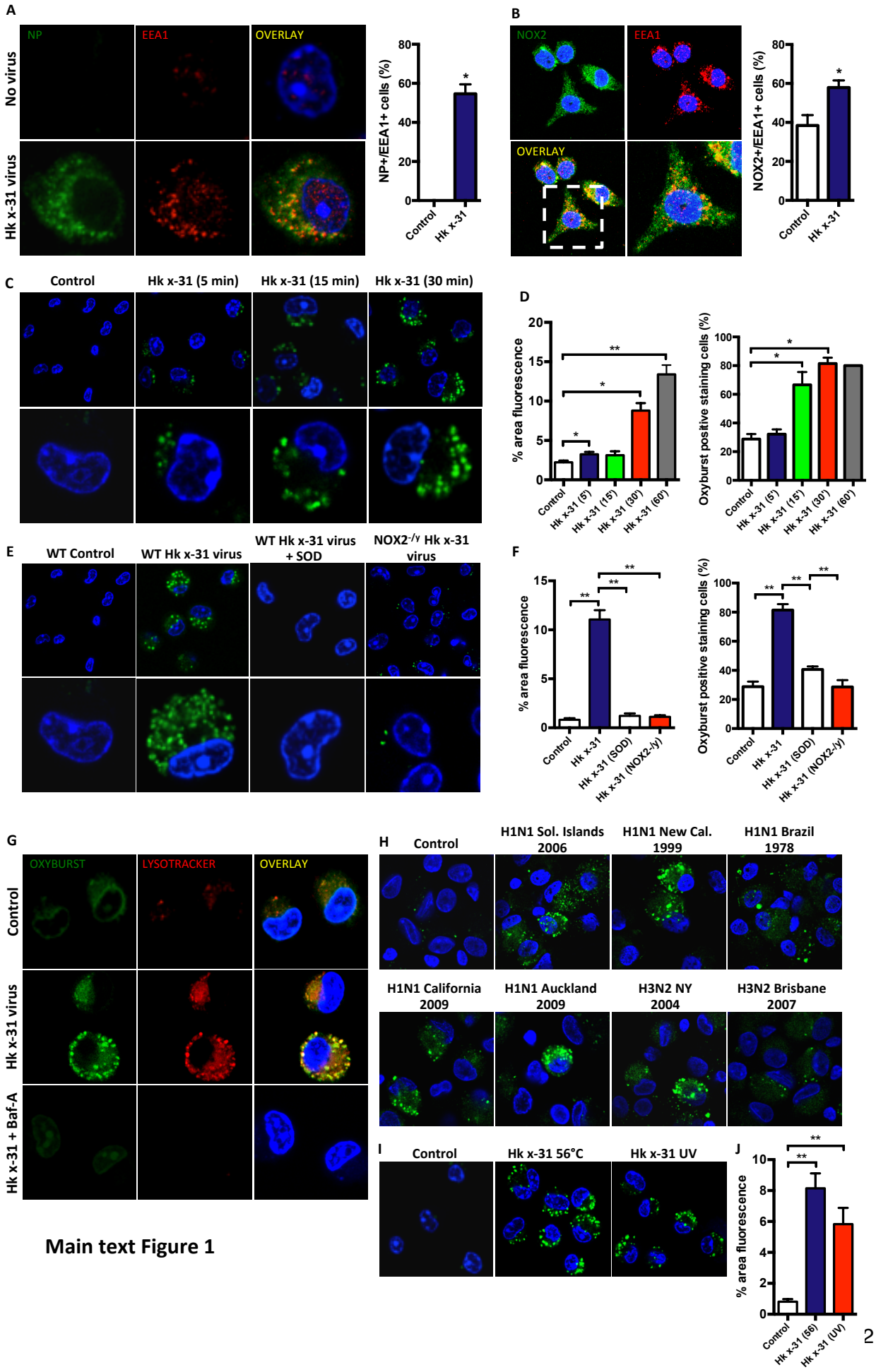

Main text Figure 1

Figure 1 Seasonal and pandemic influenza A viruses induce endosomal ROS production *via* activation of NOX2 oxidase.

(A-B) Confocal microscopy of wild-type (WT) mouse primary alveolar macrophages that were infected with influenza A virus strain HKx31 (MOI of 10) for 1hr and labeled with antibody to the early endosome antigen 1 (EEA1) and antibodies to either **A)** influenza A virus nucleoprotein (NP) or **B)** NOX2, and then with 4',6'- diamidino-2-phenylindole (DAPI; blue). Also shown is the quantification of results (n=5).

(C-D) Time-dependent elevation in endosomal ROS levels in mouse primary alveolar macrophages as assessed by OxyBURST (100μM) confocal fluorescence microscropy and labeled with DAPI (n=5).

(E-F) Endosomal ROS production in WT, $NOX2^{-/y}$ and superoxide dismutase (SOD; 300U/mL)-treated mouse primary alveolar macrophages as assessed by OxyBURST confocal fluorescence microscopy in the absence or presence of HKx31 virus and labeled with DAPI (n=5).

(G) Uninfected and HKx31 virus-infected mouse primary alveolar macrophages were labeled with OxyBURST and the acidified endosome marker Lysotracker (50 nM). Some cells were treated with bafilomycin A (Baf-A; 100 nM) to suppress acidification of endosomes (n=4).

(H) Human alveolar macrophages infected with seasonal H3N2 (A/New York/55/2004, A/Brisbane/9/2007), seasonal H1N1 (A/New Caledonia/20/1999, A/Solomon Islands/3/2006) and pandemic A(H1N1) pdm09 strains (A/California/7/2009, A/Auckland/1/2009) and labeled with OxyBURST for endosomal ROS (n=4).

(I-J) Endosomal ROS production in WT mouse primary alveolar macrophages as assessed by OxyBURST fluorescence microscopy exposed to either heat ($56^{O}C$) -inactivated HKx-31 virus (to block virus fusion) or UV-inactivated HKx-31 virus (to block replication) and labeled with DAPI (n=4).

(A, B, C, E, G, H and I) Images are representative of >150 cells analyzed over each experiment. Original magnification X100. (**A, B and D)** Data are represented as mean ± SEM. (**A and B)** Students' unpaired t-test * $P<0.05$. (**D, F and J)** One-way ANOVA followed by Dunnett's *post hoc* test for multiple comparisons. * $P<0.05$ and ** $P<0.01$.

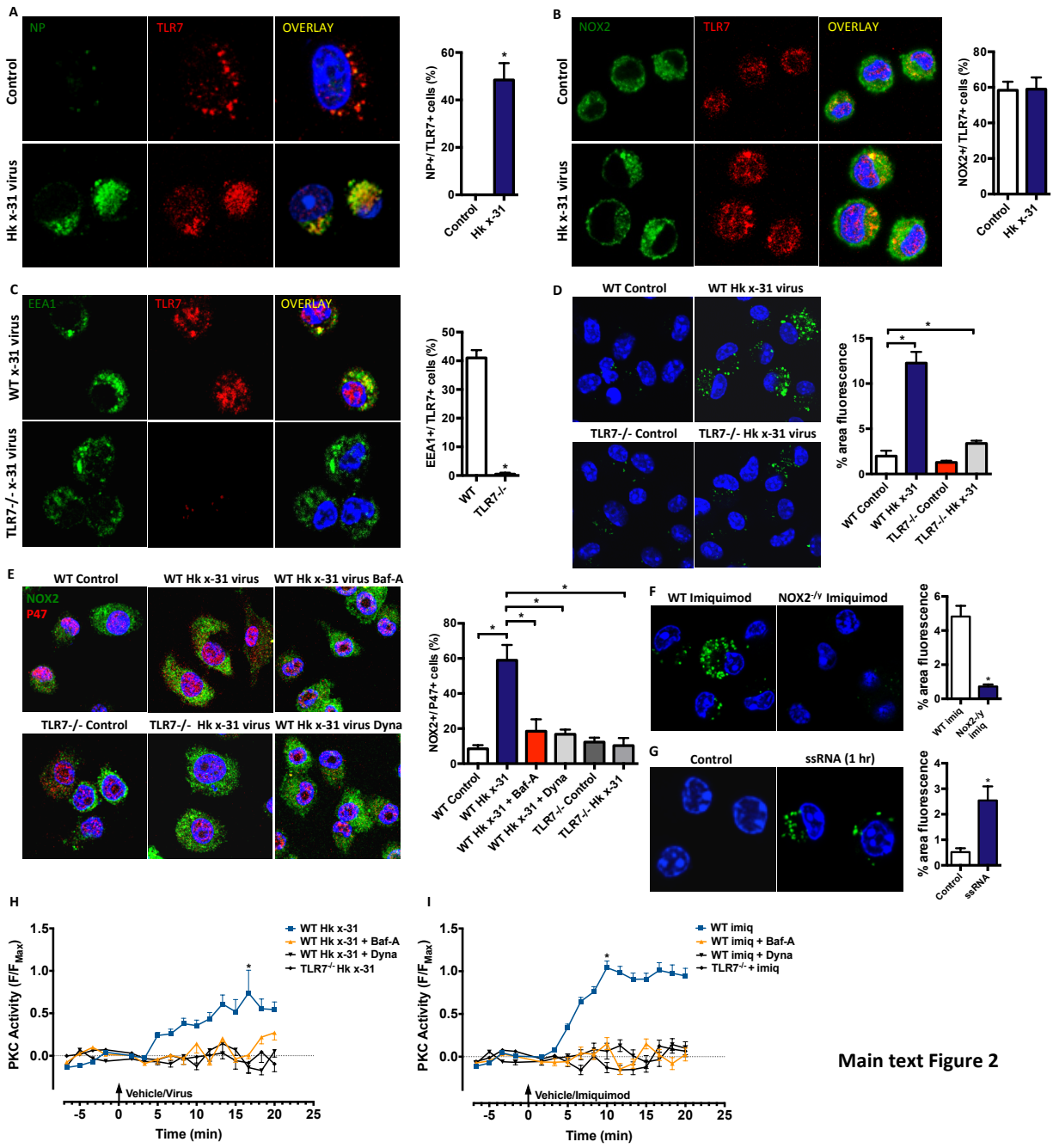

Main text Figure 2

Figure 2 Co-localization of TLR7 with influenza A virus, NOX2 and EEA1 is a signaling platform for endosomal ROS generation to influenza A virus via a TLR7 and PKC-dependent mechanism.

(A-C) Confocal microscopy of mouse primary alveolar macrophages that were untreated or infected with influenza A virus HKx31 (MOI of 10) and labeled with antibodies to TLR7 and either **A)** influenza A virus NP, **B)** NOX2 or **C)** EEA1, and then with 4',6'- diamidino-2-phenylindole (DAPI). Quantification data from multiple experiments are also shown (n=5).

(D) Endosomal ROS production in WT and TLR7$^{-/-}$ mouse primary alveolar macrophages as assessed by Oxyburst (100 μM) fluorescence microscopy in the absence or presence of HKx31 virus and labeled with DAPI (n=6).

(E) Immunofluorescence microscopy for assessment of NOX2 and p47phox association. WT and TLR7$^{-/-}$ immortalized bone marrow-derived macrophages (BMMs) were untreated or infected with HKx31 virus, (MOI of 10) in the absence or presence of dynasore (Dyna; 100 μM) or bafilomycin A (Baf-A; 100 nM), and then labeled with antibodies to NOX2 and p47phox**.** Also shown is the quantification of the results (n=5).

(F-I) Endosomal ROS production in WT and NOX2$^{-/y}$ mouse primary alveolar macrophages as assessed by Oxyburst fluorescence microscopy in the absence or presence of **F)** imiquimod (Imiq; 10 μg/ml) and **G)** ssRNA (100 μg/ml) and co-labeled with DAPI. (n=5).

(H-I) Cytosolic PKC activity as assessed by FRET analysis in WT and TLR7$^{-/-}$ BMMs. Cells were either treated with vehicle controls or with bafilomycin A (100nM) or dynasore (100μM) and then exposed for 25 min to influenza A virus (HKx31, MOI of 10) or imiquimod (10 μg/ml) (n=3).

(A-F and H) Images are representative of >150 cells analysed over each experiment. Original magnification X100. All data are represented as mean ± SEM. **(A, B, C, F and G)** Student's unpaired t-test * P<0.05. (**D, E, H and I)** One-way ANOVA followed by Dunnett's *post hoc* test for multiple comparisons. * P<0.05.

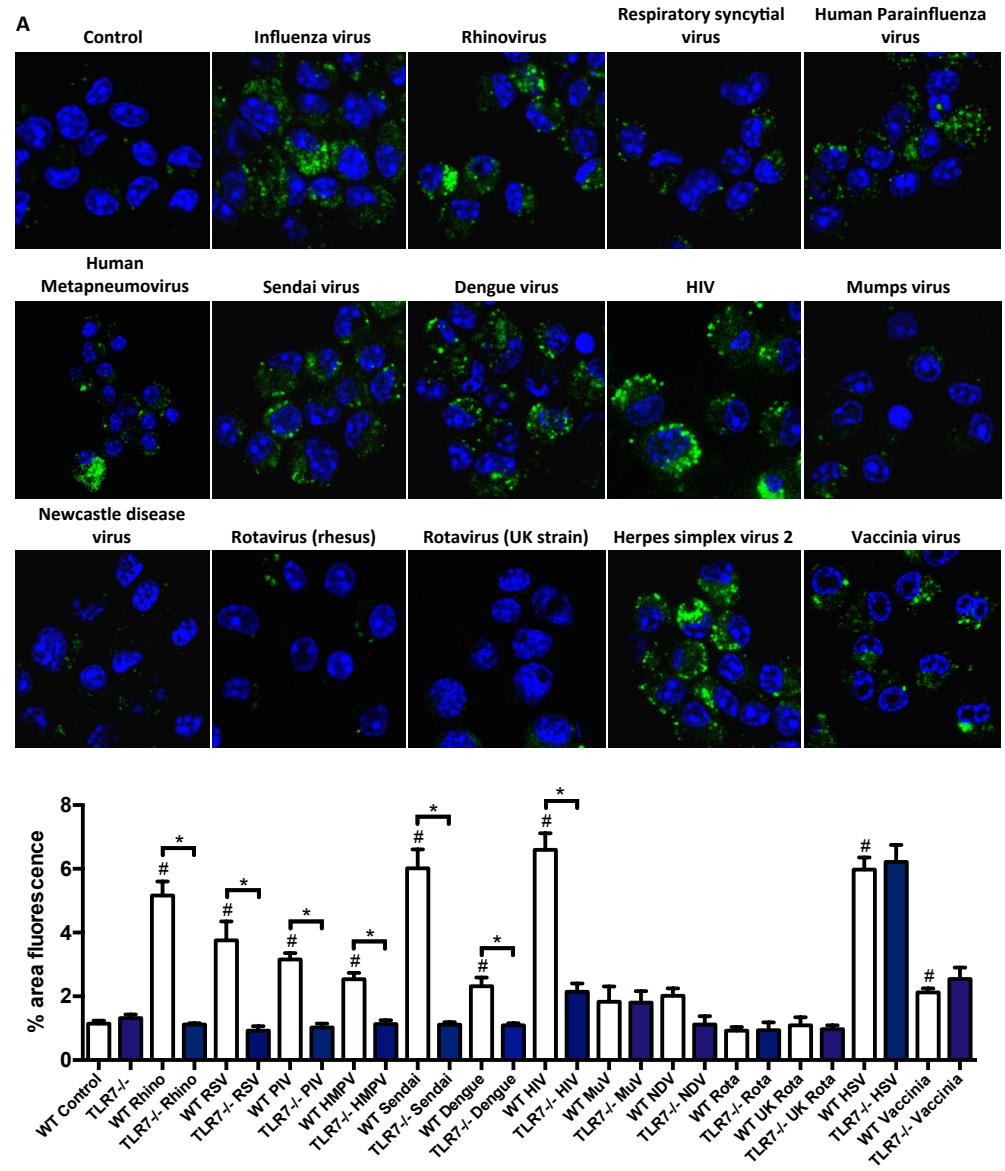

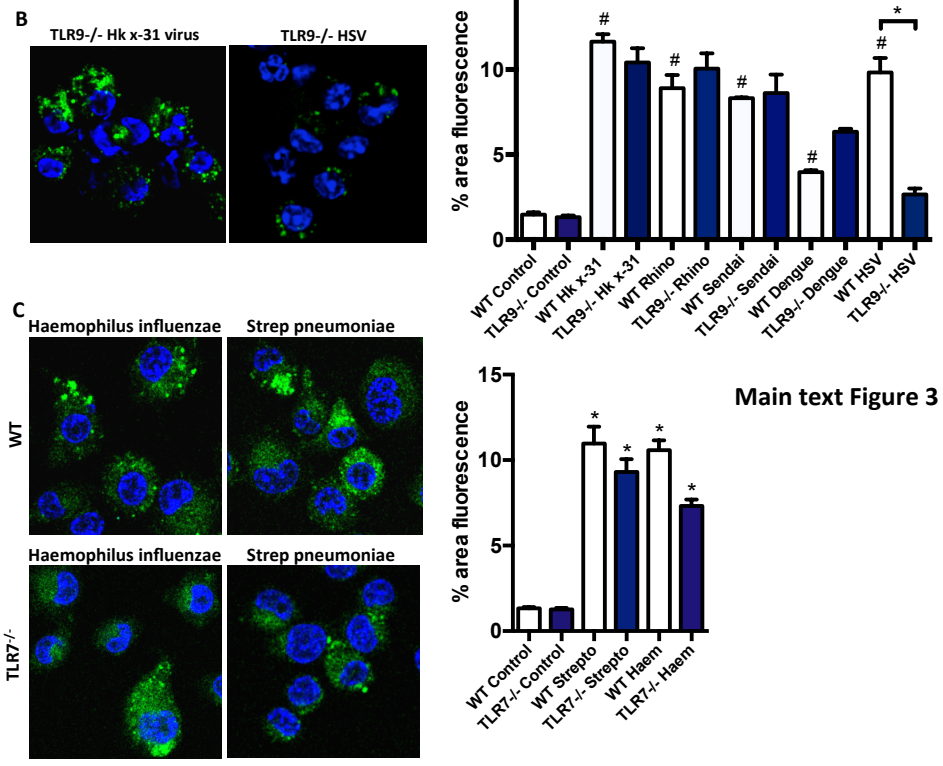

Main text Figure 3

Figure 3 Endosomal ROS production to ssRNA and DNA viruses are distinct from bacteria-induced ROS

(A) Endosomal ROS production in WT and TLR7$^{-/-}$ bone marrow-derived macrophages as assessed by OxyBURST (100 μM) fluorescence microscopy in the absence or presence of influenza A virus (HKx31 virus), rhinovirus (rhino), respiratory synctitial virus (RSV), human parainfluenza virus (PIV), human metapneumovirus (HMPV), sendai virus, dengue virus, human immunodeficiency virus (HIV), mumps virus (MuV), Newcastle disease virus (NDV), rotavirus (UK and bovine strains), herpes simplex virus 2 (HSV-2) and vaccinia virus and labeled with DAPI. Also shown is the quantification of the results (n=5).

(B) Endosomal ROS production in WT and TLR9$^{-/-}$ mouse primary alveolar macrophages as assessed by OxyBURST fluorescence microscopy in the absence or presence of HKx31 virus, rhinovirus, sendai virus, dengue virus, and herpes simplex virus 2 (HSV-2) and labeled with DAPI (n=5).

(C) Phagosomal superoxide production to *Haemophilus influenzae* and *Streptococcus pneumoniae* as assessed by OxyBURST fluorescence microscopy in WT and TLR7$^{-/-}$ immortalized bone marrow derived macrophages (n=3).

A, B and C Images are representative of >100 cells analysed over each experiment. Original magnification X100. All data are represented as mean ± SEM. One-way ANOVA followed by Dunnett's *post hoc* test for multiple comparisons. #P<0.05 compared to WT control. * P<0.05 comparisons indicated by horizontal bars.

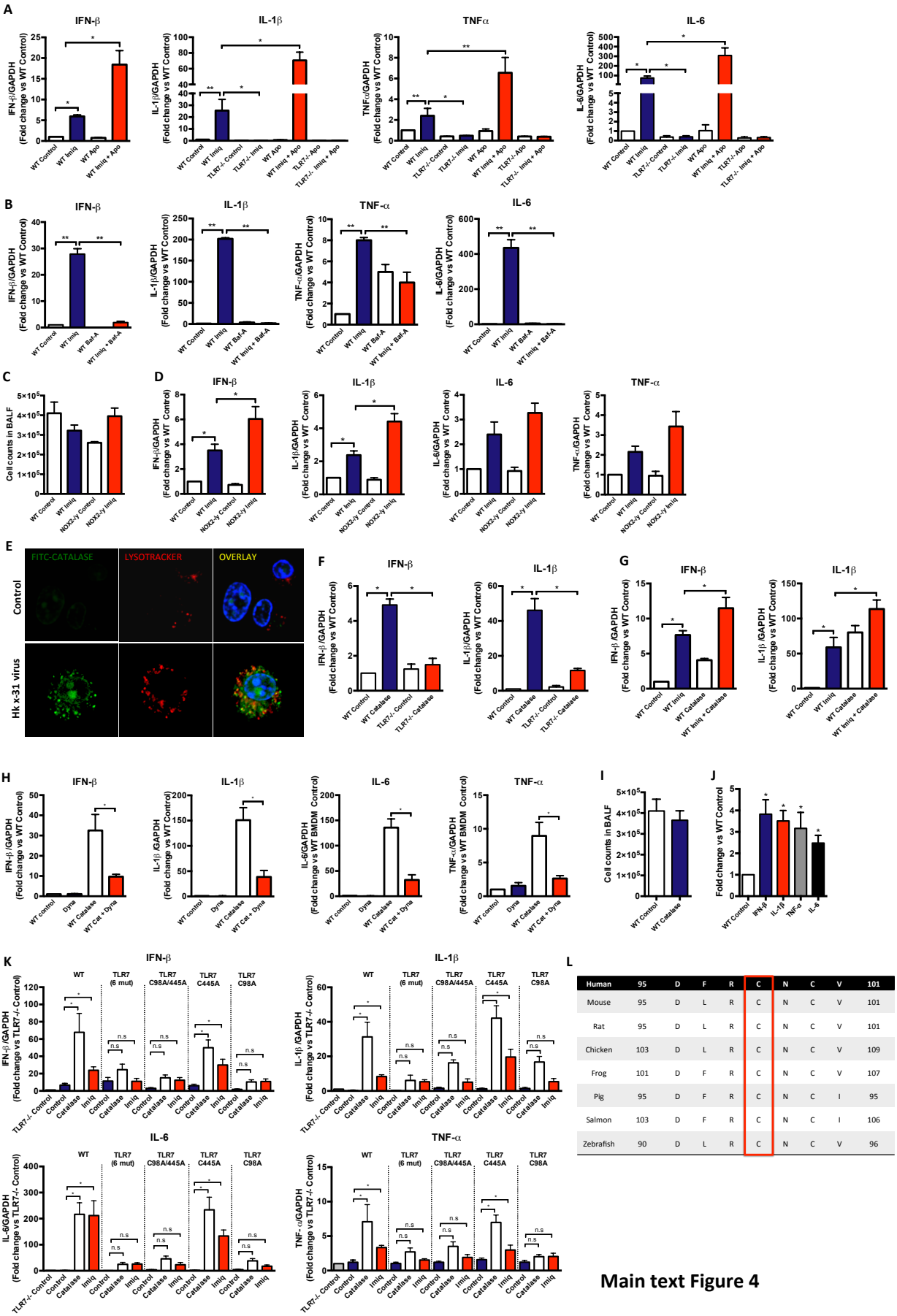

Human	95	D	F	R	C	N	C	V	101
Mouse	95	D	L	R	C	N	C	V	101
Rat	95	D	L	R	C	N	C	V	101
Chicken	103	D	L	R	C	N	C	V	109
Frog	101	D	F	R	C	N	C	V	107
Pig	95	D	F	R	C	N	C	I	95
Salmon	103	D	F	R	C	N	C	I	106
Zebrafish	90	D	L	R	C	N	C	V	96

Main text Figure 4

Figure 4 Endosomal NOX2 oxidase-derived hydrogen peroxide (H_2O_2) suppresses cytokine expression in response to TLR7 activation *in vitro* and *in vivo*.

(A-B) WT and TLR7$^{-/-}$ immortalized bone marrow-derived macrophages (BMMs) were untreated or treated with imiquimod (Imiq; 10 μg/mL) in the absence or presence of **A)** apocynin (Apo; 300 μM) or **B)** bafilomycin A (Baf-A; 100 nM), and IFN-β, IL-1β, TNF-α and IL-6 mRNA expression determined by QPCR after 24hr (n=6).

(C-D) WT and NOX2$^{-/y}$ mice were administered with imiquimod (50 μg/mouse, intranasal) and **C)** total airway inflammation and **D)** cytokine expression assessed 24 h later (n=5).

(E) WT mouse primary alveolar macrophages were either left untreated or treated with FITC-labeled catalase for 5 min prior to infection with HKx31 virus (MOI of 10). Cells were labeled for Lysotracker (50 nM) and colocalization of Lysotracker and FITC catalase assessed by confocal microscopy. Images are representative of > 50 cells analyzed over each experiment. Original magnification X100 (n=3).

(F) WT and TLR7$^{-/-}$ BMMs were left untreated or treated for 1hr with catalase (1000 U/mL) and IFN-β and IL-1β, mRNA expression determined by QPCR after 24hr (n=7).

(G) WT BMMs were left untreated or treated for 1hr with imiquimod in the absence or presence of catalase (1000 U/mL), IFN-β and IL-1β, mRNA expression assessed 24hr later by QPCR (n=6).

(H) WT immortalized bone marrow-derived macrophages were treated for 30 mins with either DMSO (0.1%) or dynasore (Dyna; 100μM) and then with catalase (1000 U/mL) for 1hr. Cytokine mRNA expression determined by QPCR after 24 h (n=6).

(I and J) Catalase (1000 U/mouse, intranasal) was administered to WT mice and I) total airway inflammation and **J)** lung cytokine expression assessed 24 h later (n=5).

(K) TLR7$^{-/-}$ BMMs were transfected with empty vector, WT TLR7 or with either TLR7 with cysteines 98, 260, 263, 270, 273 and 445 mutated to alanine (TLR7 6 mut), TLR7 with cysteines 98 and 445 mutated to alanine (TLR7C98A/445A) or with TLR7 with cysteines 445 (TLR7C445A) or 98 (TLR7C98A) mutated to alanine. After 48 h, cells were left untreated or treated for 1hr with either catalase (1000 U/mL) or imiquimod (10μg/ml) and cytokine expression assessed 24 h later (n=6). (n.s) Denotes not significant.

(L) Multiple sequence alignment with CLUSTAL OMEGA showing across species conservation of Cys 98 on TLR7.

(A, B, D, F, G, H, J) Responses are relative to GAPDH and then expressed as a fold-change above WT controls or in the case in **H)** above TLR7$^{-/-}$ controls.

(A-D, F-J) Data are represented as mean ± SEM. One-way ANOVA followed by Dunnett's *post hoc* test for multiple comparisons. Statistical significance was accepted when $P<0.05$. * $P<0.05$; ** $P<0.01$.

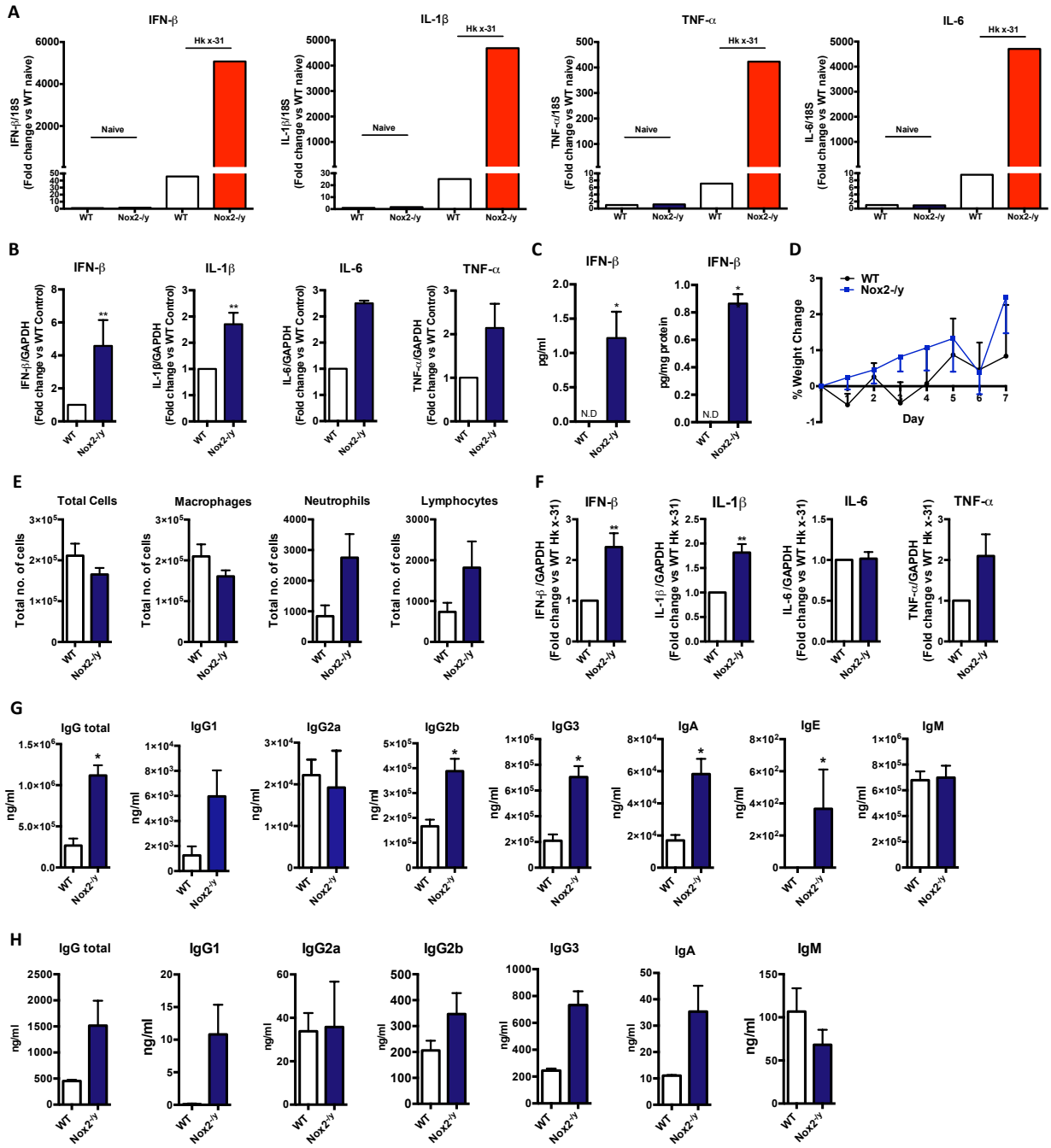

Main text Figure 5

Figure 5 Inhibition of NOX2 oxidase increases expression of Type I IFN and IL-1β, and antibody production to influenza A virus infection

(A) Alveolar macrophages from WT and Nox2$^{-/y}$ mice were left untreated or infected with HKx31 influenza A virus (MOI of 10) for analysis of IFN-β, IL-1β, TNF-α and IL-6 mRNA expression by QPCR. Data represents RNA pooled from 8 separate mice.

(B-C) WT and Nox2$^{-/y}$ mice were infected with live HKx31 influenza A virus (1×10^5 PFU per mouse) and **B)** cytokine mRNA expression and **C)** IFN-β protein expression in BALF were assessed 3 days later (n=5).

(D-H) WT and Nox2$^{-/y}$ mice were infected with inactivated HKx31 influenza A virus (equivalent to 1×10^4 PFU per mouse) for measurements at day 7 of: **D)** body weight; **E)** airway inflammation and differential cell counts (i.e. macrophages, neutrophils and lymphocytes); **F)** cytokine expression in whole lung (responses are shown as fold change relative to 18S) and **G)** serum and and **H)** BALF antibody levels (n=6).

Data are shown as mean ± SE. Unpaired t-test; statistical significance taken when the $P<0.05$. * $P<0.05$. ** $P<0.01$.

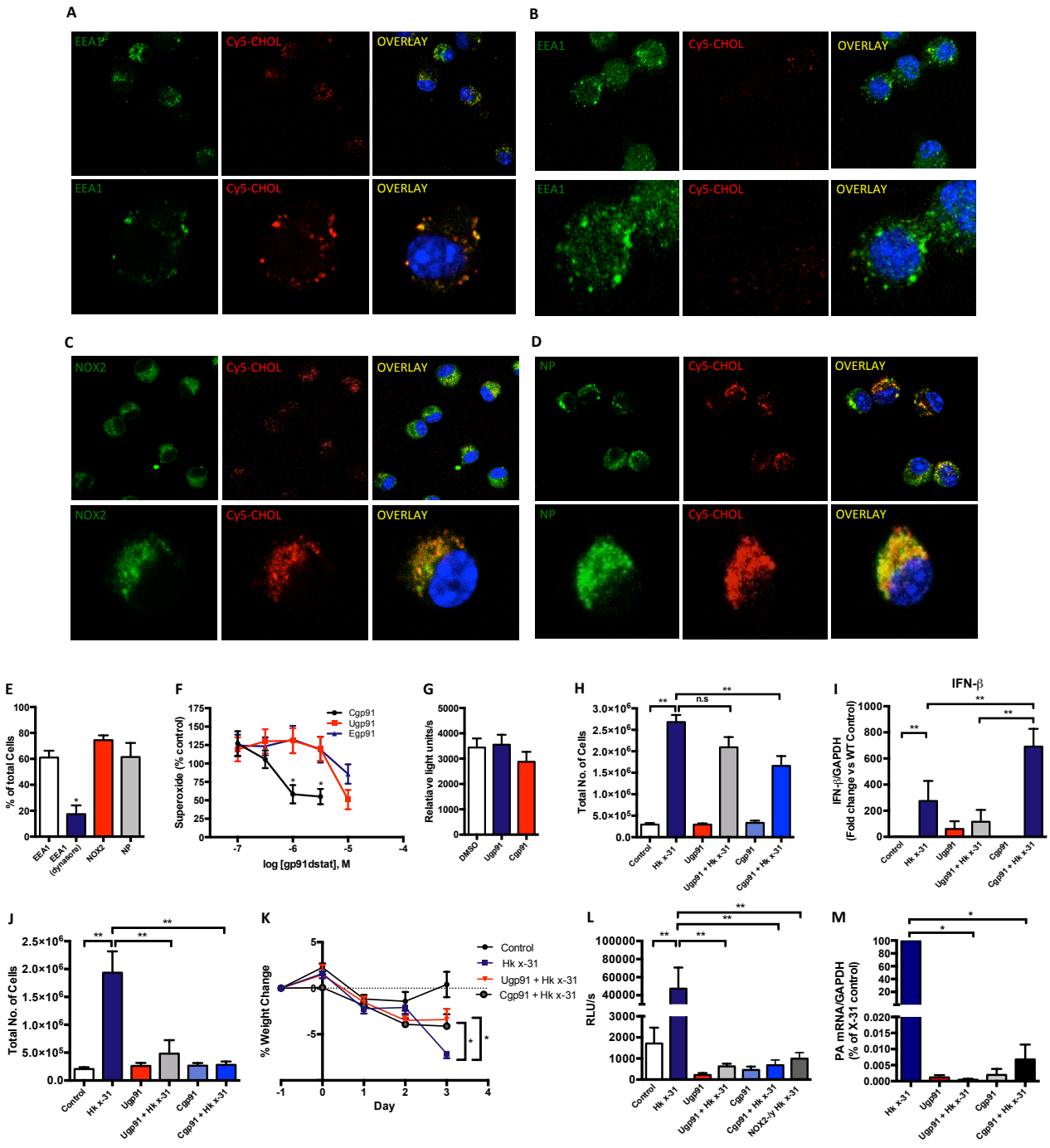
A
EEA1
Cy5-CHOL
OVERLAY
B
C
NOX2
D
NP
E
% of total Cells
EEA1
EEA1 (dynasore)
NOX2
NP
F
Superoxide (% control)
log [gp91dstat], M
Cgp91
Ugp91
Egp91
G
Relative light units/s
DMSO
H
Total No. of Cells
n.s
Control
Hk x-31
Ugp91
Ugp91 + Hk x-31
Cgp91
Cgp91 + Hk x-31
I
IFN-β
IFN-β/GAPDH
(Fold change vs WT Control)
J
K
% Weight Change
Day
Control
Hk x-31
Ugp91 + Hk x-31
Cgp91 + Hk x-31
L
RLU/s
NOX2-/y Hk x-31
M
PA mRNA/GAPDH
(% of X-31 control)

Figure 6 Endosome targeted delivery of a NOX2 oxidase inhibitor protects mice following influenza A virus infection *in vivo*

(A-E) Alveolar macrophages from WT mice were treated with the Cy5 cholestanol-PEG linker fluorophore (Cy5-chol; 100nM) for 30 min and either left untreated or infected with HKx31 influenza A virus (MOI of 10). Cells were then counter labeled with antibodies to either: **A and B)** EEA1, **C)** NOX2 or **D)** influenza A nucleoprotein (NP) and imaged with confocal microscopy. **B)** Cells were pretreated with dynasore (100μM) for 30 mins prior to exposure to Cy5-cholestanol. **E**) Quantification of these data (n=5).

(F) RAW 264.7 macrophages were either untreated or treated with various concentrations of cholestanol-conjugated gp91ds-TAT (Cgp91), ethyl conjugated gp91ds-TAT (Egp91) or unconjugated gp91ds-TAT (Ugp91) for 30 mins prior to quantifying ROS production by L-O12 enhanced chemiluminescence (n=7).

(G) Superoxide production *via* the xanthine/xanthine oxidase cell-free assay in the absence or presence of Ugp91ds-TAT, (1μM) or Cgp91ds-TAT (1μM) (n=6, RLU/s=relative light units per second).

(H-I) Ugp91ds-TAT or Cgp91ds-TAT (0.02mg/kg/day) were delivered intranasally to WT mice once daily for 4 days. At 24h after the first dose of inhibitor, mice were either treated with saline or infected with HKx31 influenza A virus (1×10^5 PFU per mouse). Mice were culled at day 3 post-infection and **H)** airway inflammation was assessed by BALF cell counts and **I)** lung IFN-β mRNA was determined by QPCR (n=7). (n.s) denotes not significant.

(J-M) Mice were subjected to the NOX2 inhibitor treatment regime and virus infection protocol as in **H)** except NOX2 inhibitors were delivered at a dose of 0.2mg/kg/day. Analysis of **J)** airway inflammation by BALF counts, **K)** body weight (% weight change from the value measured at Day -1), **L)** ROS production by BALF inflammatory cells with L-O12 enhanced chemiluminescence and **M)** viral mRNA by QPCR. Data are represented as mean ± SEM.

E) Unpaired t-test; statistical significance taken when the $P<0.05$. **(F-L)** One-way ANOVA followed by Dunnett's *post hoc* test for multiple comparisons. **M)** Kruskal-Wallis test with Dunn's *post hoc* for multiple comparisons. Statistical significance was accepted when $P<0.05$. * $P<0.05$; ** $P<0.01$.

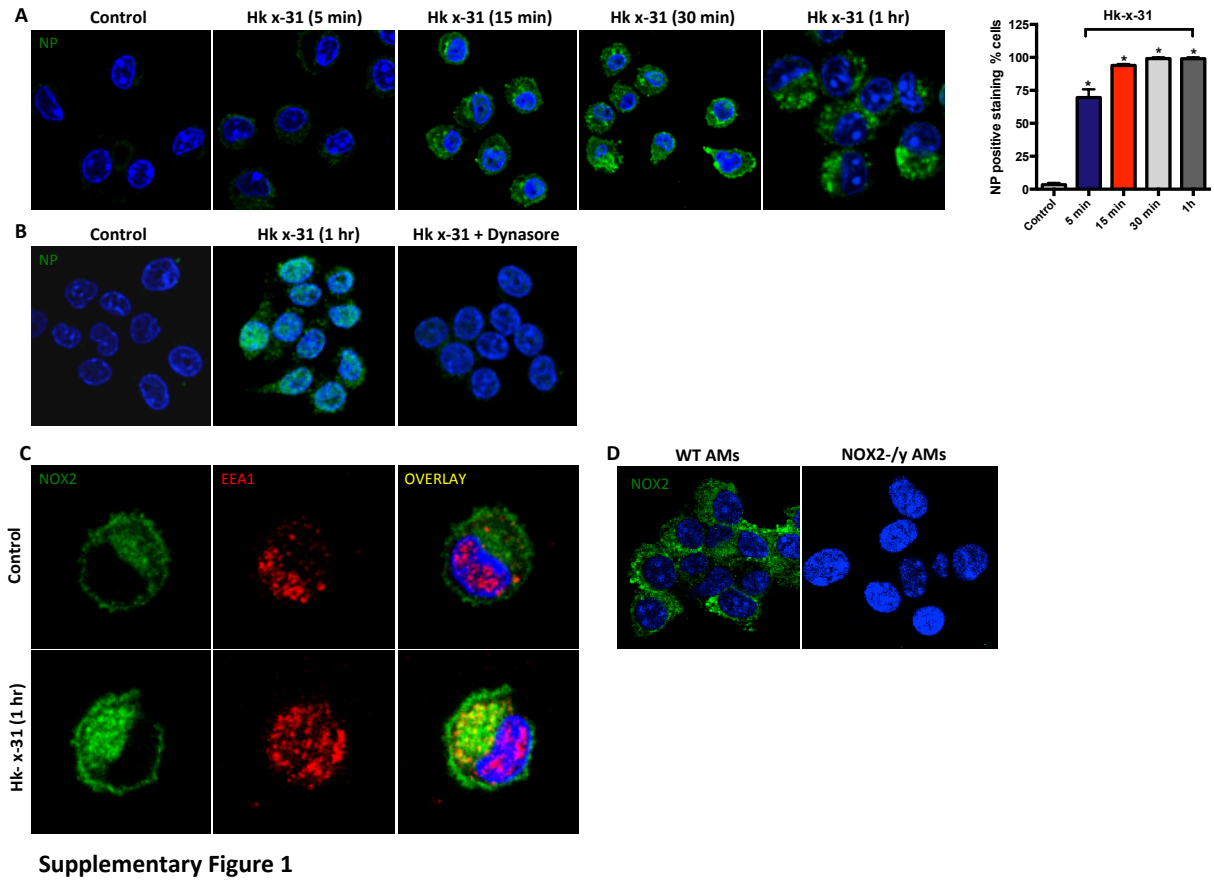

Supplementary Figure 1

Supplementary Figure S1. Dynamin-dependent endocytosis of influenza A virus and entry into early endosomes.

(A, B) Confocal microscopy of WT mouse primary alveolar macrophages that were infected with the HKx31 strain of influenza A virus (MOI of 10 at various time points) in the absence and presence of the dynamin inhibitor, Dynasore (100 μM), and then labeled as indicated with antibody to influenza A virus nucleoprotein (NP) and 4',6'- diamidino-2-phenylindole (DAPI) (n=5).

(C) Alveolar macrophages infected with influenza A virus as in A), and then labeled with the early endosome antigen 1 (EEA1) antibody and NOX2 antibody.

(D) WT and NOX2$^{-/y}$ alveolar macrophages were labeled with the NOX2 antibody and DAPI.

(A-D) Images are representative of > 100 cells analysed over each experiment. Original magnification X100.

Data are shown as mean ± SE. One-way ANOVA followed by Dunnett's *post hoc* test for multiple comparisons. * P<0.05 compared to control.

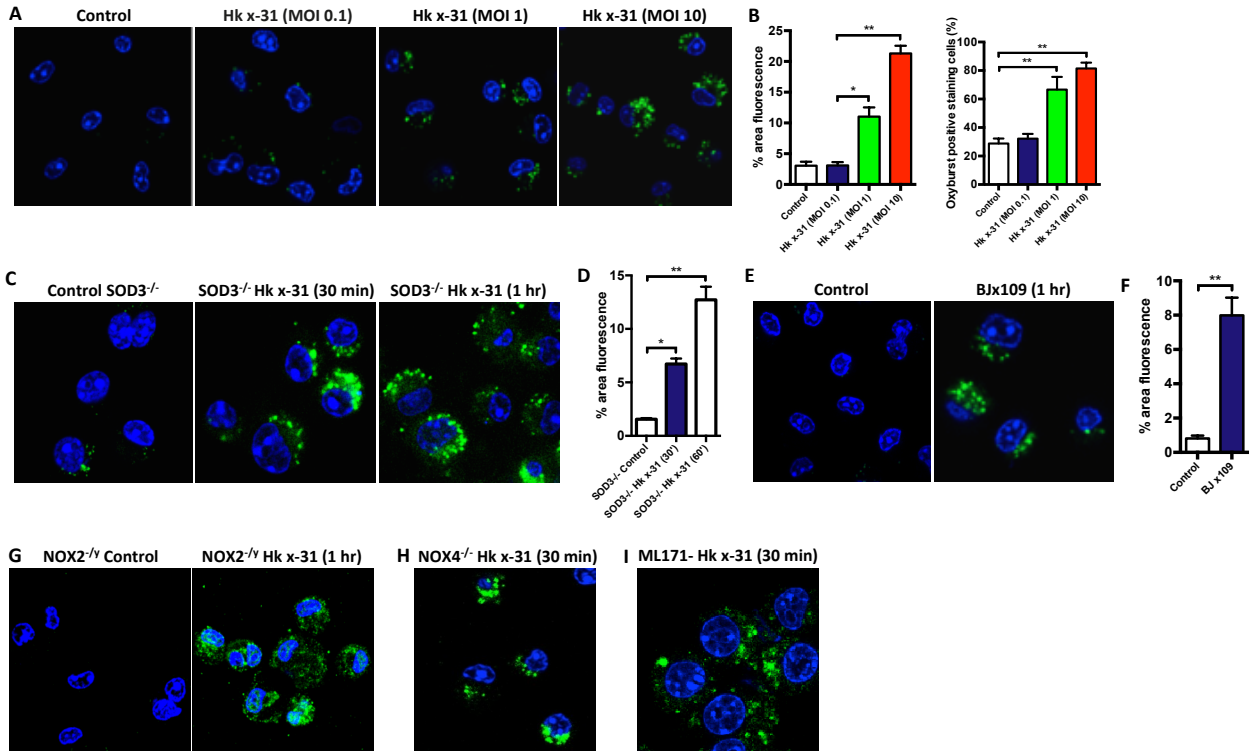

Supplementary Figure 2

Supplementary Figure S2. Influenza A viruses induce dose-dependent elevations in endosomal NOX2 oxidase-dependent ROS production.

(A, B) Endosomal ROS production in WT mouse primary alveolar macrophages as assessed by OxyBURST (100 μM) confocal fluorescence microscopy in the absence or presence of various doses of HKx31 virus (MOI of 0.1, 1 and 10) and labeled with DAPI (n=5).

(C, D) Endosomal ROS production following infection with the HKx31 virus in alveolar macrophages taken from superoxide dismutase 3 deficient ($SOD3^{-/-}$) mice (n=5).

(E, F) Endosomal ROS production in WT alveolar macrophages following infection with the BJx109 virus (n=6).

(G) Influenza NP fluorescence in alveolar macrophages taken from $NOX2^{-/y}$ mice demonstrating that influenza internalization is unaffected by the expression of NOX2 (n=3).

(H and I) Endosomal ROS production in **H)** $NOX4^{-/-}$ mouse primary alveolar macrophages or **I)** WT mouse primary alveolar macrophages treated with the NOX1 inhibitor ML171 (100nM) as assessed by OxyBURST fluorescence microscopy in the presence of HKx31 virus and labeled with DAPI (n=5).

(A, C, E, G, H, and I) Images are representative of >100 cells analysed over each experiment. Original magnification X100. All data are represented as mean ± SEM. **(B and D)** One-way ANOVA followed by Dunnett's *post hoc* test for multiple comparisons. * $P<0.05$ comparisons indicated by horizontal bars. **$P<0.01$. **(F)** Unpaired t-test; statistical significance taken when the $P<0.05$. ** $P<0.01$

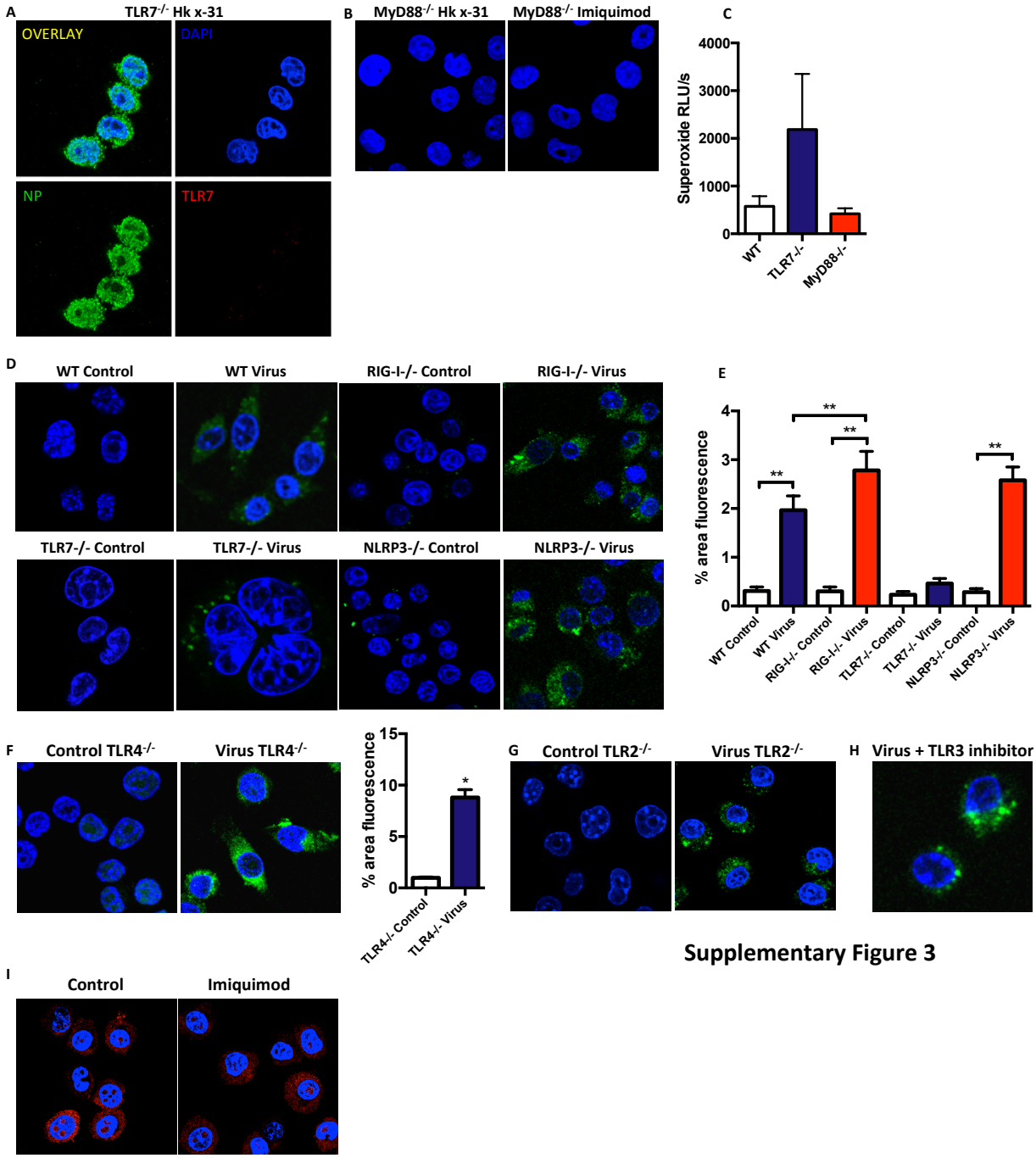

Supplementary Figure 3

Supplementary Figure S3. Endosomal ROS production to influenza A virus is dependent on MyD88 but independent of RIG-I, NLRP3, TLR2, TLR3, and TLR4.

(A) TLR7$^{-/-}$ immortalized bone marrow-derived macrophages (BMMs) were infected with HKx31 influenza A virus ((MOI of 10) and then stained with anti-TLR7 antibody and anti nucleoprotein (NP) antibody, and then DAPI (n=3).

(B) MyD88$^{-/-}$ immortalized BMMs were infected with HKx31 influenza A virus ((MOI of 10) or exposed to imiquimod (10 μg/mL) and endosomal ROS production was assessed by OxyBURST (100 μM) fluorescence microscopy (n=3).

(C) Phorbol-dibutyrate-stimulated, NOX2 oxidase-dependent superoxide production in WT, TLR7$^{-/-}$ and MyD88$^{-/-}$ immortalized bone marrow-derived macrophages measured by L-O12-enhanced chemiluminescence (n=3); RLU/s= relative light units/sec.

(D-G) Endosomal ROS production in WT, RIG-I$^{-/-}$, TLR7$^{-/-,}$ and NLRP3$^{-/-}$ and **F)** TLR4$^{-/-}$ or **G)** TLR2$^{-/-}$ BMMs, as assessed by OxyBURST fluorescence microscopy in the absence or presence of HKx31 virus and co-labeled with DAPI (n=3-5).

(H) WT mouse primary alveolar macrophages were infected with HKx31 virus (MOI of 10) in the presence of the TLR3 inhibitor (50 μM, n=3).

(I) WT mouse primary alveolar macrophages were treated with imiquimod (10μg/mL) for 60 mins and mitochondrial superoxide measured by MitoSOX confocal fluorescence microscopy and co-labeled with DAPI (n=3).

(A, B, D, F, G, H and I) Images are representative of >100 cells analyzed over each experiment. Original magnification X100. All data are represented as mean ± SEM. **(E)** One-way ANOVA followed by Dunnett's *post hoc* test for multiple comparisons. * $P<0.05$ and ** $P<0.01$ comparisons indicated by horizontal bars. **(F)** Unpaired t-test; statistical significance taken when the $P<0.05$.

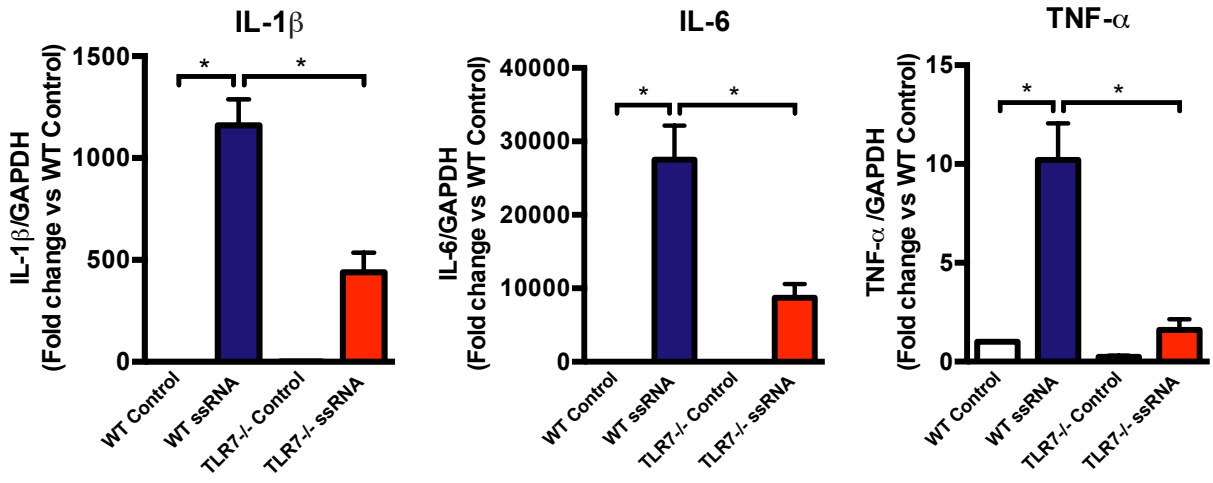

Supplementary Figure 4

Supplementary Figure S4. Single stranded RNA (ssRNA) drives IL-1β, TNF-α and IL-6 mRNA expression *via* a TLR7-dependent mechanism in macrophages.

WT and TLR7$^{-/-}$ immortalized bone marrow derived macrophages were treated with ssRNA lyoVec (100 μM) and cytokine expression was determined by QPCR after 24 h. One-way ANOVA followed by Dunnett's *post hoc* test for multiple comparisons. Statistical significance was taken when the $P<0.05$ (n=6).

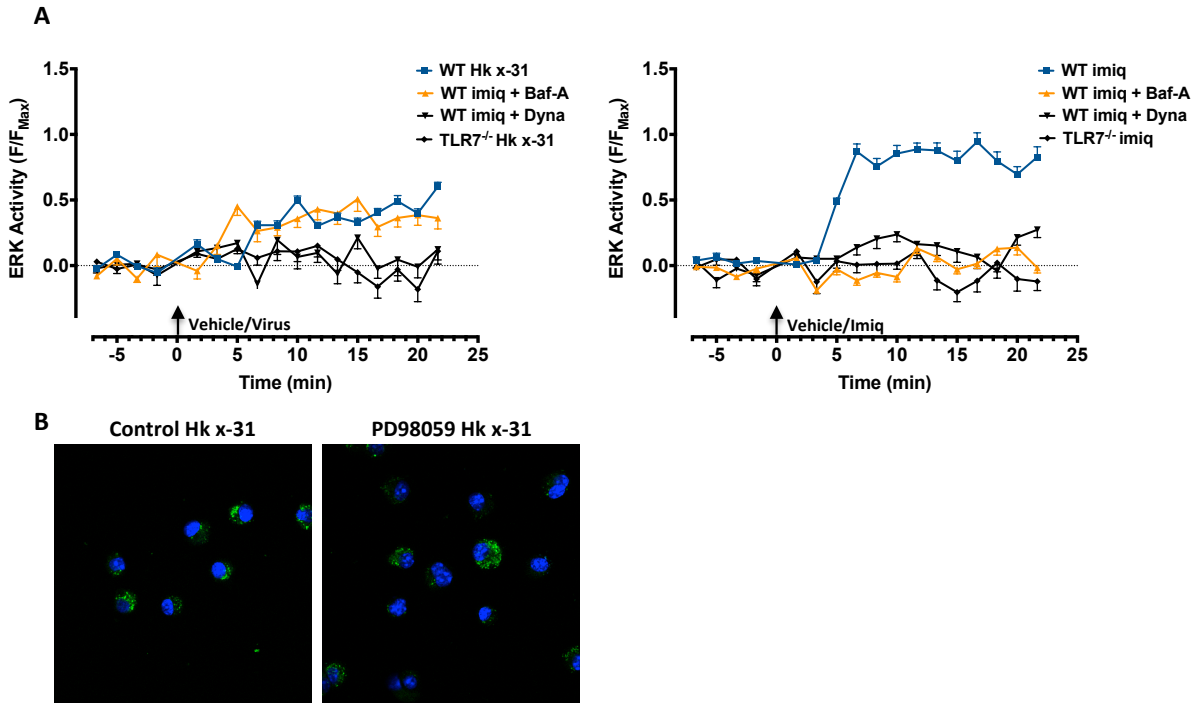

Supplementary Figure 5

Supplementary Figure S5. Influenza A virus and imiquimod trigger ERK1/2-phosphorylation in a TLR7-dependent manner whereas ERK does not contribute to activation of NOX2 oxidase.

(A) Cytosolic ERK activity as assessed by FRET analysis in WT and TLR7$^{-/-}$ bone marrow-derived macrophages. Cells were either treated with vehicle controls or with bafilomycin A (Baf-A; 100 nM) or Dynasore (Dyna; 100 μM) and then exposed for 25 min to HKx31 influenza A virus (MOI of 10) or imiquimod (imiq; 10 μg/ml) (n=3).

(B) Endosomal superoxide production to HKx31 influenza A virus in WT alveolar macrophages as assessed by OxyBURST (100 μM) fluorescence microscopy in the absence or presence of the MEK inhibitor PD98059 (30 μM).

All images are representative of >100 cells analyzed over each experiment. Original magnification X100. (n=4).

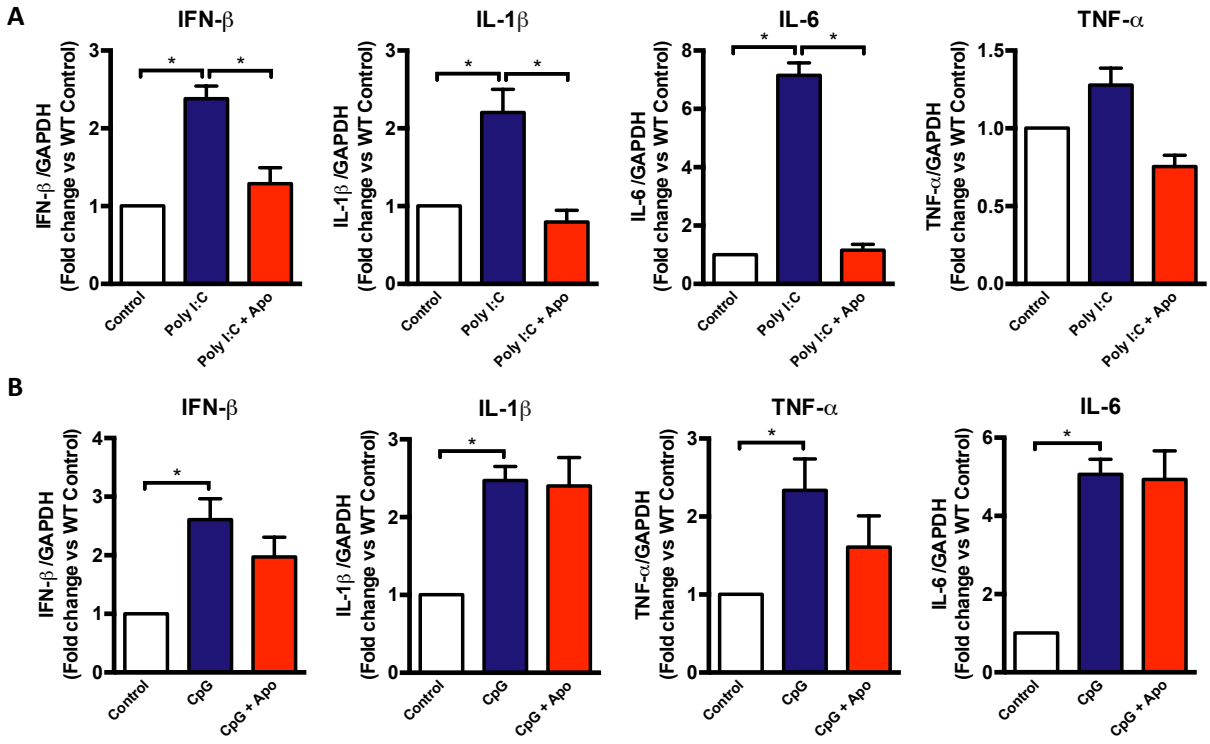

Supplementary Figure 6

Supplementary Figure S6. Effect of NOX2 oxidase inhibition on cytokine expression by TLR3 agonist, poly I:C.

or TLR9 agonist CpG. WT immortalized bone marrow derived macrophages were treated with **A)** poly I:C (25 μg/mL) or **B)** CpG (10 μg/mL) in the absence or presence of apocynin (Apo; 300 μM) and cytokine expression was determined by QPCR after 24 h (n=6). Responses are relative to GAPDH and then expressed as a fold-change above controls All data are represented as mean ± SEM. Kruskal-Wallis test with Dunn's *post hoc* for multiple comparisons. Statistical significance was taken when the $P<0.05$. * $P<0.05$.

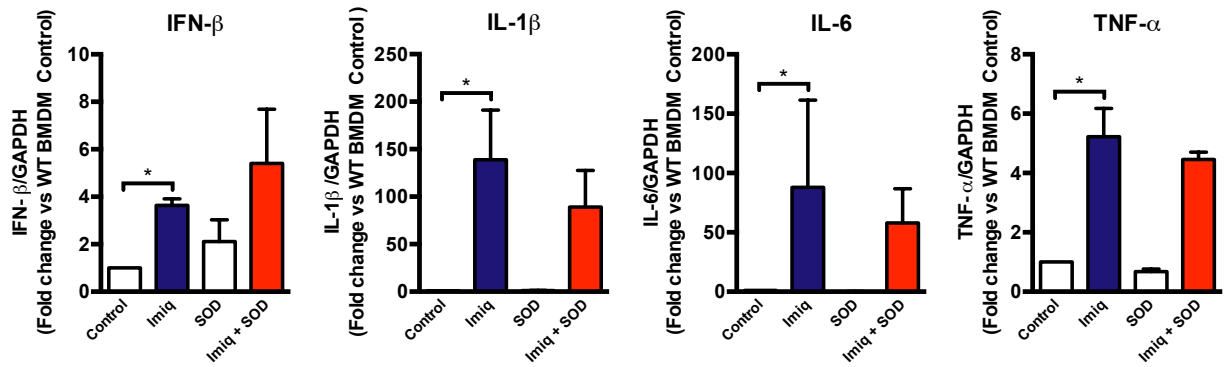

Supplementary Figure 7

Supplementary Figure S7. TLR7-dependent cytokine production to imiquimod is unaffected by endosomal superoxide production.

WT immortalized bone marrow derived macrophages were treated with imiquimod (Imiq; 10 μg/mL) in the absence or presence of superoxide dismutase (SOD; 300 U/mL) and cytokine expression was determined by QPCR after 24 h. Responses are relative to GAPDH and then expressed as a fold-change above WT controls. All data are represented as mean ± SEM. Kruskal-Wallis test with Dunn's *post hoc* for multiple comparisons. Statistical significance was taken when the $P<0.05$. * $P<0.05$ (n=6).

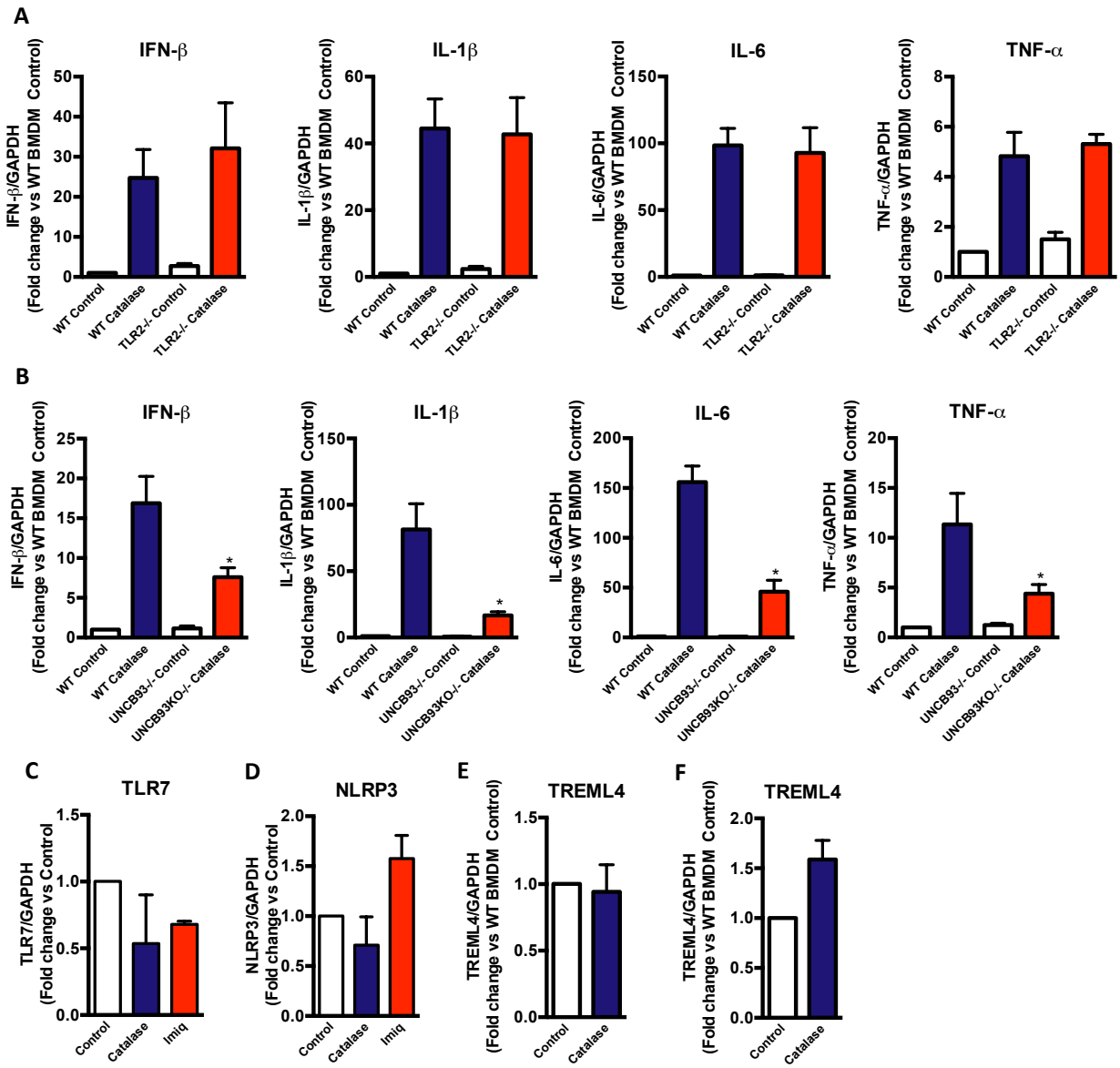

Supplementary Figure 8

Supplementary Figure S8. Catalase-dependent elevation in cytokine expression is suppressed by deletion of UNCB93 and does not involve alterations in TLR2, TLR7, NLRP3 or TREML4 expression.

(A) WT and TLR2$^{-/-}$ immortalized BMMs were treated with catalase (1000 U/mL) for 1hr and cytokine mRNA expression determined by QPCR after 24 h (n=6).

(B) WT and UNCB93$^{-/-}$ immortalized BMMs were treated with catalase (1000 U/mL) for 1hr and cytokine mRNA expression determined by QPCR after 24 h (n=6).

(C-E) WT BMMs were treated for 1hr with either catalase or imiquimod and C) TLR7, D) NLRP3 or TREML4 mRNA expression determined by QPCR after 24 h (n=6).

(F) Mice were intranasally treated with catalase (1000U/mouse) and then lung expression of TREML4 was determined by QPCR (n=5).

Responses are relative to GAPDH and then expressed as a fold-change above WT controls. All data are represented as mean ± SEM. Kruskal-Wallis test with Dunn's *post hoc* for multiple comparisons. Statistical significance was taken when the $P<0.05$. * $P<0.05$.

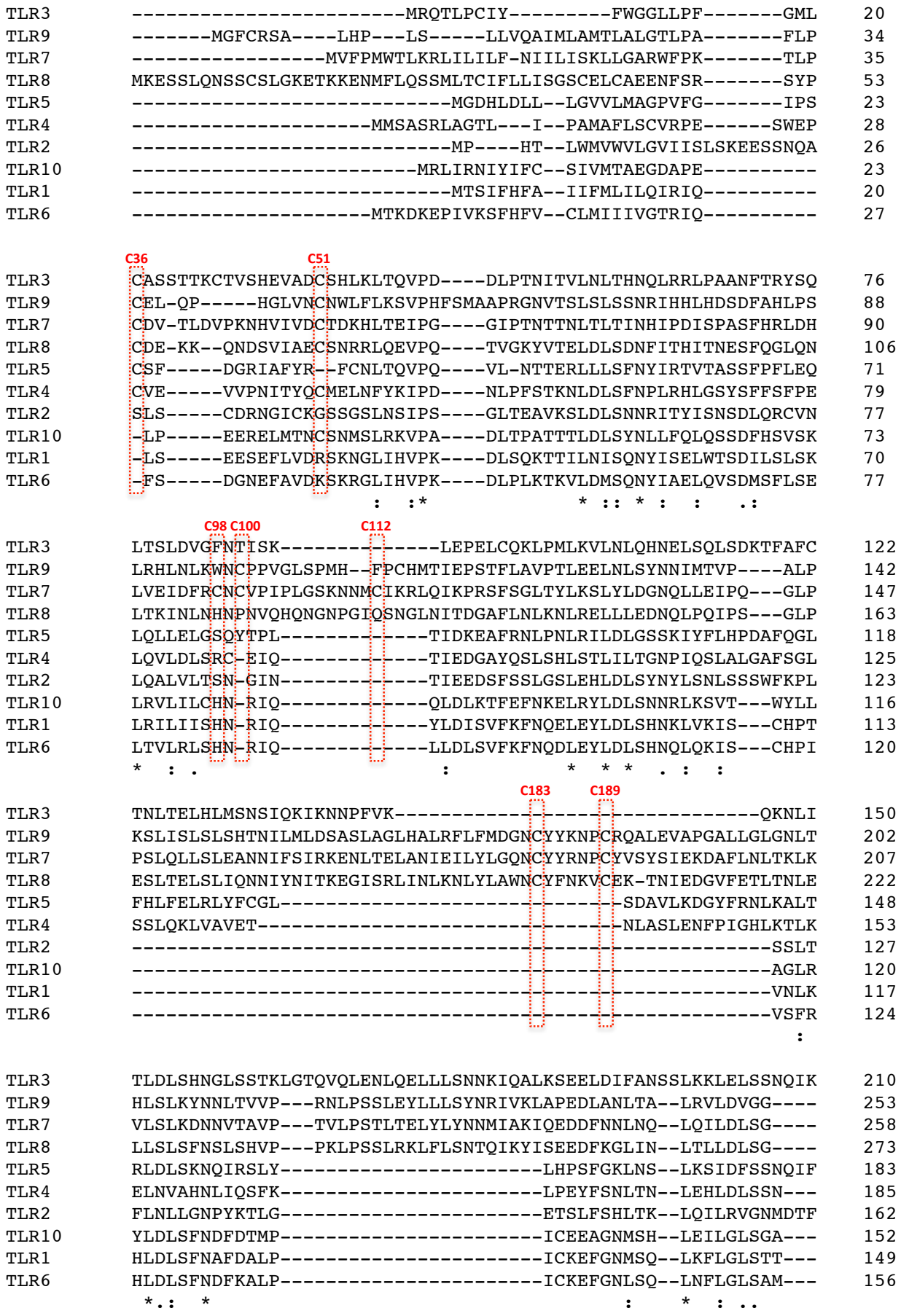
TLR3 ----------MRQTLPCIY---------FWGGLLPF-------GML 20
TLR9 -------MGFCRSA----LHP---LS-----LLVQAIMLAMTLALGTLPA-------FLP 34
TLR7 ----------------MVFPMWTLKRLILILF-NIILISKLLGARWFPK-------TLP 35
TLR8 MKESSLQNSSCSLGKETKKENMFLQSSMLTCIFLLISGSCELCAEENFSR-------SYP 53
TLR5 ----------MGDHLDLL--LGVVLMAGPVFG-------IPS 23
TLR4 ----------MMSASRLAGTL---I--PAMAFLSCVRPE------SWEP 28
TLR2 ----------MP----HT--LWMVWVLGVIISLSKEESSNQA 26
TLR10 ----------MRLIRNIYIFC--SIVMTAEGDAPE---------- 23
TLR1 ----------MTSIFHFA--IIFMLILQIRIQ---------- 20
TLR6 ----------MTKDKEPIVKSFHFV--CLMIIIVGTRIQ---------- 27
C36
C51
TLR3 CASSTTKCTVSHEVADCSHLKLTQVPD----DLPTNITVLNLTHNQLRRLPAANFTRYSQ 76
TLR9 CEL-QP-----HGLVNCNWLFLKSVPHFSMAAPRGNVTSLSLSSNRIHHLHDSDFAHLPS 88
TLR7 CDV-TLDVPKNHVIVDCTDKHLTEIPG----GIPTNTTNLTLTINHIPDISPASFHRLDH 90
TLR8 CDE-KK--QNDSVIAECSNRRLQEVPQ----TVGKYVTELDLSDNFITHITNESFQGLQN 106
TLR5 CSF-----DGRIAFYR--FCNLTQVPQ----VL-NTTERLLLSFNYIRTVTASSFPFLEQ 71
TLR4 CVE-----VVPNITYQCMELNFYKIPD----NLPFSTKNLDLSFNPLRHLGSYSFFSFPE 79
TLR2 SLS-----CDRNGICKGSSGSLNSIPS----GLTEAVKSLDLSNNRITYISNSDLQRCVN 77
TLR10 -LP-----EERELMTNCSNMSLRKVPA----DLTPATTTLDLSYNLLFQLQSSDFHSVSK 73
TLR1 -LS-----EESEFLVDRSKNGLIHVPK----DLSQKTTILNISQNYISELWTSDILSLSK 70
TLR6 -FS-----DGNEFAVDKSKRGLIHVPK----DLPLKTKVLDMSQNYIAELQVSDMSFLSE 77
C98 C100
C112
TLR3 LTSLDVGFNTISK---------LEPELCQKLPMLKVLNLQHNELSQLSDKTFAFC 122
TLR9 LRHLNLKWNCPPVGLSPMH--FPCHMTIEPSTFLAVPTLEELNLSYNNIMTVP----ALP 142
TLR7 LVEIDFRCNCVPIPLGSKNNMCIKRLQIKPRSFSGLTYLKSLYLDGNQLLEIPQ---GLP 147
TLR8 LTKINLNHNPNVQHQNGNPGIQSNGLNITDGAFLNLKNLRELLLEDNQLPQIPS---GLP 163
TLR5 LQLLELGSQYTPL---------TIDKEAFRNLPNLRILDLGSSKIYFLHPDAFQGL 118
TLR4 LQVLDLSRC-EIQ---------TIEDGAYQSLSHLSTLILTGNPIQSLALGAFSGL 125
TLR2 LQALVLTSN-GIN---------TIEEDSFSSLGSLEHLDLSYNYLSNLSSSWFKPL 123
TLR10 LRVLILCHN-RIQ---------QLDLKTFEFNKELRYLDLSNNRLKSVT---WYLL 116
TLR1 LRILIISHN-RIQ---------YLDISVFKFNQELEYLDLSHNKLVKIS---CHPT 113
TLR6 LTVLRLSHN-RIQ---------LLDLSVFKFNQDLEYLDLSHNQLQKIS---CHPI 120
C183
C189
TLR3 TNLTELHLMSNSIQKIKNNPFVK----------QKNLI 150
TLR9 KSLISLSLSHTNILMLDSASLAGLHALRFLFMDGNCYYKNPCRQALEVAPGALLGLGNLT 202
TLR7 PSLQLLSLEANNIFSIRKENLTELANIEILYLGQNCYYRNPCYVSYSIEKDAFLNLTKLK 207
TLR8 ESLTELSLIQNNIYNITKEGISRLINLKNLYLAWNCYFNKVCEK-TNIEDGVFETLTNLE 222
TLR5 FHLFELRLYFCGL----------SDAVLKDGYFRNLKALT 148
TLR4 SSLQKLVAVET----------NLASLENFPIGHLKTLK 153
TLR2 ----------SSLT 127
TLR10 ----------AGLR 120
TLR1 ----------VNLK 117
TLR6 ----------VSFR 124
TLR3 TLDLSHNGLSSTKLGTQVQLENLQELLLSNNKIQALKSEELDIFANSSLKKLELSSNQIK 210
TLR9 HLSLKYNNLTVVP---RNLPSSLEYLLLSYNRIVKLAPEDLANLTA--LRVLDVGG---- 253
TLR7 VLSLKDNNVTAVP---TVLPSTLTELYLYNNMIAKIQEDDFNNLNQ--LQILDLSG---- 258
TLR8 LLSLSFNSLSHVP---PKLPSSLRKLFLSNTQIKYISEEDFKGLIN--LTLLDLSG---- 273
TLR5 RLDLSKNQIRSLY----------LHPSFGKLNS--LKSIDFSSNQIF 183
TLR4 ELNVAHNLIQSFK----------LPEYFSNLTN--LEHLDLSSN--- 185
TLR2 FLNLLGNPYKTLG----------ETSLFSHLTK--LQILRVGNMDTF 162
TLR10 YLDLSFNDFDTMP----------ICEEAGNMSH--LEILGLSGA--- 152
TLR1 HLDLSFNAFDALP----------ICKEFGNMSQ--LKFLGLSTT--- 149
TLR6 HLDLSFNDFKALP----------ICKEFGNLSQ--LNFLGLSAM--- 156


C260
C263
C270
C273
TLR3 EFSPGCFHAIGRLFGLFLNN-VQLGPSLTEKLCLELANTSIRNLSLSNSQL-STTSNTTF 268
TLR9 -NCRRCDHAPNPCMECPRHFPQ-LHPDT------FSHLSRLEGLVLKDSSL-SWLNASWF 304
TLR7 -NCPRCYNAPFPCAPCKNNSPLQIPVNA------FDALTELKVLRLHSNSL-QHVPPRWF 310
TLR8 -NCPRCFNAPFPCVPCDGGASINIDRFA------FQNLTQLRYLNLSSTSL-RKINAAWF 325
TLR5 LVCE----HELEPLQGK----------TLSFFSLAANSLYSRVSVDWG 217
TLR4 -KIQSIYCTDLRVLHQM----------PLLNLSLDLSLNPMNF-IQ-P 220
TLR2 TKIQRKDFAGLTFLE----------EL----EIDASDLQS-YE-P 191
TLR10 -KIQKSDFQKIAHLH----------LNTVFLGFRTL--PH-YE-E 182
TLR1 -HLEKSSVLPIAHLN----------ISKVLLVLGETYGEK-ED-P 181
TLR6 -KLQKLDLLPIAHLH----------LSYILLDLRNYYIKE-NE-T 188
TLR3 LGLKWTNLT----MLDLSYNNLN--VVGNDSFAWLPQLEYFFLEYNNIQHLFSHSL---- 318
TLR9 RGL--GNLR----VLDLSENFLYKCITKTKAFQGLTQLRKLNLSFNYQKRVSFAHLSLAP 358
TLR7 KNI--NKLQ----ELDLSQNFLAKEIGDAKFLHFLPSLIQLDLSFNFELQVYRASMNLSQ 364
TLR8 KNM--PHLK----VLDLEFNYLVGEIASGAFLTMLPRLEILDLSFNYIKGSYPQHINISR 379
TLR5 KCMNPFRNMVLEI-LDVSGNGWTVDIT----------GNFSNAISKSQ 254
TLR4 GAFKEIRLHKLTL----RNNFDSLNVMKT-CIQGLAGLEVHRL----VLGEFRNE-GNLE 270
TLR2 KSLKSIQNV-SHLILHMKQHILLLEIFVD-VTSSVECLELRDT----DLDT--------F 237
TLR10 GSLPILNTTKLHIVLPMDTNFW--VLLRD-GIKTSKILEMTNI----DGKS--------- 226
TLR1 GGLQDFNTESLHIVFPTNKEFH--FILDV-SVKTVANLELSNI----KCVL--ED-SKCS 231
TLR6 ESLQILNAKTLHLVFHPTSLFA--IQVNI-SVNTLGCLQLTNI----K--L--ND-DNCQ 236
TLR3 --HGLFNVRYLNLKRSFTKQSISLASLPKIDDFSFQWLKCLEHLN-MEDNDIPGIKSNMF 375
TLR9 SFGSLVALKELDMHGIF------FRSLDETTLRPLARLPMLQTLR-LQMNFINQAQLGIF 411
TLR7 AFSSLKSLKILRIRGYV------FKELKSFNLSPLHNLQNLEVLD-LGTNFIKIANLSMF 417
TLR8 NFSKLLSLRALHLRGYV------FQELREDDFQPLMQLPNLSTIN-LGINFIKQIDFKLF 432
TLR5 AFSLILA------HHIM-GAGFGFHNIKDPDQ---------- 279
TLR4 KFDKSA---LEGLCNLT-IEEFRLAYLDYYLDDIIDLFNCLTNVSSFSLVSVTIERVKDF 326
TLR2 HF-SELS---TGETNSL-IKKFTFRNVKITDESLFQVMKLLNQIS---------- 277
TLR10 QFVSYEMQRNLSLEHAK-TSVLLLNKVDLLWDDLFLILQFVWHTS---------- 270
TLR1 YFLSILAK---LQTNPK-LSSLTLNNIETTWNSFIRILQLVWHTT---------- 272
TLR6 VFIKFLSE---LTRGPT-LLNFTLNHIETTWKCLVRVFQFLWPKP---------- 277
C445
TLR3 TGLINLKYLSLSNSFTSLRT-L---------- 396
TLR9 RAFPGLRYVDLSDNRISGASELTATMGEADGGEKV-WLQPG-------DL---------- 453
TLR7 KQFKRLKVIDLSVNKISPSGDSSEVGFCSNARTSVESYEPQVL-EQLHYFRYDKY----- 471
TLR8 QNFSNLEIIYLSENRISPLVKDTRQSYANSSSF-----QRHIRKRRSTDFEFDPH----- 482
TLR5 -------------NTFAGL----------ARS 288
TLR4 SYNFGWQHLELVNCKFGQFPTLKL----------KS---------- 352
TLR2 ----GLLELEFDDCTLNGVGNFRA----------SDNDRVIDPGKVETL 312
TLR10 -----VEHFQIRNVTFGGKAYLDH----------NS--FDYSNTVMRTI 302
TLR1 -----VWYSSISNVKLQGQ--LDF----------RD--FDYSGTSLKAL 302
TLR6 -----VEYLNIYNLTIIES--IRE----------ED--FTYSKTTLKAL 307
C475
C491
C521
TLR3 ----------TNETFVSLAHSPLHILNLTKNKISKIESDAFSWLGHLEVLDL 438
TLR9 ----------APAPVDTPSSEDFRPNCSTLNFTLDLSRNNLVTVQPEMFAQLSHLQCLRL 503
TLR7 -------ARSCRFKNKEASFMSVNESCYKYGQTLDLSKNSIFFVKSSDFQHLSFLKCLNL 524
TLR8 -------SNFYHF-----TRPLIKPQCAAYGKALDLSLNSIFFIGPNQFENLPDIACLNL 530
TLR5 SVRHLDLSHGFVFSLN-----SRVFETLKDLKVLNLAYNKINKIADEAFYGLDNLQVLNL 343
TLR4 ----------LKRLTFTSNK--GGNAFSEVDLPSLEFLDL 380
TLR2 TIRRLHIPRFYLFYDL-----STLYSLTERVKRITVENSKVFLVPCLLSQHLKSLEYLDL 367
TLR10 KLEHVHFRVFYI--QQ-----DKIYLLLTKMDIENLTISNAQMPHMLFPNYPTKFQYLNF 355
TLR1 SIHQVVSDVFGF--PQ-----SYIYEIFSNMNIKNFTVSGTRMVHMLCPSKISPFLHLDF 355
TLR6 TIEHITNQVFLF--SQ-----TALYTVFSEMNIMMLTISDTPFIHMLCPHAPSTFKFLNF 360

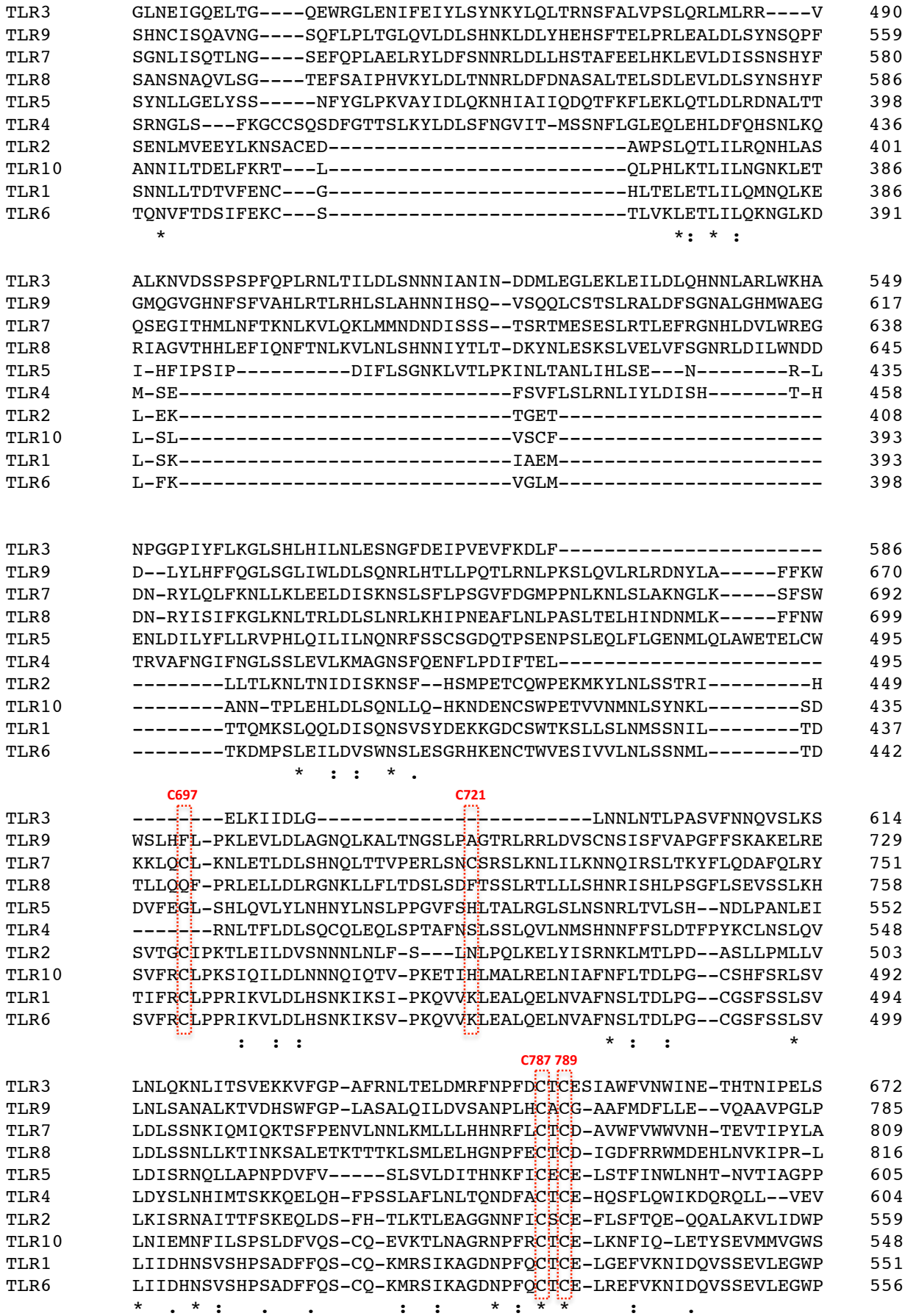
TLR3 GLNEIGQELTG----QEWRGLENIFEIYLSYNKYLQLTRNSFALVPSLQRLMLRR----V 490
TLR9 SHNCISQAVNG----SQFLPLTGLQVLDLSHNKLDLYHEHSFTELPRLEALDLSYNSQPF 559
TLR7 SGNLISQTLNG----SEFQPLAELRYLDFSNNRLDLLHSTAFEELHKLEVLDISSNSHYF 580
TLR8 SANSNAQVLSG----TEFSAIPHVKYLDLTNNRLDFDNASALTELSDLEVLDLSYNSHYF 586
TLR5 SYNLLGELYSS-----NFYGLPKVAYIDLQKNHIAIIQDQTFKFLEKLQTLDLRDNALTT 398
TLR4 SRNGLS---FKGCCSQSDFGTTSLKYLDLSFNGVIT-MSSNFLGLEQLEHLDFQHSNLKQ 436
TLR2 SENLMVEEYLKNSACED----------AWPSLQTLILRQNHLAS 401
TLR10 ANNILTDELFKRT---L----------QLPHLKTLILNGNKLET 386
TLR1 SNNLLTDTVFENC---G----------HLTELETLILQMNQLKE 386
TLR6 TQNVFTDSIFEKC---S----------TLVKLETLILQKNGLKD 391
TLR3 ALKNVDSSPSPFQPLRNLTILDLSNNNIANIN-DDMLEGLEKLEILDLQHNNLARLWKHA 549
TLR9 GMQGVGHNFSFVAHLRTLRHLSLAHNNIHSQ--VSQQLCSTSLRALDFSGNALGHMWAEG 617
TLR7 QSEGITHMLNFTKNLKVLQKLMMNDNDISSS--TSRTMESESLRTLEFRGNHLDVLWREG 638
TLR8 RIAGVTHHLEFIQNFTNLKVLNLSHNNIYTLT-DKYNLESKSLVELVFSGNRLDILWNDD 645
TLR5 I-HFIPSIP----------DIFLSGNKLVTLPKINLTANLIHLSE---N--------R-L 435
TLR4 M-SE----------FSVFLSLRNLIYLDISH-------T-H 458
TLR2 L-EK----------TGET---------- 408
TLR10 L-SL----------VSCF---------- 393
TLR1 L-SK----------IAEM---------- 393
TLR6 L-FK----------VGLM---------- 398
TLR3 NPGGPIYFLKGLSHLHILNLESNGFDEIPVEVFKDLF---------- 586
TLR9 D--LYLHFFQGLSGLIWLDLSQNRLHTLLPQTLRNLPKSLQVLRLRDNYLA-----FFKW 670
TLR7 DN-RYLQLFKNLLKLEELDISKNSLSFLPSGVFDGMPPNLKNLSLAKNGLK-----SFSW 692
TLR8 DN-RYISIFKGLKNLTRLDLSLNRLKHIPNEAFLNLPASLTELHINDNMLK-----FFNW 699
TLR5 ENLDILYFLLRVPHLQILILNQNRFSSCSGDQTPSENPSLEQLFLGENMLQLAWETELCW 495
TLR4 TRVAFNGIFNGLSSLEVLKMAGNSFQENFLPDIFTEL---------- 495
TLR2 --------LLTLKNLTNIDISKNSF--HSMPETCQWPEKMKYLNLSSTRI---------H 449
TLR10 --------ANN-TPLEHLDLSQNLLQ-HKNDENCSWPETVVNMNLSYNKL--------SD 435
TLR1 --------TTQMKSLQQLDISQNSVSYDEKKGDCSWTKSLLSLNMSSNIL--------TD 437
TLR6 --------TKDMPSLEILDVSWNSLESGRHKENCTWVESIVVLNLSSNML--------TD 442
C697
C721
TLR3 ----------ELKIIDLG----------LNNLNTLPASVFNNQVSLKS 614
TLR9 WSLHFL-PKLEVLDLAGNQLKALTNGSLPAGTRLRRLDVSCNSISFVAPGFFSKAKELRE 729
TLR7 KKLQCL-KNLETLDLSHNQLTTVPERLSNCSRSLKNLILKNNQIRSLTKYFLQDAFQLRY 751
TLR8 TLLQQF-PRLELLDLRGNKLLFLTDSLSDFTSSLRTLLLSHNRISHLPSGFLSEVSSLKH 758
TLR5 DVFEGL-SHLQVLYLNHNYLNSLPPGVFSHLTALRGLSLNSNRLTVLSH--NDLPANLEI 552
TLR4 ----------RNLTFLDLSQCQLEQLSPTAFNSLSSLQVLNMSHNNFFSLDTFPYKCLNSLQV 548
TLR2 SVTGCIPKTLEILDVSNNNLNLF-S---LNLPQLKELYISRNKLMTLPD--ASLLPMLLV 503
TLR10 SVFRCLPKSIQILDLNNNQIQTV-PKETIHLMALRELNIAFNFLTDLPG--CSHFSRLSV 492
TLR1 TIFRCLPPRIKVLDLHSNKIKSI-PKQVVKLEALQELNVAFNSLTDLPG--CGSFSSLSV 494
TLR6 SVFRCLPPRIKVLDLHSNKIKSV-PKQVVKLEALQELNVAFNSLTDLPG--CGSFSSLSV 499
C787 789
TLR3 LNLQKNLITSVEKKVFGP-AFRNLTELDMRFNPFDCTCESIAWFVNWINE-THTNIPELS 672
TLR9 LNLSANALKTVDHSWFGP-LASALQILDVSANPLHCACG-AAFMDFLLE--VQAAVPGLP 785
TLR7 LDLSSNKIQMIQKTSFPENVLNNLKMLLLHHNRFLCTCD-AVWFVWWVNH-TEVTIPYLA 809
TLR8 LDLSSNLLKTINKSALETKTTTKLSMLELHGNPFECTCD-IGDFRRWMDEHLNVKIPR-L 816
TLR5 LDISRNQLLAPNPDVFV-----SLSVLDITHNKFICECE-LSTFINWLNHT-NVTIAGPP 605
TLR4 LDYSLNHIMTSKKQELQH-FPSSLAFLNLTQNDFACTCE-HQSFLQWIKDQRQLL--VEV 604
TLR2 LKISRNAITTFSKEQLDS-FH-TLKTLEAGGNNFICSCE-FLSFTQE-QQALAKVLIDWP 559
TLR10 LNIEMNFILSPSLDFVQS-CQ-EVKTLNAGRNPFRCTCE-LKNFIQ-LETYSEVMMVGWS 548
TLR1 LIIDHNSVSHPSADFFQS-CQ-KMRSIKAGDNPFQCTCE-LGEFVKNIDQVSSEVLEGWP 551
TLR6 LIIDHNSVSHPSADFFQS-CQ-KMRSIKAGDNPFQCTCE-LREFVKNIDQVSSEVLEGWP 556

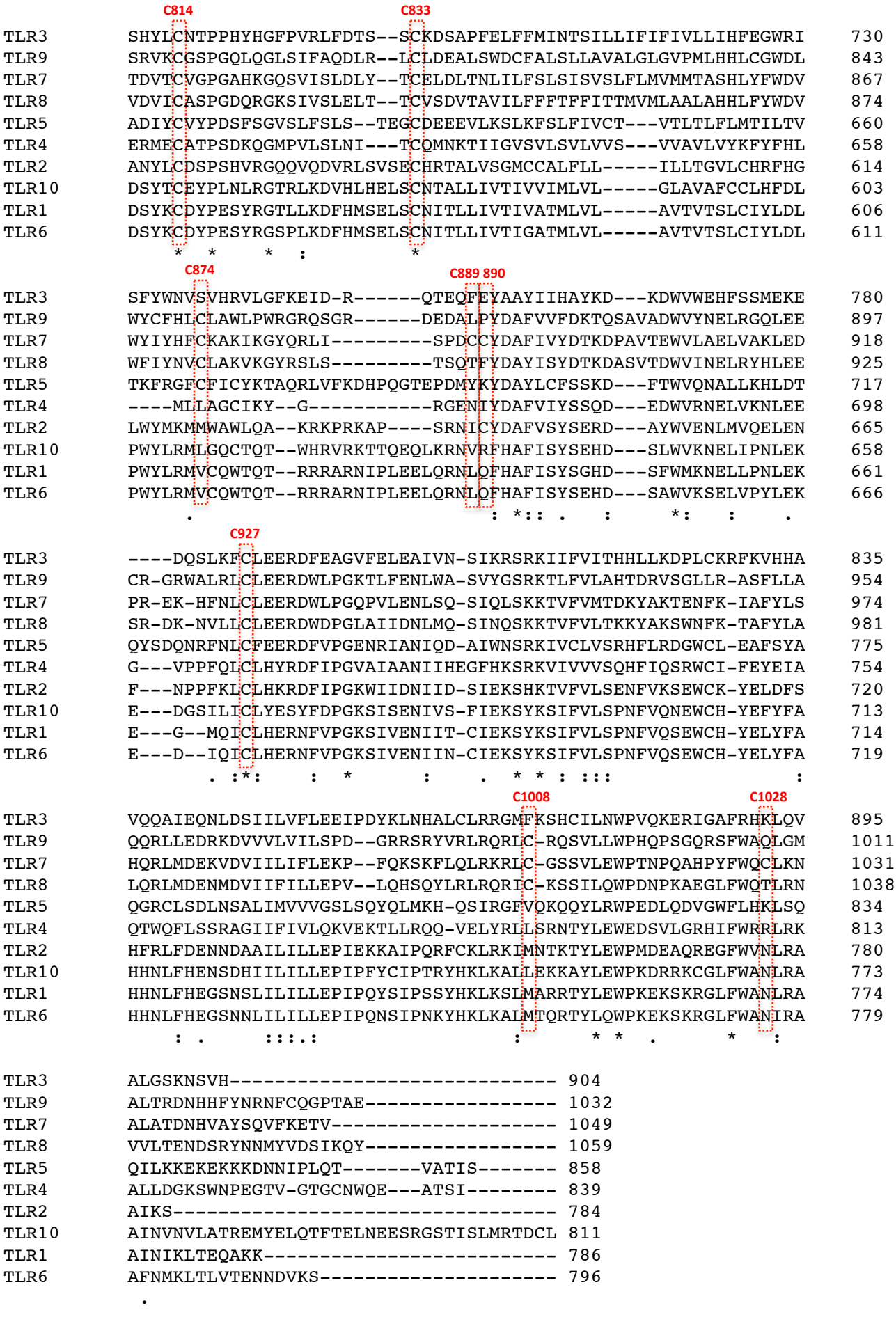
C814
C833
C874
C889 890
C927
C1008
C1028
TLR3 SHYLCNTPPHYHGFPVRLFDTS--SCKDSAPFELFFMINTSILLIFIFIVLLIHFEGWRI 730
TLR9 SRVKCGSPGQLQGLSIFAQDLR--LCLDEALSWDCFALSLLAVALGLGVPMLHHLCGWDL 843
TLR7 TDVTCVGPGAHKGQSVISLDLY--TCELDLTNLILFSLSISVSLFLMVMMTASHLYFWDV 867
TLR8 VDVICASPGDQRGKSIVSLELT--TCVSDVTAVILFFFTFFITTMVMLAALAHHLFYWDV 874
TLR5 ADIYCVYPDSFSGVSLFSLS--TEGCDEEEVLKSLKFSLFIVCT---VTLTLFLMTILTV 660
TLR4 ERMECATPSDKQGMPVLSLNI---TCQMNKTIIGVSVLSVLVVS---VVAVLVYKFYFHL 658
TLR2 ANYLCDSPSHVRGQQVQDVRLSVSECHRTALVSGMCCALFLL-----ILLTGVLCHRFHG 614
TLR10 DSYTCEYPLNLRGTRLKDVHLHELSCNTALLIVTIVVIMLVL-----GLAVAFCCLHFDL 603
TLR1 DSYKCDYPESYRGTLLKDFHMSELSCNITLLIVTIVATMLVL-----AVTVTSLCIYLDL 606
TLR6 DSYKCDYPESYRGSPLKDFHMSELSCNITLLIVTIGATMLVL-----AVTVTSLCIYLDL 611
TLR3 SFYWNVSVHRVLGFKEID-R------QTEQFEYAAYIIHAYKD---KDWVWEHFSSMEKE 780
TLR9 WYCFHLCLAWLPWRGRQSGR------DEDALPYDAFVVFDKTQSAVADWVYNELRGQLEE 897
TLR7 WYIYHFCKAKIKGYQRLI---------SPDCCYDAFIVYDTKDPAVTEWVLAELVAKLED 918
TLR8 WFIYNVCLAKVKGYRSLS---------TSQTFYDAYISYDTKDASVTDWVINELRYHLEE 925
TLR5 TKFRGFCFICYKTAQRLVFKDHPQGTEPDMYKYDAYLCFSSKD---FTWVQNALLKHLDT 717
TLR4 ----MLLAGCIKY--G-----------RGENIYDAFVIYSSQD---EDWVRNELVKNLEE 698
TLR2 LWYMKMMWAWLQA--KRKPRKAP----SRNICYDAFVSYSERD---AYWVENLMVQELEN 665
TLR10 PWYLRMLGQCTQT--WHRVRKTTQEQLKRNVRFHAFISYSEHD---SLWVKNELIPNLEK 658
TLR1 PWYLRMVCQWTQT--RRRARNIPLEELQRNLQFHAFISYSGHD---SFWMKNELLPNLEK 661
TLR6 PWYLRMVCQWTQT--RRRARNIPLEELQRNLQFHAFISYSEHD---SAWVKSELVPYLEK 666
TLR3 ----DQSLKFCLEERDFEAGVFELEAIVN-SIKRSRKIIFVITHHLLKDPLCKRFKVHHA 835
TLR9 CR-GRWALRLCLEERDWLPGKTLFENLWA-SVYGSRKTLFVLAHTDRVSGLLR-ASFLLA 954
TLR7 PR-EK-HFNLCLEERDWLPGQPVLENLSQ-SIQLSKKTVFVMTDKYAKTENFK-IAFYLS 974
TLR8 SR-DK-NVLLCLEERDWDPGLAIIDNLMQ-SINQSKKTVFVLTKKYAKSWNFK-TAFYLA 981
TLR5 QYSDQNRFNLCFEERDFVPGENRIANIQD-AIWNSRKIVCLVSRHFLRDGWCL-EAFSYA 775
TLR4 G---VPPFQLCLHYRDFIPGVAIAANIIHEGFHKSRKVIVVVSQHFIQSRWCI-FEYEIA 754
TLR2 F---NPPFKLCLHKRDFIPGKWIIDNIID-SIEKSHKTVFVLSENFVKSEWCK-YELDFS 720
TLR10 E---DGSILICLYESYFDPGKSISENIVS-FIEKSYKSIFVLSPNFVQNEWCH-YEFYFA 713
TLR1 E---G--MQICLHERNFVPGKSIVENIIT-CIEKSYKSIFVLSPNFVQSEWCH-YELYFA 714
TLR6 E---D--IQICLHERNFVPGKSIVENIIN-CIEKSYKSIFVLSPNFVQSEWCH-YELYFA 719
TLR3 VQQAIEQNLDSIILVFLEEIPDYKLNHALCLRRGMFKSHCILNWPVQKERIGAFRHKLQV 895
TLR9 QQRLLEDRKDVVVLVILSPD--GRRSRYVRLRQRLC-RQSVLLWPHQPSGQRSFWAQLGM 1011
TLR7 HQRLMDEKVDVIILIFLEKP--FQKSKFLQLRKRLC-GSSVLEWPTNPQAHPYFWQCLKN 1031
TLR8 LQRLMDENMDVIIFILLEPV--LQHSQYLRLRQRIC-KSSILQWPDNPKAEGLFWQTLRN 1038
TLR5 QGRCLSDLNSALIMVVVGSLSQYQLMKH-QSIRGFVQKQQYLRWPEDLQDVGWFLHKLSQ 834
TLR4 QTWQFLSSRAGIIFIVLQKVEKTLLRQQ-VELYRLLSRNTYLEWEDSVLGRHIFWRRLRK 813
TLR2 HFRLFDENNDAAILILLEPIEKKAIPQRFCKLRKIMNTKTYLEWPMDEAQREGFWVNLRA 780
TLR10 HHNLFHENSDHIILILLEPIPFYCIPTRYHKLKALLEKKAYLEWPKDRRKCGLFWANLRA 773
TLR1 HHNLFHEGSNSLILILLEPIPQYSIPSSYHKLKSLMARRTYLEWPKEKSKRGLFWANLRA 774
TLR6 HHNLFHEGSNNLILILLEPIPQNSIPNKYHKLKALMTQRTYLQWPKEKSKRGLFWANIRA 779
TLR3 ALGSKNSVH---------- 904
TLR9 ALTRDNHHFYNRNFCQGPTAE---------- 1032
TLR7 ALATDNHVAYSQVFKETV---------- 1049
TLR8 VVLTENDSRYNNMYVDSIKQY---------- 1059
TLR5 QILKKEKEKKKDNNIPLQT-------VATIS------- 858
TLR4 ALLDGKSWNPEGTV-GTGCNWQE---ATSI-------- 839
TLR2 AIKS---------- 784
TLR10 AINVNVLATREMYELQTFTELNEESRGSTISLMRTDCL 811
TLR1 AINIKLTEQAKK---------- 786
TLR6 AFNMKLTLVTENNDVKS---------- 796

Supplementary Figure S9. Multiple sequence alignment analysis demonstrating the position of all cysteine residues on human TLR7.

Individual sequences of human TLRs were obtained from NCBI GenBank protein databases with the following accession numbers TLR1 (CAG38593.1), TLR2 (AAH33756.1), TLR3 (ABC86910.1), TLR4 (AAF07823.1), TLR5 (AAI09119.1), TLR6 (BAA78631.1), TLR7 (AAZ99026.1), TLR8 (AAZ95441.1), TLR9 (AAZ95520.1) and TLR10 (AAY78491.1) and then sequence alignment was performed with CLUSTAL OMEGA (EMBL-EBI). Shown in red dotted rectangular boxes are the cysteines on human TLR7 and the respective position indicated.

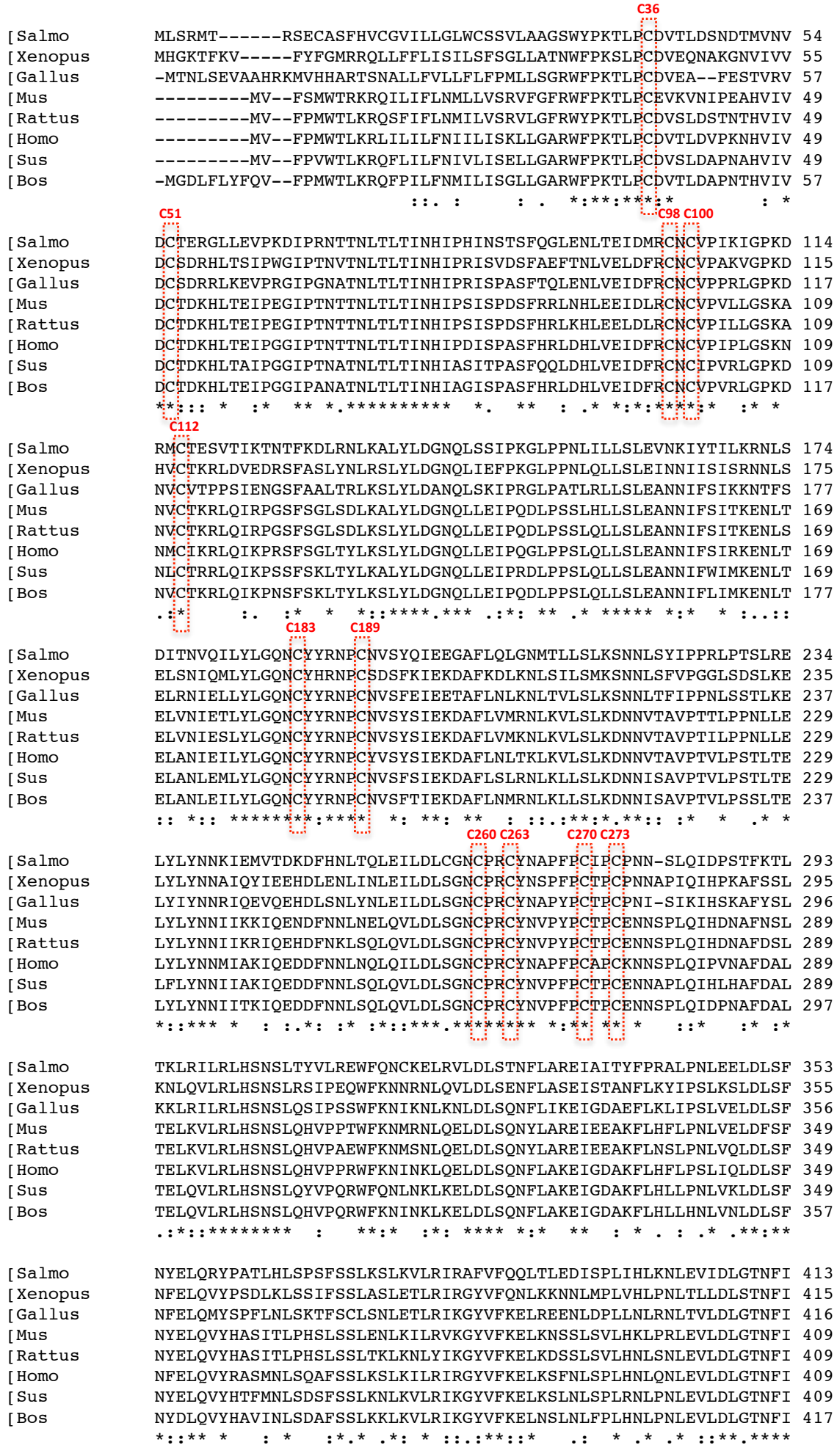
C36
[Salmo MLSRMT------RSECASFHVCGVILLGLWCSSVLAAGSWYPKTLPCDVTLDSNDTMVNV 54
[Xenopus MHGKTFKV-----FYFGMRRQLLFFLISILSFSGLLATNWFPKSLPCDVEQNAKGNVIVV 55
[Gallus -MTNLSEVAAHRKMVHHARTSNALLFVLLFLFPMLLSGRWFPKTLPCDVEA--FESTVRV 57
[Mus ---------MV--FSMWTRKRQILIFLNMLLVSRVFGFRWFPKTLPCEVKVNIPEAHVIV 49
[Rattus ---------MV--FPMWTLKRQSFIFLNMILVSRVLGFRWYPKTLPCDVSLDSTNTHVIV 49
[Homo ---------MV--FPMWTLKRLILILFNIILISKLLGARWFPKTLPCDVTLDVPKNHVIV 49
[Sus ---------MV--FPVWTLKRQFLILFNIVLISELLGARWFPKTLPCDVSLDAPNAHVIV 49
[Bos -MGDLFLYFQV--FPMWTLKRQFPILFNMILISGLLGARWFPKTLPCDVTLDAPNTHVIV 57
C51
C98 C100
[Salmo DCTERGLLEVPKDIPRNTTNLTLTINHIPHINSTSFQGLENLTEIDMRCNCVPIKIGPKD 114
[Xenopus DCSDRHLTSIPWGIPTNVTNLTLTINHIPRISVDSFAEFTNLVELDFRCNCVPAKVGPKD 115
[Gallus DCSDRRLKEVPRGIPGNATNLTLTINHIPRISPASFTQLENLVEIDFRCNCVPPRLGPKD 117
[Mus DCTDKHLTEIPEGIPTNTTNLTLTINHIPSISPDSFRRLNHLEEIDLRCNCVPVLLGSKA 109
[Rattus DCTDKHLTEIPEGIPTNTTNLTLTINHIPSISPDSFHRLKHLEELDLRCNCVPILLGSKA 109
[Homo DCTDKHLTEIPGGIPTNTTNLTLTINHIPDISPASFHRLDHLVEIDFRCNCVPIPLGSKN 109
[Sus DCTDKHLTAIPGGIPTNATNLTLTINHIASITPASFQQLDHLVEIDFRCNCIPVRLGPKD 109
[Bos DCTDKHLTEIPGGIPANATNLTLTINHIAGISPASFHRLDHLVEIDFRCNCVPVRLGPKD 117
C112
[Salmo RMCTESVTIKTNTFKDLRNLKALYLDGNQLSSIPKGLPPNLILLSLEVNKIYTILKRNLS 174
[Xenopus HVCTKRLDVEDRSFASLYNLRSLYLDGNQLIEFPKGLPPNLQLLSLEINNIISISRNNLS 175
[Gallus NVCVTPPSIENGSFAALTRLKSLYLDANQLSKIPRGLPATLRLLSLEANNIFSIKKNTFS 177
[Mus NVCTKRLQIRPGSFSGLSDLKALYLDGNQLLEIPQDLPSSLHLLSLEANNIFSITKENLT 169
[Rattus NVCTKRLQIRPGSFSGLSDLKSLYLDGNQLLEIPQDLPSSLQLLSLEANNIFSITKENLS 169
[Homo NMCIKRLQIKPRSFSGLTYLKSLYLDGNQLLEIPQGLPPSLQLLSLEANNIFSIRKENLT 169
[Sus NICTRRLQIKPSSFSKLTYLKALYLDGNQLLEIPRDLPPSLQLLSLEANNIFWIMKENLT 169
[Bos NVCTKRLQIKPNSFSKLTYLKSLYLDGNQLLEIPQDLPPSLQLLSLEANNIFLIMKENLT 177
C183
C189
[Salmo DITNVQILYLGQNCYYRNPCNVSYQIEEGAFLQLGNMTLLSLKSNNLSYIPPRLPTSLRE 234
[Xenopus ELSNIQMLYLGQNCYHRNPCSDSFKIEKDAFKDLKNLSILSMKSNNLSFVPGGLSDSLKE 235
[Gallus ELRNIELLYLGQNCYYRNPCNVSFEIEETAFLNLKNLTVLSLKSNNLTFIPPNLSSTLKE 237
[Mus ELVNIETLYLGQNCYYRNPCNVSYSIEKDAFLVMRNLKVLSLKDNNVTAVPTTLPPNLLE 229
[Rattus ELVNIESLYLGQNCYYRNPCNVSYSIEKDAFLVMKNLKVLSLKDNNVTAVPTILPPNLLE 229
[Homo ELANIEILYLGQNCYYRNPCYVSYSIEKDAFLNLTKLKVLSLKDNNVTAVPTVLPSTLTE 229
[Sus ELANLEMLYLGQNCYYRNPCNVSFSIEKDAFLSLRNLKLLSLKDNNISAVPTVLPSTLTE 229
[Bos ELANLEILYLGQNCYYRNPCNVSFTIEKDAFLNMRNLKLLSLKDNNISAVPTVLPSSLTE 237
C260 C263
C270 C273
[Salmo LYLYNNKIEMVTDKDFHNLTQLEILDLCGNCPRCYNAPFPCIPCPNN-SLQIDPSTFKTL 293
[Xenopus LYLYNNAIQYIEEHDLENLINLEILDLSGNCPRCYNSPFPCTPCPNNAPIQIHPKAFSSL 295
[Gallus LYIYNNRIQEVQEHDLSNLYNLEILDLSGNCPRCYNAPYPCTPCPNI-SIKIHSKAFYSL 296
[Mus LYLYNNIIKKIQENDFNNLNELQVLDLSGNCPRCYNVPYPCTPCENNSPLQIHDNAFNSL 289
[Rattus LYLYNNIIKRIQEHDFNKLSQLQVLDLSGNCPRCYNVPYPCTPCENNSPLQIHDNAFDSL 289
[Homo LYLYNNMIAKIQEDDFNNLNQLQILDLSGNCPRCYNAPFPCAPCKNNSPLQIPVNAFDAL 289
[Sus LFLYNNIIAKIQEDDFNNLSQLQVLDLSGNCPRCYNVPFPCTPCENNAPLQIHLHAFDAL 289
[Bos LYLYNNIITKIQEDDFNNLSQLQVLDLSGNCPRCYNVPFPCTPCENNSPLQIDPNAFDAL 297
[Salmo TKLRILRLHSNSLTYVLREWFQNCKELRVLDLSTNFLAREIAITYFPRALPNLEELDLSF 353
[Xenopus KNLQVLRLHSNSLRSIPEQWFKNNRNLQVLDLSENFLASEISTANFLKYIPSLKSLDLSF 355
[Gallus KKLRILRLHSNSLQSIPSSWFKNIKNLKNLDLSQNFLIKEIGDAEFLKLIPSLVELDLSF 356
[Mus TELKVLRLHSNSLQHVPPTWFKNMRNLQELDLSQNYLAREIEEAKFLHFLPNLVELDFSF 349
[Rattus TELKVLRLHSNSLQHVPAEWFKNMSNLQELDLSQNYLAREIEEAKFLNSLPNLVQLDLSF 349
[Homo TELKVLRLHSNSLQHVPPRWFKNINKLQELDLSQNFLAKEIGDAKFLHFLPSLIQLDLSF 349
[Sus TELQVLRLHSNSLQYVPQRWFQNLNKLKELDLSQNFLAKEIGDAKFLHLLPNLVKLDLSF 349
[Bos TELQVLRLHSNSLQHVPQRWFKNINKLKELDLSQNFLAKEIGDAKFLHLLHNLVNLDLSF 357
[Salmo NYELQRYPATLHLSPSFSSLKSLKVLRIRAFVFQQLTLEDISPLIHLKNLEVIDLGTNFI 413
[Xenopus NFELQVYPSDLKLSSIFSSLASLETLRIRGYVFQNLKKNNLMPLVHLPNLTLLDLSTNFI 415
[Gallus NFELQMYSPFLNLSKTFSCLSNLETLRIKGYVFKELREENLDPLLNLRNLTVLDLGTNFI 416
[Mus NYELQVYHASITLPHSLSSLENLKILRVKGYVFKELKNSSLSVLHKLPRLEVLDLGTNFI 409
[Rattus NYELQVYHASITLPHSLSSLTKLKNLYIKGYVFKELKDSSLSVLHNLSNLEVLDLGTNFI 409
[Homo NFELQVYRASMNLSQAFSSLKSLKILRIRGYVFKELKSFNLSPLHNLQNLEVLDLGTNFI 409
[Sus NYELQVYHTFMNLSDSFSSLKNLKVLRIKGYVFKELKSLNLSPLRNLPNLEVLDLGTNFI 409
[Bos NYDLQVYHAVINLSDAFSSLKKLKVLRIKGYVFKELNSLNLFPLHNLPNLEVLDLGTNFI 417

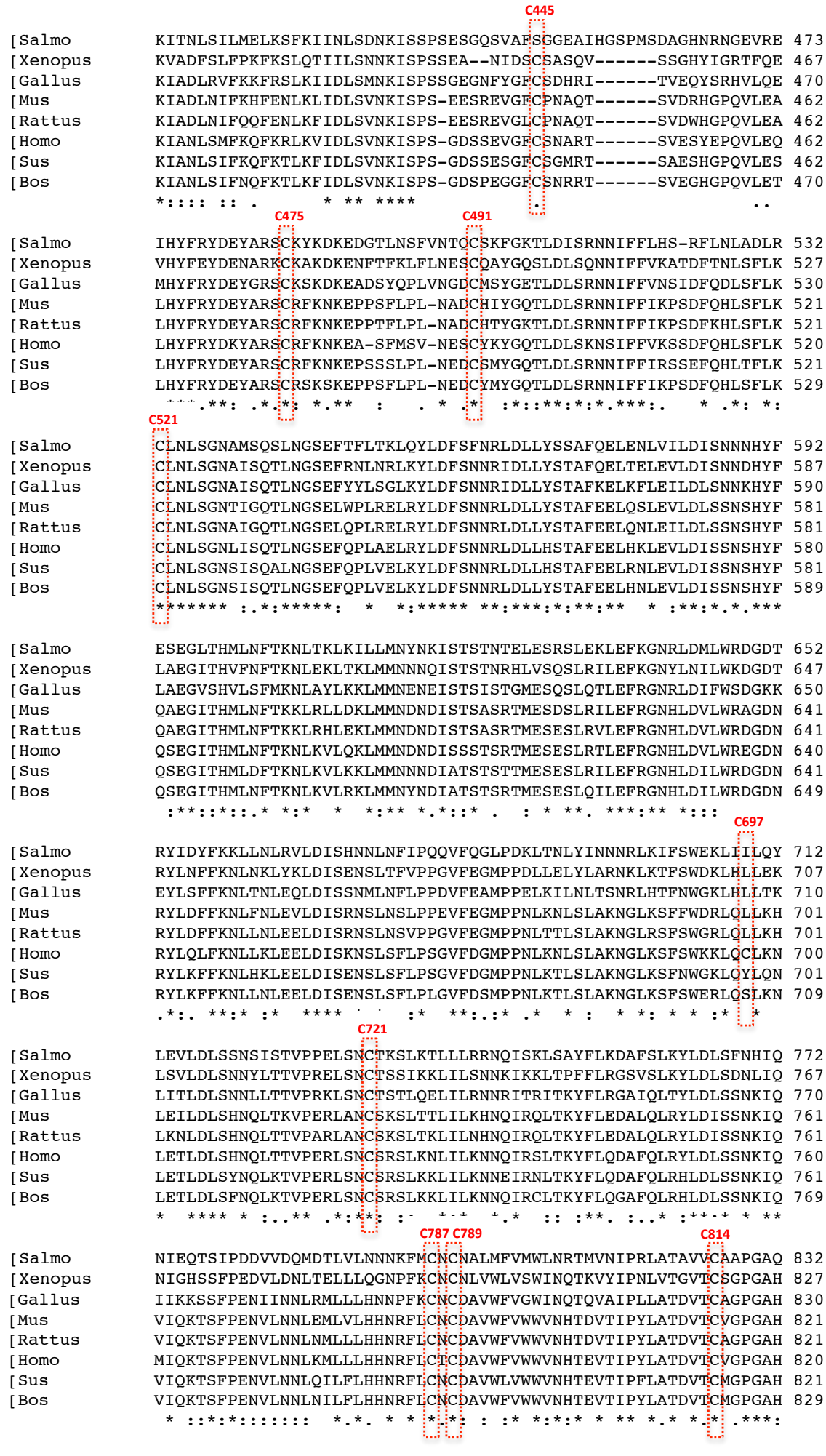
C445
[Salmo KITNLSILMELKSFKIINLSDNKISSPSESGQSVAFSGGEAIHGSPMSDAGHNRNGEVRE 473
[Xenopus KVADFSLFPKFKSLQTIILSNNKISPSSEA--NIDSCSASQV------SSGHYIGRTFQE 467
[Gallus KIADLRVFKKFRSLKIIDLSMNKISPSSGEGNFYGFCSDHRI------TVEQYSRHVLQE 470
[Mus KIADLNIFKHFENLKLIDLSVNKISPS-EESREVGFCPNAQT------SVDRHGPQVLEA 462
[Rattus KIADLNIFQQFENLKFIDLSVNKISPS-EESREVGLCPNAQT------SVDWHGPQVLEA 462
[Homo KIANLSMFKQFKRLKVIDLSVNKISPS-GDSSEVGFCSNART------SVESYEPQVLEQ 462
[Sus KIANLSIFKQFKTLKFIDLSVNKISPS-GDSSESGFCSGMRT------SAESHGPQVLES 462
[Bos KIANLSIFNQFKTLKFIDLSVNKISPS-GDSPEGGFCSNRRT------SVEGHGPQVLET 470
C475
C491
[Salmo IHYFRYDEYARSCKYKDKEDGTLNSFVNTQCSKFGKTLDISRNNIFFLHS-RFLNLADLR 532
[Xenopus VHYFEYDENARKCKAKDKENFTFKLFLNESCQAYGQSLDLSQNNIFFVKATDFTNLSFLK 527
[Gallus MHYFRYDEYGRSCKSKDKEADSYQPLVNGDCMSYGETLDLSRNNIFFVNSIDFQDLSFLK 530
[Mus LHYFRYDEYARSCRFKNKEPPSFLPL-NADCHIYGQTLDLSRNNIFFIKPSDFQHLSFLK 521
[Rattus LHYFRYDEYARSCRFKNKEPPTFLPL-NADCHTYGKTLDLSRNNIFFIKPSDFKHLSFLK 521
[Homo LHYFRYDKYARSCRFKNKEA-SFMSV-NESCYKYGQTLDLSKNSIFFVKSSDFQHLSFLK 520
[Sus LHYFRYDEYARSCRFKNKEPSSSLPL-NEDCSMYGQTLDLSRNNIFFIRSSEFQHLTFLK 521
[Bos LHYFRYDEYARSCRSKSKEPPSFLPL-NEDCYMYGQTLDLSRNNIFFIKPSDFQHLSFLK 529
C521
[Salmo CLNLSGNAMSQSLNGSEFTFLTKLQYLDFSFNRLDLLYSSAFQELENLVILDISNNNHYF 592
[Xenopus CLNLSGNAISQTLNGSEFRNLNRLKYLDFSNNRIDLLYSTAFQELTELEVLDISNNDHYF 587
[Gallus CLNLSGNAISQTLNGSEFYYLSGLKYLDFSNNRIDLLYSTAFKELKFLEILDLSNNKHYF 590
[Mus CLNLSGNTIGQTLNGSELWPLRELRYLDFSNNRLDLLYSTAFEELQSLEVLDLSSNSHYF 581
[Rattus CLNLSGNAIGQTLNGSELQPLRELRYLDFSNNRLDLLYSTAFEELQNLEILDLSSNSHYF 581
[Homo CLNLSGNLISQTLNGSEFQPLAELRYLDFSNNRLDLLHSTAFEELHKLEVLDISSNSHYF 580
[Sus CLNLSGNSISQALNGSEFQPLVELKYLDFSNNRLDLLHSTAFEELRNLEVLDISSNSHYF 581
[Bos CLNLSGNSISQTLNGSEFQPLVELKYLDFSNNRLDLLYSTAFEELHNLEVLDISSNSHYF 589
[Salmo ESEGLTHMLNFTKNLTKLKILLMNYNKISTSTNTELESRSLEKLEFKGNRLDMLWRDGDT 652
[Xenopus LAEGITHVFNFTKNLEKLTKLMMNNNQISTSTNRHLVSQSLRILEFKGNYLNILWKDGDT 647
[Gallus LAEGVSHVLSFMKNLAYLKKLMMNENEISTSISTGMESQSLQTLEFRGNRLDIFWSDGKK 650
[Mus QAEGITHMLNFTKKLRLLDKLMMNDNDISTSASRTMESDSLRILEFRGNHLDVLWRAGDN 641
[Rattus QAEGITHMLNFTKKLRHLEKLMMNDNDISTSASRTMESESLRVLEFRGNHLDVLWRDGDN 641
[Homo QSEGITHMLNFTKNLKVLQKLMMNDNDISSSTSRTMESESLRTLEFRGNHLDVLWREGDN 640
[Sus QSEGITHMLDFTKNLKVLKKLMMNNNDIATSTSTTMESESLRILEFRGNHLDILWRDGDN 641
[Bos QSEGITHMLNFTKNLKVLRKLMMNYNDIATSTSRTMESESLQILEFRGNHLDILWRDGDN 649
C697
[Salmo RYIDYFKKLLNLRVLDISHNNLNFIPQQVFQGLPDKLTNLYINNNRLKIFSWEKLIILQY 712
[Xenopus RYLNFFKNLNKLYKLDISENSLTFVPPGVFEGMPPDLLELYLARNKLKTFSWDKLHLLEK 707
[Gallus EYLSFFKNLTNLEQLDISSNMLNFLPPDVFEAMPPELKILNLTSNRLHTFNWGKLHLLTK 710
[Mus RYLDFFKNLFNLEVLDISRNSLNSLPPEVFEGMPPNLKNLSLAKNGLKSFFWDRLQLLKH 701
[Rattus RYLDFFKNLLNLEELDISRNSLNSVPPGVFEGMPPNLTTLSLAKNGLRSFSWGRLQLLKH 701
[Homo RYLQLFKNLLKLEELDISKNSLSFLPSGVFDGMPPNLKNLSLAKNGLKSFSWKKLQCLKN 700
[Sus RYLKFFKNLHKLEELDISENSLSFLPSGVFDGMPPNLKTLSLAKNGLKSFNWGKLQYLQN 701
[Bos RYLKFFKNLLNLEELDISENSLSFLPLGVFDSMPPNLKTLSLAKNGLKSFSWERLQSLKN 709
C721
[Salmo LEVLDLSSNSISTVPPELSNCTKSLKTLLLRRNQISKLSAYFLKDAFSLKYLDLSFNHIQ 772
[Xenopus LSVLDLSNNYLTTVPRELSNCTSSIKKLILSNNKIKKLTPFFLRGSVSLKYLDLSDNLIQ 767
[Gallus LITLDLSNNLLTTVPRKLSNCTSTLQELILRNNRITRITKYFLRGAIQLTYLDLSSNKIQ 770
[Mus LEILDLSHNQLTKVPERLANCSKSLTTLILKHNQIRQLTKYFLEDALQLRYLDISSNKIQ 761
[Rattus LKNLDLSHNQLTTVPARLANCSKSLTKLILNHNQIRQLTKYFLEDALQLRYLDISSNKIQ 761
[Homo LETLDLSHNQLTTVPERLSNCSRSLKNLILKNNQIRSLTKYFLQDAFQLRYLDLSSNKIQ 760
[Sus LETLDLSYNQLKTVPERLSNCSRSLKKLILKNNEIRNLTKYFLQDAFQLRHLDLSSNKIQ 761
[Bos LETLDLSFNQLKTVPERLSNCSRSLKKLILKNNQIRCLTKYFLQGAFQLRHLDLSSNKIQ 769
C787 C789
C814
[Salmo NIEQTSIPDDVVDQMDTLVLNNNKFMCNCNALMFVMWLNRTMVNIPRLATAVVCAAPGAQ 832
[Xenopus NIGHSSFPEDVLDNLTELLLQGNPFKCNCNLVWLVSWINQTKVYIPNLVTGVTCSGPGAH 827
[Gallus IIKKSSFPENIINNLRMLLLHNNPFKCNCDAVWFVGWINQTQVAIPLLATDVTCAGPGAH 830
[Mus VIQKTSFPENVLNNLEMLVLHHNRFLCNCDAVWFVWWVNHTDVTIPYLATDVTCVGPGAH 821
[Rattus VIQKTSFPENVLNNLNMLLLHHNRFLCNCDAVWFVWWVNHTDVTIPYLATDVTCAGPGAH 821
[Homo MIQKTSFPENVLNNLKMLLLHHNRFLCTCDAVWFVWWVNHTEVTIPYLATDVTCVGPGAH 820
[Sus VIQKTSFPENVLNNLQILFLHHNRFLCNCDAVWLVWWVNHTEVTIPFLATDVTCMGPGAH 821
[Bos VIQKTSFPENVLNNLNILFLHHNRFLCNCDAVWFVWWVNHTEVTIPYLATDVTCMGPGAH 829

Supplementary Figure S10. Multiple sequence alignment analysis of vertebrate TLR7.

Individual sequences of TLRs were obtained from NCBI GenBank protein databases with the following accession numbers *Salmo salar* (**CCX35457.1**), *Xenopus tropicalis* (**AAI66280.1**), *Gallus gallus* (**ACR26243.1**), *Mus musculus* (**AAI32386.1**), *Rattus norvegius* (**NP_001091051.1**), *Homo sapiens* (AAZ99026.1), *Sus scrofa* (**ABQ52583.1**) and *Bos taurus* (**NP_001028933.1**) and then sequence alignment was performed with CLUSTAL OMEGA (EMBL-EBI). Shown in red dotted rectangular boxes are the cysteines on human TLR7 and the respective position indicated.

TLR7-H	C36	C51	C98	C100	C112	C183	C189	C260	C263	C270	C273	C445	C475	C491	C521	C697	C721	C787	C789	C814	C833	C874	C889	C890	C927	C1008	C1028	Accession
TLR1-H	-	-	-	-	-	-	-	-	-	-	-	-	-	-	-	-	Yes	Yes	Yes	Yes	-	Yes	-	-	Yes	-	-	CAG38593.1
TLR2-H	-	-	-	-	-	-	-	-	-	-	-	-	-	-	-	Yes	-	Yes	Yes	Yes	-	-	-	Yes	Yes	-	-	AAH33756.1
TLR3-H	-	-	-	-	-	-	-	-	Yes	-	-	-	-	-	-	-	-	Yes	Yes	Yes	yes	-	-	-	Yes	-	-	ABC86910.1
TLR4-H	-	-	-	-	-	-	-	-	Yes	-	-	-	Yes	-	Yes	-	-	Yes	Yes	Yes	Yes	-	-	-	Yes	-	-	AAF07823.1
TLR5-H	-	-	-	-	-	-	-	-	-	-	-	-	-	-	-	-	-	Yes	Yes	Yes	Yes	Yes	-	-	Yes	-	-	AAI09119.1
TLR6-H	-	-	-	-	-	-	-	-	-	-	-	-	-	-	-	-	Yes	Yes	Yes	Yes	-	Yes	-	-	Yes	-	-	BAA78631.1
TLR8-H	Yes	Yes	-	-	-	Yes	Yes	Yes	Yes	Yes	Yes	-	-	Yes	Yes	-	-	Yes	Yes	Yes	Yes	Yes	-	-	Yes	Yes	-	AAZ95441.1
TLR9-H	Yes	Yes	-	Yes	Yes	Yes	Yes	Yes	Yes	Yes	Yes	-	-	Yes	Yes	-	-	Yes	Yes	Yes	Yes	Yes	-	-	Yes	Yes	-	AAZ95520.1
TLR10-H	-	-	-	-	-	-	-	-	-	-	-	-	-	-	-	Yes	-	Yes	Yes	Yes	-	-	-	-	Yes	-	-	AAY78491.1
TLR7 *Mus*	Yes	Yes	Yes	Yes	Yes	Yes	Yes	Yes	Yes	Yes	Yes	Yes	Yes	Yes	Yes	-	Yes	Yes	Yes	Yes	Yes	-	-	Yes	Yes	Yes	Yes	AAI32386.1
TLR7 *rattus*	Yes	Yes	Yes	Yes	Yes	Yes	Yes	Yes	Yes	Yes	Yes	Yes	Yes	Yes	Yes	-	Yes	Yes	Yes	Yes	Yes	-	-	Yes	Yes	Yes	Yes	NP_001091051.1
TLR7 *Sus*	Yes	Yes	Yes	Yes	Yes	Yes	Yes	Yes	Yes	Yes	Yes	Yes	Yes	Yes	Yes	-	Yes	Yes	Yes	Yes	Yes	Yes	-	Yes	Yes	Yes	Yes	ABQ52583.1
TLR7 *Bos taurus*	Yes	Yes	Yes	Yes	Yes	Yes	Yes	Yes	Yes	Yes	Yes	Yes	Yes	Yes	Yes	-	Yes	Yes	Yes	Yes	Yes	Yes	-	Yes	Yes	Yes	Yes	NP_001028933.1
TLR7 *Xenopus*	Yes	Yes	Yes	Yes	Yes	Yes	Yes	Yes	Yes	Yes	Yes	Yes	Yes	Yes	Yes	-	Yes	Yes	Yes	Yes	Yes	-	Yes	Yes	Yes	Yes	Yes	AAI66280.1
TLR7 *Gallus*	Yes	Yes	Yes	Yes	Yes	Yes	Yes	Yes	Yes	Yes	Yes	Yes	Yes	Yes	Yes	-	Yes	Yes	Yes	Yes	Yes	Yes	-	Yes	Yes	Yes	-	ACR26243.1
TLR7 *Salmo*	Yes	Yes	Yes	Yes	Yes	Yes	Yes	Yes	Yes	Yes	Yes	-	Yes	Yes	Yes	-	Yes	Yes	Yes	Yes	Yes	-	-	-	Yes	-	-	CCX35457.1

Supplementary Figure S11. Pairwise sequence alignment analysis of human TLR7 vs other members of the human TLR family and vs vertebrate TLR7

Individual sequences of TLRs were obtained from NCBI GenBank protein databases with the indicated accession numbers and then sequence alignment was performed with Pubmed NCBI BLAST.

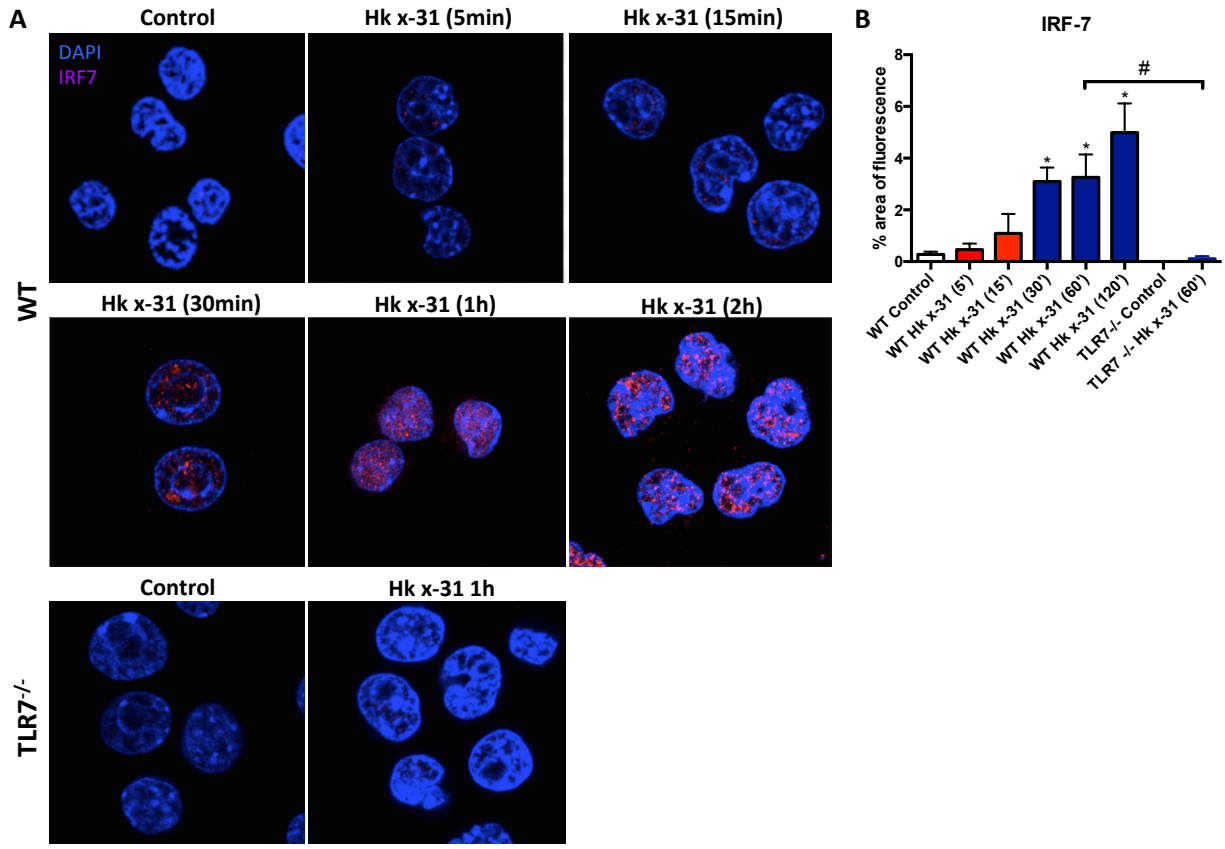

Supplementary Figure 12

Supplementary Figure S12. Influenza A virus causes interferon regulatory factor 7 (IRF-7) nuclear translocation *via* a TLR7-dependent mechanism.

(A-B) Immortalized bone marrow macrophages from WT or TLR7$^{-/-}$ mice were either left untreated or infected with HKx31 influenza A virus (HKx31, MOI of 10) for various times as indicated and then labeled with the IRF-7 antibody and 4',6'- diamidino-2-phenylindole (DAPI). Images are representative of >100 cells analyzed over 4 separate experiments. Original magnification X100. All data are represented as mean ± SEM. One-way ANOVA followed by Dunnett's *post hoc* test for multiple comparisons. *P<0.05 compared to WT controls. #P<0.05 - comparison indicated by horizontal bar.

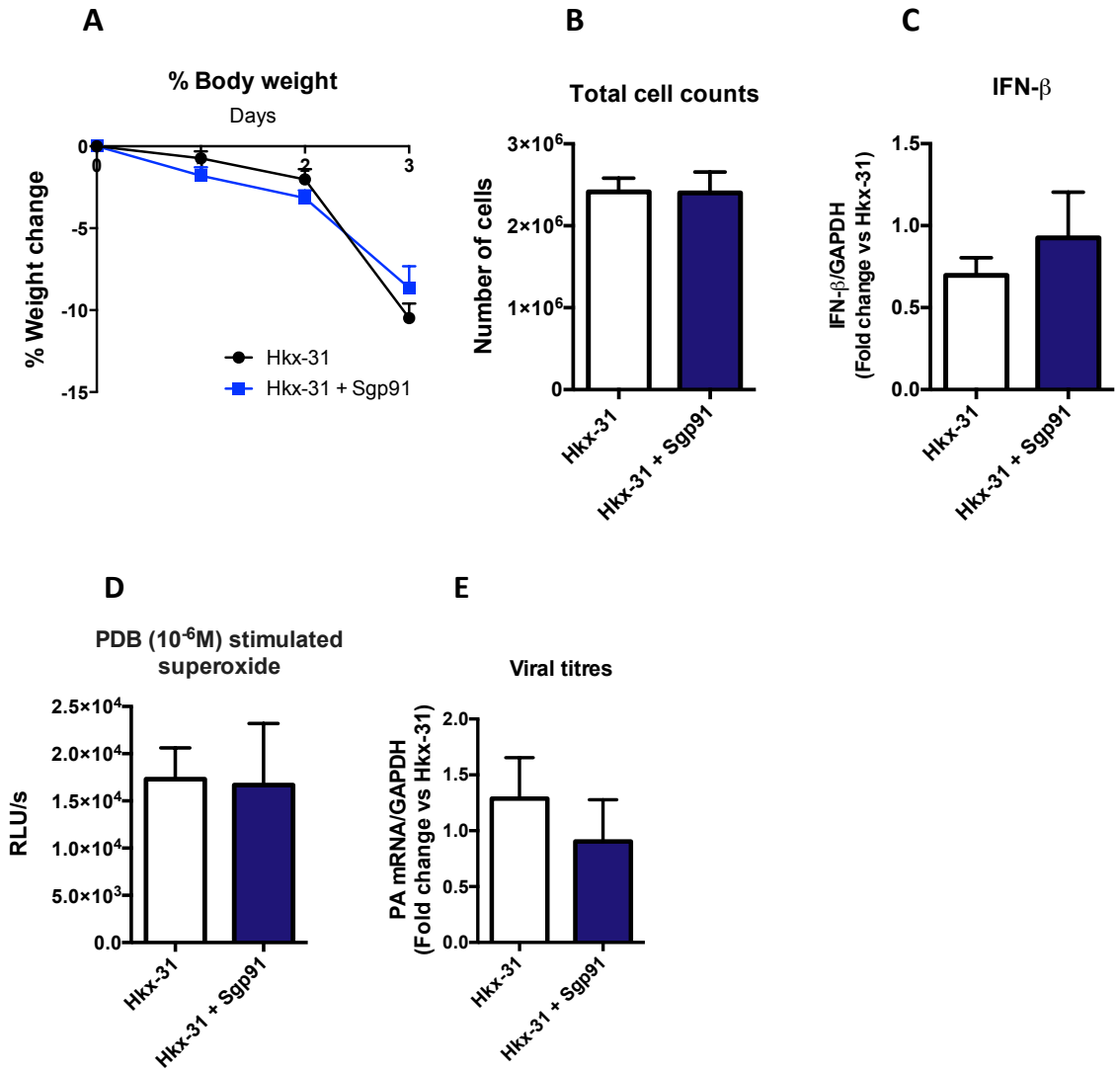

Supplementary Figure S13. Scrambled cholestanol-conjugated gp91ds-TAT failed to influence influenza A virus dependent pathology in vivo.

Scrambled gp91ds-TAT (Sgp91; 0.02mg/kg/day) was delivered intranasally to WT mice once daily for 4 days. At 24h after the first dose of inhibitor, mice were infected with HKx31 influenza A virus (1×10^5 PFU per mouse). Mice were culled at day 3 post-infection and **(A)** body weight, **(B)** airway inflammation was assessed by BALF cell counts, **(C)** lung IFN-β mRNA was determined by QPCR, **(D)** superoxide was measured from BALF inflammatory cells via L-O12 chemiluminescence and **(E)** viral titers were determined by QPCR. All data are represented as mean ± SEM, n=8.

REFERENCES

1.Kawahara T, Quinn MT, Lambeth JD. Molecular evolution of the reactive oxygen-generating NADPH oxidase (Nox/Duox) family of enzymes. *BMC evolutionary biology* 2007, **7:** 109.

2.Aguirre J, Lambeth JD. Nox enzymes from fungus to fly to fish and what they tell us about Nox function in mammals. *Free radical biology & medicine* 2010, **49**(9)**:** 1342-1353.

3.Imai Y, Kuba K, Neely GG, Yaghubian-Malhami R, Perkmann T, van Loo G*, et al.* Identification of oxidative stress and Toll-like receptor 4 signaling as a key pathway of acute lung injury. *Cell* 2008, **133**(2)**:** 235-249.

4.Snelgrove RJ, Edwards L, Rae AJ, Hussell T. An absence of reactive oxygen species improves the resolution of lung influenza infection. *Eur J Immunol* 2006, **36**(6)**:** 1364-1373.

5.To EE, Broughton BR, Hendricks KS, Vlahos R, Selemidis S. Influenza A virus and TLR7 activation potentiate NOX2 oxidase-dependent ROS production in macrophages. *Free radical research* 2014, **48**(8)**:** 940-947.

6.Vlahos R, Stambas J, Bozinovski S, Broughton BR, Drummond GR, Selemidis S. Inhibition of Nox2 oxidase activity ameliorates influenza A virus-induced lung inflammation. *PLoS pathogens* 2011, **7**(2)**:** e1001271.

7.Vlahos R, Stambas J, Selemidis S. Suppressing production of reactive oxygen species (ROS) for influenza A virus therapy. *Trends in pharmacological sciences* 2012, **33**(1)**:** 3-8.

8.Vlahos R, Selemidis S. NADPH Oxidases as Novel Pharmacologic Targets against Influenza A Virus Infection. *Molecular pharmacology* 2014, **86**(6)**:** 747-759.

9.Selemidis S, Sobey CG, Wingler K, Schmidt HH, Drummond GR. NADPH oxidases in the vasculature: molecular features, roles in disease and pharmacological inhibition. *Pharmacology & therapeutics* 2008, **120**(3)**:** 254-291.

10.Drummond GR, Selemidis S, Griendling KK, Sobey CG. Combating oxidative stress in vascular disease: NADPH oxidases as therapeutic targets. *Nature reviews Drug discovery* 2011, **10**(6)**:** 453-471.

11.Bedard K, Krause KH. The NOX family of ROS-generating NADPH oxidases: physiology and pathophysiology. *Physiological reviews* 2007, **87**(1)**:** 245-313.

12.Cossart P, Helenius A. Endocytosis of viruses and bacteria. *Cold Spring Harbor perspectives in biology* 2014, **6**(8).

13.Iwasaki A, Pillai PS. Innate immunity to influenza virus infection. *Nature reviews Immunology* 2014, **14**(5)**:** 315-328.

14.Campbell AM, Kashgarian M, Shlomchik MJ. NADPH oxidase inhibits the pathogenesis of systemic lupus erythematosus. *Science translational medicine* 2012, **4**(157)**:** 157ra141.

15.Kelkka T, Kienhofer D, Hoffmann M, Linja M, Wing K, Sareila O*, et al.* Reactive oxygen species deficiency induces autoimmunity with type 1 interferon signature. *Antioxidants & redox signaling* 2014, **21**(16)**:** 2231-2245.

16.Li Q, Harraz MM, Zhou W, Zhang LN, Ding W, Zhang Y*, et al.* Nox2 and Rac1 regulate H2O2-dependent recruitment of TRAF6 to endosomal interleukin-1 receptor complexes. *Molecular and cellular biology* 2006, **26**(1)**:** 140-154.

17.Chu Y, Piper R, Richardson S, Watanabe Y, Patel P, Heistad DD. Endocytosis of extracellular superoxide dismutase into endothelial cells: role of the heparin-binding domain. *Arteriosclerosis, thrombosis, and vascular biology* 2006, **26**(9)**:** 1985-1990.

18.Lund JM, Alexopoulou L, Sato A, Karow M, Adams NC, Gale NW*, et al.* Recognition of single-stranded RNA viruses by Toll-like receptor 7. *Proceedings of the National Academy of Sciences of the United States of America* 2004, **101**(15)**:** 5598-5603.

19.Diebold SS, Kaisho T, Hemmi H, Akira S, Reis e Sousa C. Innate antiviral responses by means of TLR7-mediated recognition of single-stranded RNA. *Science* 2004, **303**(5663)**:** 1529-1531.

20.Ichinohe T, Lee HK, Ogura Y, Flavell R, Iwasaki A. Inflammasome recognition of influenza virus is essential for adaptive immune responses. *The Journal of experimental medicine* 2009, **206**(1)**:** 79-87.

21.Allen IC, Scull MA, Moore CB, Holl EK, McElvania-TeKippe E, Taxman DJ*, et al.* The NLRP3 inflammasome mediates in vivo innate immunity to influenza A virus through recognition of viral RNA. *Immunity* 2009, **30**(4)**:** 556-565.

22.Jensen DD, Halls ML, Murphy JE, Canals M, Cattaruzza F, Poole DP*, et al.* Endothelin-converting enzyme 1 and beta-arrestins exert spatiotemporal control of substance P-induced inflammatory signals. *The Journal of biological chemistry* 2014, **289**(29)**:** 20283-20294.

23.Violin JD, Zhang J, Tsien RY, Newton AC. A genetically encoded fluorescent reporter reveals oscillatory phosphorylation by protein kinase C. *The Journal of cell biology* 2003, **161**(5)**:** 899-909.

24.Halls ML, Poole DP, Ellisdon AM, Nowell CJ, Canals M. Detection and Quantification of Intracellular Signaling Using FRET-Based Biosensors and High Content Imaging. *Methods in molecular biology* 2015, **1335:** 131-161.

25.West AP, Brodsky IE, Rahner C, Woo DK, Erdjument-Bromage H, Tempst P*, et al.* TLR signalling augments macrophage bactericidal activity through mitochondrial ROS. *Nature* 2011, **472**(7344)**:** 476-480.

26.Ramirez-Ortiz ZG, Prasad A, Griffith JW, Pendergraft WF, 3rd, Cowley GS, Root DE*, et al.* The receptor TREML4 amplifies TLR7-mediated signaling during antiviral responses and autoimmunity. *Nature immunology* 2015, **16**(5)**:** 495-504.

27.Kanno A, Yamamoto C, Onji M, Fukui R, Saitoh S, Motoi Y*, et al.* Essential role for Toll-like receptor 7 (TLR7)-unique cysteines in an intramolecular disulfide bond, proteolytic cleavage and RNA sensing. *International immunology* 2013, **25**(7)**:** 413-422.

28.Rajendran L, Schneider A, Schlechtingen G, Weidlich S, Ries J, Braxmeier T*, et al.* Efficient inhibition of the Alzheimer's disease beta-secretase by membrane targeting. *Science* 2008, **320**(5875)**:** 520-523.

29.King PT, Lim S, Pick A, Ngui J, Prodanovic Z, Downey W*, et al.* Lung T-cell responses to nontypeable Haemophilus influenzae in patients with chronic obstructive pulmonary disease. *The Journal of allergy and clinical immunology* 2013, **131**(5)**:** 1314-1321 e1314.

30.Schindelin J, Arganda-Carreras I, Frise E, Kaynig V, Longair M, Pietzsch T*, et al.* Fiji: an open-source platform for biological-image analysis. *Nature methods* 2012, **9**(7)**:** 676-682.

Chapter 4:
A novel endosomal NOX2 inhibitor protects against both low and high pathogenicity influenza A virus strains

Declaration for Thesis Chapter 4- *A novel endosomal NOX2 inhibitor protects against both low and high pathogenicity influenza A virus strains*

Declaration by candidate

In the case of Chapter 4, the nature and extent of my contribution to the work was as follows:

Nature of contribution	**Extent of contribution (%)**
Intellectual input into the design of experiments, performed all experiments (infections and treatments of animals), tissue collection, QPCR, cell culture, transfections, L-012 enhanced chemiluminsence, differential cell counts, confocal microscopy; analysed results, prepared figures and wrote the manuscript	75 %

The following co-authors have contributed to this study. If co-authors are students at Monash University, the extent of their contribution must be stated:

Name	**Nature of contribution**	**Extent of contribution (%)**
Raymond Luong Jiayin Diao	Performed and assisted the candidate with experiments	25 %
Tim Quach Christopher JH Porter	Synthesised peptides and provided intellectual advice during experimental	N/A
Stavros Selemidis	Intellectual input into the design of experiments, preparation of manuscript, management of the project and provided funding to support the project	N/A

The undersigned hereby certify that the above declaration correctly reflects the nature and extent of candidate's and co-authors' contribution to this work.

Candidates signature: Date: 17-02-2017

Main supervisor’s signature: Date: 17-02-2017

A novel endosomal NOX2 inhibitor protects against both low and high pathogenicity influenza A virus strains

Eunice E. To[1], Raymond Luong[1], Jiayin Diao[1], Ross Vlahos[5], Doug Brooks[6], John O' Leary[7,8], Tim Quach[2,3], Christopher J.H. Porter[2,4], and Stavros Selemidis[1]

1 Department of Pharmacology, Infection and Immunity Program, Biomedicine Discovery Institute, Monash University, Clayton, Victoria, Australia, 3800.

2 ARC Centre of Excellence in Convergent Bio-Nano Science and Technology, Monash Institute of Pharmaceutical Sciences, Monash University, Parkville, Victoria, Australia, 3052.

3 Medicinal Chemistry, Monash Institute of Pharmaceutical Sciences, Monash University, Parkville, Victoria, Australia, 3052.

4 Drug Delivery Disposition and Dynamics, Monash Institute of Pharmaceutical Sciences, Monash University, Parkville, Victoria, Australia, 3052.

5 School of Health Sciences and Health Innovations Research Institute, RMIT University, Bundoora, Victoria, Australia, 3083

6 School of Pharmacy and Medical Sciences, Sansom Institute for Health Research, Division of Health Sciences, University of South Australia, Australia, 5001.

7 Department of Histopathology Trinity College Dublin, Ireland, Sir Patrick Dun's Laboratory, Central Pathology Laboratory, St James's Hospital, Dublin 8, Ireland.

8 Molecular Pathology Laboratory, Coombe Women and Infants' University Hospital, Dublin 8, Ireland.

Abstract

Influenza A viruses cause respiratory tract infections that can lead to fatal outcomes when the virus spreads to the alveolar space, more predominantly observed with high pathogenic influenza virus strains. The emergence of antiviral drug-resistant strains urges the need for novel pharmacological approaches to treat influenza virus infection, regardless of the infecting strain. The excessive production of ROS by NOX2 oxidase has been widely implicated in contributing to influenza virus pathology. In Chapter 2 we showed IAV infection caused a significant elevation in ROS generation in macrophages that was dependent on serine phosphorylation. Following on from this, we demonstrated in Chapter 3 that the primary site of ROS generation is the endosome, and thus sought to design a novel endosomal NOX2 inhibitor (cholestanol-conjugated gp91ds-tat; Cgp91) that can reduce ROS-mediated inflammation and therefore alleviate the symptoms associated with influenza virus infections. Indeed, we observed treatment with Cgp91 via prevention attenuated lung inflammation and viral replication against the low pathogenic Hkx-31 strain. To further advance this work, we wanted to determine the protective effects of this novel inhibitors against a more virulent PR8 strain. In this chapter, we demonstrate in mice that Cgp91 treatment beginning one-day prior to infection with PR8 virus was effective in reducing airway inflammation, neutrophil influx, and pulmonary inflammation as measured by the degree of alveolitis, inflammatory cell influx and peribronchiolar inflammation. Additionally, Cgp91 attenuated ROS generation and viral mRNA expression in PR8-infected mice. However, when Cgp91 treatment was started one-day post virus infection there were modest reductions in the lung inflammation induced by both Hkx-31 virus and PR8 virus. These observations indicate that Cgp91 can be used as a potential adjuvant for prevention of influenza virus infections.

Introduction

Influenza epidemics and pandemics result in global morbidity and mortality, representing a major burden to the healthcare system. The currently available therapeutic approaches for influenza virus infections are vaccines and antiviral drugs, namely neuraminidase inhibitors. Despite vaccines being relatively efficacious in containing the spread of influenza viruses, the demand for mass production of vaccines in a timely manner and inaccuracies in predicting the seasonal circulating strains in turn reduce the effectiveness of the vaccination approach. Neuraminidase inhibitors interfere with newly formed virions, thus preventing the spread of the virus to neighbouring cells (Moscona, 2005). However, resistance to this drug class has also been demonstrated with some circulating influenza virus strains (Hai *et al.*, 2013; Nitsch-Osuch *et al.*, 2015). Therefore, this highlights the unmet need for the development of a novel therapeutic that can offer protection against viruses irrespective of the strain and pathogenicity.

Oxidative stress due to dysregulation in ROS generation and metabolism has been implicated in the pathogenesis of influenza virus infections (Imai *et al.*, 2008b; Schwarz, 1996). Nonetheless, there is conflicting evidence in the distinction between beneficial and harmful ROS. The general consensus is that an over exuberant ROS response triggers redox-sensitive pathways that contribute to the respiratory burst, causing inflammation and tissue injury. Therefore, targeting the ROS-generating enzyme, NOX2 to attenuate ROS levels may be an effective means for reducing the ROS burden and tissue injury. To support this, deletion of the NOX2 gene was associated with improved lung function and reduced lung tissue damage (Snelgrove *et al.*, 2006b; Vlahos *et al.*, 2011b).

In Chapter 2, we demonstrated that the oxidative burst was significantly enhanced during IAV infection in macrophages, which was reliant on Ser346 on p47phox for a functional NOX2 oxidase enzyme. In Chapter 3, we demonstrate the subcellular site of ROS generation mainly occurs within endosomes and hypothesized that endosomal ROS generation was the key culprit in contributing to disease severity. Thus, we hypothesised that targeting endosomal compartments to acutely inhibit ROS attenuates inflammation. Indeed, we demonstrate that Cgp91 treatment significantly reduces airway inflammation, viral titers and superoxide generation in Hkx-31 virus-infected mice. To advance the concept that Cgp91 blocks the pathology to IAV irrespective of pathogenicity, this present study aims to examine the effects of endosomal NOX2 inhibition through the use of a custom synthesised cholestanol-conjugated gp91ds-tat on the disease caused by the more virulent PR8 strain of IAV. A previous study has adopted this method of delivering drugs into endosomal compartments with a β-secretase inhibitor for the treatment of Alzheimer's disease (Halima *et al.*, 2011). We wanted to investigate the therapeutic potential of the endosomal NOX2 inhibitor and the non-targeted version of the NOX2 inhibitor in the PR8 virus model.

Experimental procedures

Animal ethics statement

The animal experiments described in this manuscript were approved by the Animal Experimentation Ethics Committee of Monash University (ethics number: MARP/2016/024), and conducted in compliance with the guidelines of the National Health and Medical Research Council (NHMRC) of Australia or Australian Research Council (ARC) on animal experimentation.

Animals

C57Bl/6J mice were obtained from Monash animal services (Monash University, Melbourne). Animals were housed in a high barrier facility designed for infectious experimental work with *ad libitum* access to water and standard rodent chow (4.8 % fat, 0.02 % cholesterol). All mice used in this study were males aged 8-12 weeks.

Virus infection models and treatment regimens

To investigate the potential therapeutic effect of our novel endosome NOX2 oxidase inhibitor we employed two approaches. The first approach was to model a scenario where the drug is delivered prior to virus infection to prevent the disease. The second was an interventional approach in which case the drug was delivered post infection. For the preventative studies, mice were anaesthetized by isoflurane inhalation (2-5 % isoflurane / 95 % oxygen air mixture) and then treated daily via intranasal administration with either unconjugated gp91ds-TAT (Ugp91; 0.2 mg/kg), cholestanol conjugated gp91ds-tat (Cgp91; 0.2 mg/kg) or control (DMSO; 0.2-2 %) one-day prior to infections over a 4-day period. Mice were intranasally infected with PR8 (500 PFUs) or PBS control, one-day post initial drug treatment and killed for assessment 3 days post infection. In the intervention approach, anaesthetized mice were infected with Hk-x31 (1×10^5 PFU), PR8 (50 PFUs) or control (PBS) followed by daily treatments with Ugp91 (0.2-0.5 mg/kg), Cgp91 (0.2-0.5 mg/kg) or DMSO (2-5 %) one-day post influenza infection over a 3 to 5-day period and sacrificed for assessment at 3, 5 or 6 days post influenza infection. At the end of each experiment, blood was collected via cardiac puncture, bronchoalveloar lavage fluid (BAL) was taken by a lavage technique (outlined in detail below), bodyweight was measured daily, lung weights were recorded then snap frozen for qPCR analysis and the left lung lobe was placed in 10 % neutral buffered formalin for histological purposes.

Airway inflammation and differential cell counts

Mice were killed by an intraperitoneal (i.p) injection of ketamine/xylazene (100mg/kg) mixture. An incision was made from the lower jaw to the top of the rib cage, where the salivary glands was separated to expose the surface of the trachea. The layer of smooth muscle on the trachea was removed, allowing a small incision to be made near the top of the trachea. A sheathed 21-gauge needle was inserted to the lumen and 300-400 ul of PBS was lavaged repeatedly (4

times). The total number of cells in the BALF was stained with 0.4 % trypan blue solution (Thermofisher Scientific, USA) and viable cells were evaluated using the Countess® automated cell counter (Invitrogen; Carlsbad, CA, USA). Differential cell analysis was prepared from BALF ($5x10^4$ cells) that were centrifuged at 1000 rpm for 5 min on the Cytospin 3 (Shandon, UK). Following this, slides were fixed in 100% propanol for one minute and allowed to fry overnight. Finally, samples were stained with Rapid I Aqueous Red StainTM (AMBER Scientific, Australia) and Rapid II Blue StainTM (AMBER Scientific, Australia) for 10 mins, then submerged in 70 % ethanol and absolute ethanol twice before being placed into xylene for 5 minutes (2 times). Samples were then mounted in DPX mounting medium (Labchem, NSW, Australia) and coverslips were firmly placed on top. 500 cells per sample from random fields were differentiated into macrophages, neutrophils, eosinophils and lymphocytes by standard morphological criteria. Data are represented as total cell numbers and expressed as a percentage of the cell population to analyse the different composition of inflammatory cells.

Histological analysis

The left lung lobe was contained in 10 % neutral buffered formalin for 24-28 hours prior to processing. After fixation, lung samples were embedded in paraffin wax and sections (3-4 µm thick) were cut (CM1850, Leica Microsystems, Wetzlar, Germany) longitudinally through the left lung lobe and placed on super frost slides (Menzel Gläser). Sections were de-paraffinised with xylene and a series of graded ethanol that were then stained with haemotoxylin and eosin (Sigma) and imaged by light microscopy. Samples were analysed on Imagescope (Leica Biosystems, USA) and blindly scored from 0-5 for (higher numbers indicate increased disease severity). The lung injury score was determined by a grading system that combined assessments of alveolitis, inflammatory cell infiltration and peribronchiolar inflammation by two independent assessors. A score of 0 represented was indicative of healthy lungs (ie no damage); 1-very mild damage; 2-mild damage; 3-moderate damage, 4-severe damage and 5-extremely severe histological changes.

L-O12 enhanced chemiluminescence

Extracellular ROS generation was measured using L-012 enhanced chemiluminescence. Primary alveolar macrophages taken from the BALF were seeded into a 96-well Opti Viewplate ($5x10^4$ cells/well) in Dulbecco's modified eagles medium (DMEM; supplemented with 10 % fetal bovine serum) and allowed to adhere for 3-4 hours in an incubator (37°C) with a humidified mixture of 5% CO_2 and 95 % air. Following this, cells were washed with warm 37 °C Krebs-HEPES buffer and exposed to a Krebs-HEPES buffer containing L-012 (10^{-4} mol/L) in the absence (i.e. basal ROS production) or presence (stimulated ROS production) of phorbol dibutyrate (PDB; 10^{-6} M). The same treatments were performed in blank wells to serve as controls for the background luminescence. All treatment groups were performed in triplicates.

Photon emission [relative light units (RLU/s)] was detected using the Chameleon™ luminescence detector (Hidex, model 425105, Finland) and recorded from each well for 1 s over 60 cycles. Individual data points for each group were derived from the average values of the three replicates minus the respective blank controls.

Viral and cytokine mRNA expression via quantitative polymerase chain reaction (PCR)

RNA was extracted from the lung tissue of mice for the assessment of viral mRNA and cytokine expression. The right lung lobe was placed in eppendorf tubes containing a mixture of Buffer RLT (Qiagen, USA) and β-mercaptoethanol (Sigma; 1%), which was minced into small pieces using curved scissors. Following this, lung samples were homogenized using the ultrasound homogenizer (Hielscher Ultrasonics GmBH, Teltow, Germany) and centrifuged at 14,000 rpm for 5 mins. A 1:1 ratio of lysate was mixed with 70% RNase free ethanol transferred to RNeasy spin columns (RNeasy Minikit; Qiagen, USA). Samples were spun at 10,000 rpm for 15 seconds and then washed with Buffer RW1. After discarding the flow-through, 5 μl of DNase I (Qiagen, USA) was mixed with 35 μl of Buffer RDD was pipetted directly onto the membrane of the spin column and incubated at room temperature for 15 mins. Buffer RPE was added and centrifuged for 10,000 rpm for 15 seconds. After discarding the flow-through, Buffer RPE was re-added and spun for 10,000 rpm for 2 mins. An additional spin at 14,000 rpm for 1 min was done to remove residual flow-through from the spin column. Finally, RNase free water was added and centrifuged to elute the RNA into an eppendorf tube. RNA samples were measured using the Nanodrop 1000 Spectrophotometer (Thermo Scientific, USA).

cDNA synthesis was performed using the High-Capacity cDNA RT kit (P/N4322171, Applied Biosystems, Foster City, CA, USA) using 1.0-2.0 μg total RNA. RNA was added to a mixture of reagents in the High-Capacity cDNA RT kit to make a final volume of 20 μl. This was transcribed using the BioRad MycyclerTM thermal cycler (BioRad, USA) at the following settings: 25◦C for 10 mins, 37◦C for 120 mins, 85◦C for 5 mins and 4◦C at rest. Samples were stored at -20◦C prior to use.

Quantitative polymerase chain reaction was carried out using the TaqMan Universal PCR Master Mix (Applied Biosystems, Foster City, CA, USA) or SYBR Green PCR Master Mix (Applied Biosystems, Foster City, CA, USA) and analyzed on ABI StepOneTM and StepOnePlusTM Real-time PCR Systems (Perkin-Elmer Applied Biosystems, Foster City, CA, USA). The PCR primers for TNF-α, IL-1β, IFN-β and IL-6 were included in the Assayon-Demand Gene Expression Assay Mix (Applied Biosystems, Foster City, CA, USA). Additionally, a custom designed forward and reverse primer of the segment 3 polymerase (PA) of influenza virus was used to measure viral titres. The PCR program run settings: 50◦C for 2 min, followed by 95◦C for 1 hr, then 95◦C for 15 s + 60◦C for 60 s + plate read (40 cycles). Quantitative values were obtained from the threshold cycle (Ct) number. Target gene expression level was

normalized against 18s or GAPDH mRNA expression for each sample and data was expressed relative to the control.

Statistical analysis and image analysis

Bodyweight measurements were analysed using a two-way analysis of variance (ANOVA) followed by Holm's Sidak *post-hoc* multiple comparison test. Data of the lung weights, ROS generation, cytokine expression, total and differential cell counts was analysed using one-way ANOVA followed by Tukey's *post-hoc* multiple comparison test. All data are expressed as mean ± standard error of the mean (SEM). Histological lung samples were analysed on Imagescope (Leica Biosystems, USA) and statistical comparisons were made using the non-parametric Kruskal-Wallis test, followed by the Dunn's *post-hoc* test. All statistical tests were performed using GraphPad Prism (GraphPad Software Version 6.0, San Diego CA, USA). $P<0.05$ was taken to indicate significance.

Chemicals

FBS (Sigma) was made into 50 ml aliquots and stored at -20°C. L-012 (WAKO chemicals) and PDB (Sigma) were dissolved in DMSO (100%) and prepared as 10 mM stock solutions in aliquots of 10, 25 and 50 μL, stored at -20°C. Custom designed peptides- unconjugated gp91ds-TAT and cholestanol conjugated gp91ds-TAT were dissolved in 100% DMSO in 5mM (10 μl) aliquots, and stored at -20°C.

Results

Preventative treatment with Ugp91 and Cgp91 have no effect on bodyweight and lung weight

Examining the bodyweight of mice during influenza infections is a marker used to assess disease severity. Here, we demonstrate that PR8 infected mice displayed an ~8% decrease in bodyweight 3 days post influenza virus infection, although not statistically significant from the control mice. Similarly, virus-infected mice that had daily treatments with unconjugated gp91ds-tat (Ugp91) or cholestanol-conjugated gp91ds-tat (Cgp91) lost around 7% of their bodyweight. By the third day, infected mice displayed more severe clinical signs including inactivity and poor appetite. The control mice showed no clinical signs and bodyweight was maintained during the course of the experiment (Fig. 1A). The ratio of lung weight to bodyweight was measured as an index of edema. It is evident that the lung weight to body weight ratio was increased in the virus infected mice compared to the uninfected controls but neither Ugp91 or Cgp91 treatment modified this response (Fig. 1B).

Differential cell populations are altered by treatment with Cgp91

To examine airway inflammation, the total number of cells and viable cells in the BALF were measured. There was a significant increase in cell infiltration in the PR8-infected mice compared to the controls (Fig. 2A-B). Ugp91 treated PR-8 infected mice had no effect on total or live cell counts compared to the PR8 control group. However, there does appear to be a trend for a decrease in total and live cell numbers following Cgp91 treatment (Fig. 2A-B). Since the total number of cells had increased in all virus-treated groups compared to the control, it was expected that the number of differential cells (macrophages, neutrophils, lymphocytes and eosinophils) would also increase. We demonstrate a significant increase in number of macrophages, neutrophils, lymphocytes and eosinophils in the PR8-infected mice compared to the uninfected controls (Fig. 3A-D). Strikingly, Cgp91 but not Ugp91 treatment of PR8-infected mice attenuated the increase in neutrophils by around 40% (Fig. 3B). Neither Cgp91 nor Ugp91 affected the numbers of macrophages, lymphocytes and eosinophils. If these same data where analysed to establish the proportions of inflammatory cells in the infiltrate, PR8 infection caused a dramatic decrease in the percentage of macrophages (i.e. ~80% in the uninfected controls to ~40% in the virus-infected groups) but resulted in a substantial elevation in neutrophils (~60% compared to the controls (Fig. 3A-D). The percentage of lymphocytes fell from ~17% in the control mice to 10% in the PR8-infected group. Cgp91-treated PR8-infected mice had reversed this effect and restored the lymphocyte cell population back to control levels. The percentage of lymphocytes in Ugp91-treated PR8-infected mice was similar to the PR8 alone cohort (Fig. 3C). PR8 infection resulted in a significant increase in the percentage of eosinophils that was reduced by about 40% with Ugp91 and Cgp91 treatment (Fig. 3D). It is important to note that

Ugp91 and Cgp91 treatment of naïve-uninfected mice had no effect on all cell populations examined (Figure 3A-D).

Cgp91 attenuates pulmonary inflammation

To assess the pathological changes, H&E staining alongside a scoring system was employed. The lung tissue of PR8 infected-mice displayed high levels of peribronchiolar inflammation, alveolitis and enhanced inflammatory cellular infiltrate. Treatment with Ugp91 did not alter the inflammation induced by virus infection, as it had a similar morphology to that of the PR8 control mice. However, these pathological changes were relieved in the Cgp91 treated virus-infected mice. This cohort of animals showed minor histological changes as evident by a reduction in peribronchiolar inflammation, alveolitis and enhanced inflammatory cellular infiltrate. Furthermore, both Ugp91 and Cgp91 alone had not caused any adverse inflammation, and was similar to those of the uninfected controls (Fig. 4A-B).

Cgp91 reduces ROS generation and viral titres

L-012 enhanced chemiluminescence was used to measure ROS generation in cells from the BALF of mice. Neither Ugp91 nor Cgp91 treatment of naïve-uninfected inflammatory cells taken from mice affected ROS production, as they were similar to the control group. Cells from PR8-infected mice exhibited a significant increase in ROS production compared to the controls (Fig 5). BALF inflammatory cells taken from Cgp91-treated virus-infected mice but not from Ugp91-treated mice produced ROS in levels that were lower than the PR8 control mice, although this was not statistically significant (Fig. 5). As expected the expression of viral mRNA detected in lung tissue was significantly higher in PR8-infected mice compared to the control. Also not surprising the expression of viral mRNA in both Ugp91 and Cgp91-treated naïve animals displayed no changes in expression, reflecting similar fold changes as the untreated control. Cgp91-treatment of mice infected with virus displayed a reduced level of viral mRNA expression compared to the virus control (Fig. 6).

The effect of Ugp91 and Cgp91 via intervention in Hk x-31-infected mice

Hx-31 infection caused a substantial decrease in bodyweight loss of ~8% three days post influenza infection compared to the uninfected counterparts. Both Ugp91 and Cgp91-treated virus-infected mice similarly lost ~10% of their bodyweight. Importantly, all the control groups including naïve mice that were treated with Ugp91 or Cgp91 had maintained their bodyweight throughout the course of the experiment (Fig. 7A). Importantly, the lung to body weight ratio was increased in the Hkx-31 infected mice compared to the uninfected controls. Treatment of virus-infected mice with the peptides (Ugp91 or Cgp91) failed to influence the percentage of lung weight to body weight, which was similar to the Hkx-31 virus alone group. All the uninfected control mice had lower and similar percentages (~0.8%)(Fig. 7B).

Cgp91 reduces airway inflammation and neutrophil influx

There was a significant increase in the live cell numbers in the BALF of Hkx-31-infected mice compared to the control. This inflammation was reduced by Cgp91-treatment but unaffected by Ugp91 treatment in virus-infected animals. Both Ugp91 and Cgp91 alone had no effects on inflammation, as the values were similar to the control BALF counts (Fig. 8A-B). Infection with influenza virus resulted in a significant elevation in the total macrophage, neutrophil and lymphocyte cell counts, yet eosinophils were unchanged. Cgp91 treatment had reduced neutrophil infiltration by approximately 40%, but had no impact on other cell populations including macrophages, lymphocytes or eosinophils. Treatment with Ugp91 had similar number of differential cell counts as the virus alone group (Fig. 9A-D).

Ugp91 and Cgp91 have no impact on ROS generation and cytokine expression but reduce viral titres

ROS generation was unaltered with Ugp91 or Cgp91 treatment of naïve-uninfected inflammatory cells taken from, as the superoxide levels were similar to the control group. Cells from Hkx-31-infected mice exhibited a significant increase in ROS production compared to control (Fig 10). However, BALF inflammatory cells taken from Upg91 or Cgp91-treated virus-infected mice did not alter the superoxide levels, as it was similar to the virus control group (Fig. 10). Similarly, the expression of cytokines was substantially enhanced in the lung tissue of Hkx-31-infected mice compared to the untreated control mice. Treatment with Ugp91 or Cgp91 had no impact on altering cytokine expression from the virus control. Importantly, the peptide treatments alone did not effect the expression of cytokines, showing similar fold changes as the naïve control (Fig. 11A). Despite the peptides having no impact on cytokine expressions, Cgp91 but not Ugp91 was able to reduce viral mRNA expression in virus-infected mice (Fig. 11B).

Intervention treatment with Ugp91 does not reverse clinical signs in PR8-infected mice

PR8 virus caused a significant decrease in bodyweight of 20% compared to the naïve control mice that maintained bodyweight over the course of 6-day period (Fig. 12A). Ugp91-treated PR8-infected mice showed a weight drop of ~20% (Fig. 12A). Similarly, the lung weight to body weight ratio was increased in the virus infected mice compared to the uninfected controls, however, Ugp91 treatment was not able to modify this response (Fig. 12B). At the termination of the experiment, infected mice displayed clinical signs of reduced food intake, inactivity and ruffled fur.

Airway inflammation due to PR8 infection was unaffected by Ugp91 treatment that begun 1 day post infection

Similar to our work in Figure 3(A-D) of this Chapter, this series of studies also showed that infection with PR8 resulted in marked increases in airway inflammation compared to the

uninfected controls, as assessed by BALF inflammatory cell counting (Fig. 13A-B). Differential cell populations of macrophages, neutrophils, lymphocytes and eosinophils were substantially increased after infection with PR8 virus compared to the untreated controls. However, treatment with Ugp91 failed to reverse the cell infiltration, as the cell counts were similar to the PR8 virus control (Fig. 14A-D).

ROS generation unaltered with Ugp91 treatment via intervention in Pr8 infected mice

BALF inflammatory cells from PR8-infected mice produced significantly higher levels of ROS compared to the naïve controls. Treatment with Ugp91 did not alter the superoxide levels as it similar to the virus control group (Fig. 15).

Discussion

Influenza viruses can cause severe respiratory tract infections, which is associated with lung inflammation and oxidative stress (Buffinton *et al.*, 1992; Chandler *et al.*, 2016; Vlahos *et al.*, 2011b; Vlahos *et al.*, 2012b). The emergence of drug resistant viral strains necessitates the need for novel therapeutic strategies that target influenza viruses, independent of the strain. The overproduction of ROS from NOX2 oxidase has been implicated in influenza virus infection induced disease (Snelgrove *et al.*, 2006b; Sun *et al.*, 2016; Vlahos *et al.*, 2011b). However, the underlying mechanisms of ROS generation, and their role in triggering redox-sensitive pathways have yet to be fully elucidated. This present study's major objective was to reduce ROS generation and thus airway inflammation and viral burden, which is commonly observed in influenza virus infections. Our work from Chapter 3 has identified endosomes as the key sites of ROS generation during influenza virus infections. Therefore, a custom-designed peptide to target these subcellular compartments was synthesized. The therapeutic potential of the endosome-targeted approach was compared with a non-targeted version of gp91ds-tat. In Chapter 3 it was demonstrated that endosome targeting of NOX2 oxidase reduced the severity of influenza virus infection. Specifically, the lung inflammation induced by the low pathogenic Hkx-31 virus was nearly abolished by Cgp91. Thus, we wanted to examine whether Cgp91 was also effective at suppressing disease severity in mice infected with a high pathogenic PR8 influenza A virus strain and test whether these compounds had the capacity to reduce established influenza disease.

Bodyweight loss is a key indicator of the progression and severity of influenza virus infections. Here, we demonstrate a reduction in bodyweight loss of ~ 8% in mice infected with PR8 virus at 3 days post-infection. However, both Ugp91 and Cgp91 treatment failed to suppress this bodyweight loss. This is consistent with a study conducted by Vlahos *et al.* (2011b), which demonstrated mice that were NOX2 deficient had unaffected bodyweight changes following influenza infection. Pulmonary edema is one of the contributing factors that promote respiratory distress. Evidently, we demonstrate that PR8-infected mice showed a significant increase in lung weight to bodyweight ratios, which was unaffected with treatment of either of the NOX2 inhibitors. Airway and lung inflammation is a critical feature of influenza virus infections, to serve as a protective mechanism for the host. Indeed, we demonstrate at 3 days post-infection with PR8 virus a significant increase in airway inflammation compared to the uninfected controls as assessed by BALF counting. Whilst it was clear that Ugp91 had no effect on this airway inflammation, there was a strong trend for reduction in airway inflammation in mice treated with Cgp91. This is in contrast to the dramatic reduction in airway inflammation caused by Cgp91 that we observed in Hkx-31-infected mice in Chapter 3. These differences might be explained

by the fact that PR8 virus is more virulent than the Hkx-31 virus, resulting in a stronger over exuberant inflammatory response, which overcomes the inhibition. To account for the decreased efficacy of these novel inhibitors in the PR8 infection model, it was evident that PR8 infection was associated with higher levels of virus replication compared to Hkx-31 infection (Tate *et al.*, 2011).

Pulmonary inflammation and edema are common pathological characteristics of influenza virus infections. In this present study we demonstrate that PR8 infection causes significant changes to lung morphology that was characterised by higher degrees of alveolitis, peribronchiolar inflammation and infiltrating inflammatory cells. Strikingly, Cgp91 treatment but not Ugp91 treatment attenuated both alveolitis and peribronchiolar inflammation in PR8-infected mice. This indicates that targeting endosomal ROS with Cgp91 appears to be more superior to the non-targeted version of the NOX2 inhibitor. To strengthen this idea, we show that Cgp91 is more effective than Ugp91 in reducing influenza-virus induced ROS generation and viral titres. Taken together, administration of Cgp91 via a preventative approach appears to provide protection by alleviating several symptoms induced by influenza virus infection

Neutrophil influx is a hallmark feature of the innate host immune response to influenza virus infections (Tumpey *et al.*, 2005). These inflammatory cells generate ROS as a defense mechanism to combat invading pathogens (Akaike, 2001; Akaike *et al.*, 1996). Notably, the over production of ROS released from neutrophils contributes to IAV-induced lung inflammation (Vlahos *et al.*, 2012b). Conflicting evidence reveals that neutrophil-depleted mice exhibited exacerbated levels of pulmonary inflammation and respiratory dysfunction during influenza virus infection (Tate *et al.*, 2009). It appears that the neutrophil-mediated inflammation induced by influenza viruses can possess both pathogenic and protective responses. Differences may arise from the different dose of virus used between studies, which may cause varied inflammatory responses. In this Chapter, PR8 infection resulted in a substantial increase in neutrophil influx into the airways of mice at Day 3 post infection. Cgp91 treatment reduced airway inflammation, albeit non-significantly, it resulted in a significant reduction in neutrophil infiltration following PR8 infection. It is possible that Cgp91 is causing a reduction in the circulating levels of MIP-2, a neutrophil attracting chemokine. To support this, inhibition of MIP-2 was associated with a reduction in infiltrating neutrophils and milder lung pathology, indicating that the accumulation of excessive neutrophils in the lungs contribute to severe disease (Sakai *et al.*, 2000). Overall, the role of neutrophils in influenza virus infections remains disputable. It is believed that a balance

of neutrophil influx is required for clearance of the virus, but oversaturation of neutrophil accumulation in the airways can result in damage to the surrounding tissue.

Macrophages are another critical inflammatory cell that is essential for generating type-I interferons cytokines that is necessary for viral clearance (Herold *et al.*, 2006; Hofmann *et al.*, 1997; Seo *et al.*, 2004). As expected, the number of macrophages in the BALF was significantly enhanced 3-days post-infection with PR8 virus. However, treatment with Ugp91 or Cgp91 did not alter the virus induced increases in the macrophage infiltration into the airways. In contrast, other studies demonstrate NOX2 inhibition with apocynin caused a reduction in the infiltration of macrophages in virus-infected animals (Vlahos *et al.*, 2011b). This could be due to the fact that apocynin was administered three days prior to the infection, where as in our study the NOX2 inhibitors were treated only one day prior to infection. The extra doses of apocynin could explain why it was more effective in reducing the macrophage population. It is important to note that apocynin possesses ROS scavenging properties and therefore lack in their selectivity for NOX2 oxidase (Drummond *et al.*, 2011a).

.

The adaptive immune response during a viral infection is characterized by the activation of cytotoxic T-lymphocytes (Yewdell *et al.*, 1985), which facilitate the elimination of virus-infected epithelial cells (Wijburg *et al.*, 1997). As evident in our study, PR8 infection caused a significant increase in the lymphocyte numbers. Interestingly, we also demonstrate that treatment with Cgp91 in PR8-infected mice exhibited a further elevation in lymphocyte cell numbers compared to the virus control. Consistently, Snelgrove *et al.* (2006b) reported an increase in lymphocyte cell population in NOX2 deficient mice that is likely to account for the improvement in viral clearance from this cohort of animals. Thus, it appears that Cgp91 is improving the adaptive immune response by recruiting and trafficking more lymphocytes into the airway to kill off virus-infected cells. The mechanism of regulating the leukocyte influx into the site of infection is partially regulated by chemokine receptors, specifically CXCR3. Evidently, mice deficient in CXCR3 had lower numbers of neutrophils, lymphocytes and eosinophils in the BALF 8-days post infection with virus (Wareing *et al.*, 2004). Here, we demonstrate a significant increase in eosinophil infiltration 3-days post infection with PR8 virus, which is blunted by treatment with Ugp91 and Cgp91. Increases in all the inflammatory cells post infection with PR8 virus was similar to the study conducted by Herold *et al.* (2008). It can be speculated that NOX2 inhibition could be blunting the expression of inflammatory genes to in turn reduce the amount of infiltrating eosinophils. Another possibility is that the inhibitor is attenuating airway inflammation caused by ROS, thereby inhibiting the infiltration of these inflammatory leukocytes. NOX2

inhibition with Cgp91 does not influence the adaptive immune response, which is consistent with a study conducted by Vlahos *et al.* (2011b), who demonstrated no changes in virus-specific $CD8^+$ T cells in virus-infected $NOX2^{-/y}$ mice compared to the WT counterparts. Further investigations need to be performed to fully elucidate the mechanisms by which these NOX2 inhibitors act to regulate cellular infiltration.

Having established that the endosome NOX2 oxidase inhibitor has the capacity to minimize influenza virus induced lung inflammation and oxidative stress when administered prior to virus infection, an additional clinically relevant scenario would be to administer the drug post-infection. To examine the potential of Ugp91 or Cgp91 to suppress established influenza disease mice were treated with the NOX2 inhibitor daily one-day post infection with PR8 virus until one-day prior to the end of the infection period. We wanted to determine whether these drugs were protective in relieving lung inflammation induced by the low pathogenic Hkx-31 strain. The reduction in bodyweight and the increase in lung weight to bodyweight ratio induced by Hkx-31 were similar to that seen with PR8 infection. Interestingly, treatment with Cgp91 but not Ugp91 was able to cause a modest reduction in airway inflammation. Again, this suggests that Cgp91 appears to be more effective in reducing influenza virus induced inflammation than Ugp91. Furthermore, Cgp91 had reduced the Hkx-31 induced elevation in neutrophil infiltration. This is consistent to the observation seen when Cgp91 was administered in a preventative manner in PR8-infected mice. As discussed previously, the role of neutrophils in influenza virus infection was controversial and requires more research to discover whether these inflammatory cells are harmful or beneficial.

Here, we demonstrate that mice infected with PR8 had significant bodyweight loss of 20% that was unaffected by Ugp91 treatment. Additionally, airway inflammation, differential cell populations (macrophages, neutrophils, lymphocytes and eosinophils) and ROS generation was unaffected by Ugp91 treatment. This could be attributed to the fact that the virus replication has already begun, and therefore the drug was not able to overcome the inflammation induced. Moreover, ROS are critical early activators of virus replication and inflammation and thus, our intervention approach in administering the drug one day post-infection may be too late. From this body of evidence, it appears that NOX2 inhibitors administered via intervention was not as effective in as administering the compounds in a preventative manner. Notably, we did not test Cgp91 in this prevention model due to limitations in synthesizing enough of the compound to carry out these experiments.

Influenza virus infections induce the “cytokine storm”, characterised by bursts of cytokine and chemokine release from inflammatory cells (Chan *et al.*, 2005; Perrone *et al.*, 2008). Indeed, we demonstrate a significant increase in the expression of antiviral cytokines IFN-β and IL-1β and pro-inflammatory cytokines TNF-α and IL-6 upon infection with Hk-x31 virus. Type-I interferons are produced and function by exerting anti-viral effects to aid viral clearance. Mechanistically, type-I interferons form a heterodimer with the IFN-α receptor that triggers the transcription of interferon-stimulated genes via the Jak/STAT pathway to prevent viral dissemination and spread (García-Sastre *et al.*, 2006; Schoggins *et al.*, 2011). However, it is known that interferons induce downstream activation of other cytokines to promote undesirable inflammatory responses (Hayden *et al.*, 1998). For example, TNF-α promotes tumor necrosis factor-related apoptosis-inducing ligand (TRAIL) and thus cell apoptosis in lung epithelial cells (Herold *et al.*, 2008; Ishikawa *et al.*, 2005). Additionally, TNF-α and IL-6 have been associated with the bodyweight loss observed in mice (Herold *et al.*, 2008; Xu *et al.*, 2004). Treatment with Ugp91 or Cgp91 failed to reverse the virus-induced increases in the expression of various indicated cytokines. This could be attributed to the fact that the cytokine burst occurs early on in the infection phase, therefore intervention treatment approach is too late to reduce the inflammatory responses. It is important to note that measurements were taken at Day 3 post-infection. As cytokine levels are the highest at day 3, we will need to investigate other time points such as 7-days post-infection, where the cytokine production is lowered. Perhaps, a higher dose of drug may need to be used to be more effective in attenuating the cytokine expression. This body of evidence suggests that the homeostasis of cytokines is necessary in regulating the pathogenic effects of cytokine generation in influenza infections. Moreover, the signaling pathways the lead to production of cytokines need to be further investigated, which can be used as a potential drug target in controlling viral infections.

Thus far, the observations suggest that Cgp91 is more efficacious than Ugp91 at alleviating influenza virus infection. As hypothesized, targeting the endosomal ROS appears to be an effective approach in preventing influenza virus-induced airway inflammation and lung injury. However, the pharmacokinetics of these inhibitors have not been investigated in depth, making the optimal dosing regimens difficult to predict. In our experiments, the peptides were administered once daily. As the inhibitors were relatively ineffective in the intervention models, perhaps multiple doses per day are necessary to miminise the hyper-inflammation caused by these strains of influenza viruses. Since these are newly designed inhibitors, the safety profiling needs to be properly tested. It is possible that the inhibitor has non-specific effects and it is likely that high concentrations could target other NOX isoforms or even other receptors. Once the optimal dosing has been determined, this should be compared against the current antiviral

drugs available. Furthermore, a combination therapy approach, comprising of gp91ds-tat and a TLR7 agonist (to boost immunity) may be more effective in treating viral infections. Alternatively, ROS can be inhibited via antioxidant therapy. Previous studies have inhibited ROS generation with antioxidant therapy, whereby N-acetyl-l-cysteine (NAC) was beneficial in reducing virus replication airway inflammation induced by influenza viruses (Geiler *et al.*, 2010; Zhang *et al.*, 2014). Additionally, Vitamin C was used and showed promising results by relieving influenza virus symptoms (Ely, 2007). Nonetheless, a high dose of these antioxidants are required for effective results, making them unfeasible in aiding drug design. Moreover, high doses of these antioxidants are associated with adverse effects, including stomach cramps and vomiting (Ely, 2007).

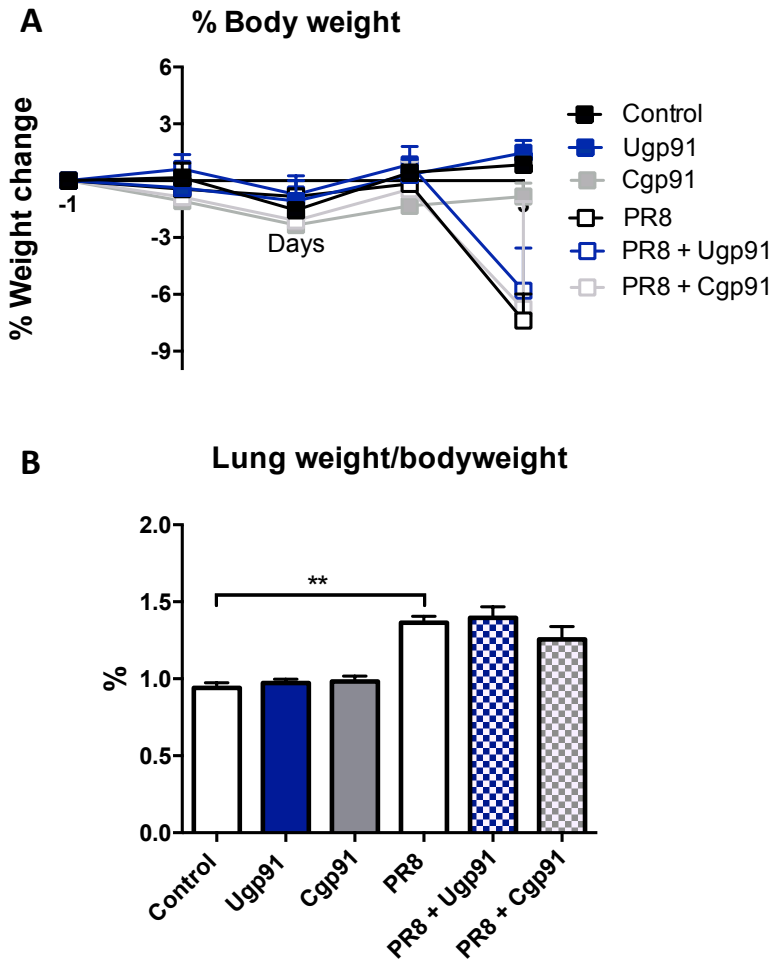

Figure 1: Delivery of Cgp91 and Ugp91 by prevention has no effect on bodyweight or lung weight in mice infected with PR8 virus. WT C57Bl/6J mice (8-12 weeks) were treated daily via intranasal administration of unconjugated gp91ds-tat (Ugp91; 0.2mg/kg), cholestanol conjugated gp91ds-tat (Cgp91; 0.2mg/kg) or DMSO (2%; control) over a 4-day period. Mice were intranasally infected with PR8 (500 PFUs) or PBS control, one-day post initial drug treatment. A) Daily bodyweight was recorded over the 4-day period. B) The weight of the lungs was measured and presented as a % of the bodyweight of each respective mouse. Data are expressed as mean ± SEM (Control, n=7; Ugp91, n=5; Cgp91, n=5; PR8, n=9, PR8 + Ugp91, n=9; PR8 + Cgp91, n=10). Statistical analysis was conducted using a two-way analysis of variance (ANOVA) followed by Holm's Sidak post-hoc multiple comparison test in 'A' and one-way ANOVA test followed by Tukey's post hoc test for multiple comparison test for 'B'. Statistical significance was taken where $P<0.05$, where ** indicates $P<0.01$.

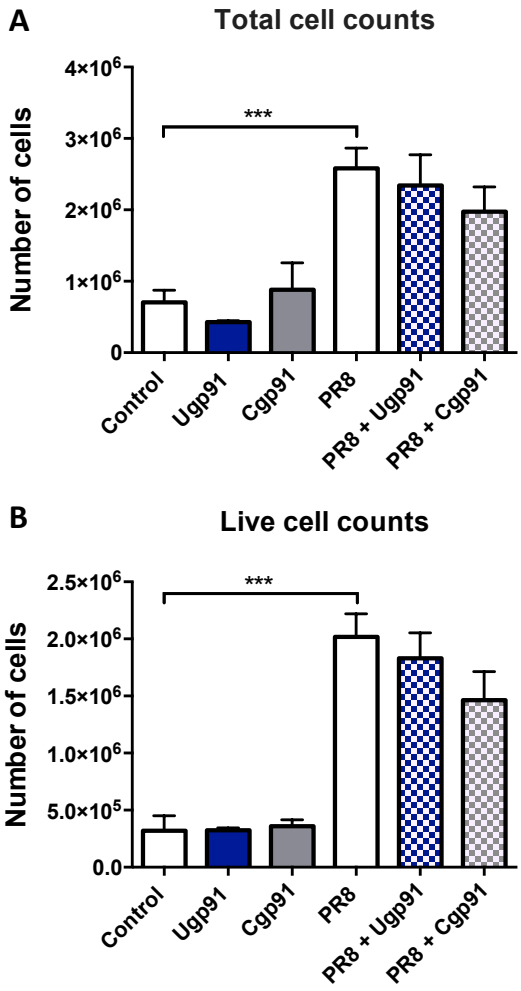

Figure 2: Cgp91 and Ugp91 by prevention had no impact on airway inflammation in mice infected with PR8 virus. Mice were treated daily via intranasal administration of Ugp91 (0.2mg/kg), Cgp91 (0.2mg/kg) or DMSO (2%; control) over a 4-day period. Mice were intranasally infected with PR8 (500 PFUs) or PBS control, one-day post initial drug treatment. Airway inflammation was assessed via counting the A) total cells and B) live cells of the BALF. Data are expressed as mean ± SEM (Control, n=7; Ugp91, n=5; Cgp91, n=5; PR8, n=9, PR8 + Ugp91, n=9; PR8 + Cgp91, n=10). Statistical analysis was conducted using one-way ANOVA test followed by Tukey's post hoc test for multiple comparison tests. Statistical significance was taken where $P<0.05$, where *** indicates $P<0.001$.

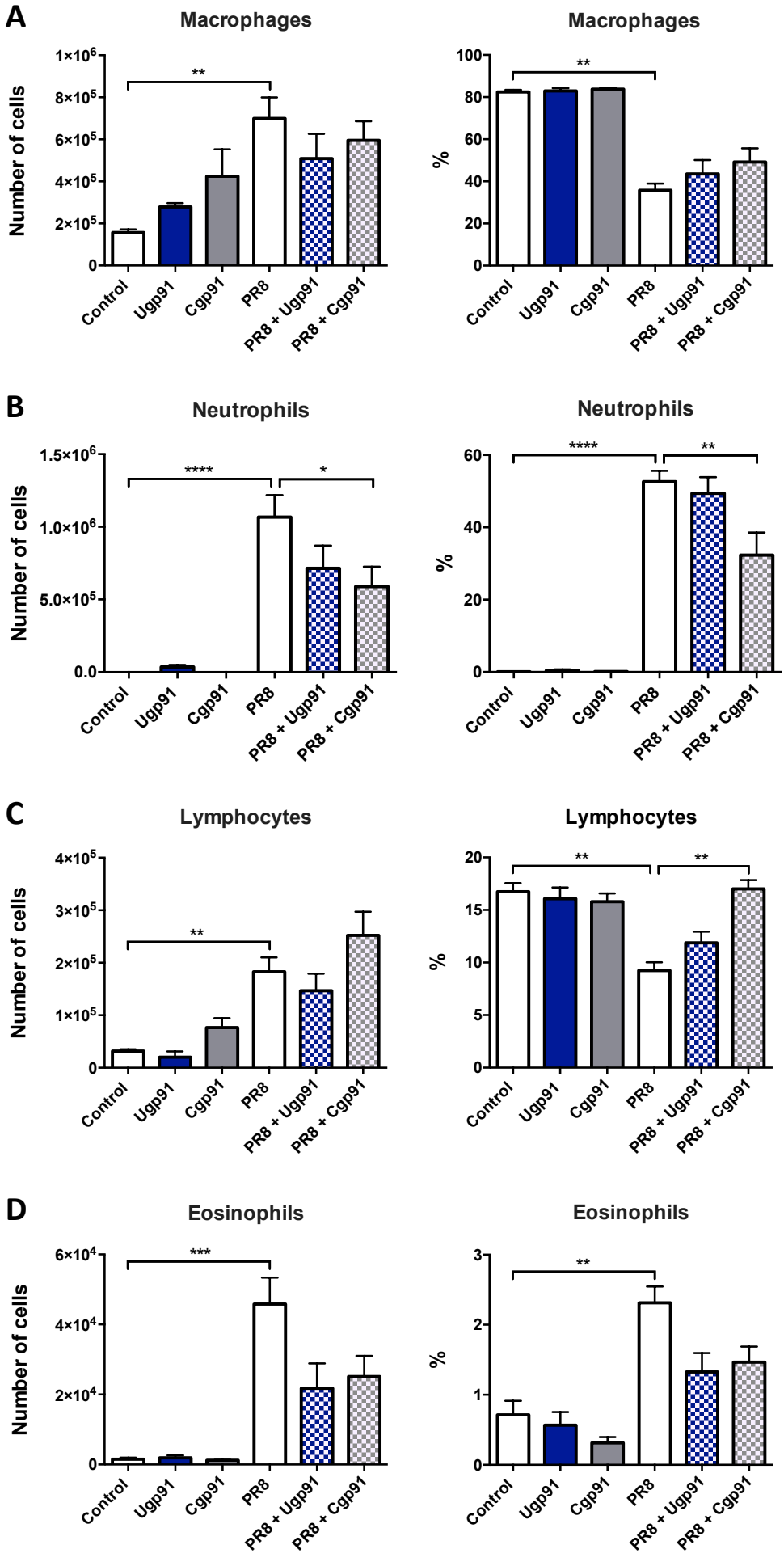
A
Macrophages
Number of cells
1×10^6
8×10^5
6×10^5
4×10^5
2×10^5
0
**
Control
Ugp91
Cgp91
PR8
PR8 + Ugp91
PR8 + Cgp91
Macrophages
%
100
80
60
40
20
0
**
B
Neutrophils
Number of cells
1.5×10^6
1.0×10^6
5.0×10^5
0.0
****
*
Neutrophils
%
60
40
20
0
****
**
C
Lymphocytes
Number of cells
4×10^5
3×10^5
2×10^5
1×10^5
0
**
Lymphocytes
%
20
15
10
5
0
**
**
D
Eosinophils
Number of cells
6×10^4
4×10^4
2×10^4
0
***
Eosinophils
%
3
2
1
0
**

Figure 3: Preventative treatment with Cgp91 reduces neutrophil infiltration induced by PR8 virus infection. Mice were treated daily via intranasal administration of Ugp91 (0.2mg/kg), Cgp91 (0.2mg/kg) or DMSO (2%; control) over a 4-day period. Mice were intranasally infected with PR8 (500 PFUs) or PBS control, one-day post initial drug treatment. BALF was collected from mice and differential cell counts A) macrophages, B) neutrophils, C) lymphocytes and D) eosinophils. 500 cells were counted from random fields by standard morphological criteria. Data are expressed as mean ± SEM (Control, n=7; Ugp91, n=5; Cgp91, n=5; PR8, n=9, PR8 + Ugp91, n=9; PR8 + Cgp91, n=10). Statistical analysis were conducted using one-way ANOVA test followed by Tukey's post hoc test for multiple comparison. Statistical significance was taken where $P<0.05$. *, $P<0.05$; **, $P<0.01$; ***, $P<0.001$; ****, $P<0.0001$.

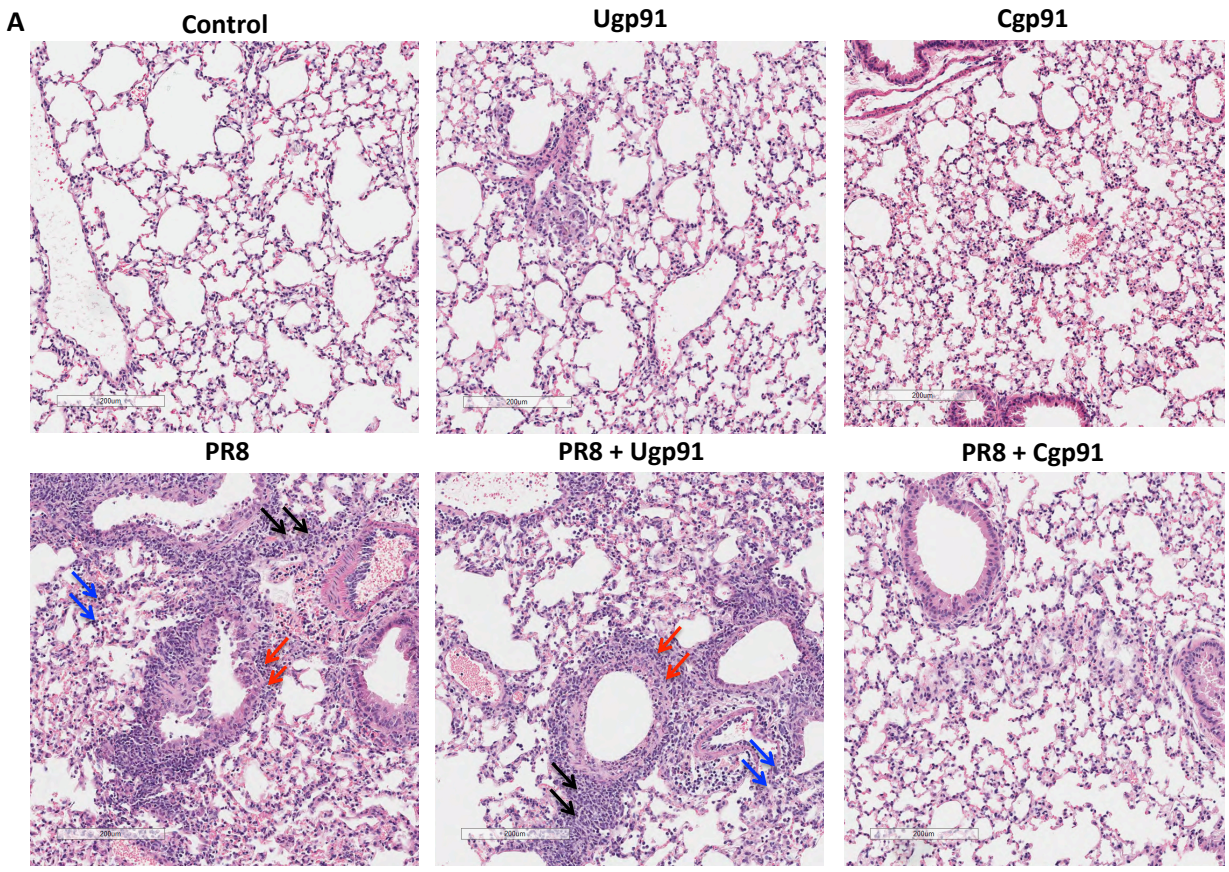
A
Control
Ugp91
Cgp91
PR8
PR8 + Ugp91
PR8 + Cgp91

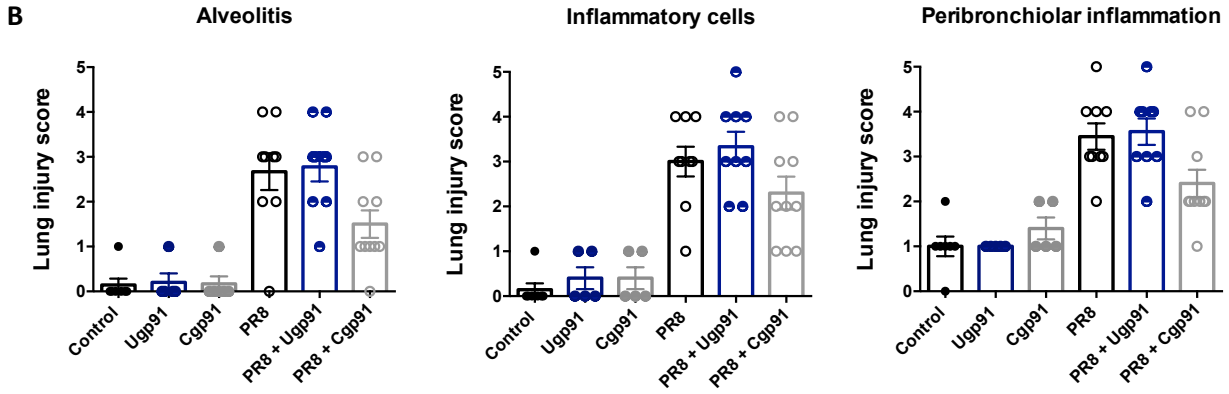
B
Alveolitis
Inflammatory cells
Peribronchiolar inflammation
Lung injury score
0
1
2
3
4
5
Control
Ugp91
Cgp91
PR8
PR8 + Ugp91
PR8 + Cgp91

Figure 4: Lung histopathological stains reveal Cgp91 reduces airway inflammation in PR8-infected mice. Histopathological analysis of lungs from WT C57Bl/6J mice treated daily via intranasal administration of Ugp91 (0.2mg/kg), Cgp91 (0.2mg/kg) or DMSO (2%; control) over a 4-day period. Mice were infected with PR8 (500 PFUs) or PBS control, one-day post initial drug treatment and analysed at day 3 post infection. A) Representative images displaying the inflammation in lung sections following H&E staining. B) Each sample was assigned a score of 0-5 for each individual mouse (higher numbers indicate increased disease severity) from two independent assessors. Sections were scored for alveolitis, inflammatory cell infiltrate and peribronchiolar inflammation. Magnifications of images are at X10. Data are expressed as mean ± SEM (Control, n=7; Ugp91, n=5; Cgp91, n=5; PR8, n=9, PR8 + Ugp91, n=9; PR8 + Cgp91, n=10). Statistical analysis was conducted using one-way ANOVA test followed by Tukey's post hoc test for multiple comparisons. Statistical significance was taken where $P<0.05$.

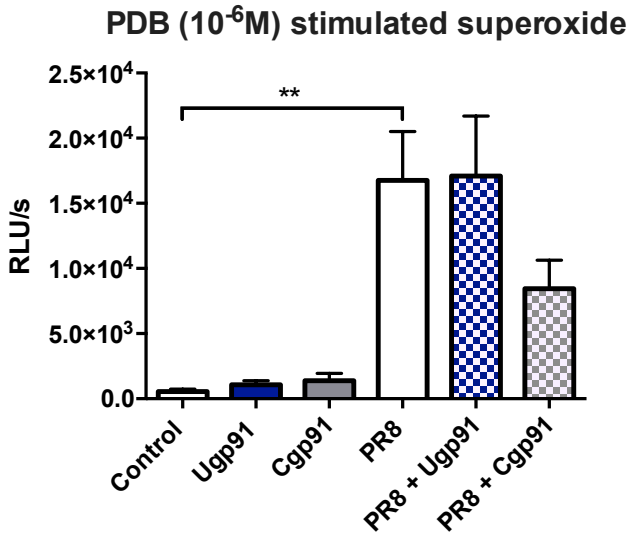

Figure 5: Preventative administration of Cgp91 is associated with a reduction in ROS generation. WT C57Bl/6J mice (8-12 weeks) were treated daily via intranasal administration of Ugp91 (0.2mg/kg), Cgp91 (0.2mg/kg) or DMSO (2%) control. Mice were intranasally infected with PR8 (500 PFUs) or PBS control, one-day post initial drug treatment. BALF was collected for PDB (10^{-6} M) stimulated ROS production that was quantified by L-O12 enhanced chemiluminescence. Data are expressed as mean ± SEM (Control, n=7; Ugp91, n=5; Cgp91, n=5; PR8, n=9, PR8 + Ugp91, n=9; PR8 + Cgp91, n=10). Statistical analysis were conducted using one-way ANOVA test followed by Tukey's post hoc test for multiple comparison. Statistical significance was taken where $P<0.05$, where ** indicates $P<0.01$.

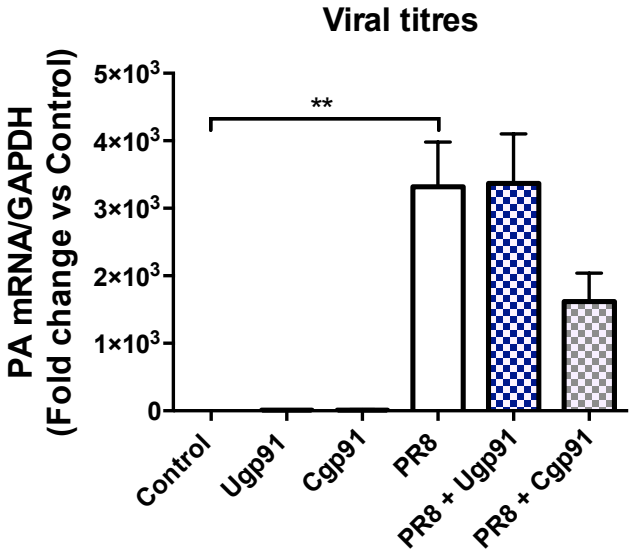

Figure 6: Cgp91 treatment reduces the expression of viral mRNA. QPCR analysis of mRNA from the gene encoding polymerase of influenza virus strain PR8 in the lungs of WT mice 3-days post infection with PR8 influenza virus; results are presented relative to those of GAPDH mRNA. Data are expressed as mean ± SEM (Control, n=7; Ugp91, n=5; Cgp91, n=5; PR8, n=9, PR8 + Ugp91, n=9; PR8 + Cgp91, n=10). Statistical analysis was conducted using one-way ANOVA test followed by Tukey's post hoc test for multiple comparisons. Statistical significance was taken where $P<0.05$. where ** indicates $P<0.01$.

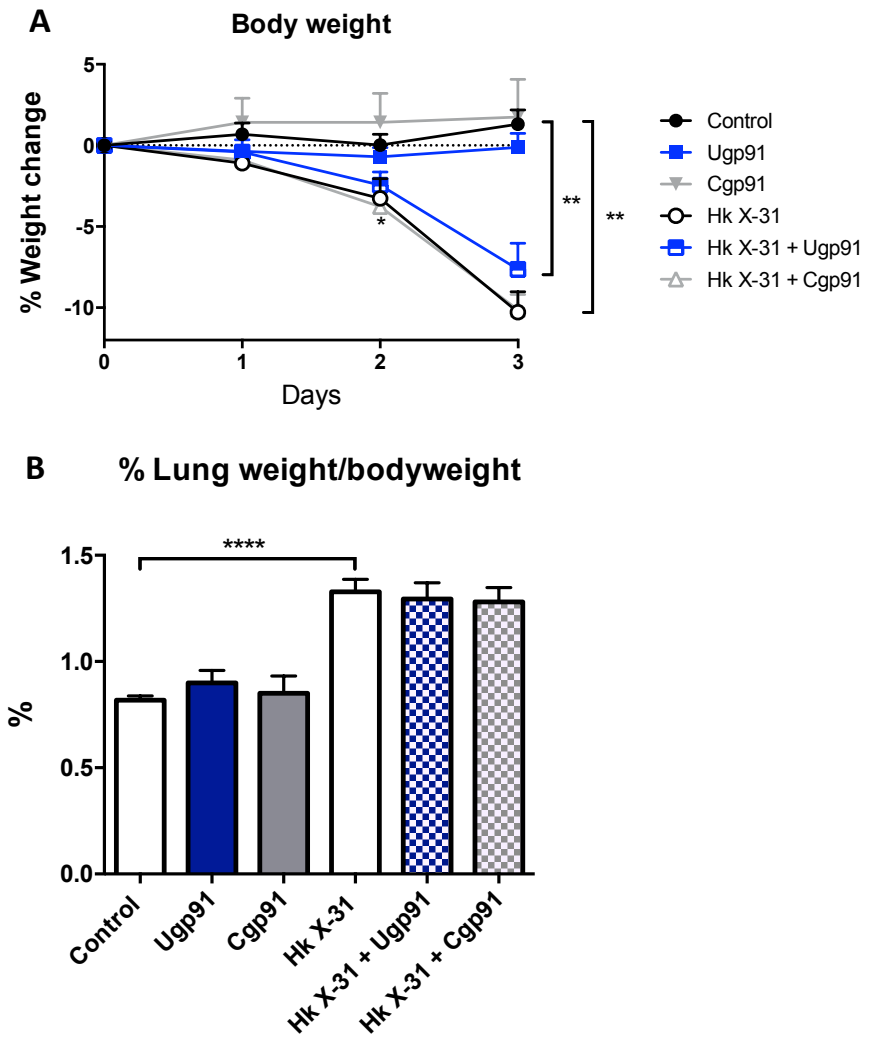

Figure 7: NOX2 inhibitors by intervention had no effect on altering bodyweight or lung weight in mice infected with low pathogenic Hk x-31 virus. WT C57Bl/6J mice (8-12 weeks) were infected with Hkx-31 ($1x10^5$ PFUs) or PBS (control) via instranal administration. One day post-infection mice were treated daily for 3 days with Ugp91 (0.2mg/kg), Cgp91 (0.2mg/kg) or DMSO (2%; control) via instranal administration for measurements at Day 3 post-infection of A) bodyweight. B) The weight of the lungs was measured and presented as a % of the bodyweight of each respective mouse. Data are expressed as mean ± SEM (Control, n=7; Ugp91, n=5; Cgp91, n=4; PR8, n=10, PR8 + Ugp91, n=10; PR8 + Cgp91, n=10). Statistical analysis were conducted using two-way ANOVA followed by Holm's Sidak *post-hoc* multiple comparison test in 'A'. One-way ANOVA test followed by Tukey's *post-hoc* test for multiple comparisons in 'B'. Statistical significance was taken where $P<0.05$. **, $P<0.01$ and ****, $P<0.0001$.

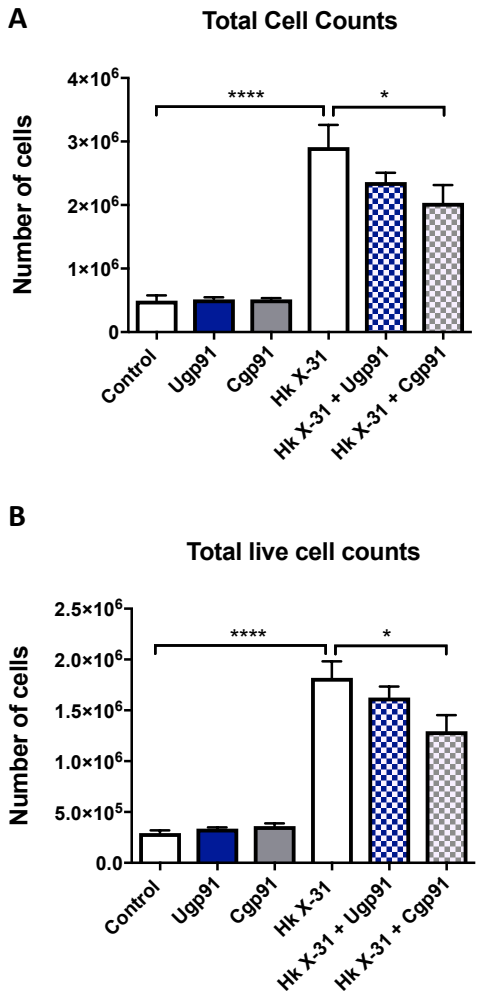

Figure 8: Cgp91 via intervention reduces airway inflammation in mice infected with PR8 virus. WT C57Bl/6J mice (8-12 weeks) were infected with Hkx-31 ($1x10^5$ PFUs) or PBS (control) via instranal administration. One day post-infection mice were treated daily for 3 days with Ugp91 (0.2mg/kg), Cgp91 (0.2mg/kg) or DMSO (2%; control) via instranal administration for measurements at Day 3 post-infection of A) total cells and B) total live cells of the BALF. Data are expressed as mean ± SEM (Control, n=7; Ugp91, n=5; Cgp91, n=4; PR8, n=10, PR8 + Ugp91, n=10; PR8 + Cgp91, n=10). Statistical analysis was conducted using one-way ANOVA test followed by Tukey's post hoc test for multiple comparison tests. Statistical significance was taken where $P<0.05$, where *, $P<0.05$ and **** , $P<0.0001$.

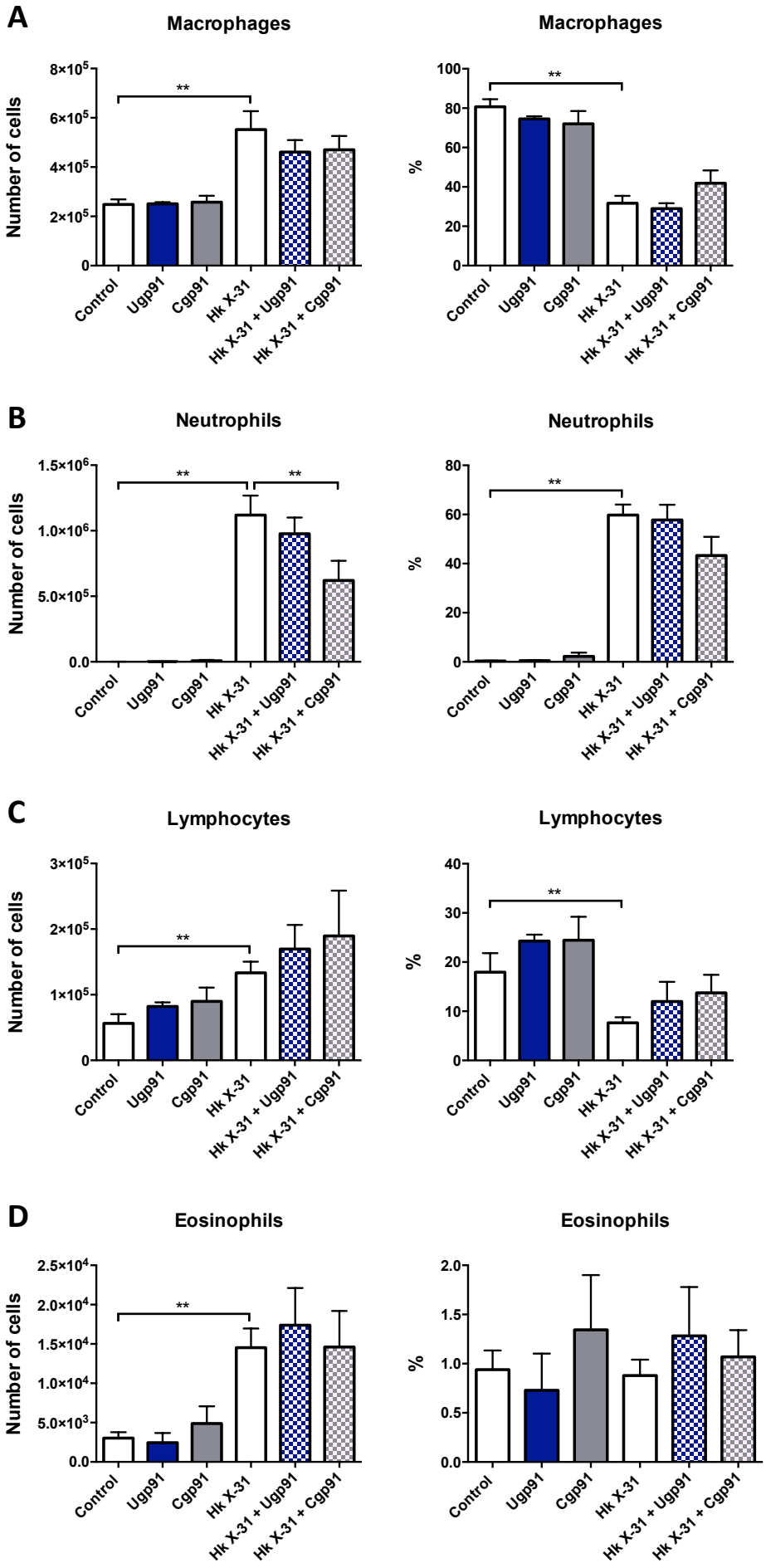
A
Macrophages
Number of cells
8×10^5
6×10^5
4×10^5
2×10^5
0
**
Control
Ugp91
Cgp91
Hk X-31
Hk X-31 + Ugp91
Hk X-31 + Cgp91
Macrophages
%
100
80
60
40
20
0
**
Control
Ugp91
Cgp91
Hk X-31
Hk X-31 + Ugp91
Hk X-31 + Cgp91
B
Neutrophils
Number of cells
1.5×10^6
1.0×10^6
5.0×10^5
0.0
**
**
Control
Ugp91
Cgp91
Hk X-31
Hk X-31 + Ugp91
Hk X-31 + Cgp91
Neutrophils
%
80
60
40
20
0
**
Control
Ugp91
Cgp91
Hk X-31
Hk X-31 + Ugp91
Hk X-31 + Cgp91
C
Lymphocytes
Number of cells
3×10^5
2×10^5
1×10^5
0
**
Control
Ugp91
Cgp91
Hk X-31
Hk X-31 + Ugp91
Hk X-31 + Cgp91
Lymphocytes
%
40
30
20
10
0
**
Control
Ugp91
Cgp91
Hk X-31
Hk X-31 + Ugp91
Hk X-31 + Cgp91
D
Eosinophils
Number of cells
2.5×10^4
2.0×10^4
1.5×10^4
1.0×10^4
5.0×10^3
0.0
**
Control
Ugp91
Cgp91
Hk X-31
Hk X-31 + Ugp91
Hk X-31 + Cgp91
Eosinophils
%
2.0
1.5
1.0
0.5
0.0
Control
Ugp91
Cgp91
Hk X-31
Hk X-31 + Ugp91
Hk X-31 + Cgp91

Figure 9: Interventional treatment with Cgp91 attenuates neutrophil infiltration induced by Hkx-31 infection. BALF was collected from infected with Hkx-31 ($1x10^5$ PFUs) or PBS (control) via instranal administration. One day post-infection mice were treated daily for 3 days with Ugp91 (0.2mg/kg), Cgp91 (0.2mg/kg) or DMSO (2%; control) via instranal administration for measurements at Day 3 post-infection. Differential cell counts and percentage of cell populations of A) macrophages, B) neutrophils, C) lymphocytes and D) eosinophils were examined. 500 cells were counted from random fields by standard morphological criteria. Data are expressed as mean ± SEM (Control, n=7; Ugp91, n=5; Cgp91, n=4; PR8, n=10, PR8 + Ugp91, n=10; PR8 + Cgp91, n=10). Statistical analysis were conducted using one-way ANOVA test followed by Tukey's post hoc test for multiple comparison. Statistical significance was taken where $P<0.05$, where ** indicates $P<0.01$.

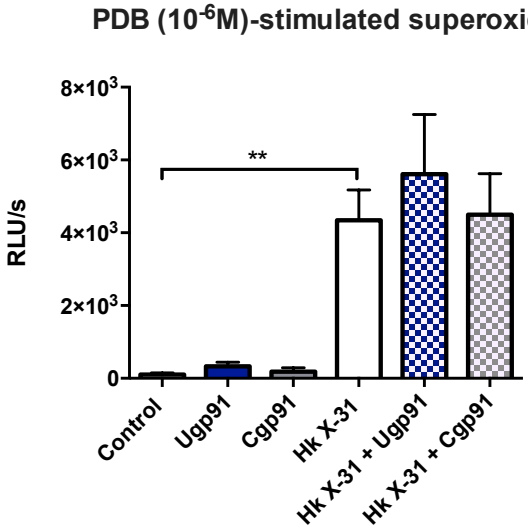

Figure 10: Intervention treatment with NOX2 inhibitors do not alter HKx-31-induced ROS generation. BALF was collected from infected with Hkx-31 ($1x10^5$ PFUs) or PBS (control) via instranal administration. One day post-infection mice were treated daily for 3 days with Ugp91 (0.2mg/kg), Cgp91 (0.2mg/kg) or DMSO (2%; control) via instranal administration for measurements at Day 3 post-infection. PDB (10^{-6} M)-stimulated ROS production that was quantified by L-O12 (10^{-4} M) enhanced chemiluminescence. Data are expressed as mean ± SEM (Control, n=7; Ugp91, n=5; Cgp91, n=4; PR8, n=10, PR8 + Ugp91, n=10; PR8 + Cgp91, n=10). Statistical analysis was conducted using one-way ANOVA test followed by Tukey's post hoc test for multiple comparison. Statistical significance was taken where $P<0.05$, where ** indicates $P<0.01$.

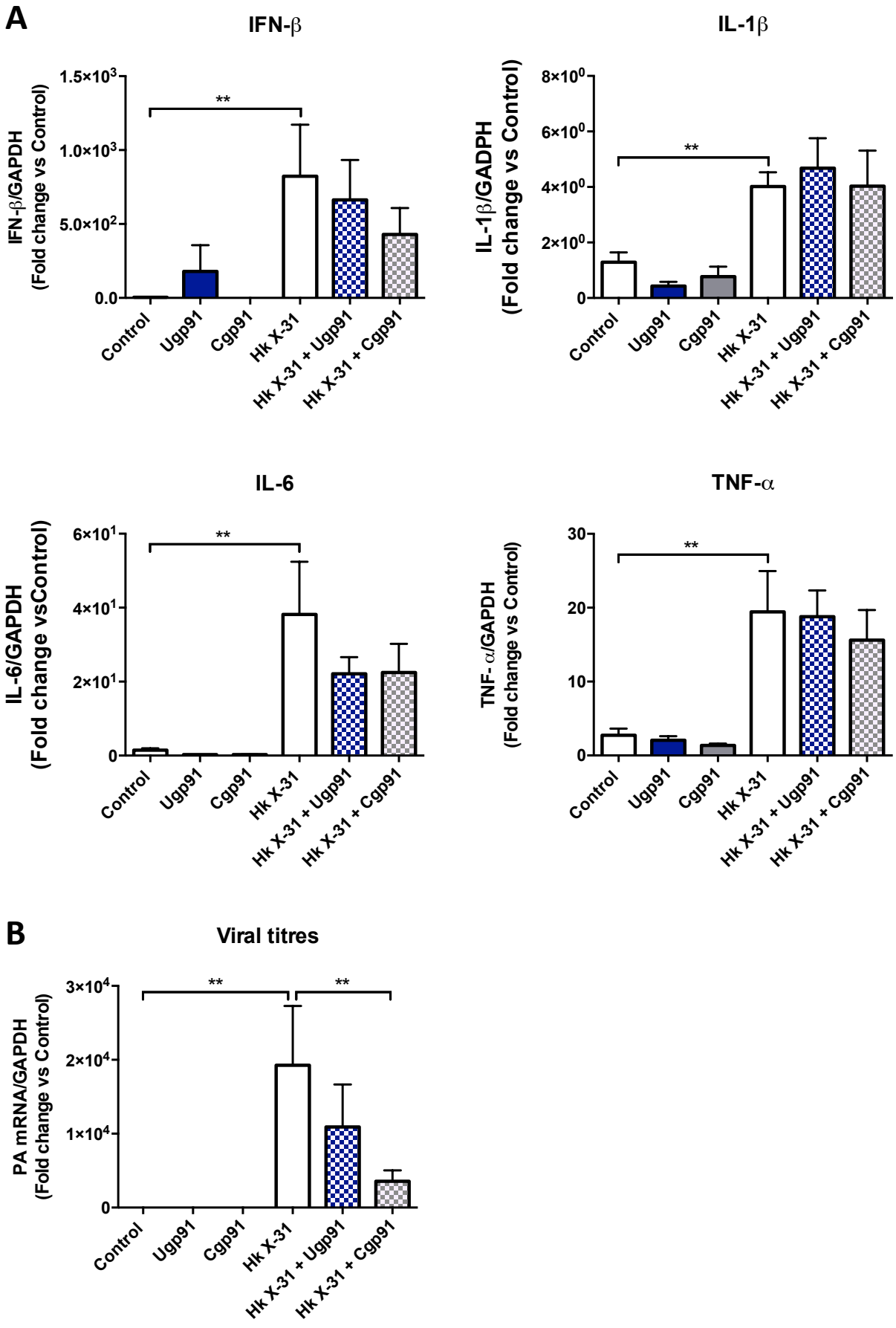
A
IFN-β
IFN-β/GAPDH
(Fold change vs Control)
1.5×10^3
1.0×10^3
5.0×10^2
0.0
**
Control
Ugp91
Cgp91
Hk X-31
Hk X-31 + Ugp91
Hk X-31 + Cgp91
IL-1β
IL-1β/GADPH
(Fold change vs Control)
8×10^0
6×10^0
4×10^0
2×10^0
0
**
Control
Ugp91
Cgp91
Hk X-31
Hk X-31 + Ugp91
Hk X-31 + Cgp91
IL-6
IL-6/GAPDH
(Fold change vsControl)
6×10^1
4×10^1
2×10^1
0
**
Control
Ugp91
Cgp91
Hk X-31
Hk X-31 + Ugp91
Hk X-31 + Cgp91
TNF-α
TNF-α/GAPDH
(Fold change vs Control)
30
20
10
0
**
Control
Ugp91
Cgp91
Hk X-31
Hk X-31 + Ugp91
Hk X-31 + Cgp91
B
Viral titres
PA mRNA/GAPDH
(Fold change vs Control)
3×10^4
2×10^4
1×10^4
0
**
**
Control
Ugp91
Cgp91
Hk X-31
Hk X-31 + Ugp91
Hk X-31 + Cgp91

Figure 11: NOX2 inhibitors by intervention reduce viral burden in mice infected with Hk x-31 virus. WT C57Bl/6J mice (8-12 weeks) were infected with Hkx-31 ($1x10^5$ PFUs) or PBS (control) via instranal administration. One day post-infection mice were treated daily for 3 days with Ugp91 (0.2mg/kg), Cgp91 (0.2mg/kg) or DMSO (2%; control) via instranal administration for measurements at Day 3 post-infection. QPCR was used to quantify expression of A) cytokines: IFN-β, IL-1β, IL-6, and TNF-α in lung tissue, and B) viral mRNA. Responses are relative to GAPDH and then expressed as a fold-change above controls. Data are expressed as mean ± SEM (Control, n=7; Ugp91, n=5; Cgp91, n=4; PR8, n=10, PR8 + Ugp91, n=10; PR8 + Cgp91, n=10). Statistical analysis was conducted using one-way ANOVA test followed by Tukey's post hoc test for multiple comparison. Statistical significance was taken where $P<0.05$, where ** indicates $P<0.01$.

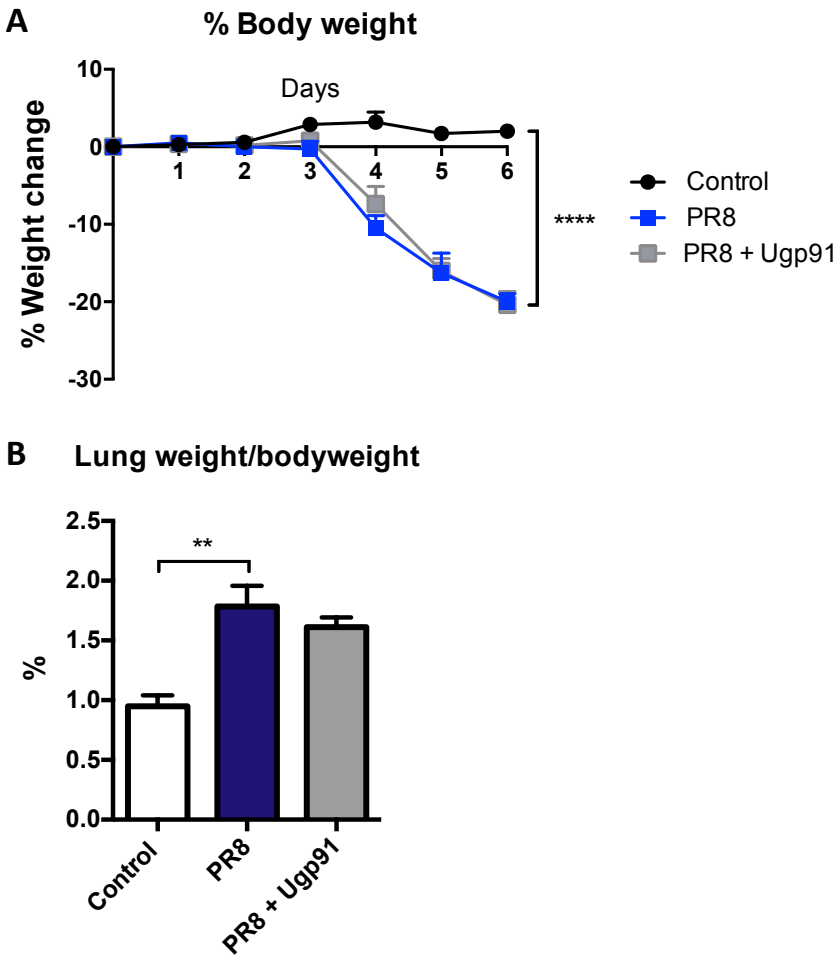

Figure 12: Delivery of Ugp91 by intervention had no effect on altering disease severity in mice infected with high pathogenic PR8 virus. WT C57Bl/6J mice (8-12 weeks) were infected with PR8 influenza A virus (50 PFUs) or PBS (control). One day post-infection mice were treated daily for 5 days with Ugp91 (0.2mg/kg) or DMSO (2%; control) for measurements at Day 6 post-infection of A) bodyweight. B) The weight of the lungs was measured and presented as a % of the bodyweight of each respective mouse. Data are expressed as mean ± SEM (Control, n=3; PR8, n=3; PR8 + Ugp91, n=4). Statistical analysis was conducted using two-way ANOVA followed by Holm's Sidak *post-hoc* multiple comparison test in 'A'. One-way ANOVA test followed by Tukey's *post-hoc* test for multiple comparisons in 'B'. Statistical significance was taken where $P<0.05$. **, $P<0.01$; ****, $P<0.0001$.

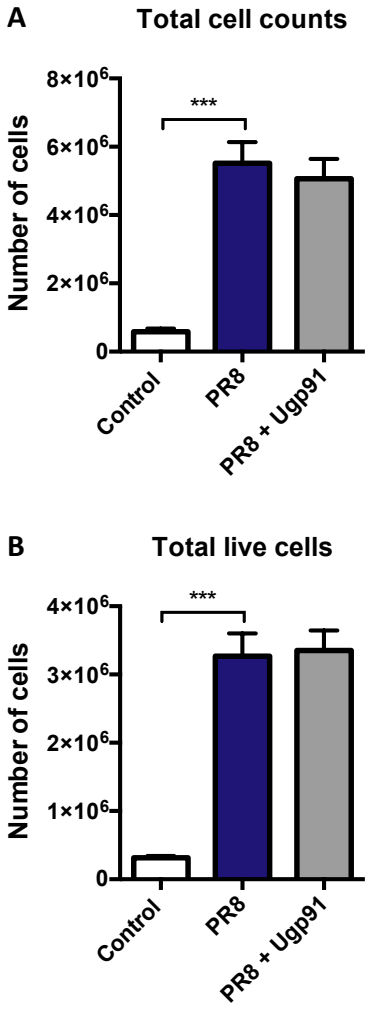

Figure 13: Ugp91 via intervention had no effect on altering disease severity in mice infected with high pathogenic PR8 virus. WT C57Bl/6J mice (8-12 weeks) were infected with PR8 influenza A virus (50 PFUs) or PBS (control). One day post-infection mice were treated daily for 5 days with Ugp91 (0.2mg/kg) or DMSO (2%; control) for measurements at Day 6 post-infection. BALF was stained with 0.4% trypan blue to measure the A) total cells and B) total live cells. Data are expressed as mean ± SEM (Control, n=3; PR8, n=3; PR8 + Ugp91, n=4). Statistical analysis was conducted using one-way ANOVA test followed by Tukey's *post-hoc* test for multiple comparisons. Statistical significance was taken where $P<0.05$, where *** indicates $P<0.001$.

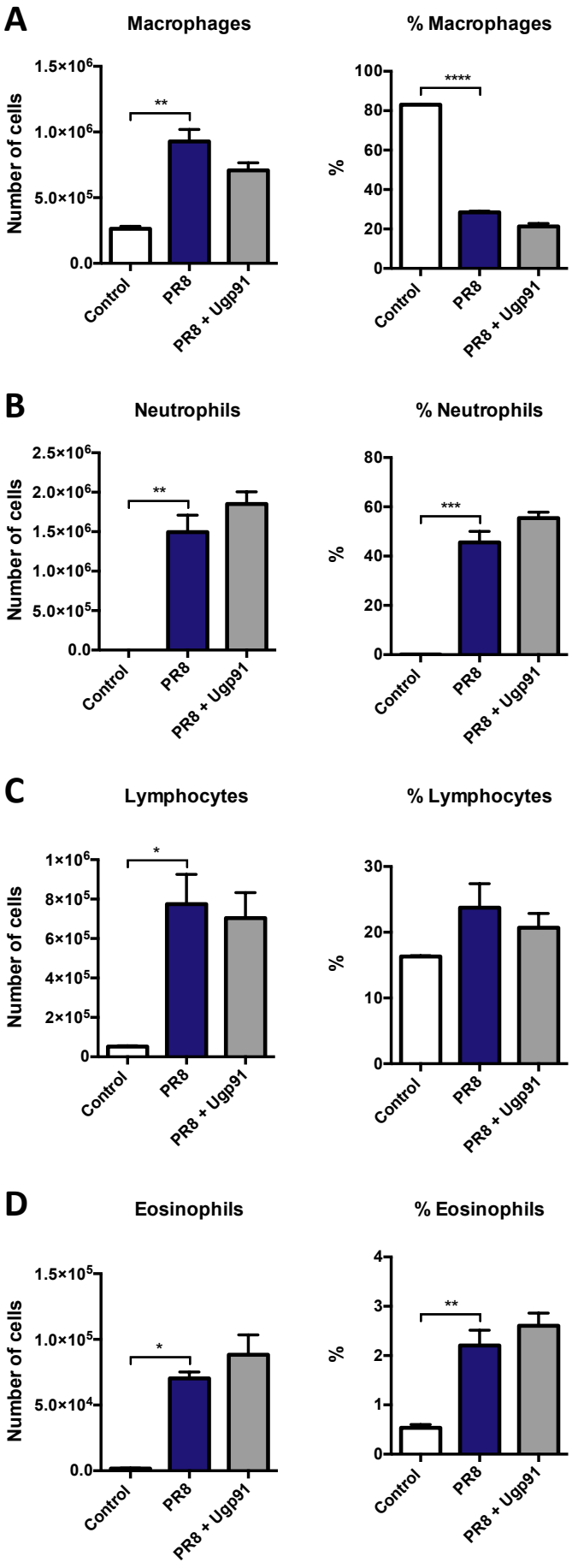
A
Macrophages
% Macrophages
Number of cells
1.5×10^6
1.0×10^6
5.0×10^5
0.0
**
100
80
60
40
20
0
****
%
Control
PR8
PR8 + Ugp91
B
Neutrophils
% Neutrophils
2.5×10^6
2.0×10^6
1.5×10^6
1.0×10^6
5.0×10^5
***
C
Lymphocytes
% Lymphocytes
1×10^6
8×10^5
6×10^5
4×10^5
2×10^5
30
D
Eosinophils
% Eosinophils
1.5×10^5
1.0×10^5
5.0×10^4

Figure 14: Ugp91 has no affect on differential cell counts in mice infected with high pathogenic PR8 virus. WT C57Bl/6J mice (8-12 weeks) were infected with PR8 influenza A virus (50 PFUs) or PBS (control). One day post-infection mice were treated daily for 5 days with Ugp91 (0.2mg/kg) or DMSO (2%; control) for measurements at Day 6 post-infection. BALF was collected from mice and differential cell counts A) macrophages, B) neutrophils, C) lymphocytes and D) eosinophils. 500 cells were counted from random fields by standard morphological criteria. Data are expressed as mean ± SEM (Control, n=3; PR8, n=3; PR8 + Ugp91, n=4). Statistical analysis were conducted using one-way ANOVA test followed by Tukey's post hoc test for multiple comparison. Statistical significance was taken where $P<0.05$. *, $P<0.05$; **, $P<0.01$; ***, $P<0.001$; ****, $P<0.0001$.

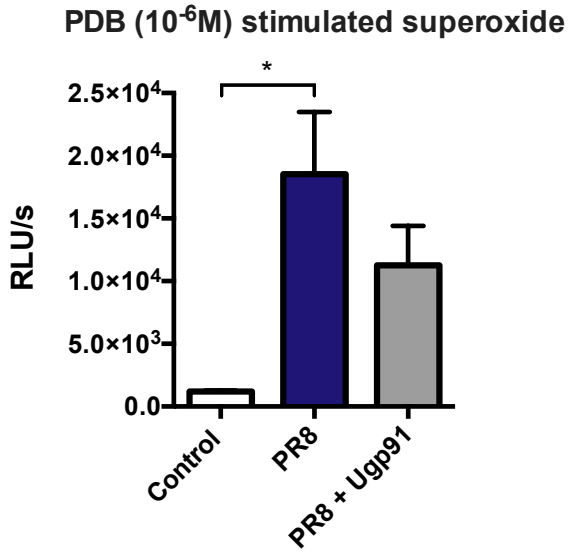

Figure 15: Intervention treatment with Ugp91 does not alter HKx-31-induced ROS generation. BALF was collected from mice infected with PR8 influenza A virus (50 PFUs) or PBS (control). One day post-infection mice were treated daily for 5 days with Ugp91 (0.2mg/kg) or DMSO (2%; control) for measurements at Day 6 post-infection. PDB (10^{-6} M)-stimulated ROS production that was quantified by L-O12 (10^{-4} M) enhanced chemiluminescence. Data is representative of n = 3-4 and expressed as mean ± SEM (Control, n=3; PR8, n=3; PR8 + Ugp91, n=4). Statistical analysis was conducted using one-way ANOVA test followed by Tukey's post hoc test for multiple comparison. Statistical significance was taken where $P<0.05$, where * Indicates $P<0.05$.

References

Abed Y, Goyette N, Boivin G (2005). Generation and characterization of recombinant influenza A (H1N1) viruses harboring amantadine resistance mutations. *Antimicrob. Agents Chemother.* **49**(2)**:** 556-559.

Akaike T (2001). Role of free radicals in viral pathogenesis and mutation. *Rev. Med. Virol.* **11**(2)**:** 87-101.

Akaike T, Noguchi Y, Ijiri S, Setoguchi K, Suga M, Zheng YM*, et al.* (1996). Pathogenesis of influenza virus-induced pneumonia: Involvement of both nitric oxide and oxygen radicals. *Proc. Natl. Acad. Sci. U. S. A.* **93**(6)**:** 2448-2453.

Buffinton GD, Christen S, Peterhans E, Stocker R (1992). Oxidative stress in lungs of mice infected with influenza a virus. *Free Radic. Res.* **16**(2)**:** 99-110.

Chan MCW, Cheung CY, Chui WH, Tsao GSW, Nicholls JM, Chan YO*, et al.* (2005). Proinflammatory cytokine responses induced by influenza A (H5N1) viruses in primary human alveolar and bronchial epithelial cells. *Respir. Res.* **6**.

Chandler JD, Hu X, Ko EJ, Park S, Lee YT, Orr M*, et al.* (2016). Metabolic pathways of lung inflammation revealed by high-resolution metabolomics (HRM) of H1N1 influenza virus infection in mice. *Am. J. Physiol. Regul. Integr. Comp. Physiol.* **311**(5)**:** R906-R916.

Ely JTA (2007). Ascorbic acid role in containment of the world avian flu pandemic. *Exp. Biol. Med.* **232**(7)**:** 847-851.

García-Sastre A, Biron CA (2006). Type 1 interferons and the virus-host relationship: A lesson in détente. *Science* **312**(5775)**:** 879-882.

Geiler J, Michaelis M, Naczk P, Leutz A, Langer K, Doerr HW*, et al.* (2010). N-acetyl-l-cysteine (NAC) inhibits virus replication and expression of pro-inflammatory molecules in A549 cells infected with highly pathogenic H5N1 influenza A virus. *Biochem. Pharmacol.* **79**(3)**:** 413-420.

German V, Chokephaibulkit K (2004). Avian influenza virus infection of children in Vietnam and Thailand. *Pediatr. Infect. Dis. J.* **23**(8)**:** 793-794.

Hai R, Schmolke M, Leyva-Grado VH, Thangavel RR, Margine I, Jaffe EL*, et al.* (2013). Influenza A(H7N9) virus gains neuraminidase inhibitor resistance without loss of in vivo virulence or transmissibility. *Nat. Commun.* **4**.

Halima SB, Rajendran L (2011). Membrane anchored and lipid raft targeted β-secretase inhibitors for alzheimer's disease therapy. *J. Alzheimer's Dis.* **24**(SUPPL. 2)**:** 143-152.

Hayden FG, Fritz RS, Lobo MC, Alvord WG, Strober W, Straus SE (1998). Local and systemic cytokine responses during experimental human influenza A virus infection. Relation to symptom formation and host defense. *Journal of Clinical Investigation* **101**(3)**:** 643-649.

He G, Dong C, Luan Z, McAllan BM, Xu T, Zhao L*, et al.* (2013). Oxygen free radical involvement in acute lung injury induced by H5N1 virus in mice. *Influ. Other Respir. Viruses* **7**(6)**:** 945-953.

Herold S, Steinmueller M, Von Wulffen W, Cakarova L, Pinto R, Pleschka S*, et al.* (2008). Lung epithelial apoptosis in influenza virus pneumonia: The role of macrophage-expressed TNF-related apoptosis-inducing ligand. *J. Exp. Med.* **205**(13)**:** 3065-3077.

Herold S, Von Wulffen W, Steinmueller M, Pleschka S, Kuziel WA, Mack M*, et al.* (2006). Alveolar epithelial cells direct monocyte transepithelial migration upon influenza virus infection: Impact of chemokines and adhesion molecules. *Journal of Immunology* **177**(3)**:** 1817-1824.

Hofmann P, Sprenger H, Kaufmann A, Bender A, Hasse C, Nain M*, et al.* (1997). Susceptibility of mononuclear phagocytes to influenza A virus infection and possible role in the antiviral response. *J. LEUKOCYTE BIOL.* **61**(4)**:** 408-414.

Ishikawa E, Nakazawa M, Yoshinari M, Minami M (2005). Role of tumor necrosis factor-related apoptosis-inducing ligand in immune response to influenza virus infection in mice. *Journal of Virology* **79**(12)**:** 7658-7663.

Leonov H, Astrahan P, Krugliak M, Arkin IT (2011). How do aminoadamantanes block the influenza M2 channel, and how does resistance develop? *J. Am. Chem. Soc.* **133**(25)**:** 9903-9911.

Li TCM, Chan MCW, Lee N (2015). Clinical implications of antiviral resistance in influenza. *Viruses* **7**(9)**:** 4929-4944.

Moscona A (2005). Neuraminidase inhibitors for influenza. *New Engl. J. Med.* **353**(13)**:** 1363-1373.

Nitsch-Osuch A, Brydak LB (2015). Treatment and prophylaxis of influenza and the problem of resistance to neuraminidase inhibitors. *Postepy Hig Med Dosw (Online)* **69:** 1087-1095.

Perrone LA, Plowden JK, García-Sastre A, Katz JM, Tumpey TM (2008). H5N1 and 1918 pandemic influenza virus infection results in early and excessive infiltration of macrophages and neutrophils in the lungs of mice. *PLoS Pathogens* **4**(8).

Schoggins JW, Wilson SJ, Panis M, Murphy MY, Jones CT, Bieniasz P*, et al.* (2011). A diverse range of gene products are effectors of the type i interferon antiviral response. *Nature* **472**(7344)**:** 481-485.

Seo SH, Webby R, Webster RG (2004). No apoptotic deaths and different levels of inductions of inflammatory cytokines in alveolar macrophages infected with influenza viruses. *Virology* **329**(2)**:** 270-279.

Snelgrove RJ, Edwards L, Rae AJ, Hussell T (2006). An absence of reactive oxygen species improves the resolution of lung influenza infection. *Eur. J. Immunol.* **36**(6)**:** 1364-1373.

Sun K, Yajjala VK, Bauer C, Talmon GA, Fischer KJ, Kielian T*, et al.* (2016). NOX2-derived oxidative stress results in inefficacy of antibiotics against post-influenza S. aureus pneumonia. *J. Exp. Med.* **213**(9)**:** 1851-1864.

Tate MD, Deng YM, Jones JE, Anderson GP, Brooks AG, Reading PC (2009). Neutrophils ameliorate lung injury and the development of severe disease during influenza infection. *Journal of Immunology* **183**(11)**:** 7441-7450.

Tate MD, Schilter HC, Brooks AG, Reading PC (2011). Responses of mouse airway epithelial cells and alveolar macrophages to virulent and avirulent strains of influenza a virus. *Viral Immunol.* **24**(2)**:** 77-88.

Tumpey TM, García-Sastre A, Taubenberger JK, Palese P, Swayne DE, Pantin-Jackwood MJ*, et al.* (2005). Pathogenicity of influenza viruses with genes from the 1918 pandemic virus: Functional roles of alveolar macrophages and neutrophils in limiting virus replication and mortality in mice. *Journal of Virology* **79**(23)**:** 14933-14944.

Vlahos R, Stambas J, Bozinovski S, Broughton BRS, Drummond GR, Selemidis S (2011). Inhibition of NOX2 oxidase activity ameliorates influenza a virus-induced lung inflammation. *PLoS Pathogens* **7**(2).

Vlahos R, Stambas J, Selemidis S (2012). Suppressing production of reactive oxygen species (ROS) for influenza A virus therapy. *Trends Pharmacol. Sci.* **33**(1)**:** 3-8.

Wareing MD, Lyon AB, Lu B, Gerard C, Sarawar SR (2004). Chemokine expression during the development and resolution of a pulmonary leukocyte response to influenza A virus infection in mice. *J. LEUKOCYTE BIOL.* **76**(4)**:** 886-895.

Wijburg OLC, Dinatale S, Vadolas J, Van Rooijen N, Strugnell RA (1997). Alveolar macrophages regulate the induction of primary cytotoxic T- lymphocyte responses during influenza virus infection. *Journal of Virology* **71**(12)**:** 9450-9457.

Xu L, Yoon H, Zhao MQ, Liu J, Ramana CV, Enelow RI (2004). Cutting edge: Pulmonary immunopathology mediated by antigen-specific expression of TNF-α by antiviral CD8+ T cells. *Journal of Immunology* **173**(2)**:** 721-725.

Yewdell JW, Bennink JR, Smith GL, Moss B (1985). Influenza A virus nucleoprotein is a major target antigen for cross-reactive anti-influenza A virus cytotoxic T lymphocytes. *Proc. Natl. Acad. Sci. U. S. A.* **82**(6)**:** 1785-1789.

Zhang RH, Li CH, Wang CL, Xu MJ, Xu T, Wei D*, et al.* (2014). N-acetyl-l-cystine (NAC) protects against H9N2 swine influenza virus-induced acute lung injury. *Int. Immunopharmacol.* **22**(1)**:** 1-8.

Chapter 5:
General discussion

Collectively, this thesis utilises a series of *in vitro* an *in vivo* clinically relevant mouse models of virus infection to unravel previously unrecognised mechanisms of viral pathology and disease progression. The main findings demonstrated for the *first time* that endosomal NOX2 oxidase is *the* primary source of ROS production following virus infection and a key modulator of anti-viral immunity. This thesis has unveiled four new paradigms of ROS biology and pathobiology. These include: 1) Influenza A virus infection potentiates NOX2 oxidase-dependent ROS production in macrophages; 2) Identification of endosomes as critical subcellular sites of ROS generation to virus infection; 3) The unravelling that critical molecular targets of endosomal ROS production are cysteine residues on proteins that reside within endosomal compartments and 4) Endosomal targeting of NOX2 oxidase protects against viral infections. In this Chapter, these 4 conceptual advancements will be further discussed.

Conceptual advancement 1: Influenza A virus infection potentiates NOX2 oxidase-dependent ROS production in macrophages

Due to their constantly changing genetic profiles, influenza viruses will inevitably continue to impose a serious threat to mankind and consequently our healthcare system. This highlights the urgency to develop new therapies to circumvent these imminent problems. Dysregulated ROS generation culminating in lung oxidative stress has been demonstrated following influenza infection (Akaike *et al.*, 1996; Imai *et al.*, 2008b; Vlahos *et al.*, 2011b). However, the mechanisms via which ROS contribute to viral pathology have up until now remained elusive. In Chapter 2, we sought to examine if ROS production in macrophages is altered by influenza A virus infection. We demonstrated that macrophages exposed to Hkx-31 IAV produced an exaggerated ROS response, which most probably involved endosomal TLR7 activation by the virus. We also demonstrated that influenza virus infection or TLR7 activation by imiquimod resulted in a "primed state" of the NOX2 oxidase. This effect of "priming" may help us understand how the NOX2 oxidase enzyme is pre-stimulated for pathogen control. In seminal previous studies key components of NOX2 oxidase were shown to be required for enzyme activation including serine residue phosphorylation on the regulatory protein p47phox (El Benna *et al.*, 1996; El-Benna *et al.*, 2008). Our data showed that serine 346 on p47phox was responsible for priming mouse NOX2 oxidase for a greater oxidative burst response, which is consistent with the study of Dang *et al.* (2006) which pinpointed the importance of serine 345 on *human* p47phox in the priming of human neutrophils. This body of evidence helps to strengthen our knowledge of signalling and transduction pathways involving NOX2 oxidase in key sentinel inflammatory cells including macrophages that are major players in the cellular and tissue injury caused by viruses. This has major implications for the over exuberant inflammatory responses occurring as a result of IAV infection that could be exploited therapeutically. However, what

remains unidentified is the subcellular compartments of ROS generation, and how this ROS modulates disease caused by viruses. These knowledge gaps therefore warranted the further investigations of Chapter 3.

Conceptual advancement 2: Identification of endosomes as the subcellular site of ROS generation to virus infection

The overproduction of ROS is a key process that occurs during influenza virus infections, consequently leading to enhanced oxidative stress that contributes to tissue injury and lung inflammation (Akaike *et al.*, 1996). However, the specific subcellular site of ROS generation during influenza infections has not been elucidated. In Chapter 3, we provided strong and unequivocal evidence for a spatially targeted platform for ROS generation, initiated within endosomes following virus infection. To support this idea, we revealed that NOX2 oxidase co-localised with early endosomes and nucleoprotein for IAV upon infection. The fact that we did not see colocalisation exclusively in early endosomes indicates that expression is likely to occur in other subcellular compartments as well, including late endosomes and lysosomes. Having established the enzymatic machinery for ROS generation is distributed in endosomal compartments, we demonstrate that infection with various ssRNA and DNA viruses that differ in genetic makeup increased the endosomal ROS and were dependent on TLR7 and TLR9, respectively. We also revealed that influenza virus activates NOX2 independently of ERK1/2 phosphorylation-independent but rather depended on cytosolic PKC activation. We have dissected the pathways involved in the signal transduction of redox dependent innate immune responses following virus infection. Undoubtedly, there are still unidentified pathways, which are redox regulated that will be discovered. However, our observations are significantly enhancing our current understanding of the complex biochemical pathways that underlie viral infections, which may be exploited therapeutically.

Conceptual advancement 3: Endosomal location of molecular targets of ROS and the consequences of ROS over production

Having established the pathways involved in regulating immunity to influenza virus infections, another important aspect arising from this study are the potential molecular targets of ROS. Indeed, we demonstrate that cysteine residues on the ectodomain of TLR7 receptor are major molecular targets of NOX2-derived H_2O_2. Specifically, we show that Cys98, in particular, to be necessary for modulating anti-viral signalling networks; as mutation of this cysteine abolished the ability of H_2O_2 to regulate cytokine expression. This builds significantly upon the study conducted by Kanno *et al.* (2013b), which demonstrated Cys98 forms an intramolecular disulphide bond with Cys475 on the TLR7 receptor that is necessary to elicit a response. Given

that proteolytic cleavage of the ectodomain of TLR7 occurs strictly in a low pH environment (Ewald *et al.*, 2011; Kanno *et al.*, 2013b) and also regulates receptor activity exemplifies that the mechanisms that underpin TLR7 activation are likely to be multiple but critically these occur in endosomes. To support the notion that Cys98 is a ROS target, it is well established that cysteine residues possess a thiol moiety in the side chain, making them particularly sensitive to oxidation (Meng *et al.*, 2013; Miki *et al.*, 2012). Given that Cys98 is a target for the redox dependent modulatory effects of H_2O_2 on antiviral signaling, whereas other conserved cysteine residues (Cys445) on the TLR7 are not raises the question of why this particular cysteine appears to be more susceptible to oxidative interaction. It is possible that the protein environment where the cysteine residues reside renders it more likely to being oxidized. For example, specific cysteine residues that are highly reactive towards ROS have demonstrated to be located within the active site of the enzyme (Fomenko *et al.*, 2008; Zhang *et al.*, 1993). The fact that this specific Cys is the only cysteine on TLR7 out of the total of 27 on the receptor to be both 1) highly conserved in eukaryotes from teleosts to man and 2) unique to this receptor within the entire 10 mammalian TLRs speaks to the importance of this receptor in mediating signaling pathways that have a functionally distinct cellular response. This phenomenon of redox regulation through cysteine oxidation occurs with other proteins. For example, the catalytic regions of PTPs possess cysteine residues that are susceptible to oxidative inactivation, where H_20_2 is capable of reducing the activity of phosphatases (Rhee, 2006; Salmeen *et al.*, 2005). It is likely that various other receptors including G-protein coupled receptors that have reactive cysteines on their complex may also signal from the endosomal compartment and potentially be targets of H_20_2. To elaborate on this, it is critical that future studies unravel the crystal structure of TLR7. This structural information will unfold the regulatory mechanisms and advance our understanding of the enzymatic activity of the protein, functionality and interactions with other proteins. Taken together, this body of evidence indicates that cysteine residues within the endosome are important for signaling downstream mechanisms to elicit a cytokine response following virus infection. This concept may be useful in regards to regulating inflammation in various diseases involving TLR7, e.g. systemic lupus erythematosus, which allow us to unveil more potential drug targets.

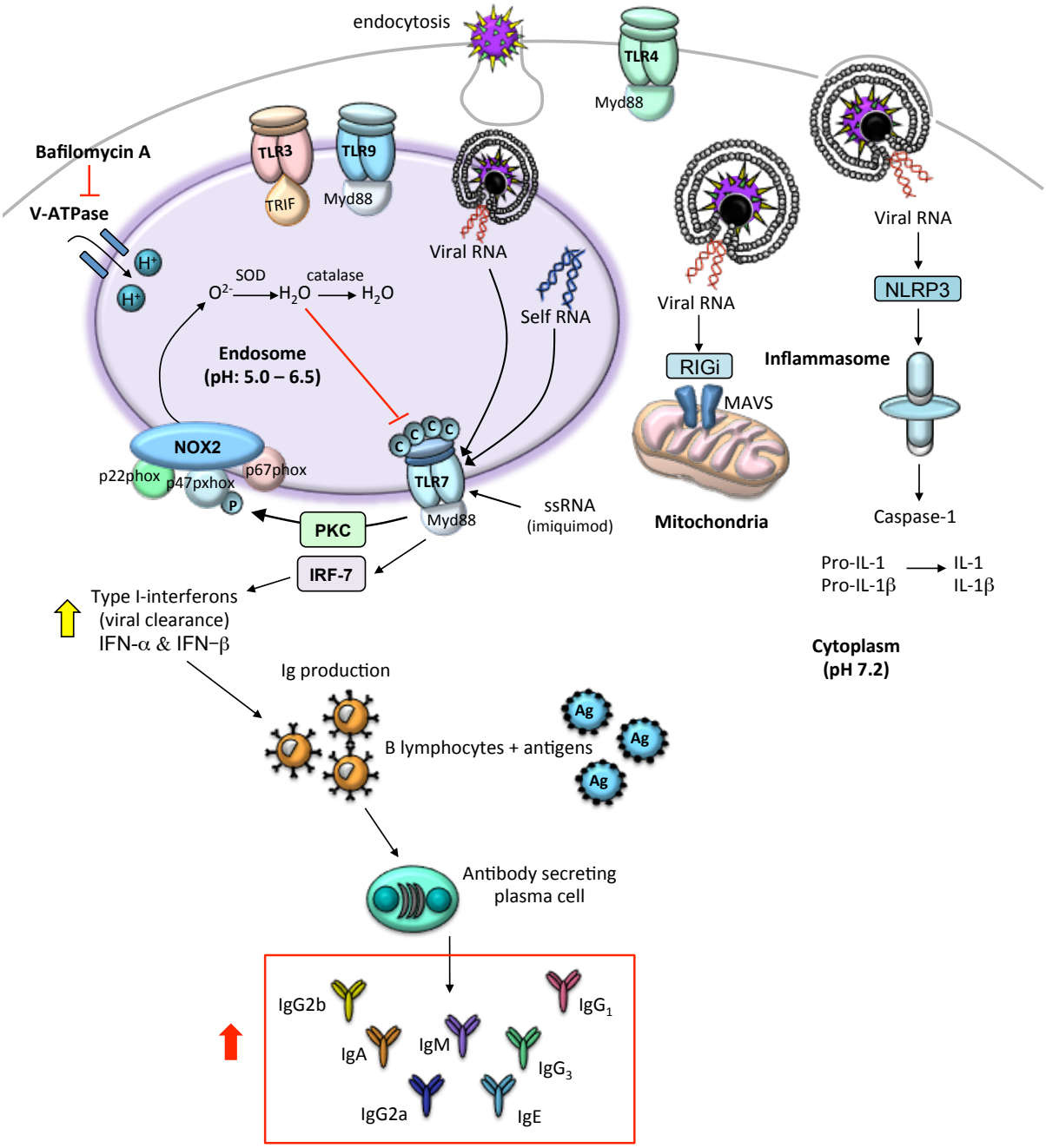

Figure 1: Proposed model of the NOX2-TLR7 signaling axis during influenza virus infection. Viruses internalize via endocytosis, resulting in acidification within endosomes and the release of ssRNA that binds onto TLR7. TLR7 signals IRF-7 to stimulate the generation of Type-1 interferons, which trigger the production of antibodies from B cells. TLR7 can also signal NOX2 oxidase that cause phosphorylation of serine residues on p47phox via a PKC-dependent mechanism, which is required for NOX2 activation and the generation of endosomal ROS. Specifically, endosomal NOX2-dervied H_20_2 negative regulates TLR7 activity via cysteine residues on the ectodomain of TLR7.

Conceptual advancement 4: A novel endosomal NOX2 inhibitor protects against both low and high pathogenicity influenza A virus strains

NOX2 derived ROS had been implicated in influenza infections, but how the spatial confinement of certain ROS modulates disease remains unidentified. In order to test the functional significance of ROS, we demonstrated that genetic deletion of NOX2 resulted in a significant increase in antiviral cytokine expression and antibody generation. Since the NOX2 enzyme is a crucial arm of innate immunity that is required for the elimination of invading pathogens, perhaps inhibiting NOX2 completely is not ideal as it mimics CGD patients who have a defective capacity to generate ROS and thus are more susceptible to developing bacterial infections (Berendes *et al.*, 1957). Indeed, we demonstrate ROS generation triggered by various pathogens to possess distinct pathways, where gram negative and positive bacterium drives phagosomal TLR4 activity and ROS production. In contrast, certain ssRNA viruses promote ROS generation via endosomal TLR7. Thus, it appears that a delicate balance of NOX2 inhibition in conjunction with the spatial targeting to endosomal compartments would be desirable in modulating the disease outcome in influenza infection. Therefore, we sought out to design a endosome-targeted NOX2 inhibitor that can acutely suppress endosomal ROS for the purpose of reducing viral pathogenesis whilst balancing the hyper inflammation often observed in IAV disease. This idea of targeting proteins within the endosome was partially derived from Rajendran *et al.* (2008b), who employed endosomal delivery of drugs for inhibition of beta secretase for the treatment of Alzheimer's disease. With striking success we showed, that administration of the endosomal NOX2 inhibitor in a manner to prevent viral disease (i.e. prior to virus infection) substantially reduced IAV severity.

Building on this framework, we wanted to examine whether the novel endosome NOX2 inhibitor provides protection against a more virulent IAV strain. In Chapter 4, we demonstrate that targeted inhibition of endosomal NOX2 provides protection against influenza infections. As evident in Chapter 3, targeted inhibition of endosomal NOX2 with Cgp91 administered in a preventative manner abolished several symptoms induced by Hkx-31 virus. Here, we show that treatment in a preventative fashion (i.e prior to virus infection) is also protective against the highly pathogenic PR8 influenza virus strain. Indeed, we demonstrate a reduction in neutrophil infiltration, pulmonary inflammation, peribronchiolar inflammation and cellular inflammatory infiltrate, as well as a trend for reduction in viral mRNA expression. However, Cgp91 was not as effective against the PR8 strain when compared with its effects against the Hkx-31 strain. This might be due to the fact that PR8 virus is substantially more virulent than Hkx31. In comparison with the Hkx-31 virus, the PR8 virus has been previously shown to induce higher levels of virus replication (Tate *et al.*, 2011), which may also account for the ineffectiveness of Cgp91 in

reducing airway inflammation. Moreover, Cgp91 was more efficacious than Ugp91 in reducing airway inflammation, pulmonary inflammation, neutrophil infiltration, viral titres and superoxide generation induced by PR8 infection. This suggests that selectively targeting endosomal ROS as opposed to targeting ROS generated in all subcellular compartments is more beneficial during an influenza virus infection. From this, it can be speculated that the endosomal ROS generated is likely to contribute, at least in part, to the lung inflammation and tissue injury observed during PR8 infection.

Given that the drug showed significant improvements in inflammation via the preventative approach, an alternative and equally important, clinically relevant model is to administer the drug in an interventional manner. Thus, we wanted to determine whether an intervention approach with the novel NOX2 oxidase inhibitor would alleviate influenza virus disease. It was apparent that treatment with the Cgp91 reduced airway inflammation, neutrophil influx and viral mRNA expression in Hkx-31-infected animals. However, the intervention approach with Ugp91 treatment did not display any benefits in the PR8-infected mice. This may be attributed by the fact that the inflammatory response and virus replication has already been initiated prior to drug administration. The early stages of IAV infection is characterised by the release of inflammatory mediators that result in the recruitment of neutrophils and macrophages into the inflamed lungs, which is necessary for viral clearance and host protection (Ada *et al.*, 1986). At the same time, ROS generation and virus replication occurs quite rapidly, usually peaking approximately 24-48 hours post infection with influenza virus (La Gruta *et al.*, 2007). The excessive production of ROS during this initial phase may explain why the intervention models with these inhibitors were not as effective in halting the progression and severity of influenza virus infections. It is probable that the timing of administration with the peptides appears to have been too late to alleviate the inflammation induced. Perhaps this particular dose (0.2mg/kg) was not enough to reduce the overactive immune responses caused by virus infection. The potential limitations associated with this study are the lack of knowledge about the pharmacokinetic properties of these inhibitors. For example, determining the half-life and absorption of the drug into the circulation would make it much easier to attain the optimal dosing regimen to treat influenza virus infected animals. Another important property of these inhibitors that requires further examination is their potential toxicity and capacity to cause adverse effects. Thus far however, we demonstrated that there were no discernible adverse reactions observed in our experimental animal model with the doses used and thus our NOX2 inhibitors are likely to be safe *in vivo*, consistent with Rey *et al.* (2001) who did not report any adverse effects in animals treated with gp91ds-tat.

Potential treatment strategy for tackling global viral disease

To this end, this thesis has contributed to a better understanding of endosome biology and cellular signalling of viruses. These concepts and observations were translated to a drug discovery approach, where the use of the custom designed drug for endosome-targeted inhibition of NOX2 proved to relieve viral pathology over and above an inhibitor of NOX2 that was not endosome targeted. These are the major findings of this thesis, giving strong rationale for future studies that examine the effects of the novel inhibitors in the context of other respiratory virus infections *in vivo*. Another interesting aspect that can be investigated is whether combined therapy of endosomal-targeted ROS inhibition will boost immunity to currently used vaccines. Moreover, the endosomal-targeted ROS inhibitor coupled with a TLR7 agonist is another possible therapeutic strategy to control viral infections. Stimulation of TLR7 with a synthetic TLR7 ligands have shown to be effective in promoting a sustained humoral immune response by generating a more potent Th1-polarised antibody production that provides protection against influenza virus infection (Chen *et al.*, 2016; Goff *et al.*, 2015). Incorporation of a synthetic TLR7 agonist as an adjuvant to improve vaccine immunogenicity has been used in other settings of viral infections, including human papillomavirus and human immunodeficiency virus (Stern *et al.*, 2012; Wille-Reece *et al.*, 2005). For this reason, we believe that acutely reducing the generation of endosomal ROS that contributes to lung inflammation, in combination with appropriate levels of TLR7 stimulation to boost Th-1 type immunogenicity, which will accelerate the onset of a protective immune response may provide a more protective outcome against influenza virus infections. Finally, uncovering the crystal structure of TLR7 will provide more information about the structural basis for cross-talk between receptors that is essential to unravelling more potential drug targets.

Concluding remarks

In conclusion, this study has provided substantial conceptual advancements in our understanding of endosome biology and cellular signalling of viruses, by identifying novel fundamental mechanisms of virus pathogenicity involving NOX2 and TLR7. The therapeutic benefit of acute endosome-targeted NOX2 inhibition may, not only be useful for the treatment of viral infections, but also in controlling other debilitating inflammatory related disorders including cancer and autoimmune disease.

References

Ada GL, Jones PD (1986). The immune response to influenza infection. *Curr Top Microbiol Immunol* **128:** 1-54.

Akaike T, Noguchi Y, Ijiri S, Setoguchi K, Suga M, Zheng YM*, et al.* (1996). Pathogenesis of influenza virus-induced pneumonia: Involvement of both nitric oxide and oxygen radicals. *Proc. Natl. Acad. Sci. U. S. A.* **93**(6)**:** 2448-2453.

Berendes H, Bridges RA, Good RA (1957). A fatal granulomatosus of childhood: the clinical study of a new syndrome. *Minn Med* **40**(5)**:** 309-312.

Chen T, Hu Y, Liu B, Huang X, Gao N, Jin Z*, et al.* (2016). Synthetic toll-like receptor 7 agonist as a conjugated adjuvant enhances the Th1 type immunogenicity of influenza virus vaccine. *Int. J. Clin. Exp. Pathol.* **9**(4)**:** 4790-4795.

Dang PMC, Stensballe A, Boussetta T, Raad H, Dewas C, Kroviarski Y*, et al.* (2006). A specific p47phox-serine phosphorylated by convergent MAPKs mediates neutrophil NADPH oxidase priming at inflammatory sites. *Journal of Clinical Investigation* **116**(7)**:** 2033-2043.

El Benna J, Faust LRP, Johnson JL, Babior BM (1996). Phosphorylation of the burst oxidase subunit p47phox as determined by two-dimensional phosphopeptide mapping: Phosphorylation by protein kinase C, protein kinase A, and a mitogen-activated protein kinase. *Journal of Biological Chemistry* **271**(11)**:** 6374-6378.

El-Benna J, Dang PMC, Gougerot-Pocidalo MA (2008). Priming of the neutrophil NADPH oxidase activation: Role of p47phox phosphorylation and NOX2 mobilization to the plasma membrane. *Seminars in Immunopathology* **30**(3)**:** 279-289.

Ewald SE, Engel A, Lee J, Wang M, Bogyo M, Barton GM (2011). Nucleic acid recognition by Toll-like receptors is coupled to stepwise processing by cathepsins and asparagine endopeptidase. *J. Exp. Med.* **208**(4)**:** 643-651.

Fomenko DE, Marino SM, Gladyshev VN (2008). Functional diversity of cysteine residues in proteins and unique features of catalytic redox-active cysteines in thiol oxidoreductases. *Mol. Cells* **26**(3)**:** 228-235.

Goff PH, Hayashi T, Martínez-Gil L, Corr M, Crain B, Yao S*, et al.* (2015). Synthetic toll-like receptor 4 (TLR4) and TLR7 ligands as influenza virus vaccine adjuvants induce rapid, sustained, and broadly protective responses. *Journal of Virology* **89**(6)**:** 3221-3235.

Imai Y, Kuba K, Neely GG, Yaghubian-Malhami R, Perkmann T, van Loo G*, et al.* (2008). Identification of Oxidative Stress and Toll-like Receptor 4 Signaling as a Key Pathway of Acute Lung Injury. *CELL* **133**(2)**:** 235-249.

Kanno A, Yamamoto C, Onji M, Fukui R, Saitoh SI, Motoi Y*, et al.* (2013). Essential role for Toll-like receptor 7 (TLR7)-unique cysteines in an intramolecular disulfide bond, proteolytic cleavage and RNA sensing. *Int. Immunol.* **25**(7)**:** 413-422.

La Gruta NL, Kedzierska K, Stambas J, Doherty PC (2007). A question of self-preservation: Immunopathology in influenza virus infection. *Immunol. Cell Biol.* **85**(2)**:** 85-92.

Meng FG, Zhang ZY (2013). Redox regulation of protein tyrosine phosphatase activity by hydroxyl radical. *Biochim. Biophys. Acta Proteins Proteomics* **1834**(1)**:** 464-469.

Miki H, Funato Y (2012). Regulation of intracellular signalling through cysteine oxidation by reactive oxygen species. *J. Biochem.* **151**(3)**:** 255-261.

Rajendran L, Schneider A, Schlechtingen G, Weidlich S, Ries J, Braxmeier T*, et al.* (2008). Efficient inhibition of the Alzheimer's disease β-secretase by membrane targeting. *Science* **320**(5875)**:** 520-523.

Rey FE, Cifuentes ME, Kiarash A, Quinn MT, Pagano PJ (2001). Novel competitive inhibitor of NAD(P)H oxidase assembly attenuates vascular O2 - and systolic blood pressure in mice. *Circ. Res.* **89**(5)**:** 408-414.

Rhee SG (2006). H2O2, a necessary evil for cell signaling. *Science* **312**(5782)**:** 1882-1883.

Salmeen A, Barford D (2005). Functions and mechanisms of redox regulation of cysteine-based phosphatases. *Antioxidants and Redox Signaling* **7**(5-6)**:** 560-577.

Stern PL, van der Burg SH, Hampson IN, Broker TR, Fiander A, Lacey CJ*, et al.* (2012). Therapy of human papillomavirus-related disease. *Vaccine* **30**(SUPPL.5)**:** F71-F82.

Tate MD, Schilter HC, Brooks AG, Reading PC (2011). Responses of mouse airway epithelial cells and alveolar macrophages to virulent and avirulent strains of influenza a virus. *Viral Immunol.* **24**(2)**:** 77-88.

Vlahos R, Stambas J, Bozinovski S, Broughton BRS, Drummond GR, Selemidis S (2011). Inhibition of Nox2 oxidase activity ameliorates influenza a virus-induced lung inflammation. *PLoS Pathogens* **7**(2).

Wille-Reece U, Flynn BJ, Loré K, Koup RA, Kedl RM, Mattapallil JJ*, et al.* (2005). HIV Gag protein conjugated to a Toll-like receptor 7/8 agonist improves the magnitude and quality of Th1 and CD8+ T cell responses in nonhuman primates. *Proc. Natl. Acad. Sci. U. S. A.* **102**(42)**:** 15190-15194.

Zhang ZY, Dixon JE (1993). Active site labeling of the yersinia protein tyrosine phosphatase: The determination of the pKa of the active site cysteine and the function of the conserved histidine 402. *Biochemistry®* **32**(36)**:** 9340-9345.

Appendix

Abstracts for conference attendance

Oral presentations

Title: Nox2 oxidase-derived reactive oxygen species (ROS) suppresses immunity to TLR7

Eunice E To[1], Keshia S Hendricks[1], Grant R Drummond[1], Steven Bozinovski[2], Ross Vlahos[2], Stavros Selemidis[1].

1. Department of Pharmacology, Infection and Immunity Program, Biomedicine Discovery Institute, Monash University, Clayton, Victoria, Australia, 3800.
2. Drug Discovery Biology, Monash Institute of Pharmaceutical Sciences, Monash University, Parkville, Victoria, Australia, 3052.

SFRRA ANNUAL SCIENTIFIC MEETING

3rd–6th DECEMBER 2014, MELBOURNE, AUSTRALIA

Title: Negative regulation of RNA immunity by endosomal reactive oxygen species

Eunice E To[1], Michelle Halls[3], Raymond Luong[1], Patrick Reading[4], Ross, Vlahos[2], Steven Bozinovski[2], Grant R Drummond[1], Stavros Selemidis[1]

1. Department of Pharmacology, Infection and Immunity Program, Biomedicine Discovery Institute, Monash University, Clayton, Victoria, Australia, 3800.
2. School of Health Sciences and Health Innovations Research Institute, RMIT University, Bundoora, Victoria, Australia, 3083.
3. Drug Discovery Biology, Monash Institute of Pharmaceutical Sciences, Monash University, Parkville, Victoria, Australia, 3052.
4. Department of Microbiology and Immunology, The University of Melbourne, The Peter Doherty Institute for Infection and Immunity, Melbourne, Victoria, Australia, 3000

ASCEPT/APSA JOINT SCIENTIFIC MEETING

29th NOV–2nd DECEMBER 2015, HOBART, AUSTRALIA

Poster presentations

Title: Negative regulation of RNA immunity by endosomal reactive oxygen species Eunice E To[1], Michelle Halls[3], Raymond Luong[1], Patrick Reading[4], Ross, Vlahos[2], Steven Bozinovski[2], Grant R Drummond[1], Stavros Selemidis[1]

1. Department of Pharmacology, Infection and Immunity Program, Biomedicine Discovery Institute, Monash University, Clayton, Victoria, Australia, 3800.
2. School of Health Sciences and Health Innovations Research Institute, RMIT University, Bundoora, Victoria, Australia, 3083.
3. Drug Discovery Biology, Monash Institute of Pharmaceutical Sciences, Monash University, Parkville, Victoria, Australia, 3052.
4. Department of Microbiology and Immunology, The University of Melbourne, The Peter Doherty Institute for Infection and Immunity, Melbourne, Victoria, Australia, 3000

ASCEPT/APSA JOINT SCIENTIFIC MEETING

29th NOV–2nd DECEMBER 2015, HOBART, AUSTRALIA

Title: NOX2 oxidase expressed in endosomes exacerbates influenza pathogenicity

Eunice E. To[1], Raymond Luong[1], Michelle L. Halls[2], Patrick C. Reading[3,6], Paul King[4], Grant R. Drummond[1], Christopher G. Sobey[1], Brad R.S. Broughton[1], Malcolm Starkey[5,6], Sharon R. Lewin[6,7], John O'Leary[8,9], Doug A. Brooks[10], Tim Quach[11,12], Christopher J.H. Porter[11,13], Steven Bozinovski[14], Ross Vlahos[14] and Stavros Selemidis[1]

1. Department of Pharmacology, Infection and Immunity Program, Biomedicine Discovery Institute, Monash University, Clayton, Victoria, Australia, 3800
2. School of Health Sciences and Health Innovations Research Institute, RMIT University, Bundoora, Victoria, Australia, 3083.
3. Drug Discovery Biology, Monash Institute of Pharmaceutical Sciences, Monash University, Parkville, Victoria, Australia, 3052.
4. Department of Microbiology and Immunology, The University of Melbourne, The Peter Doherty Institute for Infection and Immunity, Melbourne, Victoria, Australia, 3000.
5. Department of Medicine, Monash Medical Centre, Monash University, Clayton, Victoria, Australia, 3168.
6. Priority Research Centre's Grow Up Well and Lung Health, School of Biomedical Sciences and Pharmacy, Faculty of Health and Medicine, The University of Newcastle, and Hunter Medical research Institute, New South Wales, Australia, 2305.
7. The Peter Doherty Institute for Infection and Immunity, Melbourne, Victoria, Australia, 3000.
8. Department of Infectious Diseases, Alfred Hospital and Monash University, Melbourne, Australia 3004.
9. School of Biochemistry and Immunology, Trinity Biomedical Sciences Institute, Trinity College Dublin, Dublin 2, Ireland.

10. ARC Centre of Excellence in Convergent Bio-Nano Science and Technology, Monash Institute of Pharmaceutical Sciences, Monash University, Parkville, Victoria, Australia, 3052.
11. Medicinal Chemistry, Monash Institute of Pharmaceutical Sciences, Monash University, Parkville, Victoria, Australia, 3052.
12. Drug Delivery Disposition and Dynamics, Monash Institute of Pharmaceutical Sciences, Monash University, Parkville, Victoria, Australia, 3052.
13. School of Pharmacy and Medical Sciences, Sansom Institute for Health Research, Division of Health Sciences, University of South Australia, Australia, 5001.
14. Department of Histopathology Trinity College Dublin, Ireland, Sir Patrick Dun's Laboratory, Central Pathology Laboratory, St James's Hospital, Dublin 8, Ireland.

EUROPEAN RESPIRATORY SOCIETY SCIENTIFIC MEETING

3rd- 8th SEPTEMBER 2016, LONDON, UNITED KINGDOM